Deciphering the role of *tlx* in dorsal neural progenitors and its contribution to brain structure and behavior

by

Emily A. Drill

B.S. (Univ. Hons.), Carnegie Mellon University, 2003

Submitted to the Graduate Faculty of

The School of Medicine and the Center for Neuroscience

in partial fulfillment of the requirements for the degree of

Doctor of Philosophy

University of Pittsburgh

2009

UNIVERSITY OF PITTSBURGH

School of Medicine, Center for Neuroscience

This dissertation was presented

by

Emily A. Drill

It was defended on

July 8th, 2009

and approved by

J. Patrick Card, PhD, Professor, Department of Neuroscience

Laura Lillien, PhD, Associate Professor, Department of Neurobiology

Edda Thiels, PhD, Assistant Professor, Department of Neurobiology

Julie Blendy, PhD, Associate Professor, Department of Pharmacology, University of Pennsylvania

Chairperson: Cynthia Lance-Jones, PhD, Associate Professor, Department of Neurobiology

Dissertation Advisor: A. Paula Monaghan, PhD, Associate Professor, Department of Neurobiology

Deciphering the role of *tlx* in dorsal neural progenitors and its contribution to brain structure and behavior

Emily A. Drill, Ph.D.

University of Pittsburgh, 2009

Tlx (*Nr2E1*) is an orphan nuclear receptor transcription factor expressed in neural progenitor cells (PCs) in the forebrain throughout development and in regions of adult neurogenesis. *Tlx* regulates proliferation in both embryonic and adult PCs. Loss of *tlx* leads to abnormalities in limbic structures resulting in alterations in emotional and cognitive behaviors. However, the precise role of *tlx* in the developing forebrain and how *tlx* contributes to the normal development of adult anatomy and behavior are not fully understood. *Tlx* is expressed in PCs throughout the dorsal and ventral telencephalon and the diencephalon that give rise to structures including the cerebral cortex, hippocampus, amygdala, septum, striatum, and hypothalamus. Detailed examination of *tlx* expression revealed that within the dorsal PC population *tlx* is expressed specifically in radial glial progenitors but is absent from intermediate progenitor cells (IPCs). However, in the absence of *tlx* IPCs are reduced throughout development, suggesting that *tlx* promotes the production of IPCs. To examine the role of *tlx* specifically in dorsal PCs we generated mice with a conditional mutation of *tlx* in cortical, Emx1-expressing PCs (tlx^{cKO}). In these animals functional recombination of the floxed *tlx* allele occurs prior to embryonic day 12.5. Tlx^{cKO} animals show similar changes in PCs as nulls, indicating a requirement for *tlx* within dorsal PCs. The cerebral cortex of tlx^{cKO} animals is reduced in surface area and thickness from birth, persisting into adulthood. As in *tlx* null mutants, superficial layers are specifically affected and caudal functional cortical areas, including visual cortex, are disproportionately

reduced. Other dorsally-derived structures, including the hippocampus, specific nuclei of the amygdala, and the septum are reduced, whereas ventrally-derived structures are relatively unaffected. These animals exhibit a subset of the behavioral abnormalities observed in nulls, with the primary phenotype being a reduction in anxiety. Together, these findings suggest an important role for *tlx* in the regulation of dorsal PCs. I propose that *tlx* promotes divisions that produce IPCs, and that disruption of this population leads to specific alterations in adult brain structure and behavior. This model allows us to begin to make connections between early development and behavior.

TABLE OF CONTENTS

LIST OF TABLES

LIST OF FIGURES

ACKNOWLEDGEMENTS

First of all I thank Paula for all of her support and understanding throughout my time at the University of Pittsburgh. Paula, thank you for your mentorship, your time, and your patience as you have guided me through this journey, I am truly grateful for everything you have done for me. I thank the members of my thesis committee, Pat, Laura, Floh, and Cynthia, for their suggestions and guidance. I also thank my outside examiner, Julie Blendy, for taking the time to participate in my thesis defense and provide input regarding my research. I thank the past and current members of the Monaghan Laboratory for their help, support, and friendship during my time here. Susan Harrison for her advice on all things related to science and for teaching me nearly everything I know about doing *in situ* hybridization and immunohistochemistry. Heather Wilson for teaching me many things in the lab, for initiating the study of the conditional *tlx* adults, and for being the one to handle the adult *tlx* null animals. Kirsten Mauro, Liping Wang, and Jared Clemens for their assistance with my laboratory work. I thank Eloise Peet for guiding me through all of my behavior studies. I thank the members of the Lance-Jones Laboratory and the Development Journal Club for helpful discussions of my data. I thank my incredibly supportive graduate school classmates who have been right there with me since we studied together for our first-year courses. For reagents I thank Dr. R. Klein, Dr. A. McMahon, Dr. Y. Shi, and Dr. M. Takeichi. I thank Dr. G. Schütz for the *tlx* floxed mice and Dr. K Jones for the Emx1-Cre mice. I thank Dr. P. Levitt and Dr. M. Torii for hosting me at Vanderbilt University and teaching me *in utero* electroporation.

Finally, I thank my family for their love, support, and encouragement. To my parents in particular, thank you for providing me with the wonderful opportunities that have allowed me to get to this point. And to Steve: thank you for always being there for me through all of the ups and downs of my graduate career, doing your best to keep me sane and happy. I love you and I couldn't have done this without you.

1.0 INTRODUCTION

The brain begins as a single layer of proliferating cells that divide and differentiate in a precisely timed and spatially regulated manner to produce all of the neurons and glial cells that make up this complex structure. This process requires precise control over the maturation of progenitor cells (PCs), regulating their cell cycle, the types of divisions that they make, the progeny produced, and finally the appropriate migration, maturation, and connectivity of differentiated cells. This control is mediated during development by a complex network of intrinsic and extrinsic factors (reviewed by (Gupta et al., 2002; Schuurmans and Guillemot, 2002; Guillemot et al., 2006; Miller and Gauthier, 2007)). Severe perturbations to these developmental processes can lead to gross cortical malformations such as microcephaly and lissencephaly (Lian and Sheen, 2006). However, more subtle developmental changes are thought to underlie neuropsychiatric disorders such as autism, schizophrenia, bipolar disorder, and anxiety disorders (Lewis and Levitt, 2002; Rush, 2003; Levitt et al., 2004; Courchesne et al., 2007; Serene et al., 2007). Identifying the mechanisms that regulate PCs during development is critical in understanding both the normal development of brain structure and behavior, and the underlying pathology of behavioral abnormalities.

This study investigates the role of *tlx* in the development of the mouse forebrain. *Tlx* is an orphan nuclear receptor expressed in regions of neurogenesis in the developing and adult forebrain (Monaghan et al., 1995; Stenman et al., 2003a; Shi et al., 2004; Liu et al., 2008). The

human homologue of *tlx*, *NR2E1*, has been linked to developmental disorders including bipolar disorder, schizophrenia, and microcephaly (Jackson et al., 1998; Kumar et al., 2007; Kumar et al., 2008). Mice lacking functional *tlx* expression exhibit abnormalities in limbic structures, resulting in alterations in emotional and cognitive behaviors (Monaghan et al., 1997; Yu et al., 2000; Roy et al., 2002; Young et al., 2002; Land and Monaghan, 2003; Stenman et al., 2003a; Stenman et al., 2003b; Miyawaki et al., 2004; Shi et al., 2004; Zhang et al., 2006; Belz et al., 2007; Zhang et al., 2008). These abnormalities are a consequence of alterations in the properties of PCs during development and in the adult brain (Roy et al., 2002; Stenman et al., 2003b; Roy et al., 2004; Shi et al., 2004; Zhang et al., 2006; Li et al., 2008; Liu et al., 2008; Zhang et al., 2008). This study dissects the complex role of *tlx* in the developing brain, identifying a role for *tlx* in a subset of forebrain progenitors thereby regulating the development of specific brain structures and behaviors.

1.1 FOREBRAIN DEVELOPMENT

1.1.1 Patterning of the telencephalon during development

Development of the nervous system begins with the formation of the neural plate, a specialization of the ectoderm. Through a process termed neurulation the neural plate folds upwards and fuses to form the neural tube (reviewed by (Colas and Schoenwolf, 2001)). The neural tube is divided along its anterior-posterior axis into four domains: the forebrain, the midbrain, the hindbrain, and the spinal cord (reviewed by (Foley and Stern, 2001)). The anterior-most region, the forebrain, is further divided into the telencephalon, which gives rise to

structures including the cerebral cortex, hippocampus, amygdala, septum, and basal ganglia or striatum, and the diencephalon, which gives rise to structures including the thalamus and hypothalamus. Together these structures make up the limbic system, a set of structures important for the regulation of emotional behavior, learning, and memory (Kandel et al., 1995).

The telencephalon is classically divided into the dorsal pallium and ventral subpallium. More recently these domains have been further subdivided on the basis of specific molecular profiles, identifying distinct progenitor populations that produce cells destined for specific structures (Figure 1). The dorsal pallium can be further subdivided into: the medial pallium, which gives rise to the hippocampus; the dorsal pallium, which will become the neocortex; the lateral pallium, which generates olfactory cortex; and the ventral pallium, which contributes cells to parts of the amygdala (Puelles et al., 2000; Yun et al., 2001). Similarly the ventral telencephalon is divided into the lateral and medial ganglionic eminences (LGE and MGE), which give rise to the striatum as well as interneurons that migrate into both the striatum and dorsal structures (de Carlos et al., 1996; Anderson et al., 1997; Puelles et al., 2000; Yun et al., 2001). These regions are generated through the expression of secreted signaling molecules that regulate the expression of homeodomain and basic helix-loop-helix (bHLH) transcription factors (reviewed by (Wilson and Rubenstein, 2000; Schuurmans and Guillemot, 2002). Cells of the anterior neural plate are exposed to sonic hedgehog (Shh) during gastrulation, initially specifying these cells with a ventral telencephalic identity (Gunhaga et al., 2000). However, as the neural plate folds dorsal cells are exposed to Wnt and Fgf8 signaling, suppressing ventral cell fates and inducing dorsal telencephalic character (Gunhaga et al., 2003). Shh induces expression of ventral telencephalic markers, including *nkx2.1*, *gsh2*, and *dlx2* (Gaiano et al., 1999; Corbin et al., 2000; Xu et al., 2005). Specification of the dorsal telencephalon is influenced by bone

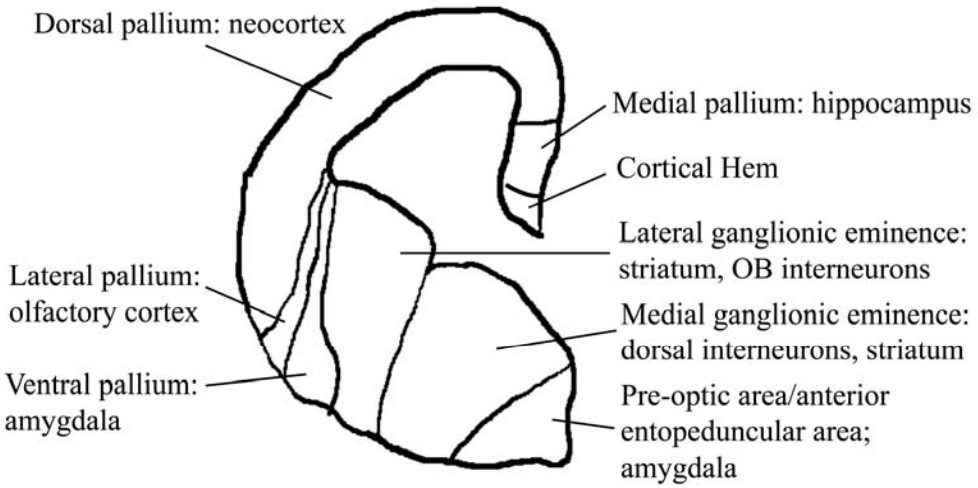

Figure 1. Regionalization of the embryonic telencephalon

This schematic coronal section through the E12.5 telencephalon shows dorsal and ventral subdomains and a partial list of their progeny. Figure adapted from (Schuurmans and Guillemot, 2002).

morphogenic proteins (BMPs) and Wnts, which have been shown to maintain pallial identity and suppress ventral telencephalic gene expression (Furuta et al., 1997; Backman et al., 2005). Wnt signaling is also important in the development of the hippocampus (Galceran et al., 2000; Lee et al., 2000b). Thus, a number of signaling molecules interact to establish different telencephalic regions; what are the downstream effectors that generate this regional identity within the cell?

Many homeodomain proteins have been shown interact to impart dorsal and ventral telencephalic identity. These include pax6, which maintains a dorsal telencephalic identity; in *pax6* mutants subpallial genes extend into the ventral pallium (Stoykova 2000, Torreson 2000, Yun 2001). In mice with a mutation in *gsh2*, which is expressed in both the LGE and MGE, dorsal cortical makers such as *pax6* extend ectopically into the subpallium (Corbin et al., 2000; Toresson et al., 2000; Yun et al., 2001). Similarly, *nkx2.1* acts downstream of Shh to specify an MGE fate and inhibits an LGE fate (Sussel et al., 1999; Xu et al., 2005). bHLH family transcription factors, including Neurogenin1 and 2 in the dorsal telencephalon and Mash1 in the

ventral telencephalon, are also important in determining dorsal versus ventral fate (Casarosa et al., 1999; Fode et al., 2000). Together, these and other genes interact to regionalize the telencephalon into distinct dorsal and ventral regions. The region where the dorsal and ventral telencephalon meet, referred to as the cortico-striatal boundary (or pallio-subpallial boundary), has been shown to contribute to specific nuclei of the developing amygdala (Puelles et al., 2000; Stoykova et al., 2000; Molnar and Butler, 2002; Carney et al., 2006). *Pax6*, *gsh2*, and *tlx* have been shown to interact in establishing this region (Corbin et al., 2000; Stoykova et al., 2000; Yun et al., 2001; Stenman et al., 2003a), although the precise regulation of this domain and its functional importance are still not entirely clear.

1.1.2 Neural cell types in the developing cortex

Progenitor cells in the telencephalon produce three main types of cells, neurons and two types of glial cells, oligodendrocytes and astrocytes, each of which derive from specific domains. Within the dorsal telencephalon progenitors mature over time, first generating excitatory glutamatergic neurons in a precisely timed manner and then transitioning into the production of astrocytes (Bayer and Altman, 1991; Levers et al., 2001). Additional populations of cells, primarily GABAergic inhibitory interneurons and oligodendrocytes, originate in ventral regions of the telencephalon and migrate into the developing cortex. This produces an adult cerebral cortex that is organized into six layers generated in an inside-out manner, each with distinct morphologies and connections (Angevine and Sidman, 1961). Many factors have been identified that regulate the proliferation, differentiation, and migration of these different populations of cells.

Glutamatergic projection neurons are born in the proliferative zone of the dorsal telencephalon and migrate radially outwards towards the pial surface. The first wave of post-mitotic neurons that migrates away from the ventricular zone (VZ) at E11 forms a layer known as the preplate. The second wave of migrating neurons splits the preplate to form the marginal zone (superficial) and subplate (deep) (Bayer and Altman, 1991; Price et al., 1997). Subsequent waves of migrating neurons exit the VZ and migrate past earlier-born layers of neurons (with the exception of the marginal zone, which will form superficial layer I) to form more superficial cortical layers (Angevine and Sidman, 1961; Rakic, 1974; Hevner et al., 2003). Normal migration depends on many different genes, including *reelin*, *doublecortin* (*dcx*), *lissencephaly 1* (*lis1*), and *cdk5* (D'Arcangelo et al., 1995; Gilmore et al., 1998; Hirotsune et al., 1998; Pilz et al., 1998; Cahana et al., 2001; Gupta et al., 2002; Bai et al., 2003). Laminar fate is closely tied to cell cycle number, with superficial layers born during the last four cell cycles, approximately E14 to E17 (Takahashi et al., 1999). The ability of PCs to contribute to different layers becomes increasingly restricted over time; heterochronic transplant studies have shown that early projection neuron precursors are multipotent and can contribute to any cortical layer, whereas later projection neurons become increasingly restricted to producing late-born superficial layer neurons (McConnell, 1988; McConnell and Kaznowski, 1991; Frantz and McConnell, 1996; Desai and McConnell, 2000). The ability of projection neurons to switch their layer commitment depends upon the progenitor cell completing the late part of its cell cycle in the host environment (McConnell and Kaznowski, 1991). Similarly, heterotopic transplant studies indicate that PCs also lose their ability to acquire different areal fates at later embryonic stages (Levitt et al., 1997).

Cortical layers can be distinguished by the expression of a number of different molecular markers (Hevner et al., 2003; Guillemot et al., 2006). Many of these genes play important roles at different stages during the specification and differentiation of these cortical layers; here I will highlight a few examples. The bHLH transcription factors *Ngn1* and *Ngn2* are important to specify a cortical, glutamatergic fate in early-born deep-layer neurons but are not required to specify upper-layer cortical neurons (Schuurmans et al., 2004). Genes *Cux2* (Zimmer et al., 2004) and *Svet1* (Tarabykin et al., 2001) identify populations of precursors in the subventricular zone (SVZ) fated to give rise to upper cortical neurons. Finally, *Fezl*, expressed weakly in early VZ progenitors and highly in layer V cells in the cortical plate, is important for the normal projections characteristic of layer V subcerebral projection neurons (Chen et al., 2005; Molyneaux et al., 2005). Cells in the cortex are also specified with an areal fate, which will be further described in Chapter 3.

GABAergic cortical interneurons derive from PCs in the ganglionic eminences of the ventral telencephalon (de Carlos et al., 1996; Anderson et al., 1997). Within the ventral telencephalon the LGE gives rise to neurons of the olfactory bulb and striatum, the MGE to cortical interneurons as well as hippocampal and striatal interneurons, and the caudal ganglionic eminence (CGE) to cortical interneurons as well as neurons of the hippocampus, amygdala, and striatum. Genetic, transplant, and cell tracing experiments suggest that the MGE is the source of most cortical interneurons (Lavdas et al., 1999; Sussel et al., 1999; Anderson et al., 2001; Wichterle et al., 2001). Interneurons expressing the calcium-binding proteins parvalbumin and somatostatin derive primarily from the MGE and require expression of MGE genes *Nkx2.1* and *Lhx6* (Xu et al., 2004; Butt et al., 2005; Xu et al., 2005; Liodis et al., 2007). In contrast, interneurons expressing calretinin originate mostly in the CGE (Xu et al., 2004; Butt et al.,

2005). Most cortical interneurons follow a restricted route of tangential migration to the cortex. Early during migration, as they leave the proliferative zone, cortical and striatal interneurons are sorted by semaphorin-neuropilin interations; only cortical interneurons express neuropilins, and therefore avoid migrating through the striatum due to a chemorepulsive signal composed of class 3 semaphorins (Marin et al., 2001). As interneurons approach the cortico-striatal boundary migration seems to be guided by a combination of diffusible attractive factors and a migration pathway defined by increasingly permissive substrates (Marin et al., 2003; Wichterle et al., 2003). Interneurons initially avoid the cortical plate, migrating through the marginal zone, intermediate zone, and subventricular zone (SVZ) (Lavdas et al., 1999; Wichterle et al., 2001; Polleux et al., 2002; Tanaka et al., 2003). Interneurons within the IZ and SVZ migrate tangentially predominantly in a lateral to medial direction but also exhibit both radial and non-radial migration towards the pial surface, eventually migrating into the cortical plate to reach their final location (Polleux et al., 2002; Tanaka et al., 2003). Similar to cortical projection neurons, cortical interneurons tend to populate the cortex in an inside-out manner (Fairen et al., 1986; Peduzzi, 1988; Valcanis and Tan, 2003; Hevner et al., 2004).

Oligodendrocytes are the myelin-forming cells in the central nervous system. Oligodendrocytes in the cerebral cortex originate from several distinct regions during development. The earliest oligodendrocytes arise from ventral precursors in the anterior entopeduncular area (or preoptic area), medial to the MGE (Spassky et al., 1998; Olivier et al., 2001; Tekki-Kessaris et al., 2001; Kessaris et al., 2006; Nakahira et al., 2006). Ventral oligodendrocyte precursor identity is specified at least in part by Shh signaling and by activity of the transcription factor Mash1 to induce expression of genes including platelet-derived growth factor receptor α (PDGFα) and Olig2 (Nery et al., 2001; Tekki-Kessaris et al., 2001). A second

wave of oligodendrocytes originates from the LGE and CGE, and postnatally a third wave originates from progenitors in the dorsal cortex, specified by FGF2 signaling (Gorski et al., 2002; Kessaris et al., 2006; Naruse et al., 2006; Yue et al., 2006). Differentiation of oligodendrocyte precursors is regulated by an intrinsic timing mechanism by which protein levels of the cyclin dependent kinase inhibitors $p27^{Kip1}$ and $p57^{Kip2}$ increase over time, promoting differentiation when a critical level is reached (Temple and Raff, 1986; Durand et al., 1997; Gao et al., 1997; Dugas et al., 2007).

Astrocytes have many roles in cortex, including regulation of synaptogenesis and synaptic plasticity, sequestering of neurotransmitters, and maintenance of the blood-brain barrier (He and Sun, 2007). At the end of neurogenesis (approximately E18), dorsal PCs that initially give rise to excitatory neurons switch to the production of astrocytes (Voigt, 1989; Gorski et al., 2002). The onset of gliogenesis is regulated by the convergence of several signaling pathways, including IL-6 cytokine, BMP, Notch, and epidermal growth factor (EGF)/FGF signaling (reviewed by (Miller and Gauthier, 2007)). The IL-6 cytokine family includes ciliary neurotrophic factor (CNTF), leukemia inhibitor factor (LIF), and cardiotrophin-1 (CT-1). These cytokines act via the JAK-STAT signaling pathway to promote astrocyte formation *in vivo* (Barnabe-Heider et al., 2005) or *in vitro* (Bonni et al., 1997; Rajan and McKay, 1998). Furthermore, mice with mutations of components in the cytokine downstream signaling pathway, coreceptors LIFRβ and gp130, show profound deficits in the generation of astrocytes (Ware et al., 1995; Koblar et al., 1998; Nakashima et al., 1999b). STATs bind directly to the promoters of astrocytic genes *gfap* and *s100β*, interacting with coactivators p300/CBP to promote transcription (Bonni et al., 1997; Nakashima et al., 1999a; Namihira et al., 2004). BMP and Notch signaling

have also been shown to promote gliogenesis, at least in part through interaction with the activated JAK-STAT pathway (Nakashima et al., 1999a; Ge et al., 2002).

Overall these findings have shown that glutamatergic neurons, GABAergic neurons, oligodendrocytes, and astrocytes have distinct spatial and temporal origins, with their generation regulated by complex signaling mechanisms involving both intrinsic and extrinsic factors. Although many of these factors involved in the specification and maturation of different populations of neurons and glia have been identified, the precise mechanisms are still not understood. Furthermore many of these cells with distinct origins converge in the dorsal telencephalon to form the adult cortex; this raises the additional question of to what degree there is interaction during development to coordinate production of these diverse populations.

1.1.3 Neural progenitor cells

All of the neurons and glia in the central nervous system are derived from neural PCs, proliferating cells with a limited capacity for self-renewal. Although the role for PCs in generating the neurons of the cerebral cortex has been recognized for some time (see (McConnell, 1995) for a review), more recent studies using novel molecular markers, cell lineage analysis, time-lapse imaging, and other techniques have changed our view of PCs and their role in neurogenesis and gliogenesis. Neural progenitors are a heterogeneous population of cells, differing in their molecular profiles and their responsiveness to environmental signals (reviewed by Lillien 1998). Prior to neurogenesis the neural tube is made up of a single layer of multipotent PCs known as neural epithelial cells (reviewed by (Gotz and Huttner, 2005)). These cells are highly polarized along the apical-basal axis, with nuclei that move up and down this axis during the cell cycle, a process known as interkinetic nuclear migration; the bodies of cells

undergoing mitosis are found at the apical surface adjacent to the ventricle while cells in S-phase are at the basal side of the progenitor region. At the onset of neurogenesis these progenitors transition into a more fate-restricted progenitor population known as radial glial cells (RGCs) (Williams and Price, 1995; Alvarez-Buylla et al., 2001). RGCs maintain radial processes to the pial and ventricular surfaces although their cell bodies remain in a layer adjacent to the ventricle known as the ventricular zone (VZ) where they go through interkinetic nuclear migration similar to neural epithelial cells (reviewed by (Rakic, 2003)). It was traditionally thought that during neurogenesis RGCs functioned as supporting cells and as a substrate for radially migrating neurons. However, it has now been well established that RGCs are proliferating cells that not only have the capacity to produce neurons and glia but in fact directly or indirectly give rise to the majority of cortical neurons (Malatesta et al., 2000; Hartfuss et al., 2001; Noctor et al., 2001; Heins et al., 2002; Noctor et al., 2002; Malatesta et al., 2003; Anthony et al., 2004). RGCs have a unique molecular profile that changes as they mature during neurogenesis (Hartfuss et al., 2001). From E12 all RGCs express the progenitor marker RC2, while a subset also express one or both of the astrocyte markers brain-lipid-binding protein (BLBP) and astrocyte-specific glutamate transporter (GLAST). As neurogenesis progresses some RGCs lose their RC2 expression but maintain BLBP and GLAST expression, and the proportion of RC2 positive cells that also express BLBP and GLAST increases. By the onset of gliogenesis all PCs express GLAST and BLBP while only about two thirds also express RC2 (Hartfuss et al., 2001). Interestingly, these different subpopulations of PCs showed differences with respect to cell cycle length (Hartfuss et al., 2001). At the end of neurogenesis RGCs begin to retract their processes, translocate outside the VZ, and transform into astrocytes (Voigt, 1989; Edwards et al., 1990).

A secondary proliferative population appears in mice at the onset of neurogenesis (Haubensak et al., 2004; Attardo et al., 2008; Noctor et al., 2008). These cells, termed intermediate progenitor cells (IPCs), are derived from PCs in the VZ and are characterized by a multipolar morphology and basal mitosis away from the ventricle (Haubensak et al., 2004; Miyata et al., 2004; Noctor et al., 2004; Attardo et al., 2008; Noctor et al., 2008). From E13.5 these cells are located basal to the VZ in a layer called the subventricular zone (SVZ) (Bayer and Altman, 1991; Bystron et al., 2008). IPCs were initially thought to produce mostly upper layer neurons (Tarabykin et al., 2001) but more recent studies have suggested that IPCs make a significant contribution to all cortical layers (Haubensak et al., 2004; Englund et al., 2005; Sessa et al., 2008; Kowalczyk et al., 2009). The control over production, proliferation, and neurogenesis of IPCs is not yet well understood; several factors that have been identified will be further discussed in Chapter 4. Furthermore, although IPCs have been shown to be involved in neurogenesis in the cortex, cerebellum, and hippocampus (Hevner et al., 2006) the role of IPCs in the development of other structures in the brain and in the normal expression of behavior have only begun to be explored. In this thesis we will address this broader role for IPCs.

1.1.4 Progenitor cell fate decisions

Throughout development, the cell cycle length, division type, and cell fate of progenitors is continuously changing (summarized in Figure 2). Numerous intrinsic and extrinsic factors interact to regulate these properties, influencing the decisions of whether to proliferate or differentiate, and whether to produce neurons or glia. Early during development divisions are predominantly proliferative, with neurogenic divisions appearing at the onset of neurogenesis (Haubensak et al., 2004). The antiproliferative gene Tis21 has been shown to be transiently

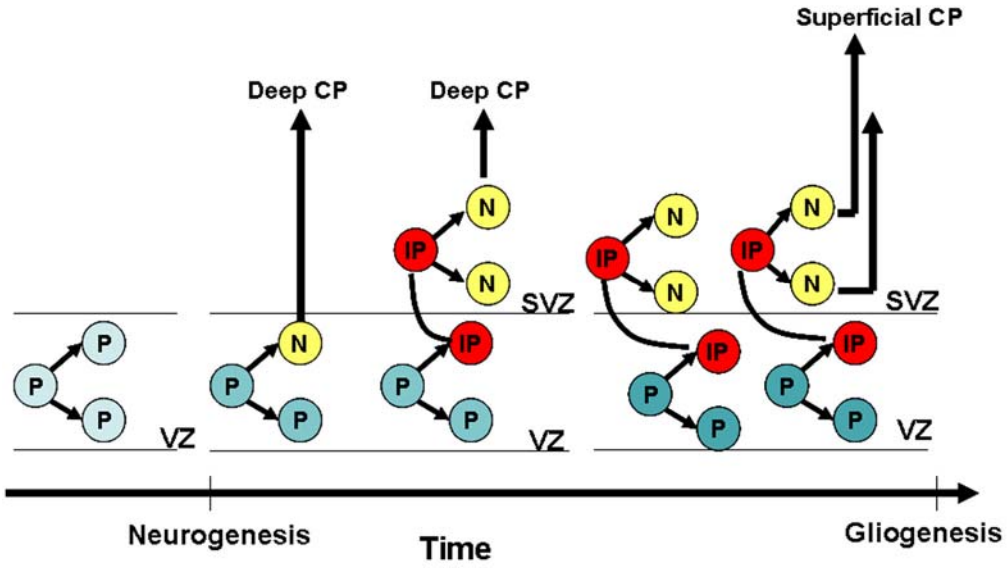

Figure 2. Progenitor cell divisions during development

As progenitor cells mature during development their division type and progeny fate change. Early during development progenitors primarily undergo symmetric proliferative divisions (P-P), expanding the progenitor population. At the onset of neurogenesis asymmetric neurogenic (P-N) and asymmetric intermediate progenitor-producing (P-IP) divisions appear. Neurons produced by both progenitor types are thought to contribute to deep layers. These IPs seed a secondary proliferative population in the subventricular zone (SVZ), apparent by mid-neurogenesis. IPs predominantly undergo symmetric neurogenic divisions (N-N) and produce most neurons of the superficial cortical plate. At the end of neurogenesis apical progenitors transition into astrocytes. A = astrocyte, CP = cortical plate, IP = intermediate progenitor, N = neuron, P = progenitor, SVZ = subventricular zone, VZ = ventricular zone. Adapted from a figure by S. Harrison.

upregulated during G1 in PCs that are fated to undergo neurogenic divisions (Iacopetti et al., 1999). As neurogenesis progresses the proportion of cells leaving the cell cycle through neurogenic divisions increases, depleting the PC population beginning from mid-neurogenesis (Caviness et al., 1999; Noctor et al., 2004). Neurogenesis is closely tied to the cell cycle number and cell cycle length; with each cell cycle the length of G1 and the proportion of cells exiting the

cell cycle increase (Takahashi et al., 1995b; Caviness et al., 1999; Takahashi et al., 1999). More recently it has been shown that neurogenic progenitors have a longer cell cycle than those undergoing proliferative divisions and that IPCs, which are neurogenic (Haubensak et al., 2004; Miyata et al., 2004; Noctor et al., 2004), have a longer G2 phase (Calegari et al., 2005). Experiments altering the length of the cell cycle suggest that increasing the length of G1 or blocking the progression from G1 to S can promote neurogenesis, indicating that the length of the cell cycle has an instructive role in PC fate ((Calegari and Huttner, 2003); reviewed by (Ohnuma and Harris, 2003; Gotz and Huttner, 2005)).

The apical-basal polarity of VZ PCs (neural epithelial cells and RGCs) is proposed to have an important role in generating symmetric versus asymmetric divisions (reviewed by (Gotz and Huttner, 2005)). VZ progenitors are highly polarized along the apical/basal axis, with certain transmembrane proteins, such as prominin-1, expressed in a putative "stem cell microdomain" localized at the apical surface adjacent to the ventricle. It has been shown that in symmetric proliferative divisions this small domain is bisected by the cleavage plane during mitosis and is divided between the two cells, whereas in asymmetric neurogenic divisions the cleavage plane bypasses this domain, which is then inherited in its entirety by the daughter progenitor (Kosodo et al., 2004). Many intrinsic factors have been shown to influence the decision to make either proliferative asymmetric divisions or neurogenic symmetric divisions, including the transcription factors Emx2 (Heins et al., 2001), which promotes a proliferative fate, and Pax6 (Heins et al., 2002), which promotes neurogenic divisions.

The Notch signaling pathway acts extrinsically to maintain the proliferative state of PCs. (reviewed by (Yoon and Gaiano, 2005)). Ligands expressed on the surface of differentiating neurons, including Delta, bind to the Notch receptor of neighboring cells. This releases the

intracellular domain of Notch, which translocates into the nucleus where it interacts with the CBF1 protein complex (also known as RBP-J or CSL) to activate transcription of pro-progenitor genes including basic helix-loop-helix (bHLH) family members such as *Hes1* and *Hes5* (Jarriault et al., 1995; Ohtsuka et al., 1999). These suppress expression of proneural bHLH genes including Mash1 and the Neurogenins. In the absence of Notch signaling these proneural genes are expressed, restricting progenitors to a neuronal fate and initiating neurogenesis (Nieto et al., 2001; Bertrand et al., 2002). It has recently been shown that although both RGCs and IPCs respond to Notch receptor activation these two populations differ in their responsiveness to CBF1 signaling (Mizutani et al., 2007). In RGCs, Notch signals through CBF1 as described above, and loss of signaling promotes neurogenesis via a conversion to IPCs. Notch signaling seems to have a role in maintaining the proliferative state of IPCs through a CBF1-independent mechanism (Mizutani et al., 2007).

During the development of the murine cortex neurons are generated first, in a specific inside-out laminar sequence, followed by the production of astrocytes (Bayer and Altman, 1991). It has been demonstrated using clonal analysis of single PCs that this specific timing, both production of deep layer neurons followed by the superficial layer neurons and production of neurons prior to glia, is intrinsically regulated (Qian et al., 2000; Shen et al., 2006). However extrinsic environmental signals also play a key role; for example, as previously discussed progenitors become increasingly restricted in their ability to produce neurons of different layers (McConnell, 1988; McConnell and Kaznowski, 1991; Frantz and McConnell, 1996; Desai and McConnell, 2000). A more recent study using constitutively active Notch signaling to force PCs to remain as proliferative PCs for several cell cycles demonstrated that once this Notch activity

was removed these PCs produced neurons with a laminar fate that matched the developmental stage, bypassing the generation of earlier-born neurons (Mizutani and Saito, 2005).

The generation of a neuronal fate is mediated within a cell by the expression of transcription factors. A transcription factor cascade involving the sequential expression of Pax6, Tbr2, NeuroD1, and Tbr1 has been proposed to control glutamatergic neurogenesis in the embryonic dorsal telencephalon as well as the developing cerebellum and adult dentate gyrus (Hevner et al., 2006). These transcription factors (see Figure 3) show sequential but overlapping expression in populations from PCs in the VZ to mature neurons in the cortical plate; Pax6 is expressed in the VZ, Tbr2 in the upper VZ and SVZ, NeuroD in the upper SVZ and lower intermediate zone, and Tbr1 in the upper intermediate zone and cortical plate (Gotz et al., 1998; Lee et al., 2000a; Hevner et al., 2001; Englund et al., 2005; Hevner et al., 2006). Within the forebrain Ngn2 regulates the program of glutamatergic differentiation in deep-layer neurons, including the expression of Tbr1 and Tbr2, while Pax6 and Tlx have been proposed to have a similar role in the specification of upper-layer neurons ((Schuurmans et al., 2004); reviewed by (Guillemot et al., 2006)). More recently Ngn2 has further been shown to have a role in the generation of IPCs, thus influencing upper layers as well (Britz et al., 2006; Hevner, 2006; Kowalczyk et al., 2009).

At the end of neurogenesis dorsal PCs switch to making glia. As previously described, this involves signaling from a variety of extrinsic signaling pathways, most notably IL-6 cytokines such as CT-1 (Barnabe-Heider et al., 2005). The extrinsic environment is critical for this neurogenic to gliogenic switch; for example, embryonic PCs taken at an age when they would normally produce neurons will instead produce astrocytes when cultured over a postnatal cortical slice (Morrow et al., 2001). However, this ability to induce astrocyte differentiation is

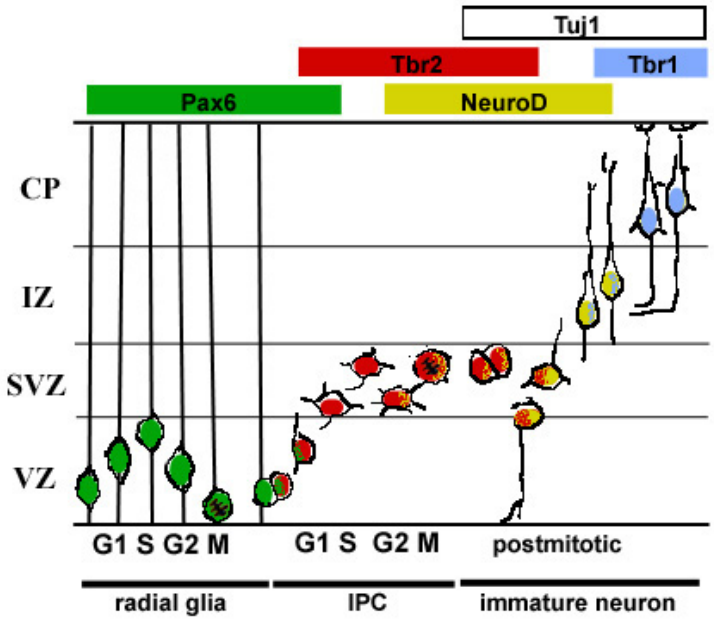

Figure 3. Transcription factor expression in neural progenitors

As cortical progenitor cells mature from radial glia to intermediate progenitor cells (IPC) to postmitotic neurons they express an overlapping series of transcription factors (colored bars). Postmitotic neurons also express neuron-specific class III β-tubulin (Tuj1). G1, S, G2, M indicate phases of the cell cycle. CP = cortical plate; IZ = intermediate zone; SVZ = subventricular zone; VZ = ventricular zone. Figure adapted from (Hevner, 2006).

age dependent (Takizawa et al., 2001; Namihira et al., 2004), suggesting that there are intrinsic factors that prevent premature gliogenesis. Indeed it has been shown that the promoters of genes expressed in glia, including *gfap* and *s100β*, as well as genes in the JAK-STAT pathway itself are methylated during early development, preventing the binding of the transcriptional activators (Takizawa et al., 2001; Namihira et al., 2004; Fan et al., 2005; He et al., 2005). As development progresses this repression is relieved to allow transcription of these genes and, hence, an astrocyte fate. A second mechanism involved in repressing gliogenesis is mediated by neurogenic bHLH proteins (Nieto et al., 2001; Sun et al., 2001; He et al., 2005). Ngn1 in particular has been shown to bind to and sequester p300/CBP, preventing it from binding to

STAT3, thereby preventing transcription of gliogenic genes (Sun et al., 2001). Thus, the downregulation of these neurogenic bHLH proteins is a critical step in the neurogenic to gliogenic transition.

Together, these studies highlight the important role of progenitor cell maturation in the development of the cortex, a role that is critical throughout the developing brain. Over time PCs mature, changing their intrinsic potential to generate different types of cells as well as changing how they respond to the external environment. These factors combine to precisely regulate the progression from proliferation to neurogenesis to gliogenesis. In the next section I will highlight several examples of how changes in the properties of PCs can lead to developmental problems.

1.1.5 Consequences of disruption of progenitor cell development

Disruption to the normal development of neural progenitor cells can lead to a wide variety of human developmental disorders. Analysis of the genes involved and the underlying molecular mechanisms has led to a better understanding of the etiology of these disorders; several examples will be described in which PC proliferation, neurogenesis, or gliogenesis are disrupted. Mutations in abnormal spindle-like microcephaly-associated (ASPM) protein are a common cause of human microcephaly (Bond et al., 2002; Bond et al., 2003). This neurodevelopmental disorder is characterized by reduced brain size at birth and mild to moderate mental retardation (Woods et al., 2005). Studies in mice have revealed that ASPM is important in maintaining the cleavage plane in dividing neuronal PCs to allow for symmetric proliferative divisions; mutations result in an increase in asymmetric neurogenic divisions (Fish et al., 2006). This suggests that microcephaly may result from a premature transition from proliferative to neurogenic divisions, thus depleting the PC pool. Specific behavioral abnormalities can also

arise from alterations in the development of specific populations of cells; mutation of the gene encoding Urokinase Plasminogen Activator Receptor disrupts the development of a subset of interneurons and results in increased anxiety and spontaneous seizures in adult mice (Powell et al., 2003). Mutations that result in increased activity of the *shp-2* (*ptpn11*) gene have been associated with Noonan Syndrome, which is associated with learning disabilities and mental retardation (Allanson, 2007). *Shp-2* encodes a protein tyrosine phosphatase that promotes neurogenesis and represses gliogenesis, in part through negative regulation of the JAK-STAT pathway (Lehmann et al., 2003; Gauthier et al., 2007). Increased activation of shp-2 in a mouse model of Noonan syndrome showed enhanced neurogenesis and decreased astrogenesis, leading to the hypothesis that perturbation of the transition from neurogenesis to gliogenesis, which results in an imbalance of the ratio of these cell types in patients with Noonan Syndrome, may underlie cognitive problems (Gauthier et al., 2007).

Animal models have also provided insight into more complex cognitive developmental disorders such as schizophrenia. Prenatal treatment with the mitotic inhibitor methylazoxymethanol acetate (MAM), which transiently halts proliferation, leads to defects in limbic structures including the cerebral cortex, entorhinal cortex, and hippocampus, and results in cognitive abnormalities that mimic symptoms of schizophrenia (Talamini et al., 1999; Flagstad et al., 2004; Gourevitch et al., 2004; Flagstad et al., 2005; Featherstone et al., 2007). Another prominent developmental model that has been used to study schizophrenia, the neonatal ventral hippocampal lesion (NVHL) model, takes a different approach in re-creating schizophrenia-like behaviors (reviewed by (Tseng et al., 2008a)). These two models converge somewhat with recent evidence that in both cases a subset of cortical interneurons are affected (Tseng et al., 2008b; Lodge et al., 2009); there is substantial evidence that interneurons are

affected in human patients with schizophrenia (reviewed by (Lewis et al., 2005)). Although the precise mechanisms underlying schizophrenia are still unclear, the ability of these different models to mimic aspects schizophrenia seems to confirm the idea that this disorder is a disruption of neural activity that can result from alterations in multiple different cell types or brain structures (Lewis and Levitt, 2002; Tseng et al., 2008a).

1.2 THE ROLE OF *TLX* IN NEURAL DEVELOPMENT

Tlx (*Nr2E1*) is a transcription factor expressed in the developing mouse forebrain (Monaghan et al., 1995). *Tlx* is a homologue of the *tailless* gene originally identified in *Drosophila*, in which it is necessary for the development of the most anterior part of the brain, the protocerebrum, as well as the posterior gut (Strecker et al., 1988; Pignoni et al., 1990; Younossi-Hartenstein et al., 1997). In addition to mouse, homologues have also been identified in chickens (Yu et al., 1994), *Xenopus* (Hollemann et al., 1998), zebrafish (Kitambi and Hauptmann, 2007), and humans (Jackson et al., 1998). *Tlx* belongs to the orphan nuclear receptor family (Yu et al., 1994; Monaghan et al., 1995), part of the nuclear receptor superfamily characterized by a central DNA-binding domain containing two conserved zinc-fingers and a putative C-terminal ligand binding domain (Mangelsdorf et al., 1995). Although in *Drosophila tailless* was originally thought to act as both a transcriptional activator and repressor, more recent studies suggest that it acts as a dedicated repressor, activating genes indirectly through repression of repressors (Moran and Jimenez, 2006). Similarly, in vertebrates *tlx* has been demonstrated to act as a transcriptional repressor (Yu et al., 1994; Yu et al., 2000; Miyawaki et al., 2004; Shi et al., 2004; Zhang et al., 2006; Sun et al., 2007; Yokoyama et al., 2008; Zhang et al., 2008).

In mice, *tlx* is first expressed in the developing forebrain adjacent to the neuroepithelium from E8 and in the dorsal midbrain from E8.75. At E12.5 and E13.5 *tlx* is expressed in dorsal PCs in a high rostral/lateral to low caudal/medial gradient, as well as in PCs in the ventral telencephalon and in parts of the diencephalon adjacent to the third ventricle (Monaghan et al., 1995; Stenman et al., 2003a). Tlx expression persists in PC populations into adulthood (Monaghan et al., 1995; Shi et al., 2004; Liu et al., 2008). However, the pattern of *tlx* expression and the specific cell types that express *tlx* have not previously been characterized in detail. To better understand the role of *tlx* in forebrain development a knock-out mouse was generated by replacing exons 2 and 3, encoding the two zinc fingers, with the *lacZ* gene (Monaghan et al., 1997). *Tlx*-deficient mice survive to adulthood, but exhibit distinct behavioral abnormalities including severe aggression, abnormal maternal instincts, impaired spatial learning, impaired memory for fear, and late-onset epilepsy (Monaghan et al., 1997; Roy et al., 2002; Young et al., 2002; Belz et al., 2007; Zhang et al., 2008). *Tlx* null animals show reductions in forebrain-derived structures including the cerebral cortex, the hippocampus, the entorhinal cortex, the amygdala, the striatum, the olfactory bulbs, and the eyes (Monaghan et al., 1997; Yu et al., 2000; Roy et al., 2002; Land and Monaghan, 2003; Stenman et al., 2003a; Stenman et al., 2003b; Miyawaki et al., 2004; Roy et al., 2004; Shi et al., 2004; Land and Monaghan, 2005; Uemura et al., 2006; Zhang et al., 2006). Further analysis shows that the adult cortex is reduced in thickness by approximately 20% due to a specific reduction in superficial cortical layers (Roy et al., 2002; Land and Monaghan, 2003).

The reduced cortex observed in *tlx* null animals arises from alterations in PC proliferation and neurogenesis during development (Roy et al., 2002; Roy et al., 2004). Early during neurogenesis (E9.5 to E14.5), *tlx* mutants show precocious neurogenesis coupled to a decrease in

the length of the cell cycle. At mid-neurogenesis the cell cycle begins to slow down (as it does in wild-type animals) but by E16.5 the cell cycle has lengthened to become longer than that of PCs in wild-type littermates. As a result of the premature neurogenesis and early decrease in cell cycle length, the cortical plate of *tlx* null animals initially shows an increase in cell number, but by E16 begins to show a decrease relative to wild-type. Progenitors in the VZ show a significant depletion at E14 only in caudal regions, but the SVZ is reduced in number at all rostrocaudal levels. Superficial cortical layers are specified prematurely, but only after the proper number of cells are committed to deep layers (Roy et al., 2004). This phenotype matches that described by Caviness et al. (Caviness et al., 2003), in which the level of the cell cycle protein p27 was manipulated in order to increase the Q fraction during early neurogenesis (E12 to E14). This indicates that a specific reduction in superficial layers could result from an early increase in the proportion of cells that differentiate. However, Schuurmans et al. (Schuurmans et al., 2004) propose that *tlx* acts in conjunction with *Pax6* to specify the differentiation of upper cortical layers.

The role for *tlx* in proliferation and neurogenesis is still not clear. Expressing *tlx* in *tlx*-null adult neural stem cells rescues the ability of these cells to maintain a proliferative stem cell phenotype (Shi et al., 2004), which could indicate an instructive role for *tlx* in promoting proliferation. *Tlx* has been shown to regulate the expression of several cell cycle genes, including p21, $p27^{Kip1}$, and *cyclinD1*, and the tumor suppressor gene *pten*, suggesting that *tlx* might exert its effect at the G1 to S transition of the cell cycle (Miyawaki et al., 2004; Zhang et al., 2006; Sun et al., 2007; Li et al., 2008; Yokoyama et al., 2008; Zhang et al., 2008). Transcriptional repression by TLX is mediated at least in part by interactions through its ligand-binding domain with corepressors such as atrophin1, histone deacetylases, and the histone

demethylase LSD1 (Zhang et al., 2006; Sun et al., 2007; Yokoyama et al., 2008). In addition, *tlx* is known in vertebrates to repress *Pax2* (Yu et al., 2000) and the glial genes *GFAP*, *S100β*, *AQP4* (Shi et al., 2004). The *Drosophila* homolog *tailless* is known to suppress expression of *empty spiracles*, the homolog of vertebrate *Emx* genes (Hartmann et al., 2001). Finally, *tlx* has been shown to genetically interact with *pax6* in formation of the pallio-subpallial boundary (Stenman et al., 2003a) and in the formation of upper cortical layers (Schuurmans et al., 2004).

In *Drosophila*, numerous proteins and pathways that regulate *tailless* expression have been identified, including Tramtrack69, which represses *tailless*, and bicoid and Torso signaling, which activate *tailless* (Pignoni et al., 1992; Chen et al., 2002; Chen et al., 2009). Less is known about the regulation of *tlx* in vertebrates, although some evidence has come from two recent studies. *Tlx* has been shown to be suppressed by the microRNA miR-9 through the TLX 3' untranslated region (Zhao et al., 2009). TLX in turn seems to be able to repress one of the three loci that encode miR-9. This suggests that miR-9 and *tlx* mediate neural stem cell proliferation and differentiation through a negative feedback loop that may allow a rapid transition from PC to differentiated cell (Zhao et al., 2009). In addition, in retinal astrocytes Bmp7 and Shh signaling have been shown to act on TLX at the *Pax2* promoter to relieve repression (Sehgal et al., 2009).

NR2E1, the human homologue of *tlx*, resides within a 6q21-22 locus for bipolar disorder and schizophrenia (Jackson et al., 1998; Kohn and Lerer, 2005; Kumar et al., 2008). Expression of *NR2E1* is observed in fetal and adult forebrain (Jackson et al., 1998; Kumar et al., 2008), similar to the expression pattern observed in other vertebrates. Association analysis indicates significant association of *NR2E1* with bipolar disorder types I and II (Kumar et al., 2008). This study further identified eight candidate mutations specific to families or patients with bipolar disorder, schizophrenia, psychopathy, or mental retardation with psychosis. Interestingly none

of these mutations are thought to result in protein coding changes; instead they are proposed to regulate transcription, with four of the mutations located in putative neural transcription factor binding sites (Kumar et al., 2008). Mutations at the *NR2E1* locus have also been identified in patients with unexplained congenital microcephaly, and again these mutations are likely regulatory rather than protein-coding (Kumar et al., 2007). As previously described, *tlx* null mice exhibit significant reductions in forebrain structures that could be analogous to human microcephaly (Monaghan et al., 1997; Roy et al., 2002; Land and Monaghan, 2003; Stenman et al., 2003b; Shi et al., 2004). One patient also exhibited optic nerve hypoplasia (Kumar et al., 2007), similar to deficits in the optic nerve observed in *tlx* null animals (Yu et al., 2000; Young et al., 2002). The human and mouse homologues have been shown to be functionally equivalent, as expression of the human *NR2E1* gene in *tlx* null mice can rescue defects in the brain development and behavior (Abrahams et al., 2005). Furthermore, highly conserved regulatory elements in non-coding regions, including within the first intron, were identified by comparison of the human, mouse, and puffer fish sequences (Abrahams et al., 2002). Together these data not only highlight the important role of *NR2E1* in the development of the human brain but further indicate significant similarity with the role of *tlx* in the developing mouse brain. Thus, better understanding of the role of *tlx* during development will yield important insight into the developmental mechanisms and pathology of human neural disorders.

1.3 OUTLINE OF STUDY

The goal of this study is to examine how changes in the development of specific PC populations affect the structure of the adult brain and associated behavioral tendencies. I will focus

specifically on the transcription factor *tlx* in the development of the forebrain, with particular emphasis on the dorsal telencephalon. I will examine the role of *tlx* in specific cellular populations in order to begin to unravel to complex role of *tlx* in forebrain development. First, Chapter 2 will provide a detailed examination of the expression of *tlx* during development, identifying the cellular subtypes that express *tlx*. Chapter 3 will examine the role of *tlx* in the development of functional cortical areas. In Chapters 4 and 5 I will utilize a conditional knock out of *tlx* in order to determine the role of *tlx* specifically in the regulation of PCs in the dorsal telencephalon (Chapter 4) and the consequences of this region-specific disruption on the development of adult brain structures and behavior (Chapter 5). Finally, in the last chapter (6), I will discuss a model of *tlx* function in the dorsal telencephalon as it relates to the development of structure and behavior, and I will describe possible future directions.

2.0 TLX EXPRESSION

2.1 INTRODUCTION

Tlx is an orphan nuclear receptor transcription factor expressed in the developing mouse forebrain. *Tlx* mRNA expression is first detected in the developing forebrain adjacent to the neuroepithelium at embryonic day 8 (E8) and in the dorsal midbrain at E8.75 (Monaghan et al., 1995). At E12.5 and E13.5 *tlx* is expressed in dorsal progenitor cells (PCs) in a high rostral/lateral to low caudal/medial gradient, as well as in PCs of the ventral telencephalon and in parts of the diencephalon adjacent to the third ventricle (Monaghan et al., 1995; Stenman et al., 2003a). *Tlx* expression persists in PC populations through development and into adulthood (Monaghan et al., 1995; Shi et al., 2004; Liu et al., 2008). Due to the lack of a commercially available antibody against TLX that could be used for immunohistochemistry these studies have either examined the expression of *tlx* mRNA or have utilized the *lacZ* gene that is fused in frame to exon two in the *tlx*-null locus (Monaghan et al., 1997) to examine β-galactosidase expression under the control of the *tlx* promoter. Recently, Shi and colleagues (Li et al., 2008) have developed an antibody against TLX and have shown that at E14.5 TLX is co-expressed with PC markers nestin and RC2 but not neuronal markers doublecortin or NeuN. TLX-positive cells also express the S-phase marker BrdU and the proliferative marker Ki67, confirming the expression of TLX in proliferating cells (Li et al., 2008). In this study I have made a detailed

characterization of the spatial and temporal pattern of *tlx* mRNA and protein expression in the developing mouse forebrain in order to better understand the role of *tlx* in cortical development.

2.2 METHODS

2.2.1 Animals

Wild type embryos and postnatal animals were obtained from timed-pregnant CD1 mice from Charles River Laboratories (Wilmington, MA). Heterozygous animals were obtained from crossings of *tlx* heterozygotes (SVE129 x C57BL/6J). Genotyping was performed by PCR as previously described (Monaghan et al., 1997). Briefly, a tail piece was digested in non-ionic detergent and proteinase K (Sigma, 0.3ng/μl) overnight at 56°C. Following heat inactivation at 96°C 50ng of DNA was amplified. Tlx PCR was performed using the following primers and conditions: Tlx1: 5'-GCC TGC TCT TTA CTG AAG GCT-3', Tlx2: 5'-ATT GGG TCC AGA CAT GGC CCT-3', Tlx3: 5'-GTT CAT GTT GAC TTC CAA ACA-3'; 94°C for 10 minutes, 35 cycles of 94°C for 30 seconds, 65°C for 1 minute, and 72°C for 1 minute, followed by 72°C for 10 minutes. PCR products were 210bp for the wild type allele and 325bp for the null allele. Embryos were collected via caesarean section at embryonic ages from E10.5 to E18.5. The morning of the vaginal plug was designated E0.5; the day of birth was designated P0. The care and handling of these animals was in accordance with the University of Pittsburgh Institutional Animal Care and Use committee and NIH guidelines.

Embryonic brains were processed by immersion fixation in cold 4% paraformaldehyde (PFA) pH7.4 (Sigma, St. Louis, MO); E10.5 for 2 hours, E12.5 to E13.5 for 4-5 hours, E16.5 to

E18.5 overnight. Postnatal brains were fixed by transcardial perfusion with cold PBS followed by 4% PFA pH7.4, dissected from the skull, and immersion fixed overnight. Brains were processed through a graded sucrose series (10-20-30%) at 4°C. Adult brains were sectioned coronally on a freezing-sliding microtome at 50μm and collected in PBS. All other brains were embedded in a 1:1 mixture of 30% sucrose and Tissue-Tek O.C.T. compound (EMS, Hatfield, PA) and sectioned on a cryostat sagitally or coronally at 14μm (E10.5 brains and E13.5 CD-1 brains) or 20μm.

2.2.2 In situ hybridization

DIG-labeled riboprobe against *tlx* (Monaghan et al., 1995) was prepared using a DIG RNA labeling kit according to the manufacturer's directions (Roche Diagnostics, Indianapolis, IN). In situ hybridization on frozen sections was performed as previously described (Schaeren-Wiemers and Gerfin-Moser, 1993) with the following modifications. The sections were treated with proteinase K (0.5 μg/ml in 50mM Tris pH 7.5 and 5mM EDTA) at 37°C for 3 min (E12.5 and E13.5), 4.5 min (E16.5), or 7.5 min (P0-P8) followed by post-fixation in 4% PFA prior to pre-hybridization. The hybridization buffer was modified to contain 50% formamide, 5X SSC, 5X Denhardt's solution, 250 μg/ml tRNA, and 250 μg/ml herring sperm DNA. Hybridization and post-hybridization washes were performed at 61°C. In addition, following hybridization the sections were treated with RNase A (20 μg/ml, in 0.5M NaCl, 10mM Tris pH7.5, 5mM EDTA) at 37°C for 30mins. After color detection slides were rapidly dehydrated through an ascending series of ethanols to xylene and coverslipped with DPX (Fluka Chemical, Ronkonkoma, NY).

2.2.3 Immunohistochemistry

Cryosections were washed in PBS and 0.1% Triton-X-100 (Fisher Scientific, Pittsburgh, PA) in PBS, blocked in 10% heat-inactivated normal goat serum (HINGS) (Jackson ImmunoResearch, West Grove, PA) in PBS, and incubated with primary antibody overnight at 4°C. Antibodies used were chicken anti-β-galactosidase (LacZ; 1:500; Abcam, Cambridge, MA); mouse anti-GFAP (1:400; Sigma); guinea pig anti-GLAST (1:4000; Chemicon, Temecula, CA); mouse anti-NeuN (1:500; Chemicon); rabbit anti-Pax6 (1:500; Covance, Berkeley, CA); rabbit anti-Sox10 (1:500; CeMines, Golden, CO); rabbit anti-Tbr2 (1:1000; Chemicon); rabbit anti-Tlx (1:1000; a gift from Y. Shi, (Li et al., 2008)); mouse anti-Tuj1 (1:1000; Sigma). For fluorescent detection of the signal tissue was washed with PBS, blocked with 10% HINGS or 10% heat inactivated normal donkey serum (HINDS) in PBS, and incubated with the appropriate Cy3 (1:400; Jackson ImmunoResearch) and/or Alexa Fluor 488 (1:1000; Invitrogen, Carlsbad, CA) secondary antibody. Sections were counterstained with 1,6-diamidino-2-phenylindole dihydrochloride (DAPI; Sigma) before mounting in fluoromount G (Southern Biotechnology Research, Birmingham, AL).

Adult sections were washed in 50% methanol/50% PBS/1% hydrogen peroxide followed by three washes with 0.1% Tween 20 (Fisher Scientific) in PBS. Sections were blocked overnight at 4°C with 10% HINGS in PBS. Sections were incubated with rabbit anti-Tlx (1:1000; a gift from Y. Shi (Li et al., 2008)) overnight at 4°C. The sections were subsequently washed in 0.1% Tween 20 in PBS, incubated with anti-rabbit biotinylated secondary antibody (1:500; Vector Laboratories, Burlingame, CA) and processed using the Vectastain(r) Elite ABC kit (Vector Laboratories) according to the manufacturer's instructions. After rinsing in PBS sections were incubated in 0.7mg/ml 3,3'-diaminobenzidine tetrahydrochloride (DAB; Sigma)

with 0.01% hydrogen peroxide. DAB stained sections were washed in PBS, mounted on slides, counterstained with 0.5% cresyl violet (Nissl; Sigma), dehydrated through alcohols, washed in xylene, and coverslipped with DPX. β-galactosidase staining was performed on frozen sections as previously described (Parrish et al., 2004). Sections were counterstained with cresyl violet or nuclear fast red (Fluka Chemical), dehydrated, and coverslipped with DPX.

Sections were visualized on a Nikon 400 (Melville, NY) fluorescent microscope, photographed with a Photometrics (North Reading, MA) Cool Snap digital camera and IP Lab software (Biovision Technologies, Exton, PA). Where indicated sections were imaged using a Nikon DF0200 confocal microscope. Composite images were prepared using Photoshop 6.0 (Adobe Systems, San Jose, CA). Contrast, color, and brightness were adjusted in Photoshop.

2.3 RESULTS

2.3.1 *Tlx* expression in the developing forebrain

Tlx mRNA is expressed in the developing forebrain from E8 (Monaghan et al., 1995). Previous studies have shown that the *tlx* gene is expressed in the PCs of the dorsal telencephalon in decreasing rostral to caudal and lateral to medial gradients at midgestation (Monaghan et al., 1995; Stenman et al., 2003a). Interestingly, cellular deficits in the absence of *tlx* are more severe caudally (Roy et al., 2004); therefore, we wanted to determine whether this gradient of transcript persists through development. Although *tlx* mRNA continues to be expressed in PCs at later embryonic and early postnatal ages (Monaghan et al., 1995), the expression pattern has not been characterized in detail. We therefore examined *tlx* mRNA expression in the dorsal telencephalon

of mice from E13.5 - P8. We initially used two different approaches to examine *tlx* expression in the developing brain. First, we used *in situ* hybridization with riboprobes directed against the entire coding sequence, as previously described (Monaghan et al., 1995) (Figure 4A-M, Figure 5). Second, we took advantage of the β-galactosidase gene that is fused in frame to exon two in the *tlx*-null locus (Monaghan et al., 1997). This places β-galactosidase expression under the control of the *tlx* promoter, allowing us to detect *tlx*-dependent cells with β-galactosidase staining in heterozygous and mutant animals (Figure 4N, O). β-galactosidase expression is similar to *tlx* expression obtained by *in situ* hybridization at embryonic ages and shows similar expression in PCs postnatally.

As previously reported (Monaghan et al., 1995), at E13.5 *tlx* mRNA is expressed in dorsal PCs in decreasing rostral to caudal and lateral to medial gradients of transcript per cell (Figure 4A-D). Interestingly, *tlx* is expressed only in a subpopulation of PCs, in some areas showing a pattern suggestive of radial clones (Figure 4M). At E16.5 *tlx* appears to be evenly expressed in the progenitor domain with no apparent rostral-caudal gradient (Figure 4E-H). At this age *tlx* is still expressed only in a subpopulation of cells in the VZ and scattered cells in the SVZ. From E18.5 *tlx* is expressed in the progenitor domain with no apparent gradient (Figure 4I-L, N, O). At the postnatal ages examined *tlx* is expressed in most cortical PCs, no longer showing the distinct clonal pattern observed at earlier ages. *Tlx* mRNA expression is also observed in the progenitor domain in the developing striatum (Figure 4A, E, I, asterisks). The PC population, and therefore the total number of cells expressing *tlx*, decrease by birth. However, examination of individual cells under high power indicates that the amount of *tlx* mRNA transcript per cell does not appear to differ from E16.5 to P8. *Tlx* mRNA expression is also observed throughout development in

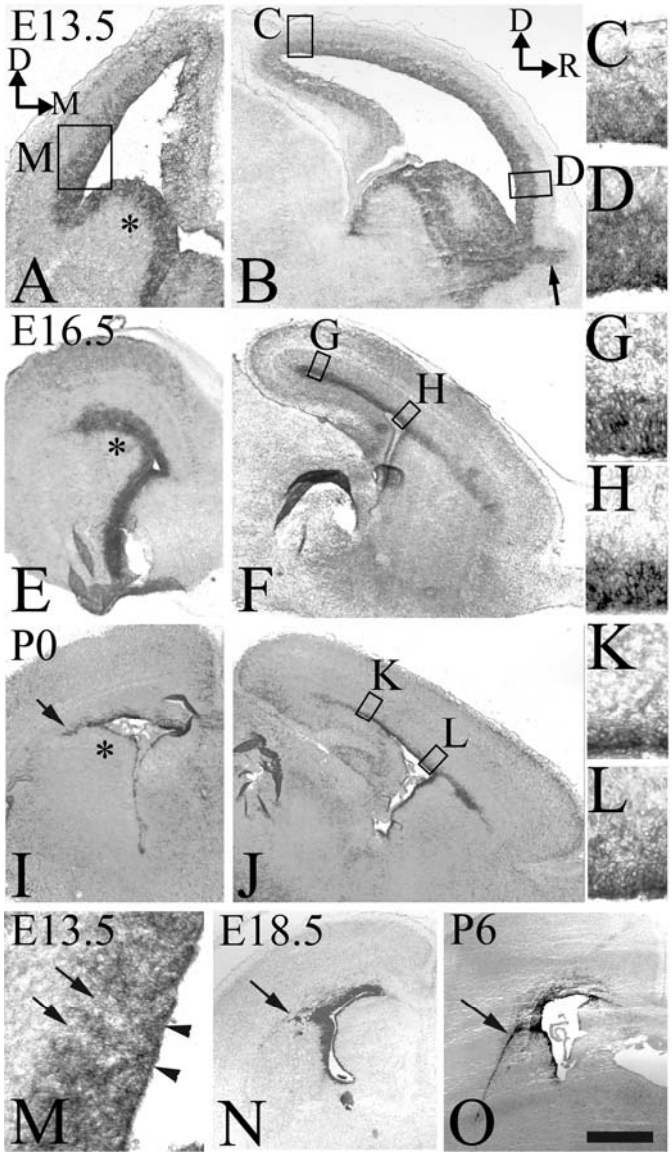

Figure 4. *Tlx* mRNA expression in the developing cortex

In situ hybridization for *tlx* in coronal (A, E, I, M) and sagittal (B-D, F-H, J-L) sections at E13.5 (A-D, M), E16.5 (E-H) and P0 (I-L). At E13.5 *tlx* is expressed in a high ventral to low dorsal gradient (A) and a high rostral to low caudal gradient (B-D) in cortical progenitor cells (PCs). *Tlx* is also expressed in the rostral migratory stream (B, arrow). C and D are higher power images of areas outlined in B, showing the difference in *tlx* expression in rostral and caudal regions. At E16.5 (E-H) there is no apparent gradient in *tlx* expression in cortical PCs. G and H are higher power images of areas outlined in F, showing the equivalent expression of *tlx* in rostral and caudal regions. Expression is maintained in cortical PCs at P0 (I-L). K and L are higher power images of areas outlined in J, showing the equivalent expression of *tlx* in rostral and caudal regions. M is a magnified view of the area boxed in

A, showing that *tlx* is expressed in a subset of PCs at E13.5. Arrowheads indicate regions of high *tlx* expression; arrows indicate regions of low or absent *tlx* expression. N and O show β-galactosidase staining in coronal sections of *tlx* null embryos at E18.5 (N) and P6 (O). Expression of β-galactosidase from the *tlx* locus mimics *tlx* expression as shown by *in situ* hybridization. *Tlx* is also expressed in the lateral cortical stream (I, N, O, arrows). Asterisks in A, E, I indicate the developing striatum. Scale bar (in O) = 280μm in A; 460μm in B; 150μm in C, D; 400μm in E; 550μm in F; 60μm in G, H, K, L; 500μm in I; 620μm in J; 85μm in M; 470μm in N; 650μm in O. D = dorsal; M = medial; R = rostral.

both the rostral migratory stream (Figure 4B, arrow) and in cells migrating in the lateral cortical stream (Figure 4I, N, O arrows).

We further examined the expression of *tlx* mRNA in ventral regions of the developing telencephalon. At E13.5 *tlx* is highly expressed in the lateral ganglionic eminence (LGE) and septal neuroepithelium (S) and more weakly expressed in the medial ganglionic eminence (MGE) (Figure 4A, Figure 5A). Expression persists in the proliferative domain of the developing septum (S) at E16.5 (Figure 5B) and at P0 (Figure 5C). In addition, *tlx*-expressing cells were observed outside of the proliferative domain at P0 in the region of the lateral septum (Figure 5C, arrows). We also observed *tlx* expression outside of the proliferative regions in the developing amygdala at E16.5 and at P0 (Figure 5D, E). Cells expressing *tlx* mRNA were observed throughout the amygdala, with clusters of *tlx*-positive cells concentrated in the regions of the medial amygdalar nucleus (M), the cortical amygdalar area (CoA), and the basal complex (BC), the latter of which includes the lateral, basolateral, and accessory basal or basomedial nuclei.

Although characterizing mRNA expression provides important information about the transcriptional regulation of *tlx*, this does not tell us whether TLX protein is present in these same populations, as mRNA might not be translated or protein might persist after

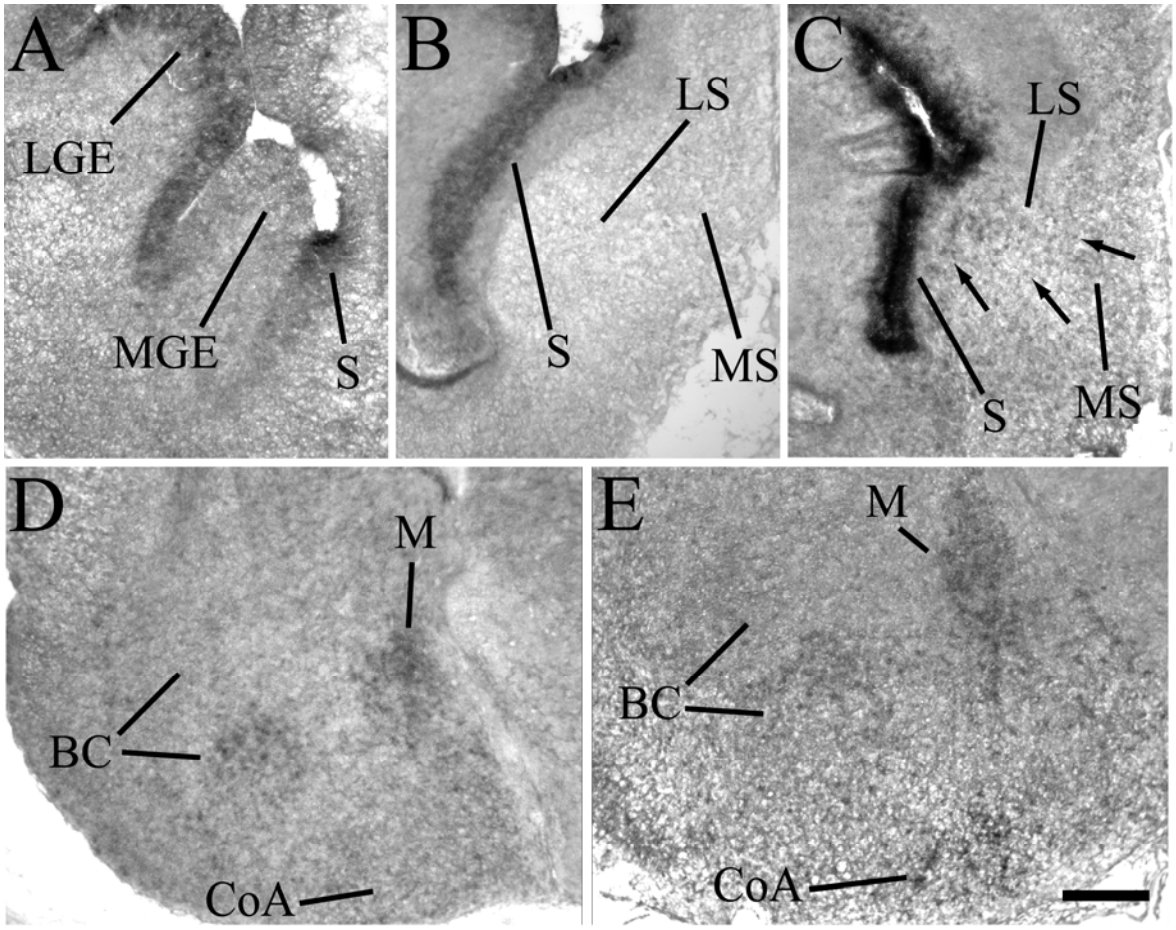

Figure 5. *Tlx* mRNA expression in the developing septum and amygdala

In situ hybridization for *tlx* in coronal sections shows staining in the developing septum (A-C) and amygdala (D, E) during development. At E13.5 *tlx* mRNA is highly expressed in the septal neuroepithelium (S) and lateral ganglionic eminence (LGE) and more weakly expressed in the medial ganglionic eminence (MGE) (A). *Tlx* expression persists in the septal proliferative zone (S) at E16.5 (B) and P0 (C). At P0 *tlx* mRNA expression is also observed in cells outside of the proliferative zone (arrows) in the region of the lateral septum (LS) (C). *Tlx* mRNA expression is observed in cells in the region of the developing amygdala at E16.5 (D) and P0 (E) in the regions of the basal complex (BC), the medial amygdalar nucleus (M), and the cortical amygdalar area (CoA). MS = medial septum. Scale bar (in E) = 200μm in A-E.

downregulation of transcription. Furthermore, protein expression, unlike mRNA expression, can show the subcellular localization of TLX. Therefore, information about TLX protein expression is critical for understanding where *tlx* is functionally relevant. It has been shown that at E14.5 TLX protein is present in nestin- and RC2-positive neural precursors in the telencephalon but not doublecortin- or NeuN-positive differentiated neurons (Li et al., 2008). However, the temporal and spatial pattern of TLX protein expression in the developing cerebral cortex has not been described in detail. Here we used an antibody specific to TLX to characterize TLX protein expression in the forebrain from E10.5 to the adult. This antibody was generated against the TLX ligand binding domain (amino acids 180-385) (Li et al., 2008). It was shown by Western blot to detect a 46-kDA protein in neural stem cells, E14.5 brain lysates, and 3T3 cells stably transfected with *tlx*, but not in parent cells that have no endogenous *tlx* expression (Li et al., 2008). In our own studies this antibody did not label any cells in brains from *tlx* null animals, which lack TLX protein expression, at any age examined (E10-P8, data not shown), further indicating that this antibody does detect the TLX protein.

Early during development TLX protein expression appears similar to *tlx* mRNA expression as previously described and shown in Figure 4 and Figure 5. TLX is highly expressed in the proliferative region adjacent to the ventricle from E10.5 (data not shown). At E13.5 TLX is robustly expressed by PCs throughout the forebrain (Figure 6). In the dorsal telencephalon TLX is expressed in a decreasing lateral to medial gradient (Figure 6A) similar to the gradient observed in mRNA expression (Figure 4A). Higher magnification examination of the dorsal telencephalon shows that TLX is unevenly expressed in cells within the VZ, with the strongest expression observed in dividing cells at the ventricular surface (Figure 6A, B). TLX expression is primarily nuclear; however, cells in M-phase in all regions examined express TLX

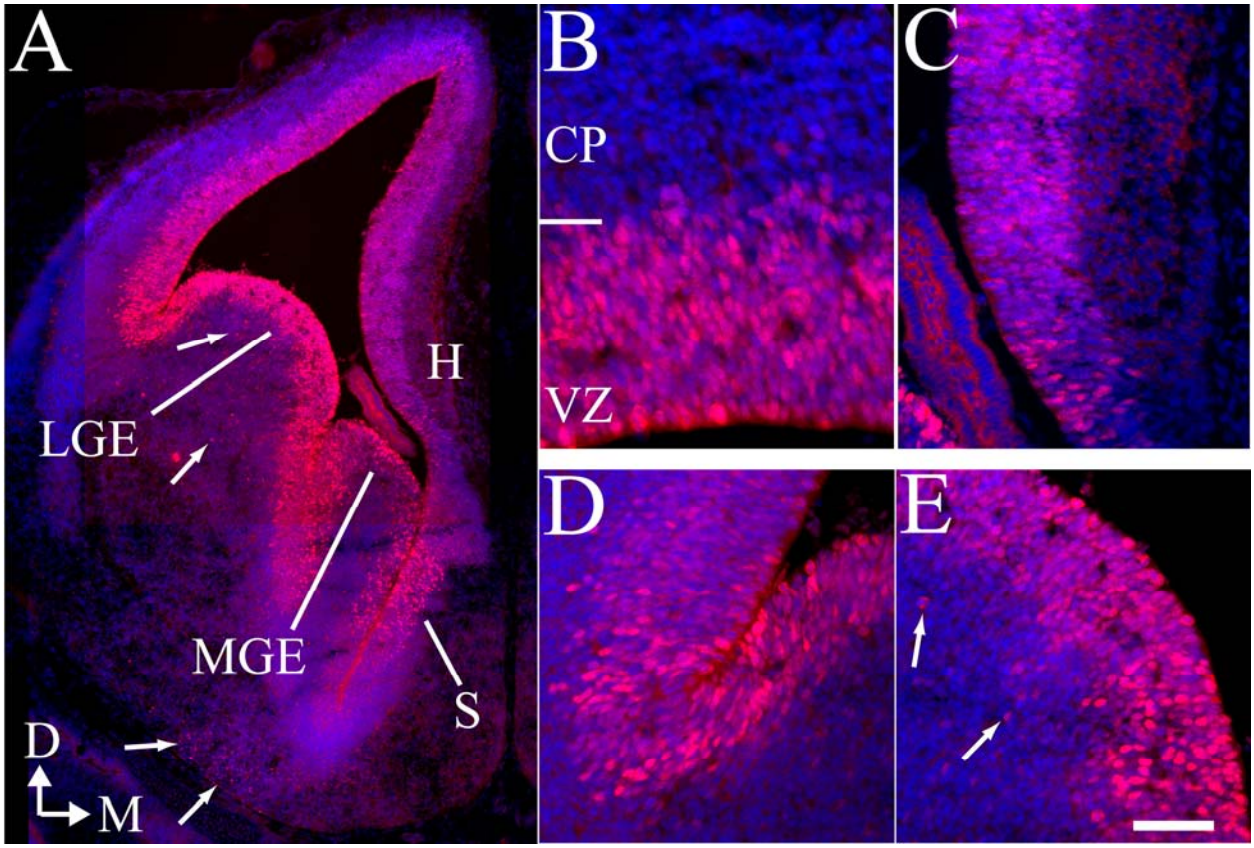

Figure 6. TLX expression at E13.5

TLX immunohistochemistry (red) in coronal sections through the telencephalon at E13.5 (A-E). In the dorsal telencephalon TLX is expressed in a high lateral to low medial gradient in progenitor cells (A), with expression extending medially into the hippocampal neuroepithelium (H). (A) High expression is observed in progenitor cells in the lateral ganglionic eminence (LGE), with lower expression in the medial ganglionic eminence (MGE) and septal neuroepithelium (S). TLX is also expressed by a subpopulation of cells in the ventral differentiating field (arrows, A, E). Higher magnification of the dorsal telencephalon (B) shows that TLX in unevenly expressed throughout the progenitor population, with particularly high expression in dividing cells at the ventricular surface. Higher magnification images of other regions indicate that TLX is similarly unevenly expressed in the proliferative zone of the hippocampal neuroepithelium (C), the corticostriatal boundary (D) and the lateral ganglionic eminence (E). Sections are counterstained for DAPI (blue). Scale bar (in E) = 200μm in A; 40μm in B; 60μm in C-E. CP = cortical plate; VZ = ventricular zone; D = dorsal; M = medial.

in a perinuclear pattern, excluded from the chromosomal material. TLX similarly shows uneven expression in the hippocampal neuroepithelium (H, Figure 6A, C), and at the corticostriatal boundary (Figure 6A, D). In the ventral telencephalon, TLX protein is highly expressed in the lateral ganglionic eminence (LGE, Figure 6A, E) and more weakly expressed in the medial ganglionic eminence (MGE) and septal neuroepithelium (S) (Figure 6A), corresponding with the described pattern of *tlx* mRNA expression (Figure 4A and Figure 5A). Uneven TLX expression is observed in the PC population of the LGE (Figure 6E). Although TLX expression is primarily restricted to progenitor domains at E13.5, TLX is expressed by a subset of cells in the differentiating field of the ventral telencephalon (Figure 6A, E, arrows).

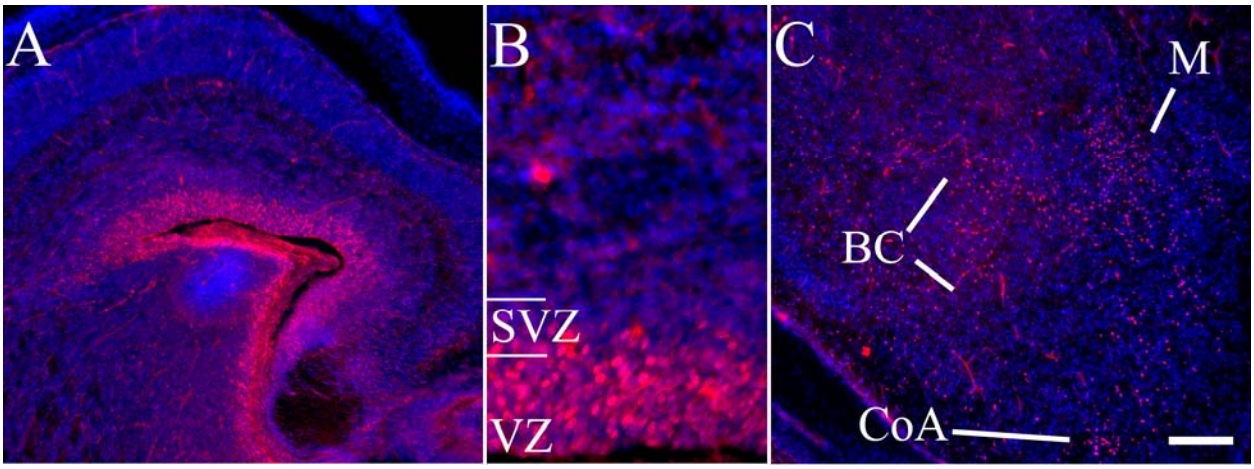

Figure 7. TLX expression at E16.5

At E16.5 TLX protein expression (red) is observed throughout the progenitor population in dorsal (A, B) and ventral (A) telencephalon. High power magnification of the dorsal cortex (B) shows that TLX is expressed by most cells in the ventricular zone (VZ) but only a subset of cells in the subventricular zone (SVZ). Cells expressing TLX (red) are also observed throughout the region of the developing amygdala at E16.5, as shown in coronal sections (C). Approximate locations of the basal complex (BC), the medial amygdalar nucleus (M), and the cortical amygdalar area (CoA) are indicated. Sections are counterstained for DAPI (blue). Scale bar (in C) = 150μm in A, C; 40μm in B.

TLX protein continues to be expressed primarily in the progenitor domain at E16.5 (Figure 7A), similar to the *tlx* mRNA expression previously described (Figure 4E). At mid-neurogenesis a second proliferative population, the subventricular zone (SVZ), arises in the developing cortex basal to the VZ (Bystron et al., 2008). We examined these two PC populations at higher magnification in the dorsal cortex and observed that, whereas TLX is expressed in most cells in the VZ, TLX is expressed only by a subset of cells in the SVZ, primarily at the VZ/SVZ boundary (Figure 7B). At E16.5, TLX expression is also observed ventrally in cells outside the progenitor domain in the region of the developing amygdala (Figure 7C). TLX-expressing cells are scattered throughout the amygdala but are more concentrated in the regions of the medial amygdalar nucleus (M), the cortical amygdalar area (CoA), and the basal complex (BC), similar to the pattern observed with mRNA expression (Figure 5D).

At E18.5 TLX continues to be expressed throughout the PC population, although increasing numbers of cells expressing TLX outside the progenitor domain are also observed (Figure 7A-C). TLX expression is observed in PCs adjacent to the lateral ventricles throughout the telencephalon, shown at both intermediate levels through somatosensory cortex (Figure 8A) and caudal levels through auditory and visual cortex (Figure 8B). TLX expression is also observed in the PC domain of the diencephalon adjacent to the third ventricle (Figure 8B, arrowhead). As seen with *tlx* mRNA expression and β-galactosidase staining, cells expressing TLX protein are observed in the lateral cortical stream (Figure 8A, A'). At E18.5 TLX-expressing cells are also apparent throughout the developing hippocampus (Figure 8A, B, B') and amygdala (Figure 8B, B"). Within the amygdala the pattern of TLX protein expression appears similar to that of *tlx* mRNA (Figure 5E). High power examination of TLX staining in the dorsal cortex at E18.5 (Figure 8C) reveals that TLX is evenly expressed in most cells in the

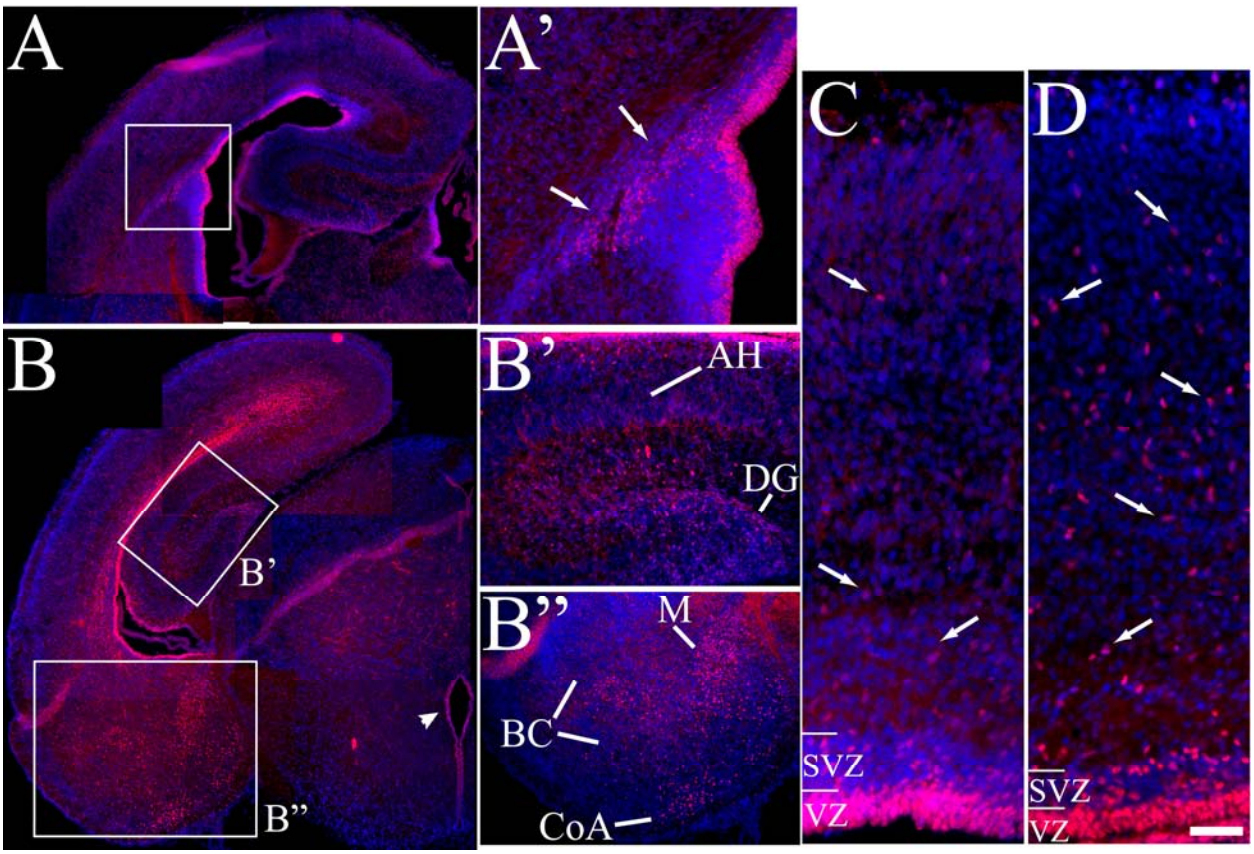

Figure 8. TLX expression at birth

TLX immunohistochemistry (red) on coronal sections at intermediate (A, A') and caudal (B-B") levels of the E18.5 brain. TLX is expressed by cells throughout the proliferative regions adjacent to the ventricles, including cells adjacent to the third ventricle (B, arrowhead). TLX expression is observed in the lateral cortical stream (A', higher power magnification of boxed area in A; arrows). TLX expression is also observed in cells in the developing hippocampus (B') and amygdala (B"). Within the amygdala expression is observed in cells in the regions of the basal complex (BC), the medial amygdalar nucleus (M), and the cortical amygdalar area (CoA). Higher power magnification of the dorsal cortex at E18.5 shows that most cells in the ventricular zone (VZ) are positive for TLX (red), while only a subset of cells in the subventricular zone (SVZ) and a few cells outside of the proliferative region (arrows) are positive for TLX (C). By postnatal day 0 TLX is expressed by numerous cells outside the proliferative region (arrows) although TLX is still expressed by cells in the VZ and SVZ (D). Sections are counterstained for DAPI (blue). AH = Ammon's horn, DG = dentate gyrus. Scale bar (in D) = 300μm in A, B; 85μm in A'; 100μm in B', B"; 45μm in C, D.

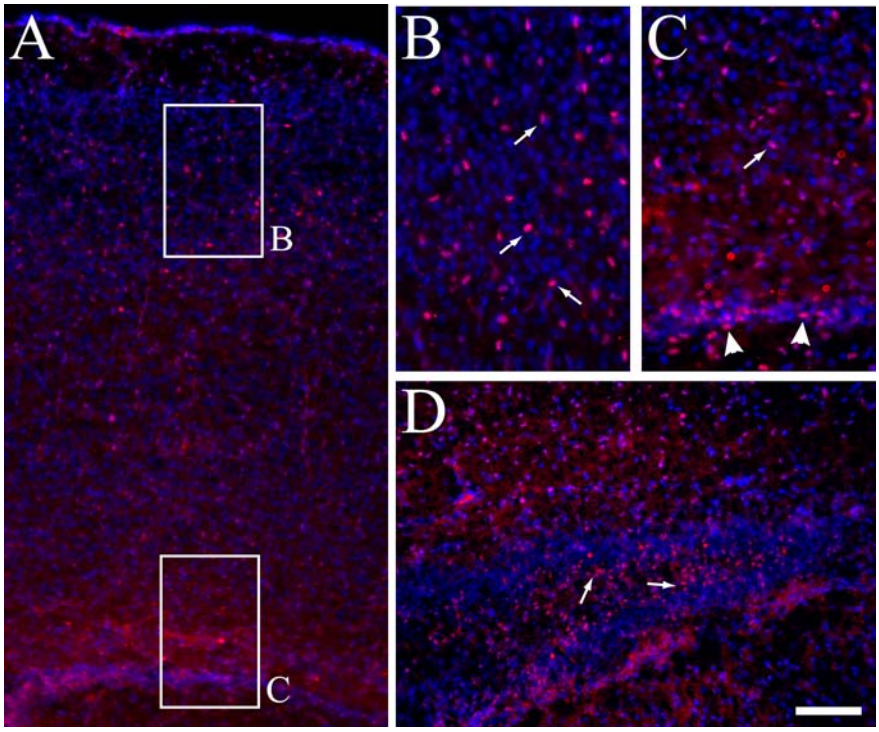

Figure 9. TLX expression at P6

Staining for Tlx (red) at P6 shows expression in a subset of cells adjacent to the ventricle (A, C, arrowheads) as well as outside of the ventricular zone in the dorsal cortex (A-C, arrows). Tlx-expressing cells are also scattered throughout the hippocampus (D), particularly in the subgranular zone of the dentate gyrus (arrows). Sections are counterstained with DAPI (blue). Scale bar (in D) = 100μm in A; 60μm in B, C; 90μm in D.

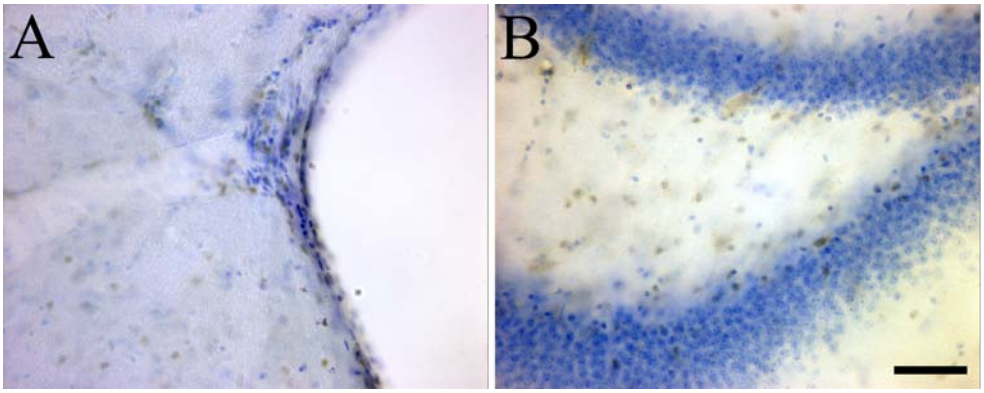

Figure 10. TLX is expressed in neurogenic regions in the adult

Tlx-expressing cells (brown) are visible in the subventricular zone (A) and subgranular zone of the dentate gyrus (B). Sections are counterstained for Nissl (blue). Scale bar = 50μm.

VZ and a subset of cells in the SVZ, as well as in cells outside of the proliferative domain (Figure 8C, arrows). By P0 even more cells expressing TLX are observed outside of the progenitor domain throughout the depth of the cortical plate (Figure 8D, arrows). Continuing this trend, at P6 cells expressing TLX are observed in the progenitor domain adjacent to the ventricle (Figure 9A, C, arrowheads) as well as outside of this region (Figure 9A-C, arrows). TLX-positive cells are also scattered throughout the hippocampus at P6 (Figure 9D) but concentrated in the subgranular zone of the dentate gyrus (arrows).

It has previously been shown that in the adult the *tlx* promoter drives gene expression in neural stem cells in the subventricular zone of the lateral ventricle and the subgranular zone of the dentate gyrus, the primary regions of neurogenesis in the adult brain (Shi et al., 2004; Liu et al., 2008). We similarly observed expression of the TLX protein in a subset of cells in both of these regions in the adult (Figure 10A, B). Overall, the presence of *tlx* mRNA and protein in PCs throughout development and in the adult support a role for *tlx* in regulating PC proliferation and neurogenesis. The nuclear localization of the TLX protein further confirms its role as a transcriptional regulator. Expression of TLX protein outside of the proliferative domains, particularly in the developing amygdala, suggests a possible novel role for tlx in specific populations of differentiated cells.

2.3.2 *Tlx* is expressed by a subset of progenitors but not by mature neurons

So far we have shown that throughout development TLX protein is expressed in the cells in the PC domain; however, TLX appears to be expressed in only a subset of cells, particularly in the SVZ where only sparse staining was observed. We therefore characterized the TLX-expressing cells in the dorsal cortex by examining colocalization of TLX with various PC and neuronal

markers. In some cases double immunohistochemistry using the TLX antibody was not possible; therefore, in order to determine whether β-galactosidase expression under the control of the *tlx* promoter mimics that of endogenous TLX protein and could therefore be used for double immunostaining experiments, we first examined the co-expression of TLX and β-galactosidase in heterozygous animals (Figure 11). Whereas TLX protein is localized to the nucleus (Figure 11A, D), β-galactosidase is localized throughout the cytoplasm reaching into cellular processes (Figure 11B, E). However, at both E12.5 (Figure 11A-C) and P0 (Figure 11D-F) TLX and β-galactosidase appear to localize to the same cells.

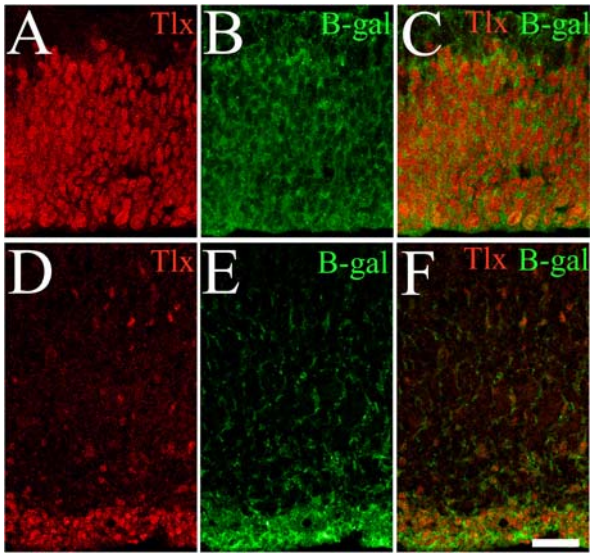

Figure 11. TLX and β-galactosidase are co-expressed in heterozygous animals

TLX (red) and β-galactosidase (green) are co-expressed in *tlx* +/- animals at E12.5 (A-C) and at P0 (D-F). Images were taken on a confocal microscope. Scale bar (in F) = 30μm in A-C; 40μm in D-F.

In order to verify that the TLX-expressing cells located in the VZ during development are PCs, we examined co-expression of TLX and the radial glia marker glutamate-aspartate transporter (GLAST) (Shibata et al., 1997; Hartfuss et al., 2001). At E13.5 TLX co-localizes

with GLAST (Figure 12A-C), indicating that TLX is expressed by radial glia. We confirmed this by examining co-expression of β-galactosidase and the radial glia marker Pax6 (Gotz et al., 1998) at E12.5 in *tlx* heterozygous animals. At this age β-galactosidase and Pax6 appear to show nearly complete co-expression (Figure 12D-F), further indicating the TLX is expressed by radial glia progenitors. This significant overlap of TLX with markers of radial glia PCs, together with its expression confined mostly to proliferative domains during early development, suggest that TLX is not expressed by differentiated neurons. In order to directly examine this idea we performed double immunostaining with an antibody against TLX and an antibody against the neuronal marker Tuj1. At E12.5 TLX does not show any co-expression with Tuj1 (Figure 12G-I). Similar results were obtained at E14.5 and E18.5 (data not shown), although occasionally a cell near the ventricle showed low levels of both TLX and Tuj1, which could reflect residual TLX expression in a cell that had just left the cell cycle to differentiate into a neuron.

We have shown that TLX is expressed in the radial glia PCs that populate the VZ; however, in the SVZ TLX expression is only observed in a subset of cells. A secondary proliferative population of cells known as intermediate progenitors (IPCs) are located primarily in the SVZ, although they are also found in the VZ, and can be identified by expression of the transcription factor Tbr2 (Englund et al., 2005). Double-immunostaining against β-galactosidase and Tbr2 at E12.5 shows that although some cells in the VZ show possible co-expression, most Tbr2-positive cells do not also express β-galactosidase (Figure 12J-L). Similarly at E14.5 (Figure 12M-O) and at E16.5 (data not shown) most Tbr2-positive cells do not express β-galactosidase, although some cells in the VZ show possible co-expression. Overall these data indicate that in the embryonic dorsal telencephalon TLX is expressed by radial glia PCs but is downregulated in IPCs and in differentiated neurons.

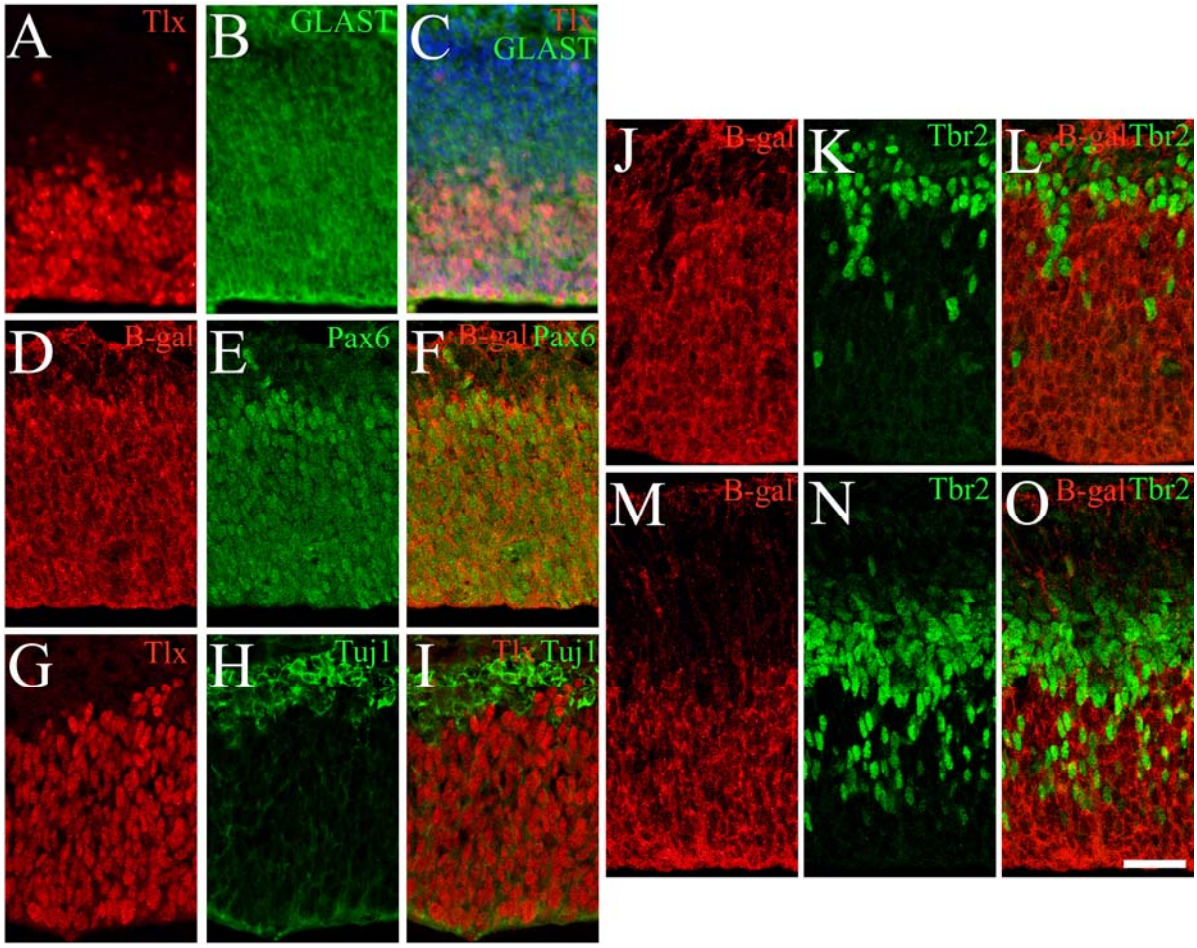

Figure 12. TLX is expressed by a subset of progenitors but not by neurons during development

TLX (red) is co-expressed with the radial glia marker GLAST (green) in the dorsal cortex at E13.5 (A-C). β-galactosidase (red) expressed under the control of the *tlx* promoter is co-expressed with ventricular zone progenitor marker Pax6 (green) at E12.5 in *tlx* +/- dorsal cortex (D-F). TLX (red) is not co-expressed with the neuronal marker Tuj1 (green) at E12.5 (G-I). β-galactosidase does not significantly overlap with intermediate progenitor cell marker Tbr2 (green) at E12.5 (J-L) or E14.5 (M-O). Section C is counterstained with DAPI (blue). Images D-O were taken on a confocal microscope. Scale bar (in O) = 50μm in A-C; 35μm in D-L; 30μm in M-O.

2.3.3 *Tlx* is expressed by oligodendrocytes and astrocytes at early postnatal ages

Expression of TLX was observed in a subset of cells outside of the progenitor domain in the dorsal telencephalon from E18.5. In order to determine whether these cells are differentiated neurons we performed double-immunostaining against TLX and the neuronal marker NeuN. At P0 most cells in the dorsal cortex that express TLX do not express NeuN (Figure 13A-C). Furthermore, the nuclei expressing TLX appear smaller than those of the NeuN-positive neurons, which suggests that these TLX-positive cells may be glial cells. There are two populations of glial cells in the cortex, oligodendrocytes and astrocytes. We examined Sox10 as a marker of oligodendrocytes (Kuhlbrodt et al., 1998). Significant co-expression of Sox10 and β-galactosidase was observed in heterozygous *tlx* brains at P0 in the progenitor domain (Figure 13D-F, arrowheads) and in a subset of cells in the differentiating field (Figure 13D-F, arrows). Although most cells that express β-galactosidase appear to express Sox10, only a subset of Sox10-positive cells outside the progenitor domain express β-galactosidase. Because Sox10 is expressed by glial progenitors as well as mature oligodendrocytes (Kuhlbrodt et al., 1998), this finding could suggest that TLX is predominantly expressed in immature or undifferentiated oligodendrocytes. To identify astrocytes we performed double immunostaining against TLX and the astrocyte marker GFAP. Although GFAP is not yet highly expressed at P0, a few cells co-expressing TLX and GFAP were observed in the dorsal cortex (Figure 13G-I, arrows).

At P8, co-expression of β-galactosidase and Sox10 is still observed in some cells near the ventricle (Figure 14A-C, arrows), although many cells in the cortex that express Sox10 do not

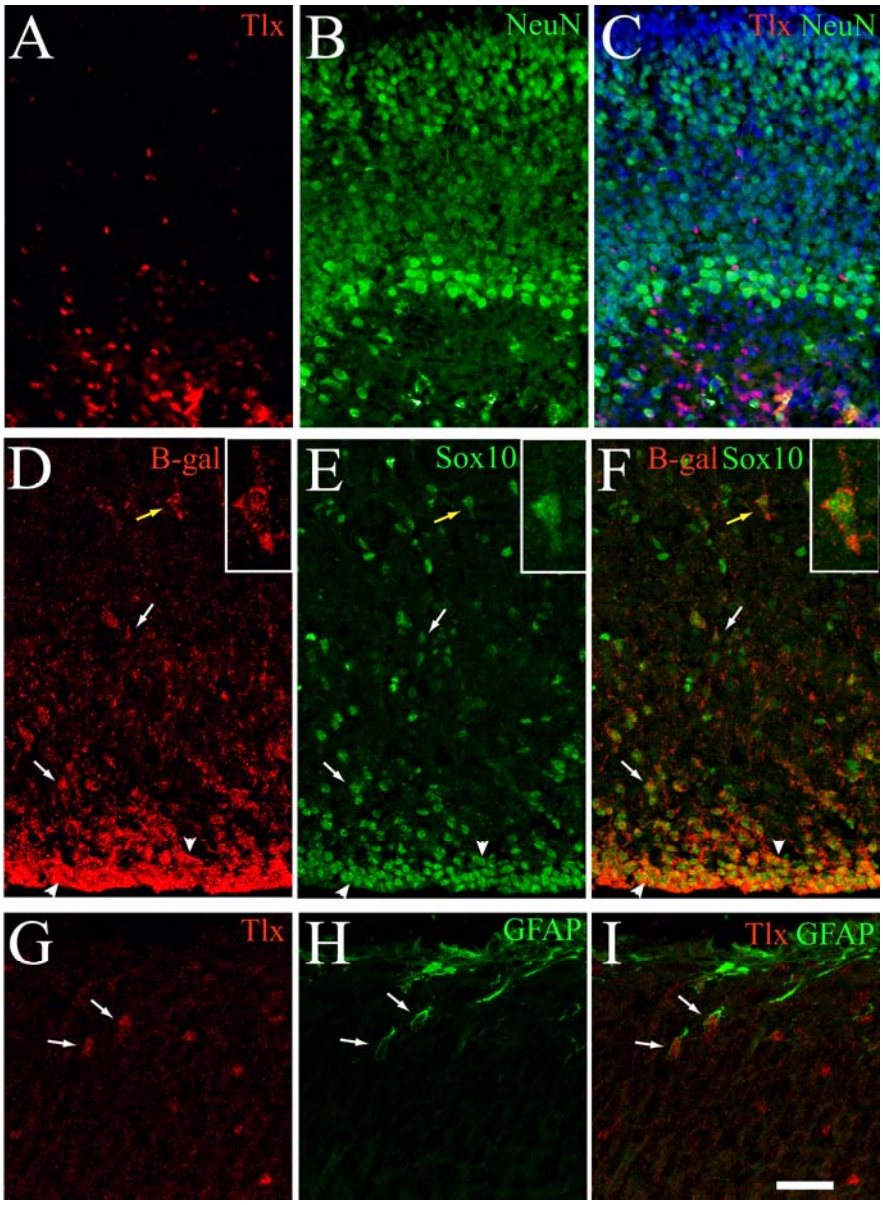

Figure 13. At P0 TLX is coexpressed with markers of glia but not neurons

TLX (red) is not co-expressed with the mature neuronal marker NeuN (green) in the dorsal cortex at P0 (A-C). β-galactosidase expressed under the control of the Tlx promoter (red) is co-expressed with the oligodendrocyte marker Sox10 (green) in cells in the *tlx* +/- dorsal cortex (D-F; arrows) as well as adjacent to the ventricle (D-F; arrowheads) at P0. The double-stained cell indicated by the yellow arrow is shown at higher power in the inset, upper right (D-F). Co-expression of Tlx (red) and the astrocyte marker GFAP (green) was observed at P0 in cells in the dorsal cortex near the pial surface (G-I; arrows). Section C is counterstained with DAPI (blue). Images D-I were taken on a confocal microscope. Scale bar (in I) = 50μm in A-C; 35μm in D-F; 30μm in G-I.

also express β-galactosidase. Co-expression of TLX and GFAP was also observed in cells in the dorsal cortex at P8 (Figure 14D-F, arrows). Many of these cells have a stellate shape, consistent with a mature astrocyte phenotype. Together these data suggest that in the early postnatal brain TLX is expressed in glial progenitors and in a subset of oligodendrocytes but not in mature neurons.

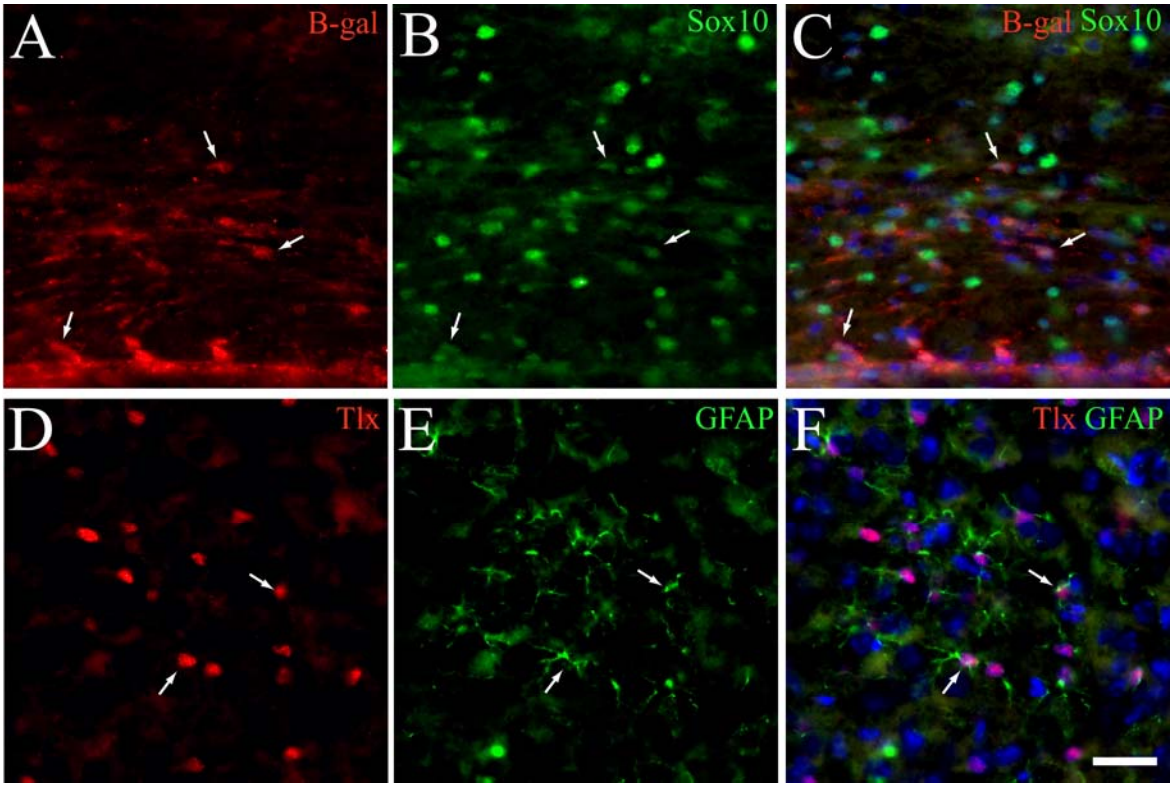

Figure 14. At P8 TLX is co-expressed with markers of glia

Co-expression of β-galactosidase expressed under the control of the *tlx* promoter (red) and oligodendrocyte marker Sox10 (green) was observed in the dorsal cortex of *tlx* +/- animals at P8 (A-C). Co-expression of TLX (red) and astrocyte marker GFAP (green) was observed in cells in the wild-type dorsal cortex at P8 (D-F). Arrows indicate examples of double-labeled cells. Sections are counterstained with DAPI (blue). Scale bar (in F) = 50μm in A-F.

2.4 DISCUSSION

In this study we have characterized the expression of *tlx* mRNA and protein during development, focusing primarily on the dorsal telencephalon. As shown in this chapter and as previously described, *tlx* is expressed in progenitor domains throughout development and in the adult (Monaghan et al., 1995; Stenman et al., 2003a; Shi et al., 2004; Li et al., 2008; Liu et al., 2008). As described here, *tlx* expression is observed in regions that give rise to forebrain structures including the cerebral cortex, hippocampus, amygdala, septum, and striatum. We have further determined that through most of embryonic development *tlx* expression within the dorsal cortex is restricted to apical radial glial PCs, showing little co-expression with the IPC marker Tbr2 or the neuronal marker Tuj1. However beginning at birth *tlx* expression is observed outside of the progenitor domain, showing co-expression with glial markers.

At E13.5 *tlx* mRNA is expressed in a subset of PCs within both the dorsal and ventral telencephalon, with a pattern that in some regions was suggestive of radial clones. Although a similar clonal pattern of TLX protein was not observed, TLX did appear to be expressed at varying levels within the VZ, with high expression in dividing cells at the ventricle. This could suggest that TLX protein is regulated with respect to the cell cycle, and perhaps that cells expressing different levels of TLX indicate different subpopulations of PCs. A similar columnar expression pattern has previously been observed in telencephalic PCs; there, the pattern reflected differential Notch signaling activity (Mizutani et al., 2007). This pattern distinguishes radial glial PCs, which respond to Notch signaling through CBF1, from IPCs, in which CBF1 activity

is reduced (Mizutani et al., 2007). We have shown that *tlx* regulates the transcription of *hes1* (Drill and Monaghan, unpublished results), a bHLH transcription factor activated by Notch signaling (Jarriault et al., 1995). This suggests a possible link between *tlx* and the Notch signaling pathway that may relate to differences between radial glial PCs and IPCs. Although most cells that express the IPC marker Tbr2 do not seem to co-express *tlx*, particularly in the SVZ, there does appear to be some overlap in cells in the VZ. This is similar to the pattern of co-expression of Pax6 and Tbr2, which are thought to be expressed sequentially in glutamatergic neurogenesis, with Pax6 downregulated in the transition from a radial glial progenitor to an IPC (Englund et al., 2005). A similar role for *tlx* in the transition from a radial glial progenitor to an IPC will be further examined in Chapter 4.

As shown previously and confirmed in this study, *tlx* mRNA is expressed in the dorsal telencephalon in decreasing rostral to caudal and lateral to medial gradients at midgestation. Here, we have shown that this graded mRNA expression results in a similar high lateral to low medial gradient of TLX protein expression at E13.5; examination of the rostral to caudal expression pattern of TLX protein was inconclusive (data not shown). However, by E16.5 these expression gradients are no longer observed. The purpose of this early graded expression pattern is unclear, although it does reflect the normal rostral to caudal and ventral to dorsal gradient of neurogenesis in the cortex (Bayer and Altman, 1991). Regional cortical identity is established in part through early gradients of transcription factors in PCs (Rash and Grove, 2006; O'Leary and Sahara, 2008), and loss of *tlx* has been shown to have different effects across cortical regions (Roy et al., 2004). The subsequent chapter (Chapter 3) will therefore investigate the role for *tlx* in the development of cortical areas.

Several subsets of TLX-positive cells were observed outside of the progenitor domain. As early as E13.5 cells were observed in the differentiating field of the ventral telencephalon. Cells expressing both *tlx* mRNA and protein were observed in the region of the developing amygdala at E16.5 and E18.5/P0, as well as in the lateral cortical stream; this latter population of migrating cells derives from the corticostriatal boundary and has been shown to contribute to the amygdala, including the basolateral nucleus (Puelles et al., 2000; Stoykova et al., 2000; Molnar and Butler, 2002; Stenman et al., 2003a; Carney et al., 2006). The lateral, basolateral, and interstitial nuclei of the amygdala have previously been shown to be altered in adult *tlx* null animals, attributed at least in part to abnormalities in the cortico-striatal boundary (Stenman et al., 2003a). The identification in this study of *tlx*-expressing cells in the differentiating field of the amygdala with a pattern indicative of specific nuclei suggests a particular function for *tlx* within the amygdala itself, possibly a novel role in differentiated cells. However, further analysis will be necessary in order to characterize these *tlx*-positive cells.

From birth, cells expressing TLX were observed in the dorsal cortex outside of the progenitor domain. Double-immunostaining indicated that these cells are glia, expressing the glial markers Sox10 and GFAP. *Tlx* expression has previously been observed in Muller glial cells and transiently in proangiogenic astrocytes in the retina, where it has a role in regulating astrogenesis (Miyawaki et al., 2004; Uemura et al., 2006). However, in adult neural stem cells *tlx* has been shown to bind to the promoters of genes expressed in glia, such as *GFAP*, and repress their transcription (Shi et al., 2004), and astrocytes are increased in the *tlx* null brain from birth (Kuznicki and Monaghan, unpublished results; (Shi et al., 2004)). Co-expression of TLX and GFAP at early postnatal ages suggests that at this stage of development TLX may not repress transcription of *gfap*. Perhaps TLX does not bind to the *gfap* promoter because it is sequestered

away from the binding site or blocked by competitive binding from another DNA-binding protein. Even if TLX is bound to the *gfap* promoter perinatally, it could require co-factors to mediate transcriptional repression that are not available at that stage of development. *Tlx* expression may persist from radial glial progenitors to mature glial cells, whereas it is downregulated in intermediate progenitors and differentiated neurons, in order to maintain the proliferative capacity of glia in the adult. Overall these findings give us a framework with which to interpret the phenotype that arises from disruption of the *tlx* allele.

3.0 TLX REGULATES EXPANSION OF VISUAL CORTICAL AREAS

3.1 INTRODUCTION

The adult cerebral cortex is divided into different functional areas that serve specialized roles in processing and integrating sensory input. Each area is characterized by distinct cytoarchitecture and connectivity. Studies in both rodents and primates have suggested that these differences arise during development through regional and temporal control of proliferation (Dehay et al., 1993; Polleux et al., 1997a; Polleux et al., 1997b; Kornack and Rakic, 1998; Lukaszewicz et al., 2005; Lukaszewicz et al., 2006). These area-specific profiles are regulated by two major mechanisms: intrinsic molecular regionalization of cortical progenitor cells (PCs) and extrinsic influence from incoming thalamocortical fibers. Together, these mechanisms are proposed to regulate both the tangential expansion of cortical regions and the differential depth of cortical layers (Rakic, 1988; O'Leary and Nakagawa, 2002). However, it is not fully understood how these area-specific proliferative profiles are generated.

Beginning as early as embryonic day 8 (E8) signaling molecules, including FGFs, Wnts, and BMPs secreted from structures at the border of the cortex, begin to establish gradients of gene expression that influence rostral-caudal, medial-lateral, and dorsal-ventral axes (Mallamaci and Stoykova, 2006). Fgf8 and Fgf17 secreted from the anterior neural ridge are required for rostral-caudal patterning (Fukuchi-Shimogori and Grove, 2001; Garel et al., 2003; Cholfin and

Rubenstein, 2007), while Wnts secreted from the cortical hem regulate dorsal-ventral patterning of the cortex (Backman et al., 2005) as well as hippocampal development (Galceran et al., 2000; Lee et al., 2000b). Wnts have also been proposed to regulate the expansion of caudal cortical areas (Muzio et al., 2005). Together, these secreted signaling molecules influence transcription factors within PCs to establish graded expression patterns across the ventricular zone (VZ) of the cortex (Bishop et al., 2000; Mallamaci et al., 2000; Muzio et al., 2002; Garel et al., 2003; Storm et al., 2006). Four key transcription factors, Emx2, Pax6, COUP-TFI, and Sp8, are expressed in cortical PCs in opposing gradients and play a critical role in the rostral-caudal arealization of the developing cortex (Bishop et al., 2000; Mallamaci et al., 2000; Zhou et al., 2001; Muzio et al., 2002; Armentano et al., 2007; Sahara et al., 2007; Zembrzycki et al., 2007). In addition to their role in regional specification, Emx2, Pax6, and COUP-TFI have been shown to influence early cortical expansion through the regulation of proliferation and differentiation (Mallamaci et al., 2000; Heins et al., 2001; Estivill-Torrus et al., 2002; Quinn et al., 2007; Faedo et al., 2008).

At mid-neurogenesis (E14.5 in mice), thalamic axons begin to arrive at the cortical plate (Molnar and Blakemore, 1995). Studies using heterotopic transplantation suggest that by this time cortical cells are already committed to their areal identity (Gitton et al., 1999; Gaillard et al., 2003). Indeed, area-specific differences in the cell cycle have been observed early during development prior to the arrival of thalamocortical projections (Polleux et al., 1997b), suggesting an early intrinsic regulation of proliferation. However, thalamocortical projections have been demonstrated in vitro to release a factor that promotes proliferation of cortical progenitors (Dehay et al., 2001), indicating a mechanism by which these inputs may further influence the development of area-specific neuronal profiles. Thus, both early intrinsic and late extrinsic mechanisms appear to operate in area-specific control of the cell cycle in PCs. Evidence from

studies of *gbx2* and *mash1* mutant mice, which fail to develop thalamocortical projections, suggests that molecular regionalization of the cortex can occur in the absence of thalamic input (Miyashita-Lin et al., 1999; Nakagawa et al., 1999). Extrinsic input from incoming thalamocortical fibers is therefore thought to contribute primarily to the refinement of the cortical map, evident in the development of sharp boundaries between areas and the specific cytoarchitecture of functional cortical areas (O'Leary and Nakagawa, 2002).

Tlx is a transcription factor expressed in PCs of the developing cortex from E8, with expression persisting in PC populations into adulthood (Monaghan et al., 1995; Stenman et al., 2003a; Shi et al., 2004). We previously generated mice carrying a targeted disruption in the *tlx* gene. *Tlx*-deficient animals survive but exhibit a variety of anatomical and behavioral abnormalities (Monaghan et al., 1997; Yu et al., 2000; Roy et al., 2002; Land and Monaghan, 2003; Stenman et al., 2003a; Stenman et al., 2003b; Miyawaki et al., 2004; Roy et al., 2004; Shi et al., 2004; Land and Monaghan, 2005; Uemura et al., 2006; Zhang et al., 2006). In the absence of *tlx*, the cortex is reduced in both surface area and depth, with the reduction in thickness due to a specific reduction in superficial cortical layers (Monaghan et al., 1997; Roy et al., 2002; Land and Monaghan, 2003). Occipital regions show a slightly greater reduction in the total depth of the cortex, 22% as opposed to 20% in frontal and parietal cortex (Land and Monaghan, 2003). These deficits arise from alterations in PC proliferation and neurogenesis during development (Roy et al., 2002; Roy et al., 2004). From E12.5 to E14.5 *tlx* mRNA is expressed in dorsal PCs in a high rostral/lateral to low caudal/medial gradient (Monaghan et al., 1995; Stenman et al., 2003a). In Chapter 2 we confirmed these gradients at E13.5, but found that from E16.5 through early postnatal development *tlx* expression no longer appears to vary along these axes. Interestingly, in the VZ caudal progenitor cells are more sensitive to the loss of *tlx*, showing a

greater reduction in PC number and rate of proliferation from E14.5 to E18.5 (Roy et al., 2004). However, the sub-ventricular zone (SVZ) is reduced at all rostro-caudal levels (Roy et al., 2004). We hypothesized that these regional alterations in PC proliferation and differentiation during development would translate to area-specific changes in functionally defined cortical areas. In order to test this hypothesis we examined markers of specific regional populations of neurons and progenitors during cortical development. We show that in the absence of *tlx* caudal functionally defined areas, including visual cortex, are specifically reduced.

3.2 METHODS

3.2.1 Animals

Wild-type, heterozygous, and mutant animals were obtained from crossings of heterozygous mice (SVE129 x C57BL/6J) from the 12th generation backcross to C57BL/6J mice. Additional animals were obtained from the 2nd generation backcross with the SVJ129 strain. Animals were genotyped by PCR as previously described in Section 2.2.1 (Monaghan et al., 1997). For all experiments, homozygous mutant embryos or mice were compared with wild-type or heterozygous littermates; we observed no significant difference between wild-type and heterozygous animals in the experiments in this study or in previous studies from E14.5 through adulthood (Land and Monaghan, 2003; Roy et al., 2004). The morning of the vaginal plug was designated E0.5; the day of birth was designated P0. The care and handling of these animals was in accordance with the University of Pittsburgh Institutional Animal Care and Use committee and NIH guidelines.

Embryonic brains were processed by immersion fixation in either cold 4% paraformaldehyde (PFA) pH7.4 (Sigma, St. Louis, MO) or cold Carnoy's fixative; E12.5 to E14.5 for 4-5 hours, E16.5 to E18.5 overnight. Postnatal brains were fixed by transcardial perfusion with cold PBS followed by 4% PFA pH7.4 and immersion fixed overnight. Some postnatal brains were dissected following perfusion and immersion fixed overnight gently flattened between glass slides. Brains intended for whole mount in situ hybridization were processed through a graded methanol series (25-50-75-100%) and stored in 100% methanol at -20°C until use. All other brains fixed with PFA were processed through a graded sucrose series (10-20-30%) at 4°C. Flattened cortices were then sectioned tangentially to the pial surface and successively through each cortical layer on a freezing-sliding microtome at 30µm (P8) or 50µm (6 weeks) and collected in PBS. All other PFA-fixed tissue was sectioned on a cryostat sagitally or coronally at 14µm (E13.5 CD-1 brains) or 20µm (all other tissue) and frozen until use. Embryos fixed in Carnoy's fixative were processed through increasing concentrations of alcohols and embedded in paraffin. Sagittal sections were cut at 10µm.

3.2.2 In situ hybridization

The following digoxigenin (DIG)-labeled riboprobes were used: *Cadherin6* (full-length coding region; obtained by RT-PCR from mouse brain using primers: forward 5'-CCA AGC AAA GAA CAT TAA GGA AG-3', reverse 5'-TTA AGA GTC TTT GTC ACT GTC CA-3'), *Cadherin8* (a gift from M. Takeichi), *Emx2* (Simeone et al., 1992), *EphA7* (a gift from R. Klein), *Id2* (1 kb fragment from +105 to +1062; obtained by RT-PCR from mouse brain using primers: forward 5'-CTC TAC AAC ATG AAC GAC TGC TAC TC-3', reverse 5'-CAA TCA ACA TTC AAT AAA CAC ACT TG-3'), *Wnt2b* (a gift from M. Takeichi), and *Wnt3a* (a gift from A.

McMahon). Probes were prepared using a DIG RNA labeling kit according to the manufacturer's directions (Roche Diagnostics, Indianapolis, IN). The *Cadherin8* was hydrolyzed to 400-bp fragments prior to use as previously described (Schaeren-Wiemers and Gerfin-Moser, 1993). Whole mount in situ hybridizations were performed as previously described (Wilkinson, 1992). Hybridization was done overnight at 70°C and the probe was used at a concentration of 1μg/ml. In situ hybridization on frozen sections was performed as described in Section 2.2.2.

3.2.3 Immunohistochemistry

Sets of paraffin-embedded sections were taken at several lateral to medial levels for processing by immunohistochemistry. Sections were dried at 56°C, de-paraffinized in xylene, rehydrated through a graded ethanol series, and washed in PBS. Antigen retrieval was performed by boiling the slides in 0.01M sodium citrate (pH 6.0); slides immersed in solution were microwaved for 3 minutes at full power followed immediately by 5 minutes at 50% power. Slides were then washed in 0.1% Triton-X-100 (Fisher Scientific) in PBS and blocked with 10% heat-inactivated normal goat serum (Jackson ImmunoResearch, West Grove, PA) in PBS. Sections were incubated with rabbit anti-Pax6 (1:500; Covance) overnight at 4°C. The tissue was then washed with PBS, incubated with Cy3 secondary antibody (1:400; Jackson ImmunoResearch), and counterstained with 1,6-diamidino-2-phenylindole dihydrochloride (DAPI; Sigma) before mounting in fluoromount (Southern Biotechnology Research, Birmingham, AL).

Tangential sections through P8 cortices were washed in 50% methanol/50% PBS/1% hydrogen peroxide followed by three washes with 0.1% Tween 20 (Fisher Scientific) in PBS. Sections were blocked overnight at 4°C with 10% heat inactivated normal goat serum/1% bovine

serum albumin (Fisher Scientific, Pittsburgh, PA) in PBS. Sections were incubated with rabbit anti-serotonin (1:20,000; ImmunoStar, Inc., Hudson, WI) for 48 hours at 4°C. The sections were subsequently washed in 0.1% Tween 20 in PBS, incubated with α-rabbit biotinylated secondary antibody (1:200; Vector Laboratories, Burlingame, CA) and processed using the Vectastain(r) Elite ABC kit (Vector Laboratories) according to the manufacturer's instructions. After rinsing in PBS, sections were incubated in nickel enhanced 0.7mg/ml 3,3'-diaminobenzidine tetrahydrochloride (DAB; Sigma) with 0.01% hydrogen peroxide. DAB stained sections were washed in PBS, mounted on slides, dehydrated, and coverslipped with DPX.

Tangential sections through layer IV of the cortex taken from 6 week old animals were stained for cytochrome oxidase activity as previously described (Land and Monaghan, 2003). All stained sections were visualized using a Nikon (Melville, NY) fluorescent microscope and photographed using a Photometrics (North Reading, MA) Cool Snap digital camera and IP Lab software (Biovision Technologies, Exton, PA).

3.2.4 Measurements

For quantification of whole mount in situs, images of the whole brain were taken at a constant magnification on a Nikon dissecting microscope using a Photometrics Cool Snap digital camera and IP Lab software. For both the left and right hemispheres of each animal, the total cortex, motor cortex, and primary visual cortex were outlined using Photoshop 6.0 (Adobe Systems, San Jose, CA) and the areas calculated using ImageJ (NIH, Bethesda, MD). Measurements for the right and left hemispheres were averaged within each individual animal, and these values were used to calculate the proportion of total cortical area occupied by motor cortex and by visual cortex. The values from three pairs of control and mutant littermates were then compared using

a paired t-test. All outlines and measurements were done blind to genotype. To confirm the results, areas were outlined by a second investigator blind to genotype and similar results were obtained by statistical analysis. Statistical analysis was done using InStat (GraphPad Software, San Diego CA). All values are written and graphed as mean ± SEM.

Id2 expression was used as a marker for caudal cortex, with layer V expression defining a caudal region extending to the border between somatosensory and motor cortex. For each brain, in situ hybridization was performed on representative sagittal sections taken at three medial to lateral levels through one cortical hemisphere. For quantification, one section each from four control and four mutant brains were matched for medial-lateral position. To draw boundaries, sections were examined under a 40X objective to identify *Id2* expressing versus non-expressing cells and boundaries were drawn using Photoshop on corresponding images taken with a 4X objective. The total length of the cortex was defined as the distance from the caudal pole to the rostral edge of the cortex at the boundary of the olfactory bulb, as traced along the pial surface of the section. This line was bisected by a perpendicular line drawn at the rostral boundary of layer V *Id2* expression. The proportion the total length caudal to this boundary was calculated for each animal and controls and mutants compared using an unpaired t-test. All boundaries and measurements were determined blind to genotype.

Quantification of serotonin immunostaining and cytochrome oxidase staining followed methods described in Hamasaki et al., (2004). Sequential images were taken of serial sections of the right cortical hemisphere through layer IV as defined by the presence of histologically identifiable whisker barrels. Images were taken at a constant magnification on a dissecting microscope as described above. For each animal, multiple adjacent sections were aligned to specific whisker-related barrels. For each section, the total cortex, posteromedial barrel subfield

(PMBSF), auditory cortex, and primary visual cortex were outlined using Photoshop and consensus outlines from multiple sections were determined for each animal. If an area could not be outlined in its entirety it was excluded from calculations. To analyze lengths, a straight line was drawn from the frontal pole to the occipital pole, and a line perpendicular to the first was drawn through whisker barrel C3. Areas and lengths were measured using ImageJ software, and statistical analysis was done using GraphPad. Measurements of area and length were compared between three to five control and three to five mutant animals using an unpaired t-test. Cortices obtained from C57BL/6J backcrossed animals and SVJ129 crosses were compared at P8 using serotonin immunostaining. No significant differences were observed for any measures tested, including the proportion of total cortical area occupied by primary visual cortex as compared between either controls of each strain ($p>0.5$, $n=3$) or mutants ($p>0.5$, $n=3$). Therefore data from both strains were pooled for all calculations.

3.3 RESULTS

3.3.1 Caudal cortical areas are specifically reduced perinatally

In Chapter 2 we showed that *tlx* is expressed in a high rostral/lateral to low caudal/medial gradient in the dorsal telencephalon at E13.5, with this gradient no longer apparent from E16.5. However, caudal PCs are more sensitive to the loss of *tlx* than rostral PCs, showing a greater reduction in number and rate of proliferation (Roy et al., 2004). To determine how the region-specific effects on cortical PCs in the absence of *tlx* impact the development of functional cortical areas, we examined the transcription pattern of genes hypothesized to be associated with

the development of functional areas (Bulfone et al., 1995; Suzuki et al., 1997; Miyashita-Lin et al., 1999; Nakagawa et al., 1999; Rubenstein et al., 1999). By P0 developing cortical areas can be identified by the distribution of genes expressed in region-specific patterns (Suzuki et al., 1997; Miyashita-Lin et al., 1999; Rubenstein et al., 1999). We first examined *cadherin8* expression in whole cortices at P0 (Figure 15A-C). *Cadherin8* is expressed throughout the cortex in layer V, but developing motor and visual areas also show high expression in layers II/III and IV (Suzuki et al., 1997; Nakagawa et al., 1999). At P0 a region of darker staining clearly demarcates a rostral motor region (Figure 15A, arrowheads). The total surface area of the cortex (both hemispheres) is reduced by 25% in *tl*x -/- animals (control: $30.7mm^2 \pm 1.1mm^2$; *tlx*-/-: $23.0mm^2 \pm 0.7mm^2$; $p<0.05$, n=3). Details of all measurements are outlined in the methods section. *Cadherin8* staining in control animals indicates that the motor region occupies 21.0% ± 0.8% of the total cortical surface area whereas in mutant animals the motor region occupies 29.3% ± 1.3%, an increase of 39.5% ($p<0.05$, n=3; Figure 15A-C). Interestingly, the actual size of the motor cortex is not altered between control and mutant brains ($p>0.5$, n=3), supporting the hypothesis of a caudal-specific reduction in functional cortical areas.

To compare cortical areas in more detail, we examined the expression of the region-specific marker *Id2* in sequential sagittal sections through control and mutant cortices at P0. *Id2* is a helix-loop-helix protein expressed in layers II/III, V, VI, and the subplate (Neuman et al., 1993). This layer-specific expression varies regionally and can be used to map developing functional areas. *Id2* expression in layer V has previously been shown to be restricted to caudal regions of the cortex, with a rostral boundary at the border between somatosensory and motor cortex (Bulfone et al., 1995; Rubenstein et al., 1999; Figure 16A, C). In *tlx -/-* animals the region caudal to this boundary occupies a significantly smaller proportion of the total rostral-caudal

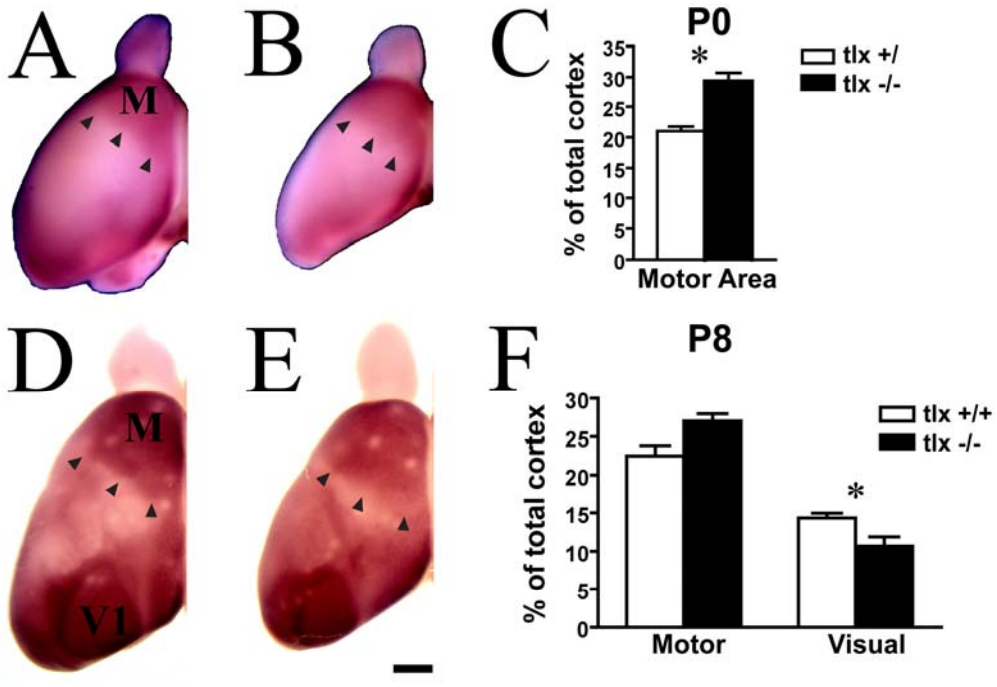

Figure 15. Visual cortex is reduced perinatally in *tlx* -/- animals while rostral motor cortex is relatively unaffected

Whole mount in situ hybridization for *Cadherin8* at P0 (A, B) and P8 (D, E). (A-C) At P0 motor cortex (M, arrowheads) occupies a significantly greater proportion of the total cortical area in *tlx* -/- animals (B) as compared to controls (A), quantified in C. (D-F) At P8 primary visual cortex (V1) occupies a significantly smaller proportion of the total cortical area in *tlx* -/- animals (E) as compared to controls (D), quantified in F. *$p<0.05$. Scale bar (in E) = 0.75mm in A, B; 1mm in D, E.

cortical length, 51.8% ± 0.8% as compared to 56.3% ± 0.7% in controls ($p<0.01$, n = 4; Figure 16A, B, boundary indicated by solid arrowhead, C, D, boundary indicated by line). *Id2* is also expressed superficially (layers II/III) in both a rostral and a caudal domain, the boundaries of which vary across the medial-lateral axis (Bulfone et al., 1995; Rubenstein et al., 1999; Figure 16A, E). At the level shown in Figure 16, the rostral superficial expression domain extends into somatosensory cortex whereas the caudal superficial expression domain is restricted to occipital cortex (Figure 16A, B, boundaries indicated by open arrowheads, E, F, boundaries indicated by

lines). In *tlx* -/- animals both boundaries are shifted farther caudally, such that the caudal superficial domain is reduced and the rostral superficial domain extends proportionately farther caudally. These results were verified by examining an independent marker of caudal cortex,

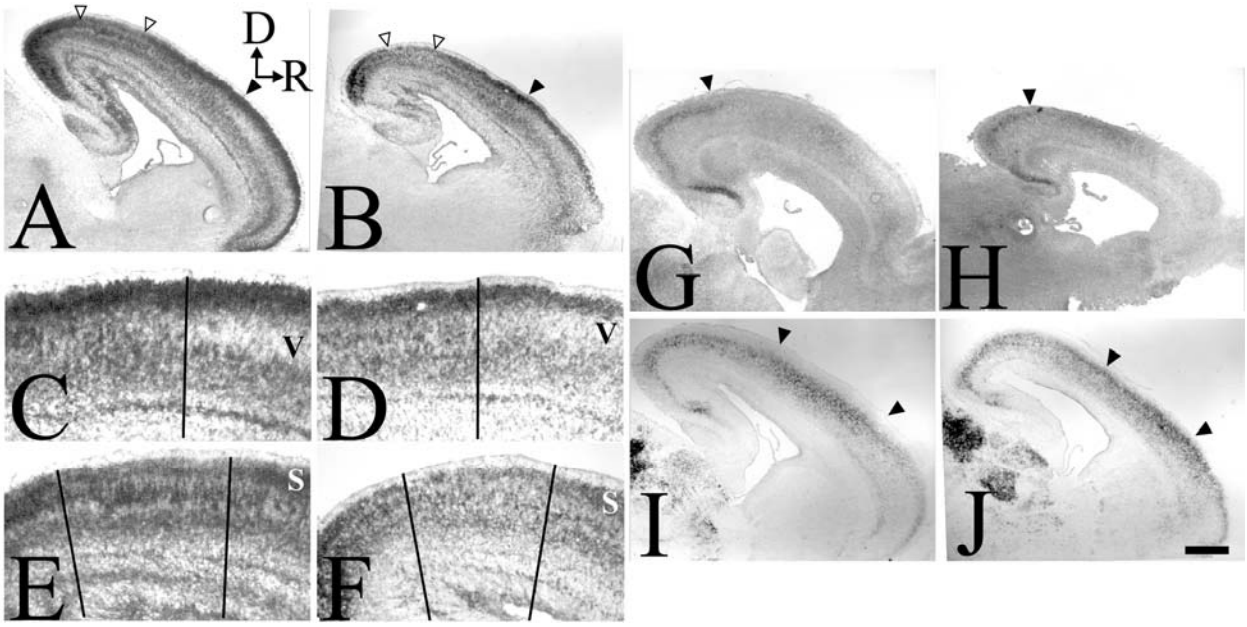

Figure 16. Caudal regions are reduced at P0 in the absence of *tlx*

In situ hybridization of sagittal sections through control (A, C, E, G, I) and *tlx* deficient (B, D, F, H, J) animals at P0. (A, B, C, D) *Id2* expression in layer V demarcates the boundary between the somatosensory and motor cortex (black arrowhead). This boundary is shifted caudally in the *tlx* -/- cortex (B). C and D are higher power images of the areas labeled with a black arrowhead in A and B respectively, showing the termination of *id2* expression in layer V (lines). (A, B, E, F) *Id2* expression in layer II/III subdivides the cortex in three rostral to caudal domains, a caudal high expression domain, an intermediate domain (open arrowheads), and a rostral high expression domain. The intermediate domain is shifted caudally in *tlx* -/- animals (B). E and F are higher power images of the areas labeled with open arrowheads in A and B respectively, with lines at the boundaries of superficial layer II/III (S) *id2* expression. (G, H) *EphA7* is highly expressed in layer IV of caudal cortex (rostral limit marked by arrowhead). This region is reduced in *tlx* -/- cortex (H) as compared to controls (G). (I, J) High *Cadherin6* expression in layers II/III, IV, and V demarcates parietal cortex (limits marked by arrowheads). This is reduced in the *tlx* -/- cortex (J) as compared to controls (I). Scale bar (in J) = 400μm in A, B, G-J; 170μm in C-F. D = dorsal; R = rostral.

ephA7. At P0 the *ephA7* receptor tyrosine kinase is expressed in layer IV with the highest expression levels in occipital cortex and very low expression in somatosensory cortex (Mori et al., 1995; Yun et al., 2003). In the absence of *tlx* the caudal cortical region demarcated by high *ephA7* expression is shifted caudally (Figure 16G, H, arrowheads; n=2). Together these findings suggest that although rostral motor areas are relatively unaffected at P0 caudal cortical areas are reduced in size.

So far, these data show that at P0 in the absence of tlx caudal cortical regions are reduced whereas rostral motor cortex is relatively unaffected. To determine whether intermediate areas are reduced we examined the expression of *cadherin6*, which is expressed in layers II/III, IV, and V with much higher expression levels in parietal cortex (Suzuki et al., 1997; Nakagawa et al., 1999). This high expression domain is reduced in length in *tlx -/-* animals (Figure 16I, J, arrowheads; n=3). Together, our data suggest that although rostral motor areas are relatively unaffected at P0, intermediate parietal cortex and caudal cortical areas are reduced in size.

Cortical areas continue to develop after birth, and by P8 *cadherin8* expression in whole mount preparations can be used to distinguish motor areas as well as visual cortex (Suzuki et al., 1997). At P8 there is no significant difference in the proportion of total cortical area occupied by motor cortex in control and mutant animals (control: 22.5% ± 1.4%; mutant: 27.0% ± 1.0%; $p=0.122$, n=3), although as at P0 the absolute area of the motor cortex appears similar between genotypes (Figure 15D-F, arrows). Primary visual cortex occupies a significantly smaller proportion of the total cortical area in mutant animals, 10.7% ± 1.1% as compared to 14.3% ± 0.7% in control animals, a reduction of 25.2% ($p<0.05$, n=3; Figure 15D-F). To verify these findings we examined cortical areas using serotonin immunostaining on tangential sections through flattened cortices at P8 (Figure 17). This marks the terminations of thalamocortical

axons in layer IV of primary sensory areas including primary somatosensory cortex, primary visual cortex (V1), and primary auditory cortex (Fujimiya et al., 1986). Serotonin staining at P8 shows that in *tlx* deficient animals V1 occupies a significantly smaller proportion of the total cortical area, 5.2% ± 0.3% as compared to 8.2% ± 0.6% in control brains, a reduction of 36.6% ($p<0.005$, n=5; Figure 17A-C). However more intermediate structures such as the posteromedial barrel subfield (PMBSF; part of somatosensory cortex) and primary auditory cortex are reduced proportionately to total cortical area (PMBSF $p>0.5$, n=3; auditory $p>0.5$, n=5).

We observed that the PMBSF appeared to be shifted medially in *tlx* deficient animals, possibly indicating changes in the medial-lateral axis. To examine this more directly we measured the medial-lateral position of the PMBSF. We arbitrarily chose the C3 barrel as the focal point for measurements due to its central location and because it was easily identifiable on several consecutive sections. To quantify the percent of the cortex located medial to the C3 barrel, we first defined a rostral-caudal axis as a straight line from the frontal pole to the occipital pole, and then drew a line perpendicular to this axis through the center of the C3 barrel (Figure 17D). In *tlx* deficient animals, the proportion of cortex medial to barrel C3 is significantly reduced, 39.4% ± 0.3% as compared to 42.7% ± 0.7% in controls, a 7.7% reduction ($p<0.005$, n=5). The segment of the rostral-caudal line posterior to C3, which bisects auditory cortex, occupies the same proportion of total rostrocaudal length in control and mutant animals ($p>0.1$, n=5), verifying our observation that auditory cortex is reduced proportionately to total cortical area. This suggests that the caudomedial cortex shows a greater reduction than caudolateral cortex.

Together, these results indicate that perinatally motor cortex is the same size in *tlx* deficient animals as in control animals and that the reduction in surface area reflects a reduction

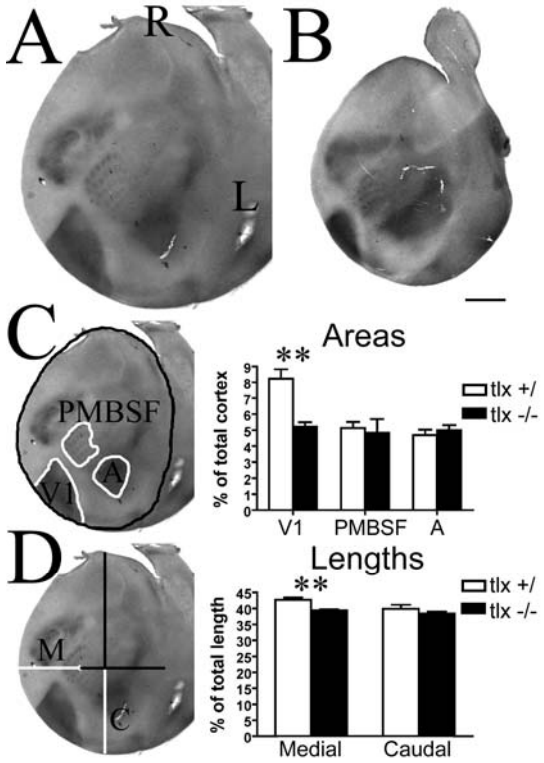

Figure 17. Primary visual cortex is disproportionately reduced in *tlx* deficient animals at P8

At P8 primary visual cortex is disproportionately reduced in the *tlx* deficient animals while auditory cortex and the posteromedial whisker barrel field are reduced proportionately to the reduction in total cortical area. Serotonin immunostaining on tangential sections through flattened *tlx* +/+ (A) and *tlx* -/- (B) cortex. (C) The regions compared between wild-type and mutant animals (posteromedial whisker barrel field, PMBSF; auditory cortex, A; primary visual cortex, V1) are outlined in white on the left. Quantification is shown on the right. (D) Caudomedial cortex is selectively reduced while caudolateral cortex is reduced proportionate to reduction in total cortical area. The medial distance M is defined as the length from barrel C3 to the medial edge of the cortex (white line). The caudal distance C is defined as the distance from the occipital pole to the point of intersection with the medial-lateral axis (white line), defined in the text. Quantification is shown on the right. ** $p<0.005$. Scale bar (in B) = 1mm in A, B. R = rostral, L = lateral.

in parietal and occipital cortex. Primary visual cortex, located the farthest caudally and medially of the functional areas examined, shows the greatest reduction.

3.3.2 Caudal cortical areas are reduced in the adult *tlx* -/- animal

It has previously been shown that in *tlx* deficient adult animals the primary somatosensory cortex whisker barrels are located in a central location along the rostral-caudal axis and the organization of the barrels into rows and arcs is similar to that of wild-type animals (Land and Monaghan, 2003). However, the size of different functional cortical areas was not examined. To determine whether the changes in functionally distinct areas observed perinatally persist in the adult we examined cytochrome oxidase staining in tangential sections through cortical layer IV of brains from 6 week old mutant and control animals. Cytochrome oxidase is an enzyme enriched in thalamocortical axon terminals in layer IV of the cortex, with higher expression in primary sensory areas (Wallace, 1987). In the mutant cortex, the PMBSF and primary auditory cortex are reduced proportionate to the reduction in total cortical area (PMBSF: $p>0.1$, $n=4$; auditory: $p>0.1$, $n=4$; Figure 18A-C). However, primary visual cortex (V1) shows a disproportionately greater reduction in the adult mutant cortex, occupying 6.0% ± 0.6% of the total cortical area in mutant animals as compared to 8.6% ± 0.4% in controls, a 30.2% reduction ($p<0.05$, $n=3$; Figure 18A-C). Thus, the pattern of reduction in functional areas observed perinatally persists in the adult, with caudal cortical areas such as visual cortex most severely affected.

As observed at P8, the PMBSF appeared to be shifted medially. Quantifying this as described previously, we found that in *tlx* deficient adults the proportion of the cortex medial to barrel C3 is significantly reduced, 30.3% ± 1.1% as compared to 39.4% ± 2.9% in controls, a 23.1% reduction ($p<0.05$, $n=4$; Figure 18D). The proportion of the rostral-caudal line posterior

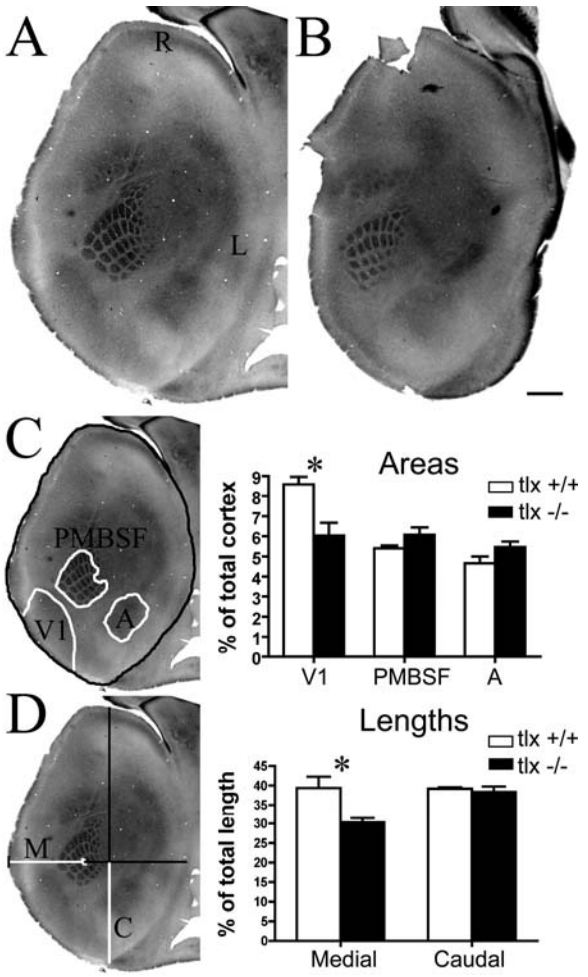

Figure 18. The specific reduction in visual cortex persists in the adult *tlx* -/- brain

Cytochrome oxidase staining on tangential sections through flattened *tlx* +/+ (A) and *tlx* -/- (B) cortex of six-week old animals. (C) The regions compared between wild-type and mutant animals (posteromedial whisker barrel field, PMBSF; auditory cortex, A; primary visual cortex, V1) are outlined in white on the left. Quantification is shown on the right. (D) The disproportionate reduction of caudomedial cortex is maintained in the adult. The medial distance M is defined as the length from barrel C3 to the medial edge of the cortex (white line). The caudal distance C is defined as the distance from the occipital pole to the point of intersection with the medial-lateral axis (white line), defined in text. Quantification is shown on the right. * $p<0.05$. Scale bar (in B) = 1mm in A; 0.6mm in B. R = rostral, L = lateral.

to barrel C3 is not significantly reduced ($p>0.5$, n=4), consistent with our observations that auditory cortex is proportionately reduced in the *tlx* deficient adult cortex. These data indicate that in the *tlx* deficient adult caudomedial functional areas continue to show the greatest reduction.

3.3.3 Early arealization is not altered in *tlx* -/- animals

To determine whether the caudal-specific reduction observed in *tlx* -/- animals is mediated by changes in early regional patterning, we examined the expression of early areal markers of the dorsal cortex at E12.5, before mutant animals begin to show a reduction in the size of the cortex. *Pax6* is expressed in a high rostral to low caudal gradient (Stoykova and Gruss, 1994). Immunostaining against *Pax6* shows a similar gradient in both control and *tlx* null animals at E12.5 (Figure 19A, B; n=3). *Emx2* is expressed in an opposing high caudal to low rostral gradient (Gulisano et al., 1996; Mallamaci et al., 1998). *In situ* hybridization with a probe directed against *emx2* shows a similar caudal to rostral gradient in control and *tlx* null animals at E12.5 (Figure 19C, D; n=3). Because we did not observe any gross differences in the expression pattern of these early markers, we conclude that cortical regions are appropriately specified at E12.5. This suggests that the deficit in functional areas observed in *tlx* null animals is the consequence of later developmental mechanisms.

In addition to a reduction in the size of caudal cortical structures, we observed a reduction in medial cortex in *tlx* null animals at P8 (Figure 17D) and in the adult (Figure 18D). Several members of the *Wnt* family are expressed by cells in the cortical hem, at the medial edge of the telencephalon, and are involved in early area patterning and neurogenesis (Grove et al., 1998; Lee et al., 2000b; Chenn and Walsh, 2002; Hirabayashi et al., 2004). Recently these *Wnts* have

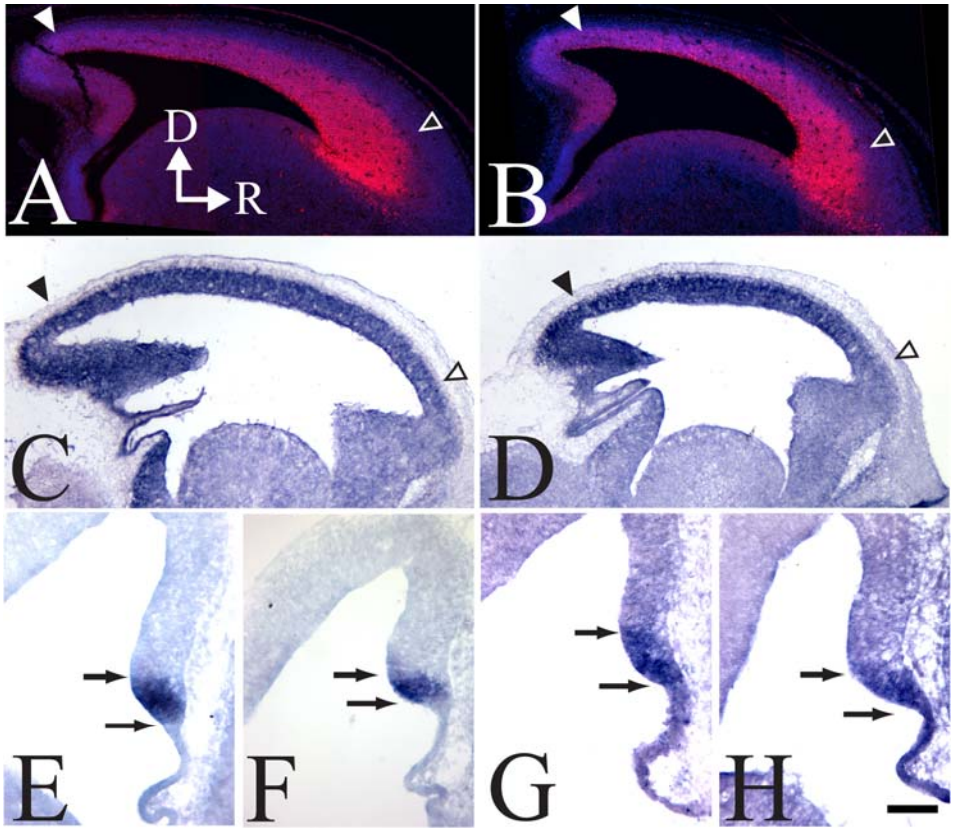

Figure 19. Early rostral-caudal patterning is not altered in *tlx*-deficient animals

Pax6 protein expression shows a high rostral (open arrowhead) to low caudal (black arrowhead) gradient (A, B) and *emx2* mRNA transcripts are expressed in a high caudal (black arrowhead) to low rostral (open arrowhead) gradient (C, D) in sagittal sections through E12.5 embryos. These gradients appear similar in *tlx* -/- animals (B, D) as compared to controls (A, C). *Wnt2b* (E, F) and *wnt3a* (G, H) expression demarcate a medial domain in the cortical hem in coronal sections of E12.5 embryos (limits marked by arrows). The expression domain of *wnt2b* and *wnt3a* is smaller in *tlx* -/- animals (F, H) as compared to controls (E, G). Scale bar = 200μm in A, B; 180μm in C, D; 100μm in E-H. D = dorsal, R = rostral.

been proposed to play a specific role in the expansion of caudal cortical areas (Muzio et al., 2005). To determine whether changes in *wnt* expression at the cortical hem could contribute to the observed caudomedial reduction, we examined the expression of *wnt2b* (Figure 19E, F, boundaries marked by arrows; n=2) and *wnt3a* (Figure 19G, H, boundaries marked by arrows;

n=5) in control and *tlx -/-* cortices at E12.5. In *tlx* null animals both *wnt2b* and *wnt3a* are more weakly expressed and do not extend as far dorsally as in mutant animals, although this is difficult to quantify. These findings suggest that changes in expression of *wnts* in the cortical hem may be involved in the reduced expansion of caudal and medial cortex in *tlx -/-* animals.

3.4 DISCUSSION

Regional regulation of PCs during development is one mechanism that is important in generating differences in functional cortical areas. In the absence of *tlx* caudal cortical areas, such as visual cortex, are reduced to a greater extent than the reduction in total cortex, while rostral areas are relatively unaffected. Medial areas, such as somatosensory cortex, show an intermediate phenotype; these areas are reduced at P0 and from P8 show a proportionate reduction relative to total cortical area. Furthermore, there are no obvious abnormalities in thalamocortical innervation in *tlx* mutants during development or in the adult (Land and Monaghan, 2003), although we cannot exclude effects due to more subtle changes in thalamocortical input. Our findings suggest that *tlx* has a regional role in cortical PCs to regulate the development of functional cortical areas.

3.4.1 *Tlx* regulates expansion of caudal cortical progenitors

Cortical areas are established in two phases. The first is an early intrinsic phase that involves regionalization of the VZ by expression of secreted signaling molecules, including FGFs and Wnts, and transcription factors, including Pax6, Emx2, COUP-TF1, and Sp8. During the second

phase, or refinement phase, input from thalamocortical fibers contributes to the transition within the cortex from broad regionalization to distinct areas defined by unique cytoarchitecture and molecular profiles (O'Leary and Nakagawa, 2002; Rash and Grove, 2006; O'Leary and Sahara, 2008). Throughout both of these phases, the size and the specific cytoarchitecture of different functional areas are determined by regulating PC output. Evidence from both rodents and primates has shown differences between cortical areas in cycle kinetics and in the proportion of PCs that make proliferative versus differentiative divisions (Dehay et al., 1993; Polleux et al., 1997b; Lukaszewicz et al., 2005). For example, in primates areas 17 (primary visual cortex) and 18 can be histologically distinguished by a greater number of supragranular neurons in area 17 (Rockel et al., 1980). This results from higher rates of neuronal production in area 17 due to a shorter cell cycle and a higher rate of proliferative divisions (Kornack and Rakic, 1998; Lukaszewicz et al., 2005). These areal differences are mediated through the regulation of important regulators of cell cycle control, cyclin-dependent kinase inhibitor $p27^{Kip1}$ and cyclin E (Lukaszewicz et al., 2006). Although expression of $p27^{Kip1}$ and other cell cycle regulators have not been examined with respect to different functional areas in rodents, manipulating levels of $p27^{Kip1}$ in mice has been shown to alter the proportion of progenitors the exit the cell cycle (Caviness et al., 2003; Tarui et al., 2005). This manipulation leads to changes in the number of neurons specifically in superficial layers (Caviness et al., 2003; Tarui et al., 2005), suggesting a mechanism that could mediate differences in layer size between functional areas in mice. These findings are consistent with the hypothesis that in rodents areal differences in cell cycle parameters and the resulting cytoarchitecture are mediated by differences in cell cycle regulators. *Tlx* has been shown in the retina and cortex to regulate proliferation through regulation of key cell cycle proteins including $p27^{Kip1}$, Pten, and cyclinD1 (Miyawaki et al., 2004; Zhang et al.,

2006; Sun et al., 2007; Li et al., 2008; Zhang et al., 2008). We hypothesize that *tlx* similarly acts through regulation of cell cycle proteins to promote proliferation in cortical PCs during development, playing a key role in the normal expansion of caudal functional areas.

During early cortical development the cortex is largely composed of a proliferative population of cells known as radial glia, which divide at the ventricular surface to produce progenitors and neurons (Malatesta et al., 2000; Noctor et al., 2001; Noctor et al., 2002). At mid-neurogenesis a second proliferative population appears. Termed intermediate progenitors, these cells are characterized by abventricular mitosis and are located predominantly within the subventricular zone (Haubensak et al., 2004; Miyata et al., 2004; Noctor et al., 2004). It is hypothesized that intermediate progenitors are the major source of cortical neurons (Haubensak 2004, Englund 2005, Sessa 2008, Kowalczyk 2009). In tlx deficient animals, the VZ is reduced in cell number only in caudal cortical regions, whereas the subventricular zone containing intermediate progenitors is reduced from E16.5 at all rostrocaudal levels (Roy et al., 2004). Further examination of this phenotype using molecular markers to specifically identify VZ progenitors and intermediate progenitor cells reveals a specific reduction in intermediate progenitors in the caudal cortex, as discussed in more detail in the following chapter (Chapter 4). This suggests a dual role for *tlx* during development. An early role in regulating proliferation and neurogenesis in the caudal VZ could result in reduced tangential expansion of the PCs that give rise to caudal cortex, leading to a disproportionate reduction in the surface area of caudal functional areas. Later, *tlx* may have a broader role in the expansion of the intermediate progenitor population in the SVZ across the entire rostrocaudal axis, leading to the reduction in the thickness of superficial layers observed across all cortical areas.

3.4.2 Early rostrocaudal patterning is not altered in the absence of *tlx*

The changes in functional cortical areas that we observed in the *tlx* mutant could result from interactions with early transcription factors that determine the regionalization of the developing cortex, such as Pax6 and Emx2 (Bishop et al., 2000). *Tlx* has been shown to interact genetically with *pax6* in the formation of the pallio-subpallial boundary (Stenman et al., 2003a) and in the formation of upper cortical layers (Schuurmans et al., 2004), and furthermore *pax6* null animals exhibit cell cycle changes early during development similar to those observed in *tlx* null animals (Estivill-Torrus et al., 2002; Roy et al., 2004). The *Drosophila* homolog *tailless* is known to suppress expression of *empty spiracles*, the homolog of the vertebrate *emx* genes (Hartmann et al., 2001). In addition, *emx2* null mice exhibit a similar cortical phenotype to *tlx* null animals, a specific reduction in caudal cortical areas (Bishop et al., 2000). However, contrary to the *tlx* null phenotype the absence of *pax6* or *emx2* leads to greater deficits where the gene is normally more highly expressed (Bishop et al., 2000). Here we have shown that the absence of *tlx* does not affect the expression patterns of *pax6* or *emx2* at E12.5, which suggests that cortical regions are specified appropriately at this age. However, one alternate possibility that we have not yet explored is that the high rostral expression of *tlx* acts to limit the expression of anterior patterning signals such as Fgf8 or Fgf17 (Fukuchi-Shimogori and Grove, 2001; Garel et al., 2003; Cholfin and Rubenstein, 2007), which would control the expansion of anterior cortical regions.

Expansion of the expression domain of Fgf8 has been shown to suppress expression of WNT proteins in the cortical hem (Shimogori et al., 2004). We did observe a reduction in the expression domains of *wnt2b* and *wnt3a* in the cortical hem at E12.5. *Wnt3a* is involved in regulating the expansion of the caudomedial region of the cortex that gives rise to the

hippocampus, with an important role in the development of the dentate gyrus (Lee et al., 2000b). Interestingly this hippocampal structure is specifically reduced in the *tlx* null adult (Monaghan et al., 1997). *Emx2* has also been shown to be required for the growth of the hippocampus (Tole et al., 2000), and animals deficient for *emx2* exhibit a pronounced downregulation of *Wnt3a* in the cortical hem (Muzio et al., 2002). Although there is not an obvious difference in *emx2* expression at E12.5 in the absence of *tlx*, there may be subtle differences that were undetected but are nonetheless sufficient to contribute to the hippocampal phenotype. It has recently been suggested that *Wnt* signaling acting in combination with *Emx2* also plays a role in the expansion of occipital cortex (Muzio et al., 2005), which could indicate that altered regulation of *Wnts* in the cortical hem contributes to the reduction of caudal and medial cortex observed in *tlx* deficient cortex postnatally. Further studies will be necessary to determine whether *tlx* is directly involved in *Wnt* signaling, indirectly affects *Wnts* through possible suppression of *Fgfs*, or whether the reduced *wnt2b* and *wnt3a* domains are simply the result of decreased progenitor proliferation in the cortical hem.

3.4.3 Functional implications

It has been shown in other systems that visual input at the appropriate developmental age can influence the proportion of the cortex occupied by primary visual cortex (Wiesel and Hubel, 1963; Berardi et al., 2000). In primates, embryonic bilateral enucleation leads to a reduction in the size of primary visual cortex without a reduction in total cortical area (Rakic, 1988; Dehay et al., 1996). Conversely, recent evidence has shown that altering in the size of somatosensory and motor cortex during development diminishes performance at sensorimotor tasks (Leingartner et al., 2007). In this study the authors examined the behavior of animals with either reduced levels

of *emx2* (heterozygous for the null allele) or elevated *emx2* (with an *emx2* transgene under the control of the progenitor-specific *nestin* promoter). These manipulations resulted in either an expansion or reduction in motor and somatosensory cortex, respectively, and in both cases sensorimotor behavioral performance was affected (Leingartner et al., 2007). Differences in proliferation are apparent in *tlx* null animals prior to ingrowth of thalamic axons, suggesting that the caudal-specific reduction observed here is independent of thalamic input. Indeed, as described in subsequent chapters conditional deletion of the *tlx* allele only in dorsal PCs results in a disproportionate reduction of primary visual cortex similar to that observed in null animals but does not appear to cause any significant visual impairment, as conditional animals perform normally in a visual placing task and in a visible version of the Morris water maze (see Chapter 5). We cannot rule out subtle deficits in vision in these mice, as it may be that altering the size of visual cortex does not show as much of a behavioral impact as altering somatosensory or motor cortex because mice rely less on vision than on other senses. However, our findings suggest that although there may be an ideal size for some functional areas, a reduced primary visual area is sufficient for normal visual function in mice.

4.0 A ROLE FOR TLX IN REGULATING THE PROPERTIES OF DORSAL PROGENITORS

4.1 INTRODUCTION

Projection neurons in the cerebral cortex are generated in a precisely timed manner from progenitor cells (PCs) located adjacent to the ventricle in the ventricular zone (VZ) and subventricular zone (SVZ) (Bystron et al., 2008). Early during development, this population consists of multipotent PCs termed neural epithelial cells (Rakic, 2003). At the onset of neurogenesis a proliferative population appears known as radial glia progenitor cells (RGCs) or, alternatively, as apical PCs. These bipolar cells extend processes to the ventricular and pial surfaces and divide at the ventricular surface to produce PCs, neurons, and later glia, directly or indirectly giving rise to the majority of cortical neurons (Malatesta et al., 2000; Hartfuss et al., 2001; Noctor et al., 2001; Heins et al., 2002; Noctor et al., 2002; Malatesta et al., 2003; Anthony et al., 2004). In mice, cortical neurons are generated between E11 and E17, during which time these apical PCs go through eleven cell cycles (Takahashi et al., 1995b). At each division the progenitor can either undergo a proliferative division, to make two progenitors, or an asymmetric neurogenic division, to make a progenitor and a neuron (McConnell, 1995). Early during development, divisions are predominantly proliferative, with neurogenic divisions appearing at the onset of neurogenesis (Haubensak et al., 2004). As neurogenesis progresses, the proportion

of cells leaving the cell cycle through neurogenic divisions increases, depleting the PC population from mid neurogenesis (Caviness and Takahashi, 1995; Noctor et al., 2004). At the end of neurogenesis (E18.5 in the mouse), RGCs begin to retract their processes, translocate outside the VZ, and transform into astrocytes (Voigt, 1989; Edwards et al., 1990).

A secondary proliferative population appears as early as E11.5 in mice (Haubensak et al., 2004; Attardo et al., 2008; Noctor et al., 2008), with this population distinguishable as the SVZ by E13.5. These cells, termed intermediate progenitor cells (IPCs) or basal PCs, are generated by asymmetric divisions of apical PCs to produce an apical PC and an IPC that migrates to the SVZ (Haubensak et al., 2004; Miyata et al., 2004; Noctor et al., 2004; Attardo et al., 2008; Noctor et al., 2008). IPCs are characterized by a multipolar morphology and basal mitosis away from the ventricle (Haubensak et al., 2004; Miyata et al., 2004; Noctor et al., 2004), and they express a unique set of genes, including *Svet1*, *Tbr2*, and *Cux1/2* (Tarabykin et al., 2001; Nieto et al., 2004; Zimmer et al., 2004; Englund et al., 2005). IPCs can undergo a limited number of symmetric proliferative divisions (1-3) to produce more IPCs, but they mainly undergo symmetric divisions to produce neurons (Haubensak et al., 2004; Miyata et al., 2004; Noctor et al., 2004). IPCs were initially thought to produce specifically upper-layer neurons, as this population undergoes significant expansion from mid-neurogenesis when upper layer neurons are being born, and genes such as *Svet1* and *Cux1/2* that are expressed by IPCs are similarly expressed by upper layer neurons (Tarabykin et al., 2001; Nieto et al., 2004; Zimmer et al., 2004; Bystron et al., 2008). Although IPCs are critical for the production of upper layer neurons, more recent studies have suggested that IPCs make a significant contribution to all cortical layers (Haubensak et al., 2004; Englund et al., 2005; Sessa et al., 2008; Kowalczyk et al., 2009).

Regulation of the type of division made by PCs, and thus the generation of different subtypes of progenitors, is clearly critical for the normal development of the cerebral cortex. Neurogenesis is closely tied to the cell cycle number and cell cycle length; with each cell cycle the length of G1 and the proportion of cells exiting the cell cycle increase (Caviness et al., 1999). Experiments altering the length of the cell cycle suggest that increasing the length of G1 or blocking the progression from G1 to S can promote neurogenesis (reviewed by (Ohnuma and Harris, 2003; Gotz and Huttner, 2005). Many molecules have been identified that influence the decision to proliferate or differentiate, including β-catenin (Chenn and Walsh, 2002), Emx2 (Heins et al., 2001), Hes1 (Ishibashi et al., 1994; Ishibashi et al., 1995), Ngn1 (Sun et al., 2001), Pax6 (Heins et al., 2002), and Sox2 (Graham et al., 2003; Bani-Yaghoub et al., 2006). Less is known about what specifically influences the production of IPCs. Tbr2 has recently been suggested to promote IPC-producing divisions, with inactivation of Tbr2 favoring a shift from these PC-IPC divisions to neurogenic PC-neuron divisions (Arnold et al., 2008; Sessa et al., 2008). Ngn2 has also been shown to promote the generation of IPCs from apical PCs as part of a transcription factor cascade involved in glutamatergic neurogenesis (Miyata et al., 2004; Britz et al., 2006; Hevner, 2006; Kowalczyk et al., 2009). Conversely, stabilized β-catenin expression in neural progenitors expands the RGC population, delaying the maturation of apical PCs into IPCs (Wrobel et al., 2007). However, the precise control of IPC generation is still unclear.

In this study, we examined the role of the transcription factor *tailless* (*tlx*) in progenitor cell regulation in the developing dorsal cortex. *Tlx* is expressed in forebrain PCs from E8, with expression persisting in progenitor populations into adulthood (Monaghan et al., 1995; Shi et al., 2004). Evidence from many systems, including adult neural stem cells, the developing retina, and the embryonic telencephalon, provide evidence for a role for *tlx* in regulating proliferation

(Stenman et al., 2003b; Roy et al., 2004; Shi et al., 2004; Zhang et al., 2006; Sun et al., 2007; Yokoyama et al., 2008; Zhang et al., 2008; Zhao et al., 2009); however, the precise nature of this regulation is unclear. As discussed in Chapter 2, in developing dorsal telencephalon *tlx* is expressed in apical PCs but appears to be downregulated in Tbr2 positive IPCs. Our lab has previously shown that in the absence of *tlx* the depth and surface area of the cortex is reduced as a result of alterations in PC proliferation and neurogenesis during development (Monaghan et al., 1997; Roy et al., 2002; Land and Monaghan, 2003; Roy et al., 2004). Early during neurogenesis (E9.5-E14.5), *tlx* null animals show precocious neurogenesis coupled to a decrease in the length of the cell cycle. At mid neurogenesis, the cell cycle begins to slow down, and by E16.5 the cell cycle has lengthened to become longer than that of PCs in control littermates. PCs in the VZ are significantly depleted in caudal regions from E14.5, but by E18.5 this reduction is no longer apparent. SVZ cells, which were histologically distinguished from E16.5, are significantly reduced at all levels (Roy et al., 2004). This reduction in the SVZ suggests a likely decrease in the IPC population. In this study, we have used new molecular markers for apical PCs and IPCs to more specifically examine changes in these populations in the absence of *tlx*. Our findings show that Tbr2 positive IPCs are reduced throughout development, suggesting a role for *tlx* in the decision to produce IPCs.

Neurons in the cortex are derived from PCs in both the dorsal telencephalon, which gives rise to glutamatergic projection neurons, and the ventral telencephalon, which gives rise to GABAergic interneurons (Marin and Rubenstein, 2001; Rice and Curran, 2001; Schuurmans and Guillemot, 2002). Loss of *tlx* has been shown to affect both dorsal and ventral PCs (Roy et al., 2002; Stenman et al., 2003b; Roy et al., 2004). Furthermore, interneurons derived from ventral PCs migrate through the SVZ and intermediate zone, where they have been shown to

molecularly interact with dorsal PCs (Marin and Rubenstein, 2001; Tiveron et al., 2006). In order to identify the role of *tlx* specifically in dorsal PCs we generated mice with a conditional knockout of *tlx* in the dorsal cortex under the control of Emx1-Cre driven recombination. We observed similar changes in PC number and proliferation in these conditional mutants as in null animals, which suggests that these effects are due to a requirement for *tlx* in dorsal PCs and do not depend on ventral influence.

4.2 METHODS

4.2.1 Animals

Embryos were obtained from crossings of *tlx* flox/flox, *tlx* flox/-, and Emx1-Cre *tlx* +/- animals (Monaghan et al., 1997; Gorski et al., 2002; Belz et al., 2007). Control animals include the genotypes *tlx* +/-, *tlx* flox/+, *tlx* flox/-, Emx1-Cre+ *tlx* +/-, and Emx1-Cre+ *tlx* flox/+. Although a transient intermediate phenotype of premature neurogenesis was observed in *tlx* +/- animals at E9.5, no differences were observed between wild-type and heterozygous animals after E11.5 (Land and Monaghan, 2003; Roy et al., 2004), which suggests the existence of a threshold requirement for *tlx* only during the earliest stages of neurogenesis. Genotyping was performed by PCR as follows: A tail piece was digested in non-ionic detergent and proteinase K (Sigma, 0.3ng/µl) overnight at 56°C. Following heat inactivation at 96°C 50ng of DNA was amplified. Tlx PCR was performed as previously described in Section 2.2.1 (Monaghan et al., 1997). Tlx-flox animals were a gift from G. Schütz (Belz et al., 2007) and were genotyped using the following primers and conditions; LoxP 399: 5'-CCT TGT GCC TCC TCT GTC TC-3', LoxP

401: 5'-TCC TTG CAG TCT CTG GGC-3', LoxP 499: 5'-TTC CCC CTG TTA AAT GCA AG-3'; 94°C for 5 minutes, 40 cycles of 94°C for 30 seconds, 63°C for 30 seconds, and 72°C for 1 minute, followed by 72°C for 10 minutes. PCR products were 181bp for the wild type allele, 312bp for the floxed allele, and 369bp for the recombined floxed allele. Emx1-Cre animals were a gift from K. Jones (Gorski et al., 2002) and were genotyped using the following primers and conditions; Cre 159: 5'-TCG ATG CAA CGA GTG ATG AG-3', Cre 160: 5'-TTC GGC TAT ACG TAA CAG GG-3', OIMR42: 5'-CTA GGC CAC AGA ATT GAA AGA TCT-3', OIMR43: 5'-GTA GGT GGA AAT TCT AGC ATC ATC C-3'; 94°C for 5 minutes, 30 cycles of 94°C for 30 seconds, 60°C for 1 minute, and 72°C for 1 minute, followed by 72°C for 10 minutes. PCR products were 300bp for the control band and 400bp for the Cre allele.

Embryos were collected via caesarian section at embryonic ages from E12.5 to E18.5 and processed for cryosectioning or paraffin sectioning as described in Section 3.2.1. Pregnant dams were injected with 5-bromo-2-deoxyuridine (BrdU) (50µg/g body weight), dissolved in sterile 0.9% NaCl and 0.007M NaOH, 60 minutes prior to embryo harvest. A single injection at 50µg/g body weight results in labeling of 100% of cells in S phase from 15 minutes to two hours following injection, without cell toxicity (Miller and Nowakowski, 1988; Nowakowski et al., 1989; Takahashi et al., 1992).

4.2.2 Immunohistochemistry

Immunohistochemistry on frozen and on paraffin sections was performed as described in Sections 2.2.3 and 3.2.3. Antibodies used were mouse anti-BrdU (1:25; Amersham Biosciences, Piscataway, NJ); rat anti-Ctip2 (1:500; Abcam); rabbit anti-Cux1 (1:500; Santa Cruz Biotechnology, Santa Cruz, CA); mouse anti-GFAP (1:400; Sigma); rabbit anti-Pax6 (1:500;

Covance); rabbit anti-Tbr1 (1:1000; Chemicon); rabbit anti-Tbr2 (1:1000; Chemicon); rabbit anti-Tlx (1:1000; a gift from Y. Shi, (Li et al., 2008)); mouse anti-Tuj1 (1:1000; Sigma).

4.2.3 Cell counts

For quantification of PC number, paraffin sections from caudal regions of the dorsal cortex were stained and imaged as described above. PCs were defined either by lack of expression of neuronal marker Tuj1 (E12.5) or by expression of PC subtype markers Pax6 or Tbr2 (E12.5, E14.5, E18.5). For all analyses a 150μm (E12.5 and E14.5) or 200μm (E18.5) wide region of the dorsal cortex from three non-adjacent sections was counted by an observer blind to genotype. The mean of the three sections per animal was compared between genotypes. For proliferation studies sections were co-labeled with BrdU and the markers described above. The number of PCs and the proportion of PCs that co-label with BrdU (labeling index) were quantified and analyzed as described previously (Roy et al., 2004). Statistical analysis was done using SPSS 14.0 (SPSS Inc., Chicago, IL). Data were compared using an unpaired t-test (E12.5) or by one-way ANOVA followed by Dunnett post-hoc analysis (E14.5, E18.5). All values are expressed as mean ± SEM. Graphs were generated using GraphPad Prism 4 (GraphPad Software, San Diego, CA).

4.3 RESULTS

4.3.1 Functional deletion of *tlx* occurs by E12.5 in *tlx*^{cKO} animals

In the absence of *tlx*, alterations in proliferation and neurogenesis are observed in both dorsal and ventral PCs (Roy et al., 2002; Stenman et al., 2003b; Roy et al., 2004). Cortical neurons derived from both of these PC populations are reduced in *tlx* null animals, as shown by a loss of superficial cortical neurons as well as specific populations of GABAergic neurons (Monaghan et al., 1997; Roy et al., 2002; Land and Monaghan, 2003). Early during neurogenesis (E9.5-E14.5) dorsal PCs show precocious neurogenesis coupled to an increased rate of proliferation. At mid-neurogenesis the rate of proliferation begins to slow down, and by E18.5 has lengthened to become longer than that of PCs in wild type littermates in the caudal VZ and in the SVZ at all rostro-caudal levels. Late PCs (E15.5-birth) become depleted, particularly in the SVZ (Roy et al., 2004). It is unclear whether these changes reflect a role for *tlx* solely in dorsal PCs or whether dorsal PCs are influenced by changes in ventral telencephalon. In order to address this question we generated mice with a conditional knockout of *tlx* in the dorsal cortex. This was achieved by crossing mice with a conditional *tlx* allele in which exon 2 is flanked by loxP sites (Belz et al., 2007; Figure 19A) to the *Emx1-IRES-cre* line, which has been shown to drive recombination in the dorsal pallium from E10.5 (Gorski et al., 2002). Exon 2 of *tlx* encodes part of the zinc-finger DNA-binding domain (Monaghan et al., 1995), and as a result deletion of this exon is expected to prevent the protein from binding to DNA and mediating transcription. When crossed to the R26R reporter strain Emx1-Cre driven recombination is observed in dorsally-derived PCs and projection neurons but not in ventrally-derived cortical interneurons (Gorski et al., 2002). The conditional *tlx* mutant mice used in this study will be referred to as *tlx*^{cKO}.

Tlx is expressed in the dorsal telencephalon from E8 (Monaghan et al., 1995). *Emx1* is expressed from E9.5 (Simeone et al., 1992), while Emx1-Cre driven recombination is observed from E10.5 (Gorski et al., 2002). Therefore in *tlx*^{cKO} animals there will likely be some early expression of *tlx* in the dorsal telencephalon prior to Cre-mediated deletion. In order to determine whether cre-mediated recombination of the floxed *tlx* allele had occurred in embryonic *tlx*^{cKO} brains, we first examined the *tlx* locus using genomic PCR on tissue from the dorsal and ventral telencephalon at E12.5 (Figure 20A); lines in Figure 20B indicate the regions from which tissue samples were collected. Band 2 corresponds to the non-recombined floxed allele, depicted in the upper part of Figure 20A, and is present in every tissue sample. Band 1, which corresponds to the recombined floxed allele, is detected only in the presence of the Emx1-Cre transgene. Samples from the dorsal telencephalon do not show complete recombination at least in part because they also include tissue from outside of the brain. The recombined band corresponding to the floxed allele present in the sample from the ventral telencephalon likely reflects the small areas of recombination observed near the corticostriatal boundary (Gorski et al., 2002) (also see Figure 20C, arrow). In order to verify that Cre-mediated deletion of the *tlx* floxed allele results in the absence of protein, we stained for TLX protein expression in the telencephalon at E12.5 (Figure 20B, C). Staining for TLX reveals that, while TLX expression extends into the dorsal cortex in control animals (Figure 20B), in *tlx*^{cKO} animals TLX expression is restricted to the ventral telencephalon (Figure 20C) (n=3). Patchy expression of TLX is observed at the corticostriatal boundary (arrow, Figure 20C). This TLX antibody was generated against the ligand-binding domain of the protein (Li et al., 2008), and therefore the observed

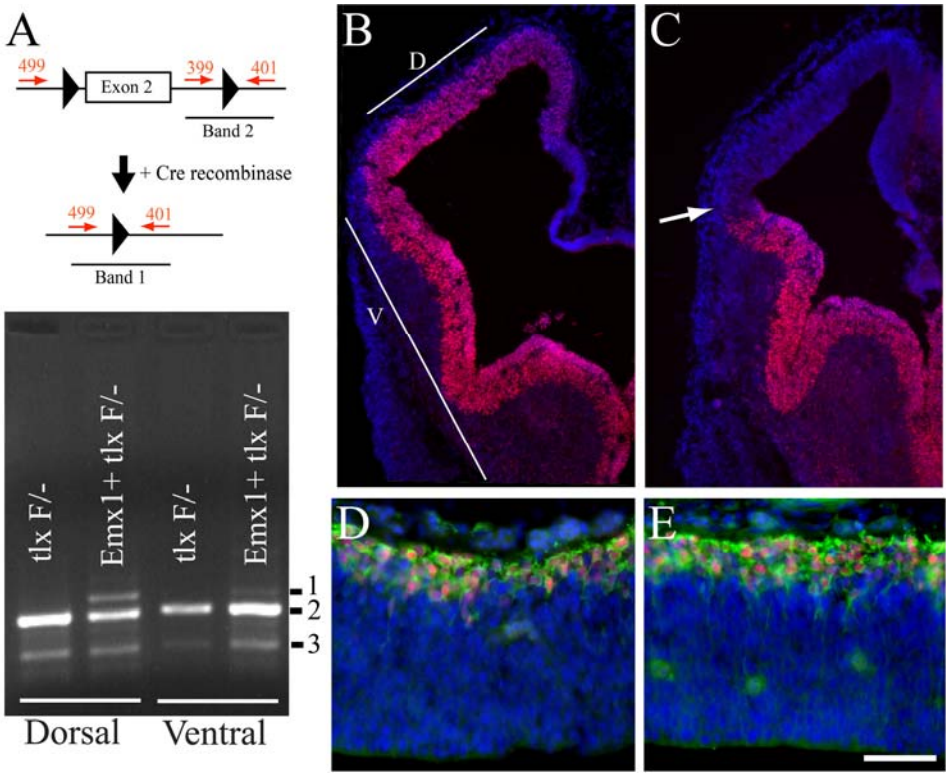

Figure 20. Emx1-Cre mediated recombination of the *tlx* floxed allele occurs by embryonic day 12.5

Cre-mediated recombination of the *tlx* floxed allele results in excision of exon 2, as diagrammed in the upper part of A. Primers used for genomic PCR are indicated in red; triangles indicate loxP sites. Genomic PCR on dorsal and ventral forebrain collected from E12.5 embryos (A, bottom) shows the recombined floxed allele (Band 1) in the telencephalon of tlx^{cKO} (Emx1+ *tlx* F/-) animals but not in that of animals without the Emx1-Cre allele (*tlx* F/- shown here). The band corresponding to the non-recombined floxed allele (Band 2) is present in all samples; Band 3 is a non-specific PCR product. The regions from which dorsal (D) and ventral (V) tissue samples were collected for PCR are indicated in B. Tlx protein expression (red) in the cortex of control (B) and tlx^{cKO} (C) animals at E12.5. Tlx is absent from cells in the dorsal cortex of tlx^{cKO} animals with patchy expression at the corticostriatal boundary (arrow). Staining for neuronal markers Tuj1 (green) and Tbr1 (red) in the dorsal cortex at E12.5 shows an increase in differentiated neurons in tlx^{cKO} animals (E) as compared to controls (D). Sections are counterstained with DAPI (blue). Scale bar (in E) = 200μm in B, C; 50μm in D, E.

absence of TLX protein expression in conditional mutants indicates that Cre-mediated recombination of the floxed allele results in a truncated TLX protein. In addition, the complete deletion of *tlx* apparent in the dorsal telencephalon suggests that *tlx* and Emx1-Cre must show complete overlap in cells in this region.

We have shown that TLX protein is absent from the dorsal telencephalon of tlx^{cKO} animals at E12.5, which suggests that Cre-mediated recombination of the *tlx* allele occurs prior to this age. To determine whether functional recombination of *tlx* has occurred by E12.5 we stained for the neuronal markers Tuj1 and Tbr1. Complete deletion of *tlx* results in an early increase in the size of the preplate that is apparent at E12.5 (Roy et al., 2004). We observed a similar increase in differentiated neurons in the preplate in tlx^{cKO} animals as compared to controls (Figure 20D, E) (n=2); whereas the preplate in controls generally contained two to three layers of cells, the preplate in tlx^{cKO} animals contained three to four layers of cells with more Tuj1-positive cells apparent in the VZ. This finding indicates that functional recombination of the *tlx* floxed allele has occurred in the dorsal telencephalon prior to E12.5, early enough in tlx^{cKO} animals to show a phenotype by this age.

4.3.2 *Tlx* expression in dorsal progenitor cells regulates progenitor cell dynamics

In *tlx* null animals, total PCs are decreased from E12.5 in intermediate and caudal regions, coupled to an increase in the rate of the cell cycle (Roy et al., 2004). To determine whether this is the result of the absence of *tlx* specifically from dorsal PCs, we counted the number of PCs in tlx^{cKO} and control brains at E12.5. These and all subsequent counts were done in caudal regions of the dorsal cortex, which have been shown to be most sensitive to the loss of *tlx* (Roy et al., 2004). At this age total PCs were identified as DAPI-stained cells that do not label with the pan-

neuronal marker Tuj1 (Figure 21A, B). Total PCs were reduced in number by 12% in *tlx*^{cKO} animals (283.1 ± 12.4 in controls versus 250.2 ± 2.3 in *tlx*^{cKO} animals, n=5, $p<0.05$; Figure 21C), similar to the 12% reduction in caudal PCs previously reported for *tlx* null animals (Roy et al., 2004). Previous studies identified a significant reduction in cells in the SVZ from E16.5 (Roy et al., 2004), which suggests a particular deficit in the production of intermediate progenitor cells (IPCs). With the molecular markers now available we were able to examine this population much earlier during development. At E12.5, Tbr2 expression labels IPCs as well as a subset of preplate neurons (Figure 21D, E) (Bulfone et al., 1999; Englund et al., 2005). Tbr2-positive cells are reduced by 35% in *tlx*^{cKO} animals as compared to controls (80.2 ± 10.3 in controls versus 52.1 ± 2.3 in *tlx*^{cKO} animals, n=4, $p<0.05$; Figure 21C). Given that the preplate has been shown to be increased in the absence of *tlx*, this reduction is likely due to a decrease in IPCs; this conclusion is supported by comparing the absolute reduction of total PCs and Tbr2-positive cells, both approximately 30 cells. However, to directly test the hypothesis that apical PCs are not altered at E12.5 we counted Tbr2-negative PCs as an approximation of the apical PC population. Although the Tbr2-negative population showed a slight reduction in number, the difference was not significant (230.5 ± 6.8 in controls versus 216.3 ± 7.3 in *tlx*^{cKO} animals, n=4, $p=0.20$; Figure 21C). These results therefore suggest that at E12.5 Tbr2-positive IPCs are significantly reduced in the *tlx*^{cKO} dorsal telencephalon while apical PCs are unaffected.

Changes in the size of the PC population could result from changes in proliferation, differentiation, or cell death. Previous studies have associated this reduction in the PC population with an early increase in neurogenesis and in the rate of proliferation (Roy et al., 2004). To determine whether PCs in *tlx*^{cKO} animals show changes in proliferation, timed-pregnant dams were given short-term injections of BrdU, a thymidine analog that is incorporated

into cells in S phase (Miller and Nowakowski, 1988; Nowakowski et al., 1989; Takahashi et al., 1992). This was used to determine the proportion of cells in S-phase during the labeling period (defined as the labeling index, LI). No significant difference in the LI of total PCs was observed at E12.5 in *tlx*^{cKO} animals as compared to controls (n=5, p=0.40; Figure 21F). Previous studies have found no changes in cell death in *tlx* null animals (Roy et al., 2004; Li et al., 2008); therefore, although cell death was not examined in *tlx*^{cKO} animals, we propose that it is unlikely

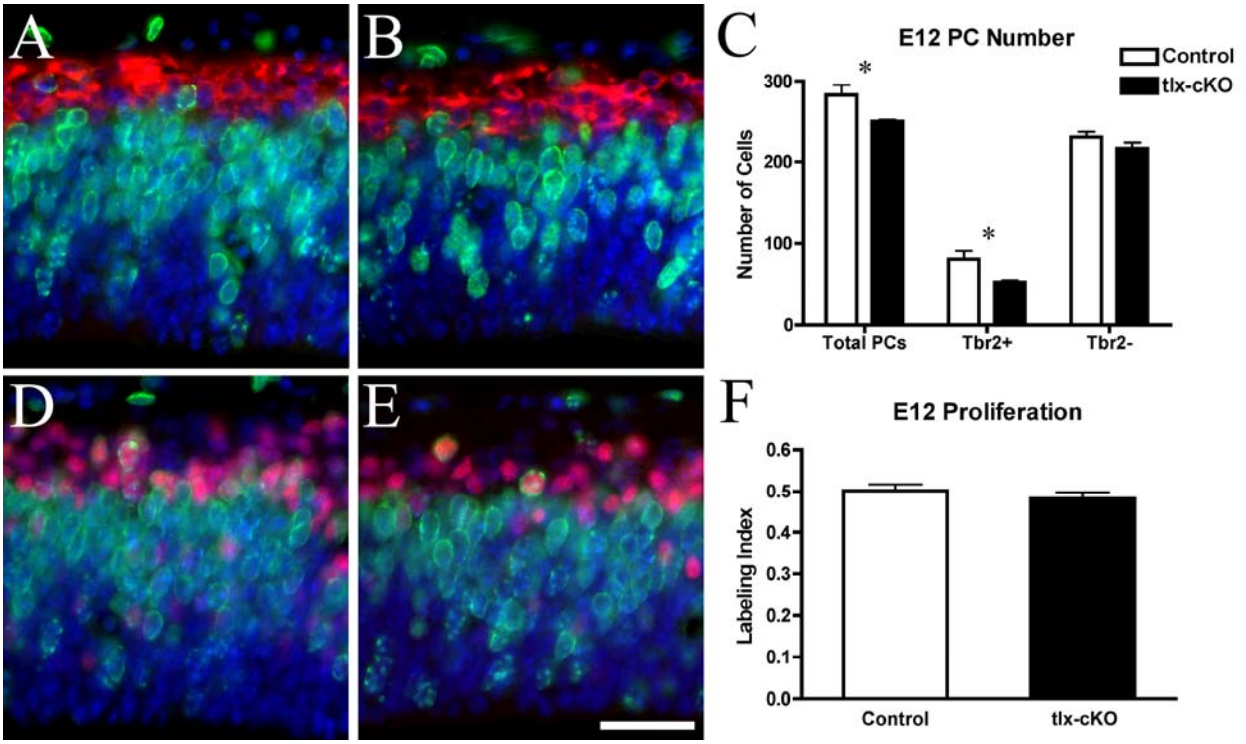

Figure 21. Progenitor cells are decreased in *tlx*^{cKO} animals at E12.5

Sections through control (A, D) or *tlx*^{cKO} (B, E) brains at E12.5 show staining for BrdU (green) to label proliferating cells and either Tuj1 (red, A, B) to label cortical neurons or Tbr2 (red, D, E) to label intermediate progenitor cells and a subset of preplate neurons. Both total progenitor cells (Tuj1-negative) and Tbr2-positive cells are significantly decreased in number at E12.5 (C). The labeling index of total progenitor cells is not altered in *tlx*^{cKO} animals as compared to controls (F). Sections are counterstained with DAPI (blue). *$p<0.05$. Scale bar (in E) = 30μm.

to be altered. Hence, we propose that the observed reduction in Tbr2 positive cells, coupled with the increase in differentiated neurons, is due to a change in differentiation; we hypothesize that at this age neurogenic divisions are being made at the expense of IPC-producing divisions.

In *tlx* null animals the PC population continues to be depleted as the brain develops, with the reduction in total PC number even greater by E14.5. Previous studies of PC number and proliferation did not differentiate between the VZ and SVZ until E16.5, as these populations can be difficult to distinguish earlier using histological methods due to mixing of these populations at the boundary (Takahashi et al., 1995a). Furthermore, the SVZ is a mixed population, containing migrating excitatory and inhibitory interneurons in addition to IPCs (Marin and Rubenstein, 2001; Tarabykin et al., 2001; Haubensak et al., 2004; Noctor et al., 2004; Bystron et al., 2008). Therefore, we used molecular markers to specifically identify apical PCs and IPCs in both tlx^{cKO} and *tlx* null animals as compared to controls. Apical PCs can be identified using the marker Pax6 (Figure 22A-C) (Gotz et al., 1998), and by E14.5 IPCs can be identified using the marker Tbr2 (Figure 22E-G) (Englund et al., 2005). Neither Pax6-positive cell number nor Tbr2-positive cell number showed a significant effect of genotype as determined by one-way ANOVA (Pax6: $F_{2,6}$=2.43, p=0.17, n=3; Tbr2: $F_{2,6}$=1.31, p=0.34, n=3; Figure 22D). The n of three may be too low to see a significant effect, as there appears to be a trend towards a decrease in Tbr2-positive cells in both conditionals and nulls (control: 150.0 ± 9.5; tlx^{cKO}: 126.0 ± 8.6; null: 132.0 ± 13.9). Proliferation was examined by determining the LI, as previously described. No difference in LI was observed for either Pax6-positive or Tbr2-positive cells (Pax6: $F_{2,6}$=1.49, p=0.30, n=3; Tbr2: $F_{2,6}$=1.86, p=0.23, n=3; Figure 22H).

At E18.5 reductions in cell number are observed in the SVZ of *tlx* null animals at all rostrocaudal levels, while changes in VZ cell number are only observed at intermediate levels

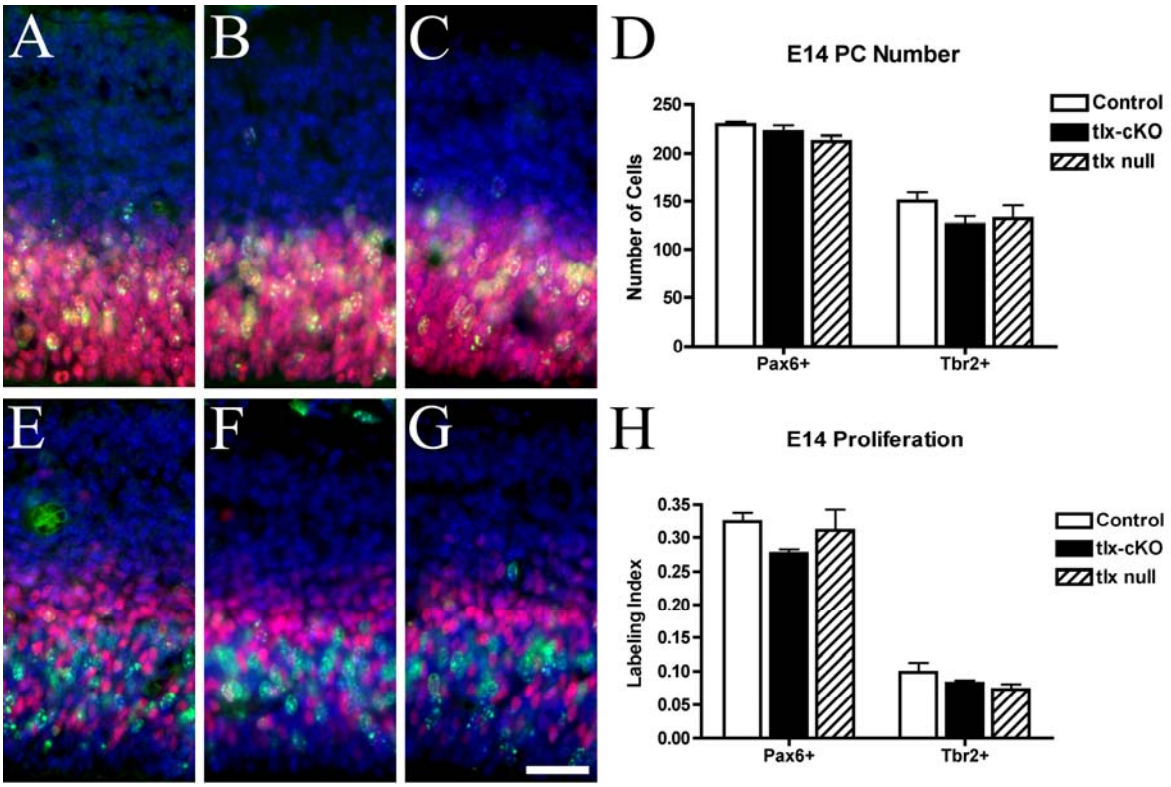

Figure 22. Progenitor cells at E14.5

Sections through control (A, E), *tlx*^{cKO} (B, F), and *tlx* null (C, G) brains at E14.5 show staining for BrdU (green) to label proliferating cells and either Pax (red, A-C) to label ventricular zone progenitors or Tbr2 (red, E-G) to label intermediate progenitors. No significant differences by genotype were observed either for number of Pax6- or Tbr2-positive cells (D) or labeling index (H). Sections are counterstained with DAPI (blue). Scale bar (in G) = 30μm.

(Roy et al., 2004); this is consistent with our observations at E12.5 and E14.5 that Tbr2 positive IPCs seem to be specifically affected in the absence of *tlx*. Interestingly, in *tlx* null animals the rate of proliferation, which is increased early, slows down such that by E18.5 cells in the caudal VZ and all regions of the SVZ are cycling more slowly than those of control littermates (Roy et al., 2004). We examined PC number and proliferation at E18.5 in the dorsal cortex of both *tlx*^{cKO} and *tlx* null animals using Pax6 as a marker for apical PCs (Figure 23A-C) and Tbr2 as a marker for IPCs (Figure 23E-G). No significant difference by genotype was observed for the total

number of Pax6-positive cells ($F_{2,9}$=1.673, p=0.24, n=4; Figure 23D). However Tbr2-positive IPCs did show a significant effect of genotype ($F_{2,9}$=8.15, p<0.01, n=4; Figure 23D). Post-hoc analysis identified a significant 32% decrease in Tbr2-positive cells in *tlx* null brains as compared to controls (p<0.01, n=4), whereas the 18% decrease in tlx^{cKO} brains as compared to controls is not quite significant (p=0.09, n=4) (control: 40.4 ± 3.1; tlx^{cKO}: 33.2 ± 2.0; null: 27.4 ± 1.3). Although Pax6-positive cells did not differ in cell number, a significant effect of genotype was observed for the LI ($F_{2,9}$=7.70, p<0.05, n=4; Figure 23H). Post-hoc analysis showed a significant 29% decrease in the LI of Pax6-positive cells in tlx^{cKO} animals as compared to controls (p<0.01, n=4) and a 21% decrease in *tlx* null animals as compared to controls (p<0.05, n=4) (control: 0.21 ± 0.01; tlx^{cKO}: 0.15 ± 0.01; null: 0.16 ± 0.01).

Overall these studies indicate that tlx^{cKO} and *tlx* null animals show similar changes in PC number and proliferation during development, which suggests that these effects are due to a requirement for *tlx* in dorsal PCs. This study used molecular markers to specifically identify and characterize apical PCs and IPCs. To summarize, total PCs are reduced at E12.5 in tlx^{cKO} animals as compared to controls, similar to the decrease previously reported for *tlx* null animals. At later ages no difference in the cell number of Pax6-positive apical PCs was observed, while Tbr2-positive IPCs seem to be reduced throughout development. A significant decrease in LI was observed in Pax6-positive cells at E18.5 for both tlx^{cKO} and *tlx* null animals as compared to controls, suggesting that the cell cycle of apical PCs is longer. Together with the finding that *tlx* is not coexpressed with Tbr2 (see Chapter 2), these results suggest that *tlx* has a role in dorsal VZ PCs in promoting divisions that produce IPCs.

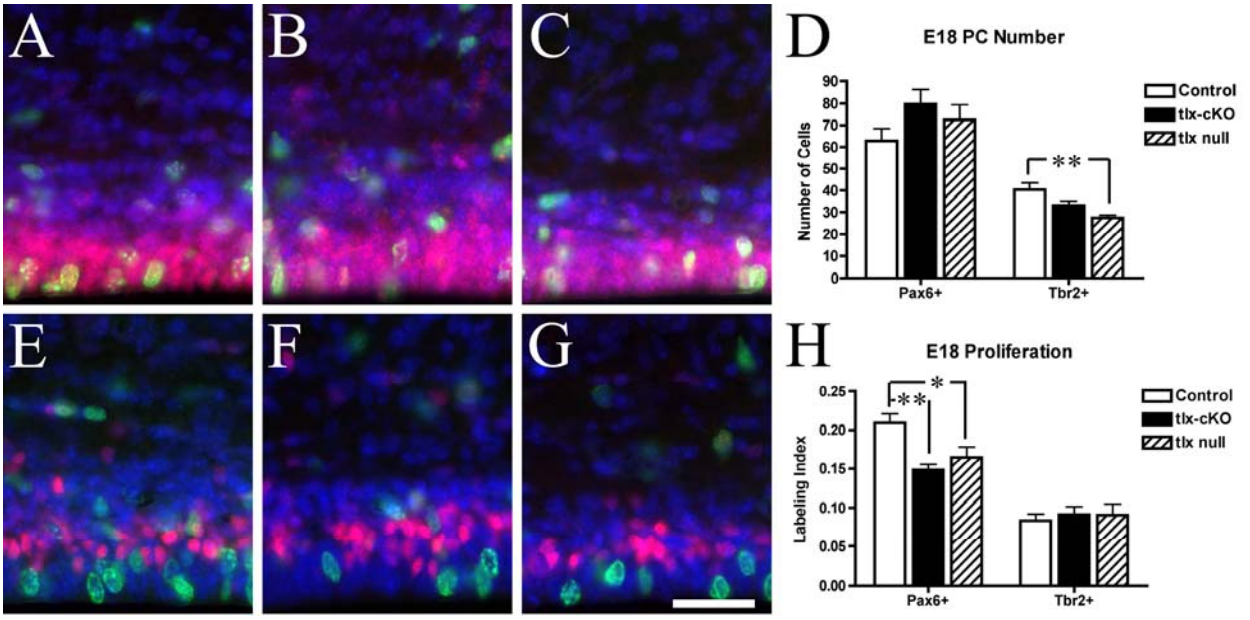

Figure 23. Progenitor cells at E18.5

Sections through control (A, E), *tlx*^{cKO} (B, F), and *tlx* null (C, G) brains at E18.5 show staining for BrdU (green) to label proliferating cells and either Pax (red, A-C) to label ventricular zone progenitors or Tbr2 (red, E-G) to label intermediate progenitors. Although no difference was observed in number of Pax6-positive cells, Tbr2-positive cells were significantly reduced in *tlx* null animals as compared to controls (D). The labeling index of Pax6-positive cells was significantly decreased in both *tlx*^{cKO} and *tlx* null animals as compared to controls (H). No significant differences were observed in the labeling index of Tbr2-positive cells. Sections are counterstained with DAPI (blue). * $p<0.05$; ** $p<0.01$. Scale bar (in G) = 30μm.

4.3.3 Deletion of *tlx* from dorsal progenitors results in decreased cortical thickness by birth

The reduction in the number of IPCs observed in both *tlx*^{cKO} and *tlx* null animals led us to hypothesize that the cortical plate would be reduced in size, with superficial layers specifically affected. Indeed, it has previously been shown that, although lamination in the cortical plate of *tlx* null animals appears to be normal, the cortex is decreased in thickness at all rostrocaudal

levels from E16.5 with superficial layers specifically affected (Roy et al., 2002; Land and Monaghan, 2003; Roy et al., 2004). However a reduction in ventrally-derived interneurons could contribute to this decrease. To determine the role of *tlx* specifically in dorsal PCs in the formation of the cortical plate, we examined cortical thickness and lamination of both tlx^{cKO} and *tlx* null animals at E18.5 using several layer-specific markers (Figure 24). The transcription factor Tbr1 is strongly expressed by glutamatergic cells in the subplate and layer VI of the cerebral cortex (Figure 24A-C) (Bulfone et al., 1995; Hevner et al., 2003; Kolk et al., 2005). Ctip2 is a C_2H_2 zinc finger protein highly expressed by a subset of cells in layer V (Figure 24A-C) (Avram et al., 2000; Arlotta et al., 2005). No difference was observed in the expression pattern of these genes, and these layers appear similar in size in both tlx^{cKO} and null animals as compared to controls (Figure 24A-C; n=3), which indicates that deep layers are appropriately specified. We examined superficial layers using immunostaining against the transcription factor Cux1, which at E18.5 is expressed by cells in upper cortical layers II/III and IV as well as cells in the intermediate zone and proliferative region (Figure 24D-F) (Nieto et al., 2004; Zimmer et al., 2004). The position of Cux1-positive cells is similar across all genotypes, which indicates that superficial layers are appropriately specified (Figure 24D-F; n=3). However, superficial layers appear reduced in size in both tlx^{cKO} and null animals as compared to controls. Therefore, as predicted, the cortex is reduced in thickness at E18.5 in both conditional and null mutants, with superficial layers specifically affected.

As PCs mature they produce cells in a specific order, first deep layer neurons, then upper layer neurons, and finally astrocytes (Bayer and Altman, 1991). At the end of neurogenesis near birth, as PCs transition into the production of glia, we observed co-expression of *tlx* with markers of glia (Chapter 2), which suggests a possible role in gliogenesis. Furthermore, we have shown

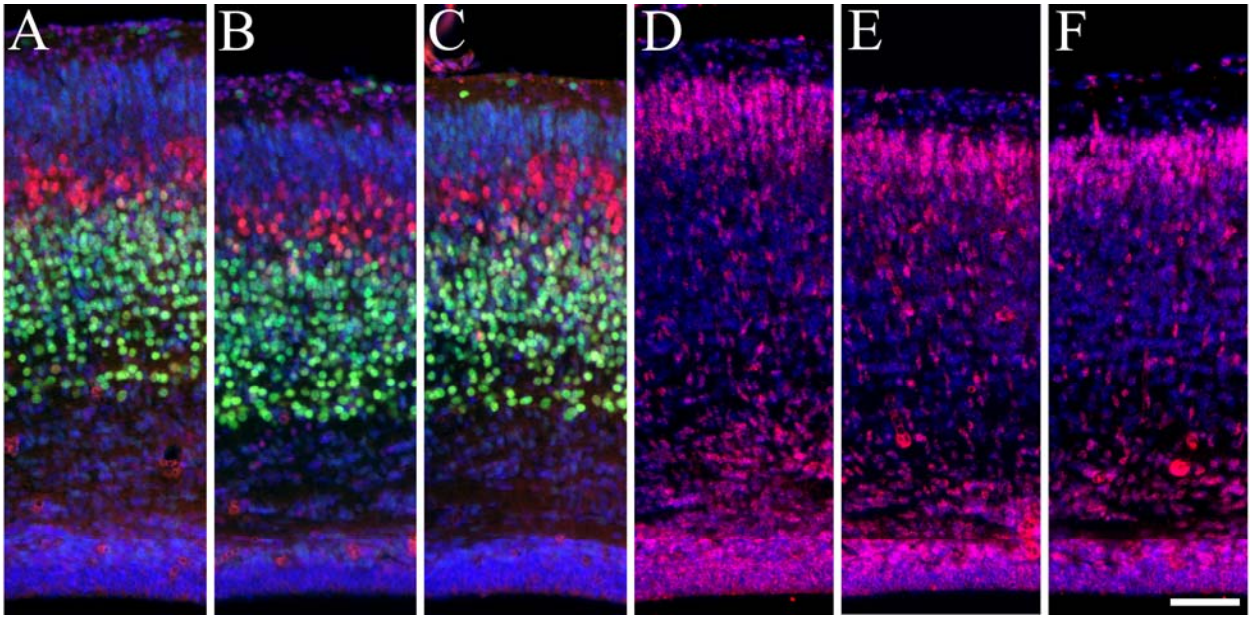

Figure 24. Cortical thickness and lamination at E18.5

At E18.5 the thickness of the cerebral wall is similarly reduced in both *tlx*^{cKO} (B, E) and *tlx* null (C, F) animals as compared to controls (A, D). Deep layers, as shown by Tbr1 (green, A-C) staining of subplate and layer VI cells and Ctip2 (red, A-C) staining of layer V cells, appear similar in size for all genotypes. Superficial layers, as shown by Cux1 (red, D-F) staining for superficial layers II/III and IV, is reduced in size in both *tlx*^{cKO} and *tlx* null brains as compared to controls. Sections are counterstained with DAPI (blue). Scale bar (in F) = 50μm.

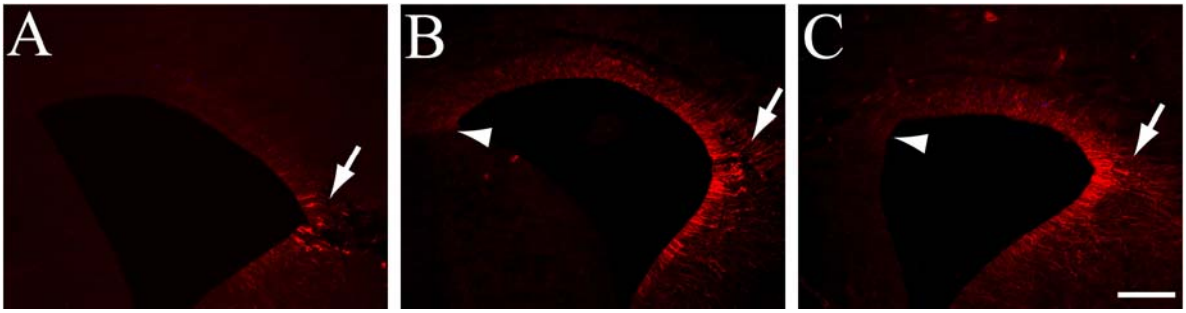

Figure 25. GFAP is prematurely expressed in the cortex in the absence of *tlx*

In controls animals at E18.5 GFAP expression (red) is only detected in midline glia (arrow). In both *tlx*^{cKO} (B) and *tlx* null (C) animals GFAP expression is detected throughout the ventricular zone of the dorsal cortex (lateral extent of expression marked by arrowhead). Scale bar (in C) = 100μm.

here that at E18.5 the cell cycle is increased in apical PCs in both *tlx*^{cKO} and *tlx* null animals, which indicates that the PCs that produce astrocytes are in some way altered in the absence of *tlx*. It has previously been shown that astrocytes are increased in the subventricular zone and the dentate gyrus of adult *tlx* null animals (Shi et al., 2004). Results from our lab show that this effect is of developmental origin, as in the absence of *tlx*, radial glia prematurely express mature glial markers and a significant increase in astrocytes is apparent from as early as postnatal day 2 (Kuznicki and Monaghan, unpublished results). In order to determine whether this is due to a role for *tlx* in dorsal progenitors, we examined the expression of the astrocyte marker glial fibrillary acidic protein (GFAP) at E18.5. Whereas GFAP expression is restricted to midline glia in controls (Figure 25A, arrow), GFAP is expressed by radial glia in the dorsal VZ in both *tlx*^{cKO} and *tlx* null brains, extending across to the corticostriatal boundary (Figure 25B, C, arrowheads) (control, *tlx*^{cKO} n=3; null, n=2). This finding suggests that the premature activation of GFAP in radial glia is due to the absence of TLX from dorsal PCs.

4.4 DISCUSSION

The formation of the mature cerebral cortex requires precise control of generation and proliferation of different subtypes of neural progenitor cells (PCs). In the absence of *tlx* changes in both dorsal and ventral PC number and proliferation during development lead to reductions in adult structures including the cerebral cortex and hippocampus (Monaghan et al., 1997; Roy et al., 2002; Land and Monaghan, 2003; Stenman et al., 2003b; Roy et al., 2004). In this study we have shown that absence of *tlx* specifically from dorsal PCs results in a reduction in total PC number at E12.5, with Tbr2-positive intermediate progenitor cells (IPCs) reduced throughout

embryonic development. Proliferation of Tbr2-positive cells was not altered in the absence of *tlx*, although a significant decrease in LI was observed in Pax6-positive cells at E18.5 in tlx^{cKO} and *tlx* null animals as compared to controls. By E18.5, these changes in PC dynamics have resulted in a reduction in the thickness of the cortical plate, specifically superficial layers. Together with the finding that *tlx* is not coexpressed with Tbr2 (see Chapter 2), this outcome suggests that *tlx* has a role in dorsal apical PCs in the decision to produce IPCs and in the normal development of the cerebral cortex.

At all ages examined, similar changes in PC number and proliferation were observed in both tlx^{cKO} and *tlx* null animals. Animals of both genotypes furthermore showed a reduction in cortical thickness by E18.5 as compared to controls, with superficial cortical layers specifically affected, and premature expression of astrocyte marker GFAP. This suggests a requirement for *tlx* expression specifically in dorsal PCs, and further indicates that ventrally-derived cells do not have a significant impact on PC dynamics during embryogenesis in *tlx* null animals. Specific changes in cell number and proliferation have previously been described in *tlx* null animals throughout development (Roy et al., 2004). Unlike this previous study, which histologically identified the VZ and from E16.5 the SVZ, we used the molecular markers Pax6 and Tbr2 to specifically identify apical PC and IPC populations, respectively. This is an important difference because, in addition to IPCs, the SVZ also contains radially migrating glutamatergic neurons and tangentially migrating interneurons (Marin and Rubenstein, 2001; Tarabykin et al., 2001; Haubensak et al., 2004; Noctor et al., 2004; Bystron et al., 2008). Furthermore, recent evidence has shown that some Tbr2-positive IPCs are located within the VZ (Englund et al., 2005; Noctor et al., 2008; Kowalczyk et al., 2009). However, despite these differences, similar changes in PC number were observed for each study. At E12.5 we identified a 12% reduction in total PCs in

tlx^{cKO} animals, similar to the 12% reduction previously reported in *tlx* null animals (Roy et al., 2004). We found that this reduction is due at least in part to a significant reduction in Tbr2-positive IPCs. By E14.5 Tbr2-positive cells seem to be reduced while Pax6-positive apical PCs are unaffected, although increasing the N and confirming these findings by examining the late G_2-M phase marker phosphohistone H3 (Zeitlin et al., 2001) will help to elucidate these results. A 23% decrease in the number of cells in the VZ at E14.5 was previously reported in nulls, although at this age the SVZ was not separately quantified (Roy et al., 2004). At E18.5 we identified a significant decrease in the Tbr2-positive population (18% in conditional animals, 32% in null animals, as compared to controls), with no change in apical Pax6 positive progenitors. This result again matches the previously reported 21% decrease in the SVZ of *tlx* null animals at E18.5 (Roy et al., 2004).

Our findings differ from those previously reported with respect to proliferation, as determined by the labeling index (LI). The LI can be affected due to changes in either the rate of the cell cycle or in the number of cells that are cycling. The LI was previously shown to be significantly increased in the caudal VZ at E12.5 and E14.5 in *tlx* null animals as compared to controls, but significantly decreased in both the VZ and SVZ by E18.5 (Roy et al., 2004). This was interpreted to indicate that the cell cycle is faster during early neurogenesis but slows to become slower than that of control PCs by E16.5. We observed a significant decrease in the LI of Pax6 positive cells at E18.5, with no change in the LI of Tbr2 positive cells. No significant changes were observed at any other age. At early stages, differences between our results for conditional anumals and previously reported changes in the LI for nulls could be due to the fact that *tlx* is not knocked out quite as early in conditionals. Early expression of *tlx* in *tlx*^{cKO} animals might therefore result in a less robust phenotype. In support of this hypothesis, the early increase

in neurogenesis does not seem as dramatic in conditional mutants as in *tlx* null mutants. At E14.5 our data show a trend towards a decrease in the LI in both populations. A recent study from another group found a similar decrease in the LI of total PCs at E14.5 (Li et al., 2008), supporting our current results. This second study identified PCs using the proliferative marker Ki67, whereas Roy and colleagues identified the proliferative region histologically (Roy et al., 2004). The total cell counts used by Roy and colleagues to calculate the LI at E14.5 could therefore have included migrating neurons and interneurons. A decrease in migrating interneurons in *tlx* null brains could decrease the total cell count, resulting in an increase in the calculated LI. Overall, the increased length of the cell cycle in apical PCs later during neurogenesis in *tlx* mutants, together with the premature expression of GFAP at E18.5, suggests that in the absence of *tlx* PCs mature faster.

Tlx is expressed in apical Pax6-positive PCs but not Tbr2-positive IPCs (see Chapter 2), but in the absence of *tlx* the most significant effect is the reduction of IPCs throughout development. We therefore propose that *tlx* has an important role during development in determining the type of division made by apical PCs, in particular promoting divisions that produce IPCs. Early during development, we have shown that neurons are increased, IPCs are reduced, and apical PCs are unaffected in both number and rate of the cell cycle. Based on these findings we propose that early during neurogenesis *tlx* acts to promote the production of IPCs (Figure 26). It has been shown that knocking out the transcription factor Tbr2 results in a phenotype strikingly similar to that observed in *tlx* mutants. Inactivation of Tbr2 has been suggested to favor a shift from IPC-producing divisions to neurogenic divisions, resulting in an early increase in neurogenesis followed by a later decrease in neuronal production due to the reduced number of proliferative IPCs (Arnold et al., 2008; Sessa et al., 2008). The cortex in

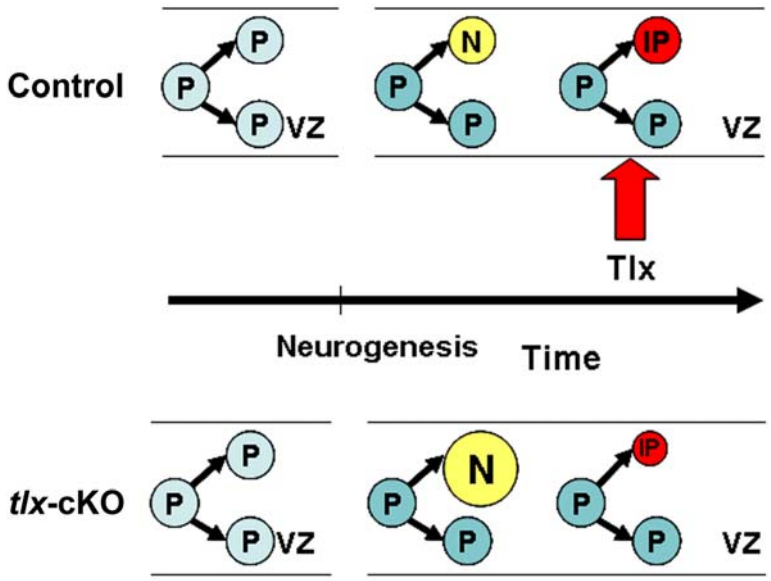

Figure 26. *Tlx* promotes the production of IPCs early during development

Early during neurogenesis in tlx^{cKO} animals neurons (N) are increased, intermediate progenitor cells (IP) are reduced, and radial glia progenitors (P) are unaffected in cell number and proliferation. We propose that *tlx* has a role in promoting the production of intermediate progenitor cells, and in the absence of *tlx* neurons are produced at the expense of intermediate progenitors.

Tbr2 mutants is reduced in surface area and thickness, with a specific reduction in superficial cortical layers although in one study reductions were also seen in deep layers (Arnold et al., 2008; Sessa et al., 2008). The olfactory bulbs, commissures, and dentate gyrus are reduced, and adult animals exhibit severe aggression and hyperactivity (Arnold et al., 2008). These findings support the hypothesis that much of the phenotype observed in the absence of *tlx* could be explained by a role in promoting divisions that produce IPCs. We plan to test this hypothesis using 24 hour BrdU injections to examine PC divisions at E14.5. Li and colleagues examined cell cycle exit using a similar method, injecting BrdU on E14.5 and quantifying cell cycle exit 24 hours later on E15.5, and observed a decrease in the proportion of PCs that re-entered the cell cycle in *tlx* null animals (Li et al., 2008). However, they quantified total PCs rather than PC

subtypes, so their results could either indicate that fewer cells are re-entering the cell cycle as apical PCs, or that fewer IPCs are being generated. We hypothesize that in the absence of *tlx* a greater proportion of PCs will produce neurons (Tuj1-positive cells) at the expense of producing IPCs (Tbr2-positive cells).

By the end of neurogenesis (E18.5) the number of apical radial glia PCs is still unaffected, whereas both IPCs and neurons are reduced. This could reflect a continued role for *tlx* in promoting divisions that produce IPCs over those that produce neurons directly (Figure 27). However, we have also shown that at this age apical PCs cycle more slowly. This would

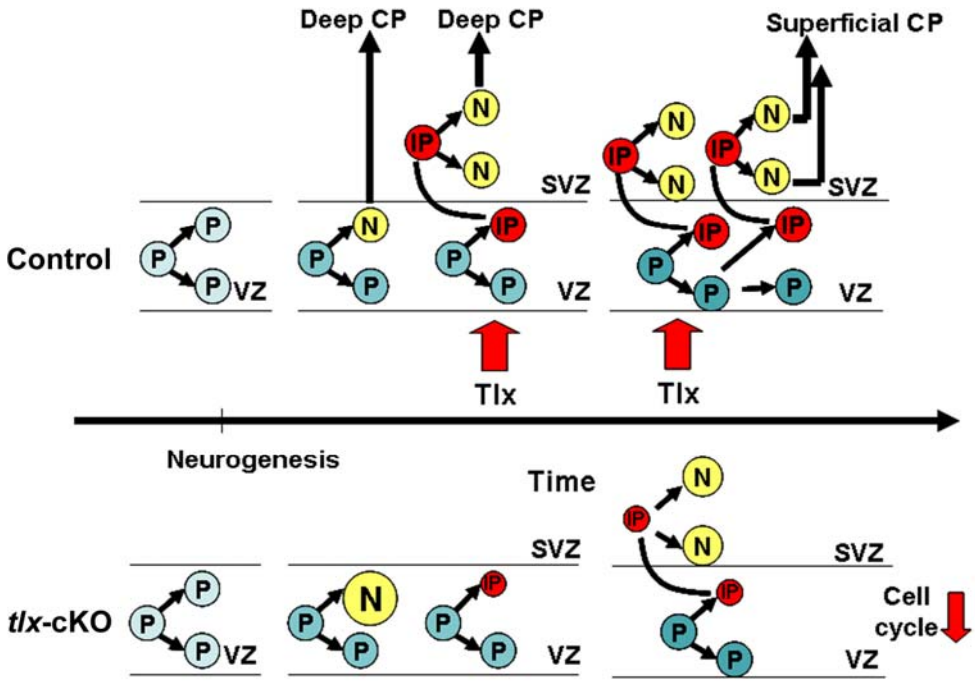

Figure 27. *Tlx* promotes the production of IPCs throughout neurogenesis

During late neurogenesis in *tlx*^{cKO} animals, intermediate progenitor cells (IP) and neurons (N) are decreased while apical radial glia progenitors (P) are unaffected in number. In addition at this later stage radial glia progenitors cycle more slowly. We propose that *tlx* has a role during late neurogenesis in promoting the production of intermediate progenitors, as described during early neurogenesis. This is likely due to a role in both influencing cell division type and, either directly or indirectly, regulating proliferation.

also contribute to decreased production of both IPCs and neurons, because a progenitor cycling more slowly would divide fewer times and produce fewer progeny. It is not clear whether this change in the cell cycle is due to a direct role for *tlx* or is a secondary effect of early changes in PCs. Regardless, our data indicate that there is an important role for *tlx* in the production of IPCs throughout development (Figure 27).

How might *tlx* influence PC divisions? *Tlx* has been shown in the retina and cortex to regulate proliferation through the transcriptional repression of cell-cycle proteins, including cyclin-dependent kinase inhibitors p21 and $p27^{Kip1}$, and the tumor suppressor gene Pten (Miyawaki et al., 2004; Zhang et al., 2006; Sun et al., 2007; Li et al., 2008; Yokoyama et al., 2008; Zhang et al., 2008). These proteins negatively regulate stem cell proliferation in part through the repression of downstream targets such as CyclinD1, which is important for the G1 to S transition of the cell cycle (Sherr and Roberts, 1995). In *tlx* null animals these negative cell cycle regulators are upregulated, and CyclinD1 is decreased (Miyawaki et al., 2004; Zhang et al., 2006; Sun et al., 2007; Li et al., 2008; Yokoyama et al., 2008; Zhang et al., 2008). Repression by TLX is mediated by interactions through its ligand-binding domain with co-repressors, such as atrophin1, histone deacetylases (HDAC3 and HDAC5), and the histone demethylase LSD1 (Zhang et al., 2006; Sun et al., 2007; Yokoyama et al., 2008). An increase in p21 expression has been shown to correlate with exit from the cell cycle during cortical development (Siegenthaler and Miller, 2005). *Foxg1* haploinsufficient mice exhibit a decrease in the production of Tbr2-positive IPCs that is associated with an increase in the expression of p21 predominantly in the VZ (Siegenthaler et al., 2008). The number of apical PCs is unaffected, leading the authors to conclude that p21 expression promotes neurogenic divisions at the expense of IPC-producing divisions. These results suggest that repression of p21 by TLX in apical PCs is one potential

mechanism by which TLX could promote the production of IPCs. Repression by TLX of $p27^{Kip1}$, which is also known to promote cell cycle exit (Caviness et al., 2003; Tarui et al., 2005), could be a factor as well.

In addition to an important role in the production of IPCs *tlx* appears to have an additional role in delaying the maturation of RGCs, as evidenced by the premature expression of glial markers in the absence of *tlx*. This premature gene expression is coupled to an increase in the length of the cell cycle in apical RGCs at E18.5. It is unclear whether this later phenotype is due to a direct role for *tlx* or a secondary effect due to an altered environment. *Tlx* has been shown in the retina to directly regulate astrogenesis (Miyawaki et al., 2004; Uemura et al., 2006), which suggests that *tlx* may have a similar function in regulating astrogenesis in the embryonic cortex. Although *tlx* has been shown to suppress transcription of glial genes such as *GFAP* in adult neural stem cells, the observed coexpression of *tlx* with these same glial markers (Chapter 2) suggests that *tlx* may prevent premature gliogenesis through other mechanisms. Ngn1, which promotes neurogenesis through its function as a transcriptional activator, has been shown to repress gliogenesis by binding and sequestering p300/CBP, a complex necessary for the transcription of gliogenic genes, and by suppressing the JAK-STAT glial signaling pathway (Sun et al., 2001). *Tlx* could similarly have a dual role, perhaps preventing gliogenesis through an as of yet unidentified mechanism apart from its role as a transcriptional repressor.

Here we have identified *tlx* as an important regulator of the production of intermediate progenitor cells as well as the maturation of RGCs in the dorsal telencephalon. Although *tlx* is not coexpressed with IPC marker Tbr2, Tbr2-positive cells are significantly reduced from E12.5. We propose that during development *tlx* acts in apical PCs through regulation of cell cycle

proteins to promote divisions that produce IPCs, thus indirectly regulating the number of neurons in the cerebral cortex.

5.0 TLX EXPRESSION IN DORSAL PROGENITORS IS REQUIRED FOR THE DEVELOPMENT OF DORSALLY DERIVED STRUCTURES AND FOR THE NORMAL EXPRESSION OF ANXIETY

5.1 INTRODUCTION

Alterations in brain development leading to abnormalities in brain structure, connections, and function have been associated with a wide variety of neuropsychiatric disorders, including schizophrenia, autism, and mood disorders such as anxiety and depression (Holmes et al., 2003a; Levitt et al., 2004; Chen et al., 2006a; Chen et al., 2006b; Clapcote et al., 2007; Courchesne et al., 2007; Geschwind and Levitt, 2007; Serene et al., 2007; Chubb et al., 2008; Tseng et al., 2008a). Although modeling symptoms of these and other disorders in rodents have identified many structures and neurotransmitter systems that are involved in specific behaviors, the precise mechanisms underlying the development of behavior are still unclear. Many of the studies identifying brain regions involved in behavior have either used lesions, which can disrupt not only the targeted cells but fibers that pass through the area or other connected cells due to the indirect effects of cell death, or localized drug injection (Moser and Moser, 1998; Bannerman et al., 2004b; Sheehan et al., 2004). Importantly, such perturbations in a fully developed adult animal may not entirely reflect the developmental mechanisms that underlie pathological behavior.

In order to examine how subtle changes during development can lead to the deficits in specific brain structures and behaviors, we focused on the role of the nuclear receptor *tlx* (*Nr2e1*). Disruption of the *tlx* locus in mice results in a broad array of both anatomical and behavioral deficits reflecting the critical role for *tlx* in the development of adult brain structures derived from these regions. In the absence of *tlx*, alterations in progenitor cell proliferation and neurogenesis during development results in a reduction in the surface area and thickness of the cerebral hemispheres, with the 20% reduction in thickness due to a specific reduction in superficial cortical layers (Monaghan et al., 1997; Roy et al., 2002; Land and Monaghan, 2003; Roy et al., 2004). As described in detail in Chapter 3, caudal areas of the cortex, such as primary visual cortex, are disproportionately reduced relative to the reduction in total surface area. Similarly, the striatum is reduced in size due to impaired proliferation in the ventral telencephalon during development (Stenman et al., 2003b). Loss of *tlx* also results in a reduction in limbic and rhinencephalic structures, including the olfactory, infrarhinal, and entorhinal cortex, the islands of Calleja, the amygdala, and the dentate gyrus (Monaghan et al., 1997; Stenman et al., 2003a; Shi et al., 2004). Within the amygdala, the lateral and basolateral nuclei are substantially decreased in size and the morphology of the interstitial nucleus is altered, but the size of the central nucleus seems relatively normal (Stenman et al., 2003a). Granule cells in the *tlx* null dentate gyrus are reduced in number and connect abnormally to CA3, resulting in an ectopic infrapyramidal mossy fiber projection (Monaghan et al., 1997). Dentate gyrus granule cells also show changes in dendritic structure and impairment in long-term potentiation, both of which are observed in the dentate gyrus but not in area CA1 (Christie et al., 2006). Hence, global deletion of *tlx* during development leads to profound changes in adult anatomy, in particular many limbic structures.

The limbic system is important for the control of emotional behavior as well as learning and memory (Kandel et al., 1995). The disruption to many components of the limbic system as well as other brain structures in *tlx*-deficient animals results in distinct behavioral abnormalities, including severe aggression, hyperexcitability, abnormal maternal instincts, reduced anxiety, reduced spatial learning, deficits in contextual and cued fear conditioning, and late-onset epilepsy (Monaghan et al., 1997; Roy et al., 2002; Young et al., 2002; Belz et al., 2007; Zhang et al., 2008). Study of behavior in *tlx*-deficient animals is complicated by defects in the development of the retina and the optic nerve that result in severe visual deficits (Yu et al., 2000; Young et al., 2002; Miyawaki et al., 2004; Zhang et al., 2006). To identify behaviors that result from changes in the brain itself, as opposed to behaviors that result from blindness, Belz and colleagues (2007) generated *tlx* mutant mice with intact vision by using a calcium/calmodulin-dependent protein kinase II alpha (CAMKIIα) gene-driven Cre recombinase to delete *tlx* from the developing brain but not the eye. CAMKIIα-Cre driven recombination was observed throughout the brain from embryonic day 12.5 (E12.5) but was absent from the eye, and in mutant animals *tlx* mRNA was strongly reduced at E12.5 and hardly detectable by E14.5. The brains of *CAMKIIα-tlx*^{cKO} conditional animals showed the same structural abnormalities as previously observed in null animals, however eye morphology and vision appeared normal (Belz et al., 2007). These mice retained the severe aggression and reduced anxiety observed in *tlx* null mutants but did not show any impairment in either contextual or cued fear conditioning or spatial learning as assayed by the Morris water maze (Belz et al., 2007). The finding that blindness of the *tlx* null mutants was the cause of poor performance in fear conditioning was confirmed by another group using a Nestin-driven Cre, which drives recombination in progenitors throughout the developing CNS as early as E9 (Zimmerman et al., 1994; Tronche et al., 1999). These

Nestin-tlx^{cKO} conditional mutants showed normal retinal morphology and vision but deficits in brain development similar to null mutants (Zhang et al., 2008). However, despite intact vision these mice showed impaired performance in the Morris water maze similar to that of *tlx* null animals (Monaghan et al., 1997; Zhang et al., 2008). This difference could be due to *tlx* being deleted earlier in *Nestin-tlx*^{cKO} animals (promoter drives expression from E9, but knockout not characterized in detail (Zimmerman et al., 1994)) than in *CAMKIIα-tlx*^{cKO} animals (E12.5), resulting in a more severe phenotype. In addition, the *Nestin-tlx*^{cKO} mice were tested with a more challenging version of the Morris water maze than the *CAMKIIα-tlx*^{cKO} mice, which could also explain this discrepancy. The *CAMKIIα-tlx*^{cKO} mice were trained for one day on a visible platform version of the Morris water maze followed by training with a hidden platform, with a trial length of 120 seconds (Belz et al., 2007). *Nestin-tlx*^{cKO} mice began with hidden platform training, and were allowed only 40 seconds per trial to find the hidden platform (Zhang et al., 2008). This suggests that mice deficient for *tlx* in the developing brain can show some degree of spatial learning but it is impaired. Overall, *tlx* has been shown to have an important role in the development of a variety of behaviors. However, the precise nature of this role, and the link between anatomical and behavioral abnormalities in the absence of *tlx*, have not yet been determined.

In addition to its role during development, *tlx* has also been shown to regulate the proliferation of adult neural stem cells in both the subgranular zone of the dentate gyrus and the subventricular zone (Shi et al., 2004; Liu et al., 2008; Zhang et al., 2008). Adult neurogenesis has been implicated in a variety of neurological disorders and treatments, with a particular role in learning and memory (Sahay and Hen, 2007; Kaneko and Sawamoto, 2009). In order to examine the role of *tlx*-expressing adult neural stem cells in behavior Zhang and colleagues (2008) used a

tamoxifen-inducible Cre to remove *tlx* in the adult animal, resulting in reduced proliferation and neurogenesis in the dentate gyrus but otherwise normal brain morphology. These animals exhibit normal contextual fear conditioning and anxiety but show delayed learning in the Morris water maze task as well as the reversal version of the task. Given the role for *tlx* in maintaining adult neural stem cells (Shi et al., 2004; Liu et al., 2008; Zhang et al., 2008), these results suggest that these *tlx*-positive neural stem cells have a role in spatial learning.

During development *tlx* is expressed throughout the forebrain, with expression identified in PCs in the dorsal and ventral telencephalon and in the diencephalon as well as in a subset of cells in the differentiating field (Chapter 2) (Monaghan et al., 1995; Stenman et al., 2003a). Consequently, global disruption of *tlx* affects a wide variety of structures derived from these different regions, including from the dorsal telencephalon the cerebral cortex, the hippocampus, and parts of the amygdala; from the ventral telencephalon the striatum, cortical interneurons, and the amygdala; and from the diencephalon the hypothalamus (Monaghan et al., 1997; Roy et al., 2002; Land and Monaghan, 2003; Stenman et al., 2003a; Stenman et al., 2003b; Roy et al., 2004; Shi et al., 2004)(Monaghan et al., unpublished results). All of the *tlx* mutants generated previously have knocked out *tlx* from PCs throughout the forebrain. The association between distinct behavioral abnormalities and specific anatomical deficits is therefore still very much unclear. Our goal in this study was to dissect the developmental and anatomical origin of specific behaviors by generating mice in which *tlx* is deleted only from a subset of cells, specifically from the dorsal telencephalon. We therefore hypothesized that dorsally-derived structures, such as the cerebral cortex and the hippocampus, would be specifically affected. Loss of *tlx* from dorsal PCs could also indirectly affect structures derived from other parts of the brain

through changes in development or in connectivity. It will thus be important to consider these possible effects when interpreting the anatomical and behavioral phenotype of dorsal *tlx* deletion.

We generated mice in which *tlx* is deleted from dorsal cortical PCs using Emx1-Cre driven recombination (*tlx*^{cKO}; described in chapter 4). Emx1 expression is observed as early as E9.5, with Emx1-driven Cre recombination evident from E10.5 (Gorski et al., 2002). Crossing these Emx1-Cre mice to the R26R reporter strain shows extensive, reproducible Cre-mediated recombination in derivatives of the lateral, dorsal, and medial pallium (Gorski et al., 2002). Extensive recombination was observed in the hippocampus, entorhinal cortex, and parts of the piriform and endopiriform cortex as well as in excitatory neurons and glia but not GABAergic neurons in the cerebral cortex. In the septum, recombination was observed in the septohippocampal, septofimbrial, and lateral septal nuclei, with no recombination observed in the medial septal area. In the amygdala, recombination was observed primarily in the lateral, basolateral, and basomedial nuclei, with little to no recombination in other areas. Little recombination was observed in subcortical structures, such as the striatum or in regions outside of the telencephalon (Gorski et al., 2002).

Here we show that Emx1-Cre mediated deletion of *tlx* from dorsal progenitors results in deficits in a subset of the structures affected in the adult null mutant, including the cerebral cortex, the hippocampus, the basolateral amygdala, and the septum, with other structures such as the striatum and the hypothalamus relatively unaffected. These conditional mutants exhibit behavioral abnormalities including reduced anxiety, reduced depression-like behavior, and impaired behavioral flexibility. However, these animals do not show the hyperexcitability or severe aggression characteristic of null mutants, and show no deficits in spatial learning. This

provides a developmental model that allows us to refine our views on the association between specific brain structure and behavior.

5.2 METHODS

5.2.1 Animals

Animals were obtained from crossings of *tlx* heterozygote, *tlx* flox/flox, and Emx1-Cre *tlx* +/- animals (Monaghan et al., 1997; Gorski et al., 2002; Belz et al., 2007). Control animals include the genotypes *tlx* flox/+, *tlx* flox/-, and Emx1-Cre *tlx* flox/+. Genotyping was performed by PCR as described in Sections 2.2.1 and 4.2.1. Mice were housed in groups of 2-5 under standard laboratory conditions on a 12-hour light/dark cycle with light onset at 7am. Standard mouse food pellets and water were available ad libitum. The care and handling of these animals was in accordance with the University of Pittsburgh Institutional Animal Care and Use committee and NIH guidelines.

Postnatal brains were fixed by transcardial perfusion with cold PBS followed by 4% PFA pH7.4, dissected from the skull, and immersion fixed overnight. Brains were processed through a graded sucrose series (10-20-30%) at 4°C. Adult brains were sectioned coronally on a freezing-sliding microtome at 50μm and collected in PBS. A subset of brains was dissected following perfusion and immersion fixed overnight gently flattened between glass slides. Flattened cortices were then sectioned tangentially on a freezing-sliding microtome at 30μm.

5.2.2 Immunohistochemistry

Sections were washed in 50% methanol/50% PBS/1% hydrogen peroxide followed by three washes with 0.1% Tween 20 (Fisher Scientific) in PBS. Sections were blocked overnight at 4°C with 10% HINGS in PBS and then incubated with primary antibody overnight at 4°C. Antibodies used were mouse anti-calbindin (1:1000; Sigma); rabbit anti-calretinin (1:2500; Chemicon); rabbit anti-CGRP (1:2000; Abcam); rabbit anti-Cux1 (1:1000; Santa Cruz Biotechnology); rabbit anti-DARPP-32 (1:500; Chemicon); rabbit anti-GABA (1:1000; Sigma); mouse anti-GFAP (1:1000; Sigma); rabbit anti-GFAP (1:1000; Sigma); mouse anti-parvalbumin (1:2000; Sigma); rabbit anti-Tbr1 (1:2000; Chemicon); rabbit anti-Tbr2 (1:2000; Chemicon); rabbit anti-serotonin (1:20,000; ImmunoStar, Inc.); rabbit anti-vasopressin (1:2000; Chemicon). The sections were subsequently washed in 0.1% Tween 20 in PBS, incubated with biotinylated secondary antibody (1:500; Vector Laboratories) for 1.5 hours and processed using the Vectastain(r) Elite ABC kit (Vector Laboratories) according to the manufacturer's instructions. After rinsing in PBS, sections were incubated in 0.7mg/ml 3,3'-diaminobenzidine tetrahydrochloride (DAB; Sigma) with 0.01% hydrogen peroxide, in some cases nickel enhanced. DAB stained sections were washed in PBS, mounted on slides, counterstained with 0.5% cresyl violet (Nissl; Sigma), dehydrated through alcohols, washed in xylene, and coverslipped with DPX.

All sections were visualized on a Nikon 400 (Melville, NY) fluorescent microscope, photographed with a Photometrics (North Reading, MA) Cool Snap digital camera and IP Lab software (Biovision Technologies, Exton, PA). Composite images were prepared using Photoshop 6.0 (Adobe Systems, San Jose, CA). Contrast, color, and brightness were adjusted in Photoshop.

5.2.3 Measurements

For whole brain measurements, PFA-fixed brains were imaged on a Nikon dissecting microscope and photographed with a Photometrics Cool Snap digital camera and IP Lab software. Total brain area, cortical hemispheres, and olfactory bulbs were outlined, and the surface areas calculated using Photoshop 6.0. Quantification of serotonin staining on tangential sections was performed as described in Section 3.2.4 following methods used in (Hamasaki et al., 2004). Cortical thickness was measured as previously described (Land and Monaghan, 2003). Briefly, the thickness of cortical layers was measured along a radial line extending from the pial surface to the white matter in parietal and occipital regions, defined histologically. Layers were identified histologically using either Nissl-stained sections or sections stained with laminar markers Tbr1 or Cux1. All analyses were performed by an observer blind to genotype. Statistical analysis was performed using unpaired t tests with SPSS 14.0 software (SPSS, Inc., Chicago, IL). All values are expressed as mean ± SEM.

5.2.4 Behavioral experiments

Mutant and control mice were matched for sex and age, and littermates were housed together in groups of 2-5. Experimental animals were between 3 and 14 months (see Table 1 for cohort details, including order of experiments). Prior to the start of behavioral testing, animals were handled daily for 5 days. Behavioral analyses were carried out between noon and 7pm. The home cage was brought to the test room at least 15 minutes before each experiment, and each apparatus was cleaned with Quatricide PV (Pharmacal Research Laboratories, Inc., Naugatuck, CT) before releasing each animal. Mice were observed in a clean cage for 3 minutes to examine

general physical characteristics (whiskers, presence of bald spots) and behavior (wild running, freezing, posture, excessive grooming). Mice were tested for eye blink, ear twitch, and whisker-orienting reflexes. Vision was informally tested using the visual placing task, in which mice are lowered by their tail towards the edge of a table, and if they extend their forepaws prior to touching the table it is assumed they can see.

Activity and motor function were assessed by placing the animals into a test arena equipped with infra-red light beams and sensors for a 15 minute test period (arena size: 10 inches by 10 inches, with infra-red beams spaced 0.6 inches apart; Coulbourn Instruments, Whitehall, PA). The box is housed in a sound-attenuating chamber, and no illumination was provided. Data was collected using Tru Scan 2.0 software (Coulbourn Instruments). Measures analyzed include number of movements, total time spent moving, total distance traveled, average ambulatory velocity, frequency of rearing (vertical plane entries), and frequency of "stereotypic" movement.

Motor function was also examined using a rotarod treadmill (IITC Life Science, Woodland Hills, CA). Mice were placed on the stationary rod for 60 seconds to acclimatize to the equipment, followed by 5 minutes in the home cage. Mice then were given two 3-minute learning trials with a 5-minute inter-trial interval during which the rod moved at 10rpm and mice were replaced if they fell. This was followed by three test trials for a maximum length of 5 minutes with 5-minute inter-trial intervals. During each trial the speed of the rod increased gradually from 5rpm to 40rpm, reaching maximum speed at 260 seconds. The latency to fall was recorded, and the average of the three test trials calculated for each mouse to be compared by genotype. Trial data was thrown out if the mouse fell in less than 10 seconds (occurred rarely).

Acoustic startle reactivity and prepulse inhibition were examined as described by Geyer and Dulawa (Geyer and Dulawa, 2003) using the StartleMonitor apparatus and software from Kinder Scientific (Poway, CA). Continuous background noise level was set at 65dB. For acoustic startle, the maximal response was measured following 40msec bursts of semi-randomly presented sound intensities of either no pulse, 78dB, 82dB, 86dB, 90dB, 100dB, 110dB, or 120dB separated by inter-trial intervals ranging from 8 to 23 seconds with an average of 15 seconds. Data were averaged for each intensity level and compared across genotype by repeated measures ANOVA. For prepulse experiments 120dB pulses were used. The experiment was organized into four blocks, with the first and last blocks consisting of six 120 dB pulse-only trials and blocks 2 and 3 consisting of a mix of no-pulse, pulse-only, and prepulse + pulse trials. During prepulse + pulse trials, 20msec prepulses 4, 8, or 16dB above background noise level (69dB, 73dB, or 77dB) were presented 100msec prior to a 40msec pulse at 120dB. Data were combined from blocks 2 and 3 and were averaged for each intensity level and compared across genotype by repeated measures ANOVA. Percent prepulse inhibition was calculated as 100 x [(pulse-only) – (prepulse + pulse)] / (pulse-only).

Anxiety was tested using the light-dark box paradigm. The same chamber used for activity monitoring was divided in half using a dark insert with a small hole to allow mice to move between sides (Coulbourn Instruments). The light half of the box was brightly illuminated. Mice were placed in the light half of the chamber and allowed to freely explore for 5 minutes. Time spent in each half (light or dark) was determined using Tru Scan 2.0 software and compared across genotype by unpaired t-tests.

Nose pokes were examined by placing mice into an open 41cm by 32cm chamber for 10 minutes. Nose pokes into small holes (1.1cm) equally spaced 2cm above the floor along two

opposite walls of the chamber (5 holes on each wall) were counted by an observer hidden from view. Mice were recorded and tracked using LimeLight (Actimetrics Software, Wilmette, IL). Nose pokes were compared across genotypes using an unpaired t-test.

The apparatus used for the elevated plus maze consisted of four arms, 35cm long by 5.2cm wide, oriented in a cross shape elevated above the ground and constructed out of smooth white plastic. Two opposing arms were enclosed by 15cm walls, with the other two arms left open. Lamps were positioned at either end of the open arms in order to enhance the difference between open and closed arms; average light intensity was approximately 180 lux at the ends of open arms, 110 lux at the center of the maze, and 35 lux at the ends of the closed arms. Mice were placed on an open arm facing the center and allowed to freely explore the maze for 5 minutes. LimeLight software was used to track the mice and determine the number of visits to each arm and time spent in each arm. The percent time spent in the open arms, closed arms, and center were calculated and compared across genotype using unpaired t-tests.

For the forced swim task, mice were placed in a plastic cylinder (20cm diameter) filled with water (22.5-23°C) up to a height of 10cm. Mice were observed for 6 minutes to determine the percent of time spent floating, with data reported for the last 4 minutes of the task. Floating was defined as immobility in the water, except for movements necessary for the animal to keep its head above water, as opposed to active swimming or attempts to escape. Limelight software was used to record and track the mice.

The Morris water maze, including spatial acquisition and spatial reversal, was conducted as described by Vorhees and Williams (Vorhees and Williams, 2006). A blue plastic tank 4 feet in diameter was filled with water (22.5°C ± 0.5°C), which was made opaque by a combination of whole milk and non-toxic white paint (RichArt, Northvale, NJ). A circular white platform 10cm

in diameter was located in the center of one of the four virtually divided quadrants submerged 0.5cm below the surface of the water. Distal cues, such as a dark curtain, a shelf, and a printed rectangular pattern taped to a white wall were provided as spatial references and remained constant throughout the experiment. Mice were given four 1-minute training trials per day with 4-minute inter-trial intervals during which mice were returned to the home cage. Four different start positions were used, with the mice released from each these four positions in a different semi-random order on each training day. Mice were allowed to swim for up to 1 minute, after which mice were placed on the platform if they had not yet reached it on their own. Once on the platform, mice were left for 15 seconds before being returned to their home cage. During probe trials, the mice were allowed to swim for 1 minute without the platform. The SMART video tracking system (Panlab, Barcelona, Spain) was used during training and probe trials to record and analyze the latency to reach the platform, swim path, average distance from target, velocity, and time spent in each quadrant. For reversal learning the hidden platform was moved to the opposite quadrant from the original location without changing any distal cues. Mice were trained as with spatial learning, with four new start positions. For the visible version of the water maze (after spatial and reversal training and testing) the water was lowered to 33.5cm (halfway down the tank) so that spatial cues would not be easily visible. The platform was positioned so that it was visible above the waterline. Mice were given three trials of the visible version of the water maze, with a novel platform location and start site for each trial.

Spontaneous alternation was tested as described by Ragozzino et al. (Ragozzino et al., 1998). The apparatus used was a radial arm maze made by Lafayette Instrument Company (Lafayette, IN) and modified to function as a four-arm plus maze with arms 25cm in length. The surface of the maze was constructed out of black coated aluminum with 20cm walls made of

clear polycarbonate. The test was conducted under low overhead illumination. Mice were placed in the center of the maze and allowed to freely explore for 15 minutes, during which LimeLight software was used to track the mice and determine the number and sequence of arm entries, with an entry defined by the placement of all four paws in the arm. An alternation was defined as a set of five consecutive arm entries that included entry into all four arms, with percent alternation calculated as the proportion of actual alternations divided by the total number of five-arm sets (total number of arm entries minus four). Repetitive or perseverative behavior (triplets) was defined as sets of three consecutive arm entries during which the same arm was entered twice, with percent triplets defined as the proportion of triplets divided by the total number of three-arm sets (total number of arm entries minus two).

Statistical analysis was performed using SPSS 14.0 software (SPSS, Inc.). Data were compared between genotypes using t-tests or ANOVA followed by Dunnett's post-hoc analysis as indicated. All values are expressed as mean ± SEM. Graphs were generated using GraphPad Prism 4 (GraphPad Software).

5.3 RESULTS

5.3.1 Cortical surface area is reduced in *tlx*^{cKO} animals postnatally with a disproportionate reduction in caudal areas

In the complete absence of *tlx*, many adult brain structures are altered, resulting in a complex behavioral phenotype. In order to examine the role of *tlx* in the development of a subset of brain structures and to identify the behavioral abnormalities associated with these changes, we

generated mice with a conditional deletion of *tlx* in dorsal progenitor cells using Emx1-Cre driven recombination; these mice will be referred to as conditional mutants or tlx^{cKO}. Emx1 expression initiates at E9.5 (Gorski et al., 2002), and, as we showed in Chapter 4, functional deletion of *tlx* occurs by E12.5 (Figure 20). Just before birth (E18.5), the cerebral cortex of tlx^{cKO} animals is visibly reduced in surface area and thickness (Chapter 4 and data not shown). Conditional mutant animals are born in normal Mendelian ratios and are indistinguishable from littermates, with no significant difference in adult body weight (data not shown). Examination of the gross anatomy of the brain of adult tlx^{cKO} animals revealed that total brain surface area is decreased by 7.1% ($p<0.05$, n=6; Figure 28). This is largely due to a 15.3% decrease in the surface area of the cerebral hemispheres (C), $52.1mm^2 \pm 1.4mm^2$ as compared to $61.6mm^2 \pm 1.4mm^2$ in controls ($p<0.001$, n=7; Figure 28), which exposes more of the superior colliculi (SC). The olfactory bulbs (O) also show a 26.3% decrease in area, $6.0mm^2 \pm 0.3mm^2$ as compared to $8.1mm^2 \pm 0.4mm^2$ in controls ($p<0.001$, n=6; Figure 28). Similar to *tlx* null animals, the gross morphology of the cerebellum appears relatively unaffected. These data suggest that, as expected, absence of TLX from dorsal progenitors specifically affects forebrain-derived structures.

In *tlx* null animals, the surface area of the cerebral cortex is reduced, with a disproportionate reduction in caudal cortical areas ((Monaghan et al., 1997; Land and Monaghan, 2003); Chapter 3). In order to determine whether this disproportionate reduction is an intrinsic effect due to the loss of TLX from dorsal progenitors, we examined functional cortical areas in tlx^{cKO} animals at P8. Serotonin immunostaining, which marks the terminations of thalamocortical axons in layer IV of primary sensory areas including primary somatosensory cortex, primary visual cortex (V1), and primary auditory cortex (Fujimiya et al., 1986), was used

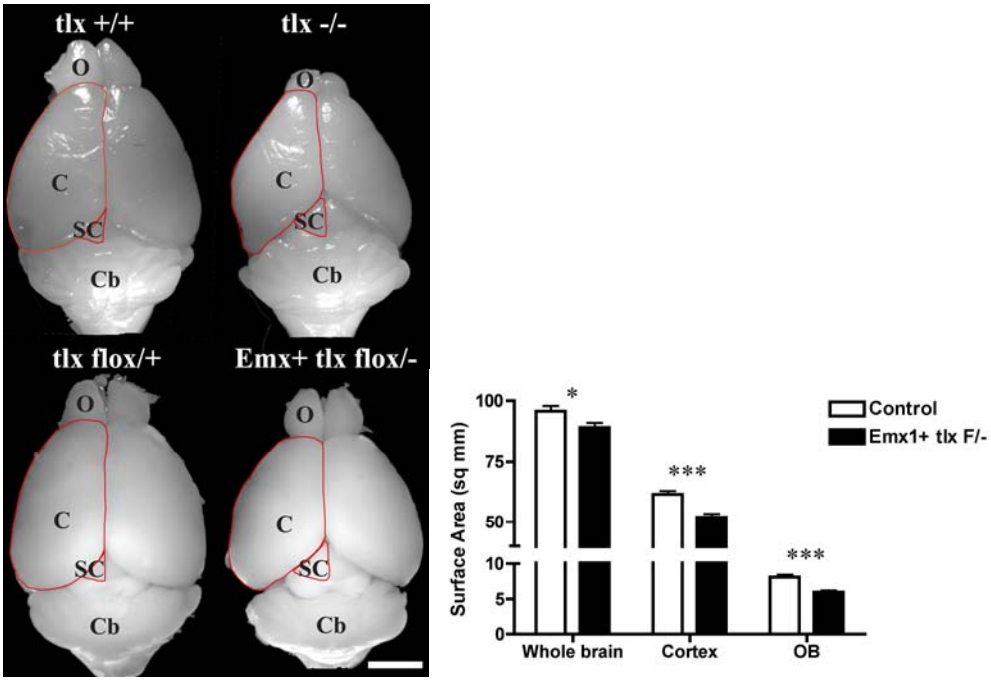

Figure 28. Cortical surface area is reduced in *tlx*^{cKO} animals

Similar to *tlx*-/- mice, the whole brain is reduced in surface area in *tlx*^{cKO} adults as compared to controls (tlx F/+ shown here). The hemispheres of the cerebral cortex (C, outlined in red) are reduced in size, exposing more of the superior colliculi (SC, outlined in red). The olfactory bulbs (O or OB) are also significantly reduced in size in *tlx*^{cKO} animals as compared to controls. The gross morphology of the cerebellum (Cb) is relatively unaffected. Quantification is shown in the right. * $p<0.05$; *** $p<0.001$. Scale bar = 0.5cm.

on tangential sections through flattened cortices to determine the relative proportion of total cortical area occupied by each of these sensory areas. The proportion of total cortical area occupied by primary visual cortex (V1) in *tlx*^{cKO} animals is decreased by 29.3%, 5.2% ± 0.5% as compared to 7.4% ± 0.6% in control brains ($p<0.05$, n=4; Figure 29A-C). More intermediate structures, such as the posteromedial barrel subfield (PMBSF; part of somatosensory cortex) and auditory cortex (A), are reduced proportionately to total cortical area in *tlx*^{cKO} animals (PMBSF $p=0.68$, n=4; auditory $p=0.54$, n=3). These results are similar to those observed for null animals, which showed a 36.6% decrease in the proportion of total cortex occupied by V1 and

proportionate reductions in the PMBSF and auditory cortex (see Chapter 3). These findings suggest that *tlx* is required in dorsal progenitors for the normal expansion of caudal cortical areas, although we cannot rule out a contribution from ventral regions to account for the small difference in size of V1 in conditionals as compared to nulls. Furthermore, as *tlx* should be expressed normally in the developing eye in *tlx*^{cKO} animals, our findings suggest that the reduction in primary visual cortex is likely not due to deficits in development of the retina or optic nerve or reduced visual input but rather due to intrinsic changes in cortical development.

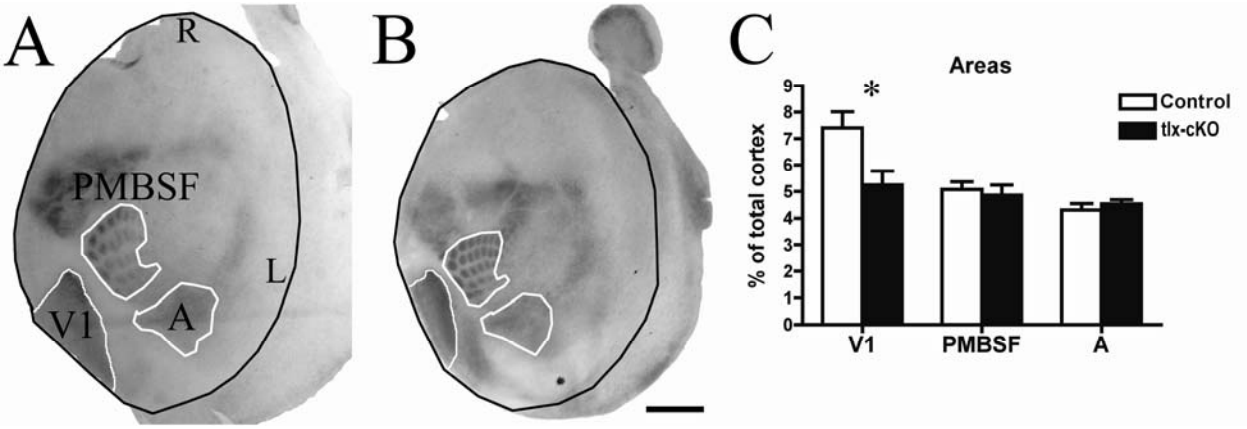

Figure 29. Primary visual cortex is disproportionately reduced in *tlx*^{cKO} animals

Serotonin immunostaining on tangential sections through flattened control (A) and *tlx*^{cKO} (B) P8 cortex. Primary visual cortex (V1) is disproportionately reduced in the tlx deficient animals while auditory cortex (A) and the posteromedial whisker barrel field (PMBSF) are reduced proportionately to the reduction in total cortical area (quantified in C). The regions compared between wild-type and mutant animals are outlined in white, with total cortical area outlined in black. * $p<0.05$. Scale bar (in B) = 1mm in A, B. R = rostral, L = lateral.

5.3.2 Cortical thickness is reduced but glia are increased in *tlx*^{cKO} animals

In *tlx* null animals the cerebral cortex is reduced in thickness due to a specific reduction in superficial cortical layers (Roy et al., 2002; Land and Monaghan, 2003). To determine whether this phenotype is due to a requirement for *tlx* is dorsal progenitors, we examined cortical thickness in *tlx*^{cKO} animals. The cortex was examined on adult coronal sections stained with Nissl alone or with either an antibody against Cux1, a transcription factor expressed by cells in upper cortical layers II/III and IV (Nieto et al., 2004), or an antibody against Tbr1, a transcription factor highly expressed by glutamatergic cells in layer VI and more weakly expressed by cells in layers II/III and IV and a small subset of cells in layer V (Bulfone et al., 1995; Hevner et al., 2003; Kolk et al., 2005). The total thickness of the cerebral cortex (from the white matter to the pial surface) is reduced by 13.4% in parietal regions (1319.7μm ± 33.8μm in controls versus 1142.2μm ± 38.6μm in *tlx*^{cKO} animals, n=4, $p<0.05$) and by 9.3% in occipital regions (869.9μm ± 27.4μm in controls versus 788.9μm ± 17.7μm in *tlx*^{cKO} animals, n=4, $p<0.05$) (Figure 30). We separately quantified the thickness of superficial layers (II/III and IV) and deep layers (V and VI), identified by histological examination in combination with layer-specific Tbr1 and Cux1 staining. We found that the reduction in cortical thickness in *tlx*^{cKO} animals is due to a specific reduction in superficial cortical layers in both parietal ($p<0.001$, n=4) and occipital regions ($p<0.001$, n=4) (Figure 30). No significant difference in the thickness of deep cortical layers was observed in the regions examined (parietal $p=0.85$, n=4; occipital $p=0.14$, n=4).

In addition to changes in excitatory neurons, *tlx* null adults have previously been shown to have reductions in specific populations of cortical GABAergic interneurons, in particular calretinin- and somatostatin-expressing cells (Monaghan et al., 1997; Roy et al., 2002). The Emx1-Cre that we used to generate our conditional mutants is not expressed in GABAergic cells

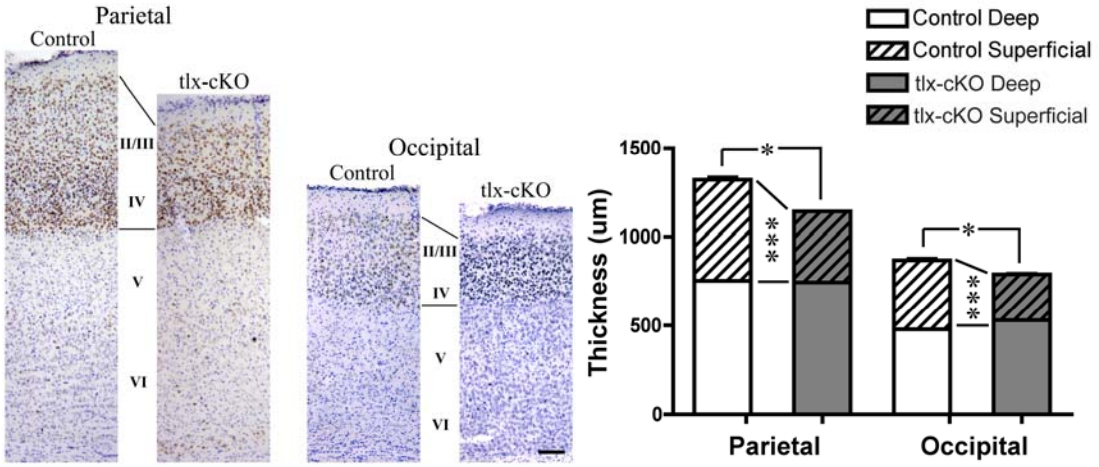

Figure 30. Cortical thickness is reduced due to a specific reduction in superficial cortical layers

The cerebral cortex of adult *tlx*^{cKO} mice is reduced in thickness as compared to controls at both parietal and occipital levels. Cux1 expression (brown or black) in superficial layers II/III and IV shows that superficial layers are specifically affected. Sections are counterstained for Nissl (blue). * $p<0.05$; *** $p<0.001$. Scale bar = 100µm.

in the cerebral cortex (Gorski et al., 2002), which derive from progenitor populations in the ventral forebrain (de Carlos et al., 1996; Anderson et al., 1997). However, cells in the dorsal cortex could influence the migration or maturation of cortical interneurons, and thus indirect changes in interneuron populations might be observed in *tlx*^{cKO} animals. Immunostaining against GABA to label all interneurons did not reveal any gross differences in number or distribution of GABA-positive cells in parietal or occipital regions of *tlx*^{cKO} cortex as compared to controls (Figure 31A-D; n=2), although this was not quantified. Specific interneuron populations were identified using the expression of the calcium binding proteins calbindin, parvalbumin, and calretinin (Kubota et al., 1994; Gonchar and Burkhalter, 1997). Visual inspection revealed no differences in interneurons in *tlx*^{cKO} parietal cortex expressing calbindin (Figure 31E, F; n=5) or parvalbumin (Figure 31G, H; n=1), populations that are similarly unaltered in *tlx* null animals (Monaghan et al., 1997; Roy et al., 2002). Although calretinin-positive cortical interneurons are

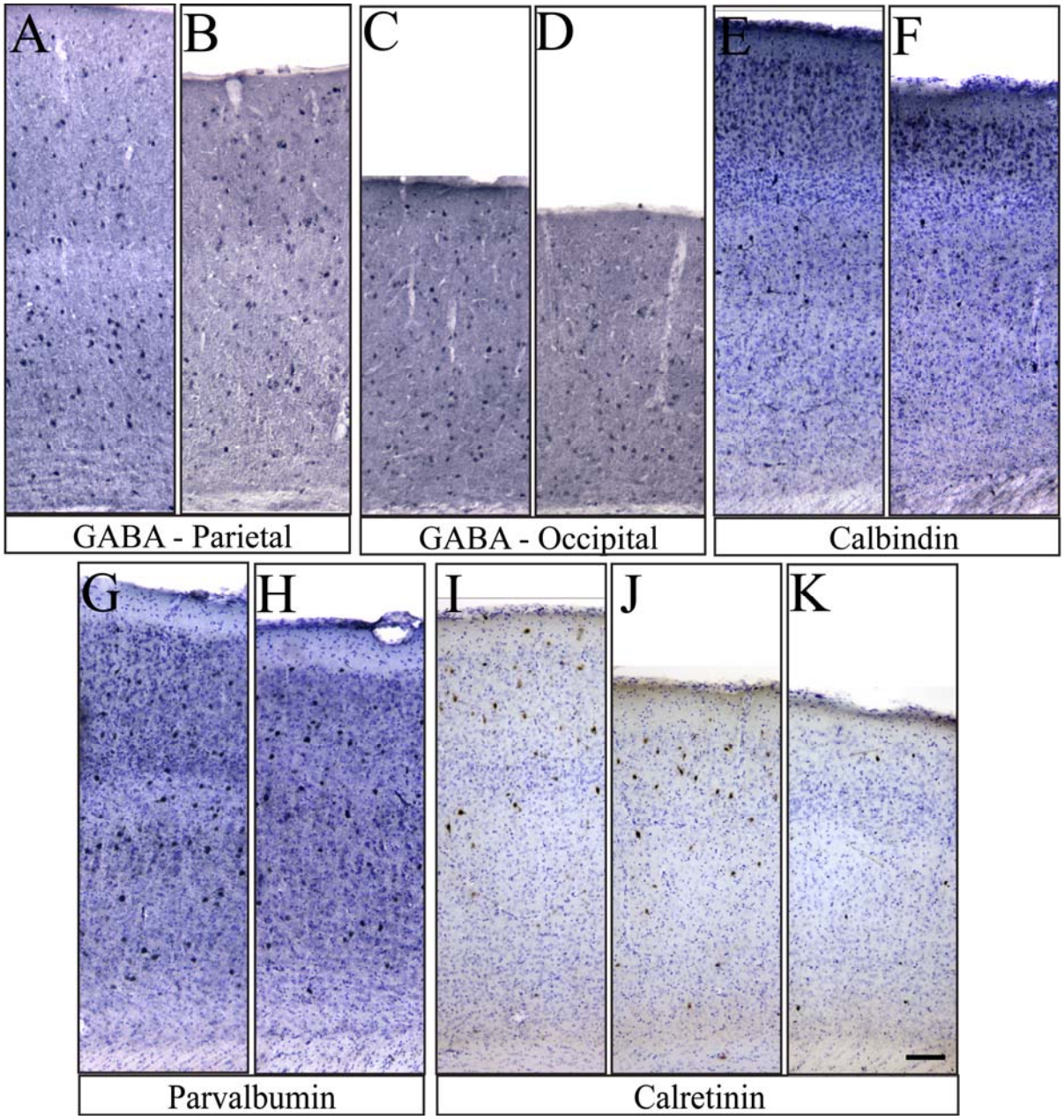

Figure 31. Interneurons are relatively unaltered in the *tlx*^{cKO} adult cortex

GABA expression (black) in the cerebral cortex of adult control (A, C) and *tlx*^{cKO} (B, D) animals at parietal (A, B) and occipital (C, D) levels shows no difference in total interneurons. Expression of calbindin (E, F; brown) and parvalbumin (G, H; black), in adult control (E, G) and *tlx*^{cKO} (F, H) parietal cortex shows no difference in these interneuron populations. Calretinin (I-K, brown) expression in adult parietal cortex is relatively unaltered in *tlx*^{cKO} (J) animals as compared to controls (I), whereas calretinin is significantly reduced in *tlx* null cortex (K). Sections E-K are counterstained for Nissl (blue). Scale bar (in K) = 100μm.

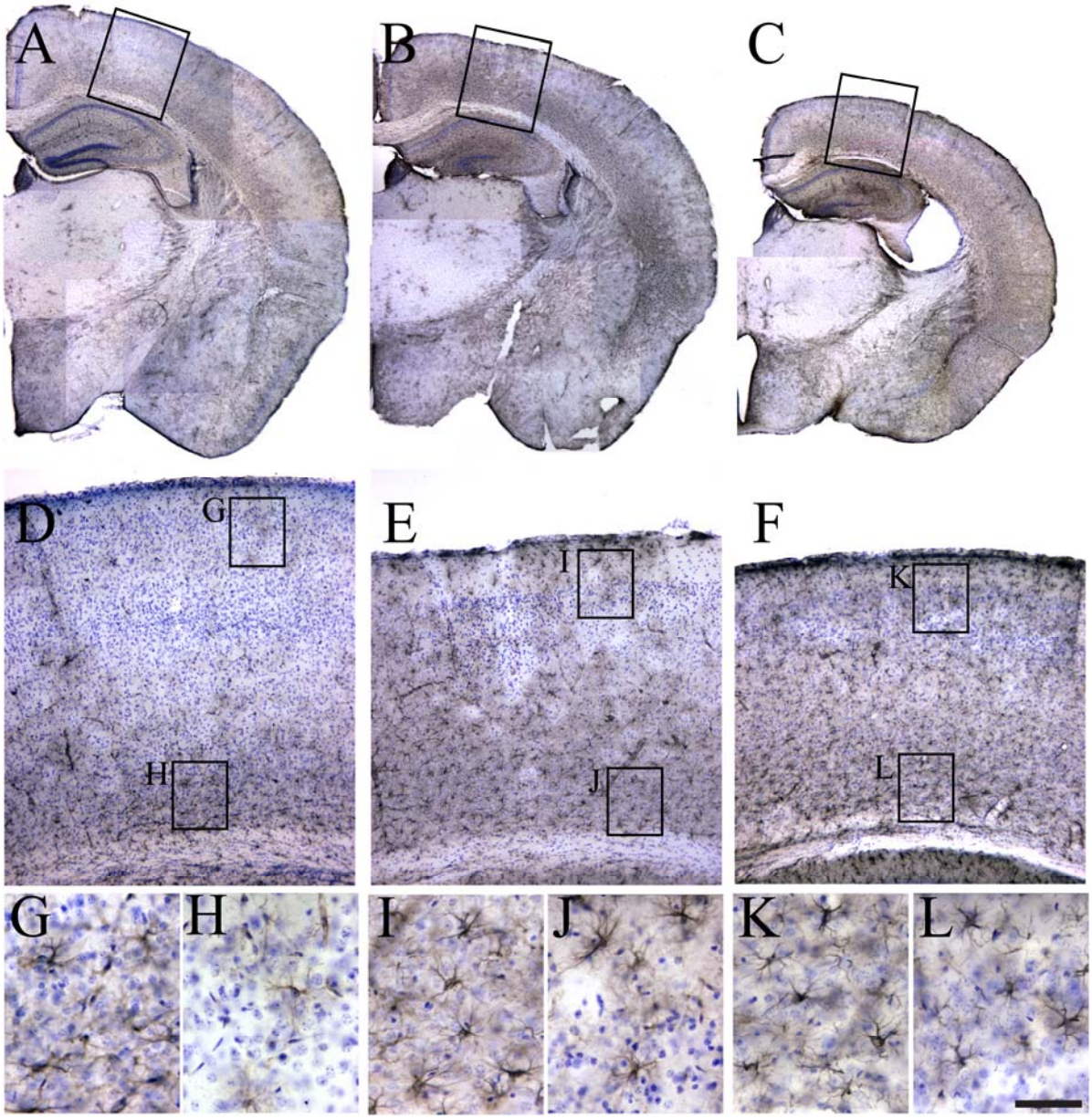

Figure 32. GFAP+ glia are increased in both the *tlx*^{cKO} and *tlx* null adult cortex

GFAP expression (black) in coronal sections from control (left column; A, D, G, H), *tlx*^{cKO} (center column; B, E, I, J), and tlx null animals (right column; C, F, K, L) shows in increase in glia in the cerebral cortex of both conditional and null mutants. D, E, and F are higher power images of the boxed areas in A, B, and C, respectively. G-L are high power images of the boxed areas in D-F as indicated. Sections are counterstained with Nissl (blue). Scale bar (in L) = 1mm in A-C; 200µm in D-F; 50µm in G-L.

decreased in null animals (Figure 31K) (Monaghan et al., 1997; Roy et al., 2002), no difference was observed in this population in *tlx*^{cKO} animals as compared to controls (Figure 31I, J; n=4). These findings suggest that deletion of *tlx* from dorsal progenitors does not indirectly alter development of cortical interneurons.

The third cell type present in the cerebral cortex in addition to excitatory neurons and interneurons is glia. Although the cerebral cortex is reduced in the absence of *tlx*, astrocytes have been shown to be increased from birth, with greater numbers still apparent in the adult (Shi et al., 2004) (Kuznicki and Monaghan, unpublished results). As described in Chapter 4, premature expression of the astrocyte marker glial fibrillary acidic protein (GFAP) was observed in the dorsal VZ of both *tlx*^{cKO} and null brains at E18.5 (Figure 25). Examination of GFAP expression in the adult reveals a similar increase in GFAP-positive cells in the cerebral cortex of both *tlx*^{cKO} and *tlx* null animals as compared to controls (Figure 32A-F; n=4). In control cortex GFAP positive cells are located primarily in the white matter and deep cortical gray matter, with few positive cells in the upper cortical layers (Figure 32D). In both the conditional and null mutant brains GFAP-positive cells are observed throughout the cortical layers (Figure 32E, F). Higher power examination of GFAP staining at both the pial and ventricular surface indicates that for all genotypes the GFAP positive cells appear to have fine processes extending from the main processes in a stellate shape, consistent with a mature astrocyte phenotype (Figure 32G-L). Together these results suggest that *tlx* is involved in repressing gliogenesis, a role intrinsic to dorsal progenitors.

5.3.3 Dorsally-derived structures, including the hippocampus, amygdala, and septum, are reduced in *tlx*^{cKO} animals

In addition to the cerebral cortex, many other structures are derived from Emx1-expressing cells, as shown by crossing Emx1-Cre mice to the R26R reporter strain (Gorski et al., 2002). These structures include the hippocampus and parts of the amygdala and septum, of which the former two have been shown to be affected in *tlx* null knock out animals (Monaghan et al., 1997; Stenman et al., 2003a; Shi et al., 2004). Here we will analyze each structure in turn to identify any anatomical deficits as a result of the dorsal-specific deletion of *tlx*. We first examined the hippocampus, which shows extensive Cre-mediated recombination in Emx1-Cre animals (Gorski et al., 2002). In order to examine the hippocampus as a whole, this structure was dissected from the brains of adult control and *tlx*^{cKO} mice. Visual examination of the whole hippocampus with dissecting microscope showed a reduction in width in *tlx*^{cKO} animals as compared to controls across the entire length of the hippocampus (Figure 33; n=2).

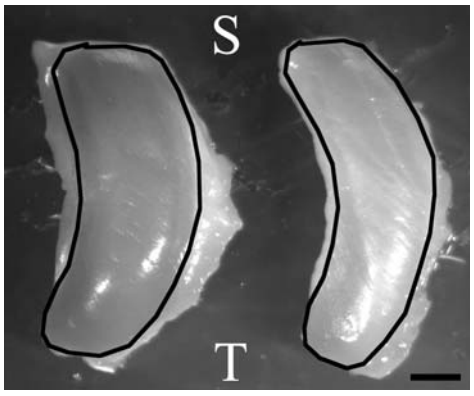

Figure 33. The whole hippocampus is reduced in conditional mutant animals

The hippocampus of *tlx*^{cKO} mice (right) is decreased in size as compared to controls (left) across its length from the septal (S) to the temporal (T) pole. Scale bar = 1mm.

We more carefully examined this general reduction in size of the hippocampus through histological examination of coronal and horizontal sections through the adult brain. For coronal sections, every twelfth section was stained with an antibody against the calcium binding protein calbindin to specifically label granule cell somata and molecular layer dendrites (Sloviter, 1989). Visual examination revealed an overall reduction in the dorsal hippocampus of both *tlx*^{cKO} and *tlx* null animals as compared to controls (Figure 34A-C; n=5). Both conditional and null mutants showed a marked reduction in the size of the dentate gyrus, with the infrapyramidal blade particularly affected (DGi, Figure 34A-C; n=5). In order to specifically examine dorsal and ventral regions of the hippocampus, we prepared a series of horizontal Nissl-stained sections through the hippocampus (every fourth section) from dorsal (Figure 34D-F) to ventral (Figure 34M-O) levels. Visual examination of these horizontal sections indicated a reduction at all levels in both *tlx*^{cKO} and null animals as compared to controls (Figure 34D-O; control, *tlx*^{cKO}, n=2; null, n=1). The dentate gyrus appears reduced at all levels, whereas the subiculum (S) shows a more pronounced reduction at more ventral levels. Overall this pattern suggests a role for *tlx* in dorsal PCs in the development of the hippocampus, in particular of the dentate gyrus.

The subgranular zone (SGZ) of the dentate gyrus is one of the primary regions of adult neurogenesis (reviewed by (Duan et al., 2008)). Therefore, in light of the reduction in the dentate gyrus in *tlx*^{cKO} adults and the known role of *tlx* in the maintenance of adult neural stem cells (Shi et al., 2004; Liu et al., 2008; Zhang et al., 2008), we decided to look specifically at markers of adult neurogenesis in the SGZ of the dorsal hippocampus. Initial examination of higher power images of Nissl staining of the dentate gyrus revealed that granule cells, in addition to being fewer in number, are less tightly packed in *tlx*^{cKO} animals as compared to controls

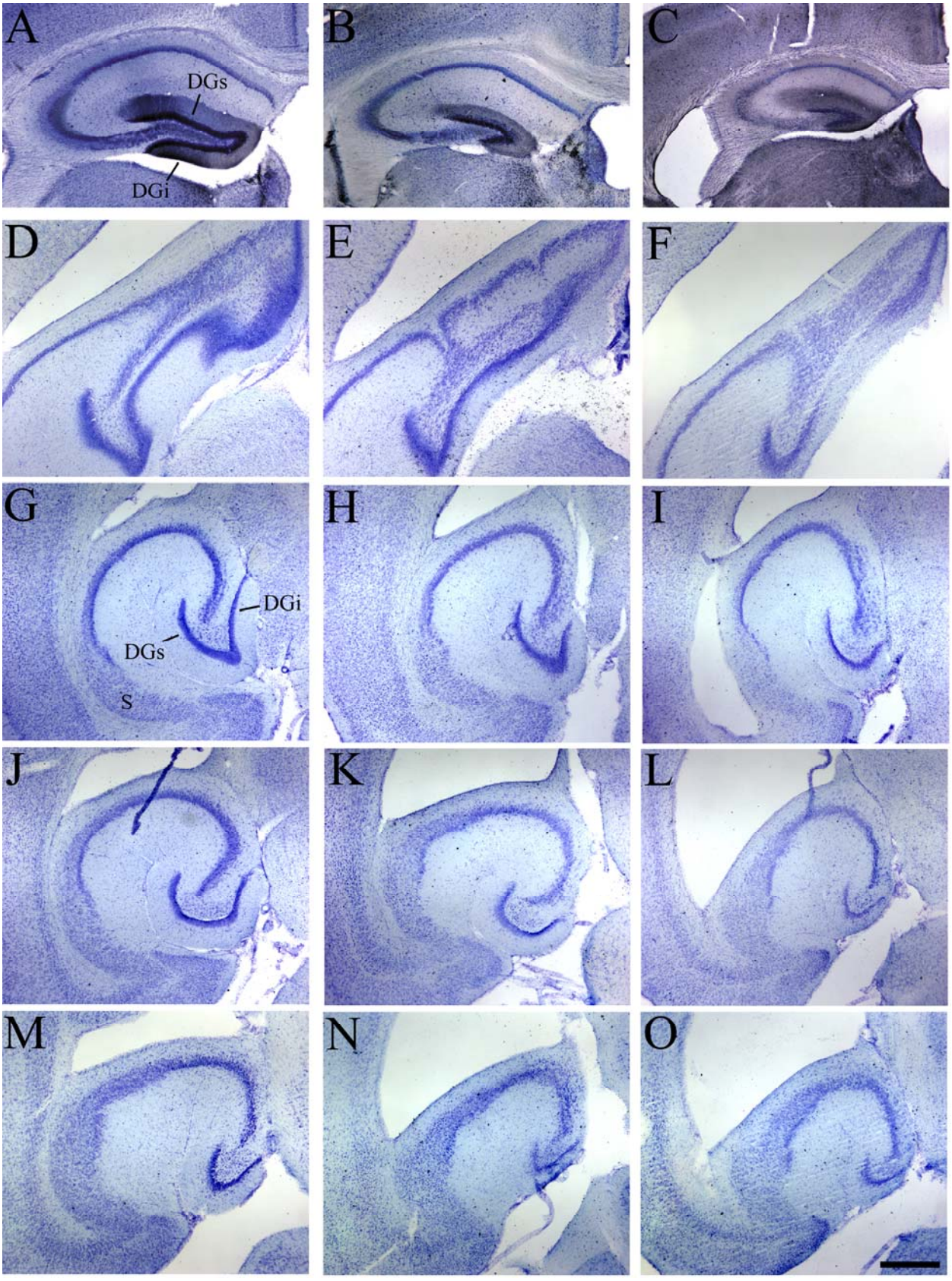
A
DGs
DGi
B
C
D
E
F
G
DGi
DGs
S
H
I
J
K
L
M
N
O

Figure 34. The hippocampus is reduced in size in *tlx*^{cKO} animals

Staining for calbindin (black) in coronal sections through adult dorsal hippocampus (A-C) shows a reduction in the size of the dentate gyrus in both *tlx*^{cKO} (B) and tlx null (C) brains as compared to controls (A), with the infrapyramidal blade (DGi) particularly affected. Nissl staining (blue) on a series of horizontal sections through the adult hippocampus from dorsal (D-F) to ventral (M-O) levels shows a reduction in size at all levels for both *tlx*^{cKO} (center column; E, H, K, N) and tlx null (right column; F, I, L, O) animals as compared to controls (left column; D, G, J, M). Horizontal images are taken from every sixteenth section through the hippocampus of control and *tlx*^{cKO} animals, approximately every twelfth section of *tlx* null animals at anatomically-matched levels. This plane of sectioning also reveals the greater reduction of the infrapyramidal blade of the dentate gyrus (DGi) relative to the suprapyramidal blade (DGs) at more dorsal levels (G-I). S = subiculum. Sections in A-C are counterstained for Nissl (blue). Scale bar (in O) = 535μm in A-C; 500μm in D-O.

(Figure 35A-F). Generation of new neurons from SVZ precursors can be divided into distinct developmental stages that can be identified by the expression of various markers (reviewed by (von Bohlen Und Halbach, 2007; Duan et al., 2008)). A subset of GFAP-expressing cells located in the SGZ has been shown to be an early radial glia-like precursor population that divides to give rise to new granule cells in the adult dentate gyrus (Seri et al., 2001). Numerous radial glia-like GFAP positive cells, with cell bodies at the border of the granule cell layer and a single apical dendrite, are apparent in the SGZ of the control dentate gyrus (Figure 35A, A', arrows). In contrast, although high GFAP expression is observed in the *tlx*^{cKO} hippocampus, these GFAP positive cells have a stellate shape suggestive of mature astrocytes and are not as specifically localized to the SGZ (Figure 35B, B'; n=3). These early precursors give rise to transient amplifying cells (or intermediate progenitor cells, IPCs) that express the transcription factor T-box brain gene 2 (Tbr2) (Hodge et al., 2008). Tbr2-positive cells are located in the SGZ of the control dentate gyrus (Figure 35C, C', arrows) but are absent from the *tlx*^{cKO} dentate gyrus

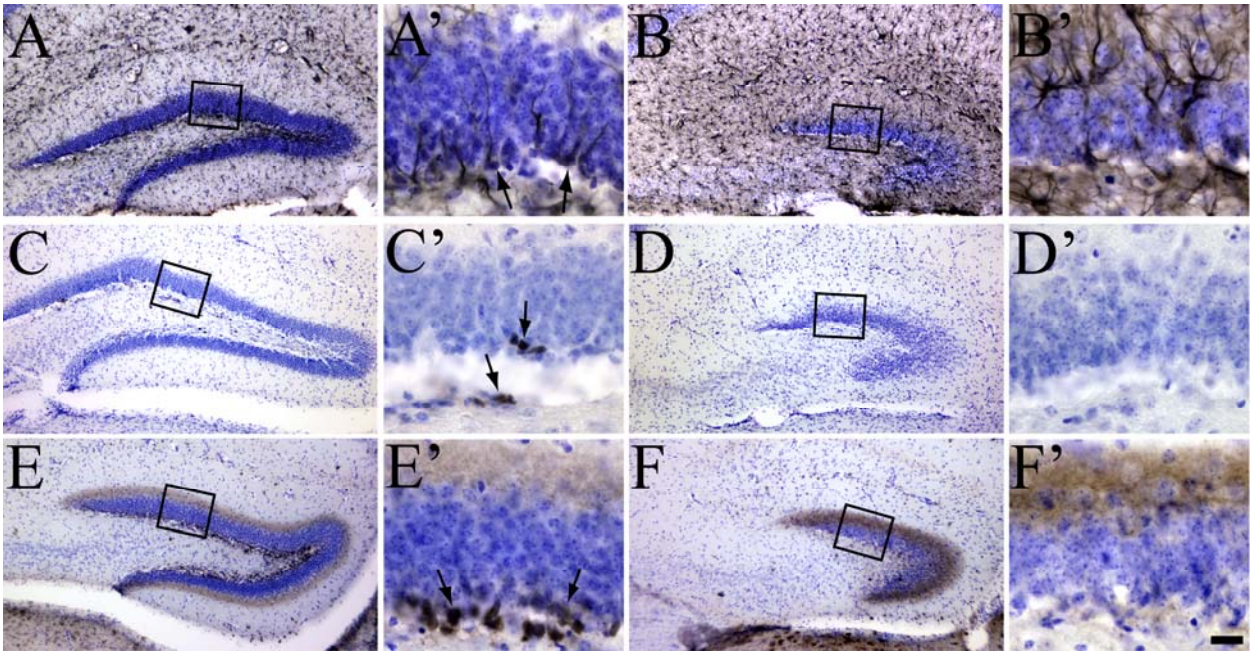

Figure 35. Adult neurogenesis in the dorsal SGZ is impaired

Immunostaining (black) against markers for neurons at different stages of adult neurogenesis on coronal sections through the dorsal hippocampus of control (left columns; A, A', C, C', E, E') and *tlx*^{cKO} (right columns; B, B', D, D', F, F') adults. Radial glia-like GFAP-expressing cells in the SGZ (arrows) are reduced in *tlx*^{cKO} adults (B, B') as compared to controls (A, A'), although GFAP positive astrocytes are increased in the *tlx*^{cK} dentate gyrus. Tbr2-expressing cells are observed in the SGZ of controls (C, C', arrows) but are absent from *tlx*^{cKO} animals (D, D'). Calretinin+ cells in the SGZ are reduced in *tlx*^{cKO} adults (F, F') as compared to controls (E, E', arrows). A' is a higher power image of the boxed region in A, etc. Sections are counterstained for Nissl (blue). Scale bar (in F') = 100μm in A-F; 18μm in A'-F'.

(Figure 35D, D') (n=2). These cells in turn give rise to immature postmitotic granule cells, that transiently express the calcium-binding protein calretinin (Liu et al., 1996; Brandt et al., 2003). There are numerous calretinin-positive cells located in the SGZ of control animals (Figure 35E, E', arrows) whereas there are few in *tlx*^{cKO} animals (Figure 35F, F') (n=4). Calretinin-positive fibers, however, are apparent in the inner molecular layer of both genotypes. Together, these

data indicate that *tlx* is required in dorsal progenitors for the development or maintenance of adult neural stem cells in the SGZ.

The amygdala is also affected in *tlx* null animals, with the lateral (LA) and basolateral (BLA) nuclei substantially reduced relative to controls (Monaghan et al., 1997; Stenman et al., 2003a). These nuclei derive in part from the cells at the cortico-striatal boundary, a region that shows partial recombination in Emx1-Cre animals crossed to the R26R reporter strain (Gorski et al., 2002) as well as in tlx^{cKO} animals (Figure 20, Chapter 4). In Chapter 2, we showed expression of *tlx* in the amygdala in the developing embryo, which could indicate an additional role for *tlx* in the development of this structure. Furthermore, the amygdala is highly interconnected both between amygdaloid nuclei and with many other brain structures, receiving significant input from the cerebral cortex, entorhinal cortex, perirhinal cortex, hippocampus, thalamus, and hypothalamus, with efferent connections to many of these same structures (reviewed by (Sah et al., 2003)). Therefore, in addition to a direct role for *tlx* in the development of the amygdala, there could be indirect effects in *tlx* null animals due to changes in connecting structures. Only a subset of cells within the amygdala (specifically within the LA/BLA nuclei and the corticomedial nuclei) and a subset of connecting structures derive from a dorsal, Emx1-expressing lineage (Gorski et al., 2002). We examined the amygdala of tlx^{cKO} and control animals using immunostaining for specific cell populations on every twelfth section of coronally cut adult brains. Because the size of the amygdalar nuclei can vary along the rostral-caudal axis, sections were carefully matched for anatomical level. We found that the teardrop shape of the LA/BLA is clearly defined in tlx^{cKO} animals but appears reduced in size by visual inspection as compared to controls (Figure 36A-J). Staining for Tbr1, to label pallial-derived glutamatergic cells (Puelles et al., 2000) (Figure 36A-D; n=2), or for calbindin, to label a subset

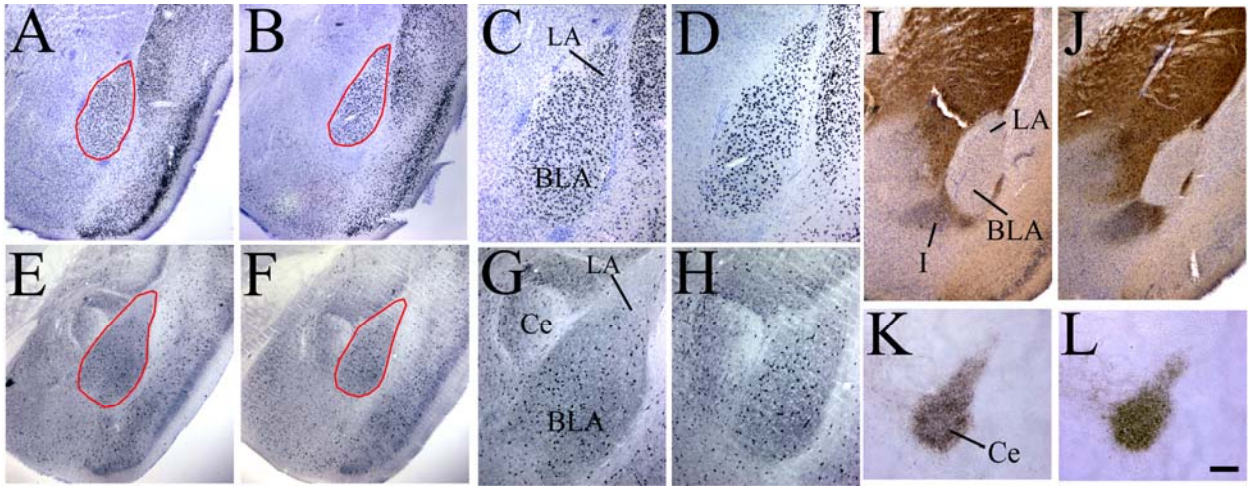

Figure 36. The basolateral nucleus of the amygdala is reduced while the central and interstitial nuclei are unaffected

Tbr1 expression (A-D; black) in excitatory neurons in the basolateral (BLA) and lateral (LA) amygdala (outlined in red in A, B) shows a decrease in the size of the BLA in *tlx*^{cKO} animals (B, D) as compared to controls (A, C). Calbindin expression (E-H; black) shows that the central nucleus (Ce) of the amygdala appears similar in control (E, G) and *tlx*^{cKO} (F, H) brains, whereas the BLA/LA (outlined in red in E, F) is decreased in size. DARPP-32 expression (I, J; brown) in the interstitial nucleus (I) and parts of the Ce delineates the teardrop shape of the BLA and LA. The BLA/LA appears reduced in *tlx*^{cKO} (J) animals as compared to controls (I), whereas the interstitial nucleus appears to be unaltered. CGRP expression (K, L; brown) in the Ce shows no difference between control (K) and *tlx*^{cKO} (L) animals. Sections in A-J are counterstained for Nissl (blue). Scale bar (in L) = 300µm in A, B, E, F; 150µm in C, D, G, H, K, L; 220µm in I, J.

of interneurons as well as some pyramidal-like cells (Kemppainen and Pitkanen, 2000) (Figure 36E-H; n=3), showed a qualitative reduction in the size of the LA/BLA. Staining for the phosphoprotein DARPP-32, which outlines the teardrop shape of the BLA/LA, also shows a reduction in these nuclei (Figure 36I, J; n=3). The central nucleus (Ce), which can be identified by expression of calbindin (Figure 36E-H; n=2) or calcitonin gene-related peptide (CGRP) (Figure 36K, L; n=2) appears similar in *tlx*^{cKO} and control animals. The interstitial nucleus (I),

which shows altered morphology in *tlx* nullanimals (Stenman et al., 2003a), appears similar in control and *tlx*^{cKO} animals, as shown by DARPP-32 expression (Figure 36I, J; n=3). Overall these data show that loss of *tlx* from dorsal progenitors directly or indirectly leads to a reduction in but not absence of pallial-derived nuclei of the amygdala.

The septum has been implicated in many of the behaviors characteristic of *tlx* null animals, including aggression, fear, anxiety, spatial learning, and maternal instincts (reviewed by (Chozick, 1985; Sheehan et al., 2004)). Furthermore, as shown in Chapter 2, during development *tlx* is expressed in regions that will give rise to the septum (Figure 5 and Figure 6). However, the septum has not been specifically studied in *tlx* null animals. Therefore, we examined the septum in both *tlx*^{cKO} and null animals as compared to controls. Every twelfth brain section cut in the coronal plane and every fourth section cut in the horizontal plane were stained with Nissl, and sections through the septum matched histologically for visual comparison. A reduction in the size of the septum (S) in both *tlx*^{cKO} and *tlx* null animals as compared to controls was observed in coronal (Figure 37A-C; n=4) and horizontal (Figure 37D-F; control and *tlx*^{cKO}, n=2; null, n=1) sections, although this was not quantified. Interestingly, the reduction in the septum in conditional mutants appears less severe than in null mutants, which could be explained by the finding that only a subset of cells in the lateral septum derive from an Emx1-expressing lineage (Gorski et al., 2002). Also apparent in these sections is a reduction in the thickness of the corpus callosum in both *tlx*^{cKO} and *tlx* null animals as compared to controls (CC; Figure 37A-F; (Land and Monaghan, 2003)). However, the ventral hippocampal commissure appears relatively similar for all genotypes (vhc; Figure 37D-F).

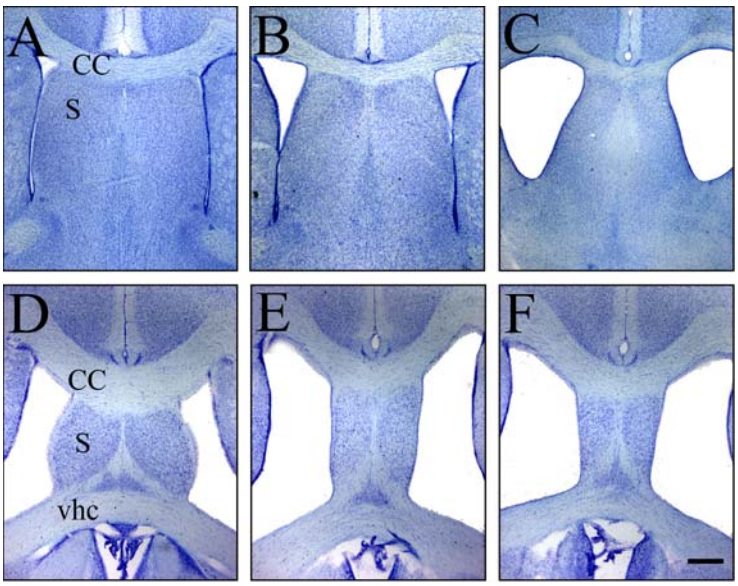

Figure 37. The septum is reduced in conditional and null mutant animals

Coronal (A-C) and horizontal (D-F) sections through control (A, D), *tlx*^{cKO} (B, E), and *tlx* null (C, F) adult brains show a reduction in the size of the septum (S) as well as a reduction in the thickness of the corpus callosum (CC) in both conditional and null mutants. The ventral hippocampal commissure (vhc) appears relatively normal (D-F). Sections are stained for Nissl (blue). Scale bar (in F) = 300μm.

5.3.4 Ventrally-derived structures, including the striatum and hypothalamus, are relatively unaltered

Tlx is required for the normal development of the lateral ganglionic eminence, leading to a smaller striatum in *tlx* null animals (Stenman et al., 2003b). In order to determine whether changes in dorsal PCs and their derivatives has a secondary effect on the development or maturation of the ventrally-derived striatum, we examined this region in *tlx*^{cKO} animals using staining against DARPP-32 (Figure 38A-C; n=3), which labels the patch compartment (Ouimet et al., 1984), and calbindin (Figure 38D-F; n=3), which labels the matrix compartment (Gerfen et

al., 1985). Although the striatum is reduced in size in *tlx* null animals (Figure 38C, F), it appears relatively normal in *tlx*^{cKO} animals (Figure 38B, E) as compared to controls (Figure 38A, D). The islands of Calleja appear as dense Nissl-stained patches in both the control and *tlx*^{cKO} brains but are absent in *tlx* null brains (IC, Figure 38A-C). The anterior wings of the anterior commissure are reduced in both conditional and null mutant brains as compared to controls (AC, Figure 38A-F).

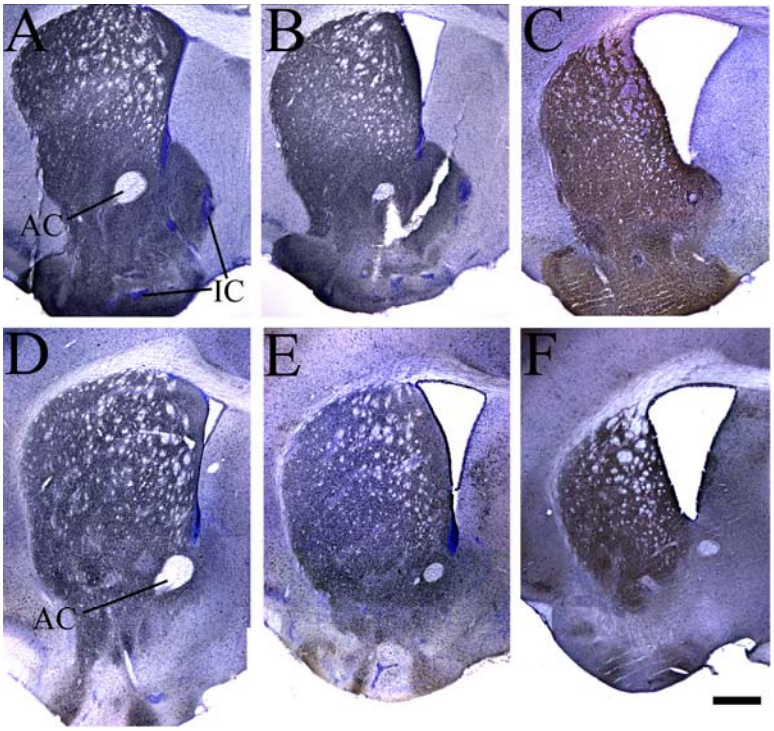

Figure 38. The striatum is relatively unaffected in *tlx*^{cKO} animals

DARPP-32 (A-C; black or brown) and calbindin (D-F; black or brown) expression show that while the adult striatum is reduced in tlx -/- animals (C, F) as compared to controls (A, D), the striatum appears relatively normal in *tlx*^{cKO} animals (B, E). The anterior wings of the anterior commissure (AC) are reduced in both *tlx*^{cKO} animals (B, E) and nulls (C, F). The islands of Calleja (IC) are visible as dense Nissl-stainined patches (blue) in control (A) and *tlx*^{cKO} (B) animals but are absent in *tlx* null animals (C). Sections are counterstained for Nissl (blue). Scale bar (in F) = 500μm.

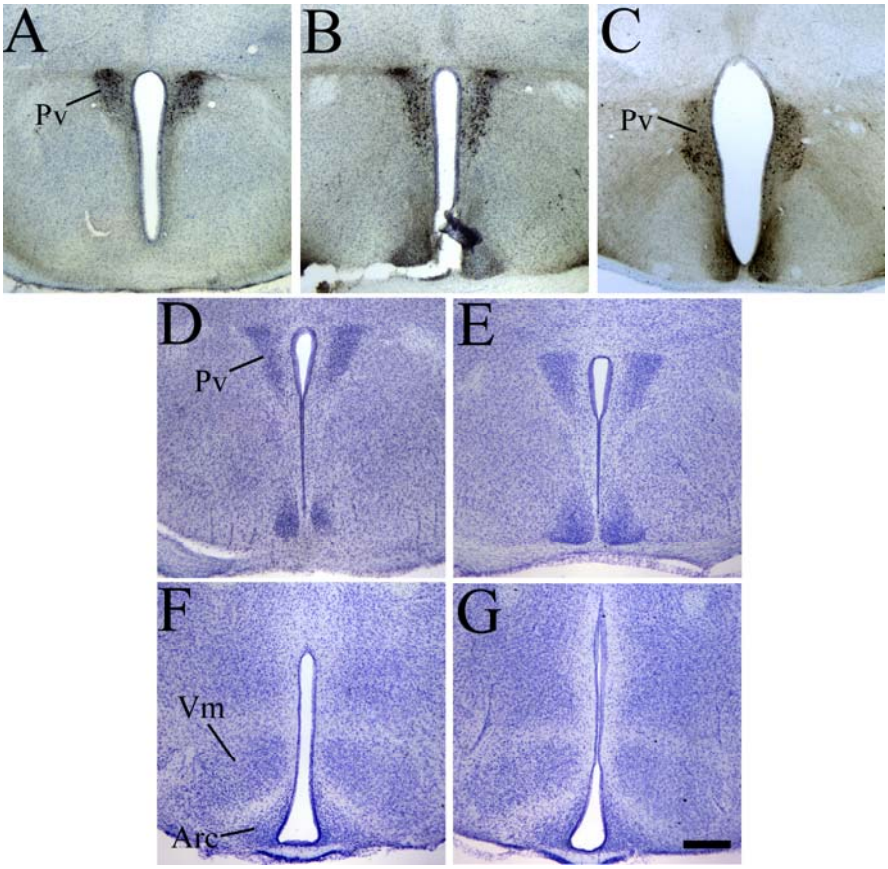

Figure 39. The hypothalamus is relatively unaffected in *tlx*^{cKO} animals

Vasopressin staining (A-C, brown) shows that whereas the paraventricular nucleus (Pv) is disorganized in *tlx* null animals (C) as compared to controls (A) it appears relatively normal in *tlx*^{cKO} animals (B). Nissl staining (blue) through the hypothalamus at two different levels shows that the Pv, the ventromedial nucleus (Vm) and the arcuate nucleus (Arc) appear similar in control (D, F) and *tlx*^{cKO} (E, G) animals. Sections in A-C are counterstained for Nissl (blue). Scale bar (in G) = 300μm.

Similarly, although the hypothalamus does not derive directly from an Emx1 lineage, its development could be influenced through changes in the circuitry of the *tlx*^{cKO} brain. In the absence of *tlx*, abnormalities are seen in the hypothalamus, including abnormal localization of the vasopressin-expressing cells in the paraventricular nucleus of the hypothalamus (Pv, Figure 39C; Monaghan et al., unpublished results). In contrast, the paraventricular nucleus appears

similar in *tlx*^{cKO} and control animals as shown by staining for vasopressin (Figure 39A, B; n=2) or Nissl (Figure 39D, E; n=4). The ventromedial (Vm) and arcuate (Arc) nuclei of the hypothalamus also appear unaltered in *tlx*^{cKO} animals as compared to controls (Figure 39F, G). Overall, these data indicate that structures derived from the ventral telencephalon and the diencephalon (specifically the striatum, the central nucleus of the amygdala, and the hypothalamus) are relatively unaffected in *tlx*^{cKO} animals. Although we cannot rule out indirect effects, such as altered connections, it appears that the structures that are affected in *tlx*^{cKO} animals are those that derive from the dorsal PCs from which *tlx* is deleted.

5.3.5 *Tlx*^{cKO} animals are indistinguishable from littermates during handling or in tests of basic motor or sensory function

Here we have shown that dorsal specific deletion of *tlx* leads to reductions in only a subset of the brain structures altered in the complete absence of *tlx*. To determine how this impacts the behavior of *tlx*^{cKO} animals, we screened adult conditional mutants using a variety of behavioral paradigms, focusing primarily on the behaviors that have previously been shown to be altered in *tlx* null mutants. All animals used in this study have been backcrossed for at least 7 generations to C57Bl/6 mice, and thus are effectively on a C57Bl/6 background (animals with the *tlx* null or floxed allele have been backcrossed for more than 10 generations, animals with the *Emx1-Cre* allele for 7 generations). This is the genetic background that has primarily been used to study behavior in *tlx* null animals (Monaghan et al., 1997; Roy et al., 2002; Young et al., 2002; Belz et al., 2007). Although *tlx* null animals are difficult to handle from birth, exhibiting severe aggression and hyperexcitability (Monaghan et al., 1997; Young et al., 2002), *tlx*^{cKO} animals were indistinguishable during handling or home cage observation. Furthermore, although adult

tlx null males will mutilate or kill littermates and must therefore be housed individually, tlx^{cKO} adult males could be housed in littermate groups. This absence of signs of aggression suggests that in *tlx* null animals aggressive behavior is mediated by changes in ventrally-derived structures. We first assessed general and sensorimotor behavior by observing each mouse in an empty cage for three minutes. Conditional mutant mice showed no gross differences during this observation period in locomotion, posture, ear twitch reflex, or whisker response. tlx^{cKO} and control mice were then put through a battery of tests in order to examine behaviors including basic motor and sensory function, anxiety and depressive-like behaviors, and spatial learning, as outlined in Table 1. The second cohort of animals tested showed abnormal results in the light-dark experiment due to an undetermined technical error; therefore, their data were excluded from this analysis and the data reported here will be pooled from cohorts 1 and 3 pooled together, unless otherwise specified.

To determine whether tlx^{cKO} animals show any differences in activity level, each mouse was tested in an activity monitor chamber in near-darkness for fifteen minutes. No difference from controls was observed in any measure recorded, including total distance traveled ($p=0.31$, $n=19$; Figure 40A) and vertical plane entries ($p=0.58$, $n=19$; Figure 40B), indicating that these animals are not hyperactive. Motor coordination and balance were normal in tlx^{cKO} mice, as indicated by similar latency to fall in the rotarod test ($p=0.74$, $n=19$; Figure 40C). Auditory reflexes were evaluated using acoustic startle response. tlx^{cKO} mice did not differ from controls in maximum startle response over the range of sound levels tested ($F_{1,34}=0.006$, $p=0.94$, $n=18$; Figure 40D). Although it was not examined in tlx^{cKO} animals, we do not expect the development of the retina to be altered because Emx1-driven Cre expression is not observed in the eye

Table 1. Cohort information and behavior test sequence for *tlx*^{cKO} animals

Cohort 1	Cohort 2	Cohort 3
Age: 12-14 months n = 7 7 male, 7 female	Age: 3-4 months n = 7 7 male, 7 female	Age: 4-6 months n = 12 20 male, 4 female
Activity monitor	Light-dark	Activity monitor
Elevated plus maze	Nose poke	Elevated plus maze
Spontaneous alternation	Elevated plus maze	Spontaneous alternation
Light-dark	Spontaneous alternation	Light-dark
Nose poke	Activity monitor	Nose poke
Rotarod	Rotarod	Rotarod
Acoustic startle/PPI	Forced swim	Acoustic startle/PPI
Forced swim	Water maze (w/reversal)	Forced swim
	Acoustic startle/PPI	Water maze (w/reversal)

(Gorski et al., 2002). We qualitatively tested vision using the visual placing task, in which mice are lowered by their tail towards the edge of a table, and, if they extend their forepaws prior to touching the table, it is assumed they can see. Both *tlx*^{cKO} and control animals showed this forepaw extension. Furthermore, *tlx*^{cKO} animals showed similar performance to controls in a visible-platform version of the Morris water-maze (data not shown). Therefore, we conclude that *tlx*^{cKO} animals have no major deficits in basic motor function, sensory function, or startle reflex and have relatively intact vision.

Prepulse inhibition (PPI) of the startle response, the phenomenon by which a weak prepulse suppresses the response to a startling stimulus, is regulated by many forebrain structures that require *tlx* for normal development, including the hippocampus, amygdala, medial prefrontal cortex, striatum, and ventral pallidum (Swerdlow et al., 2001). However, PPI has not previously been examined in *tlx* mutant animals. PPI is considered to provide a measure of sensorimotor

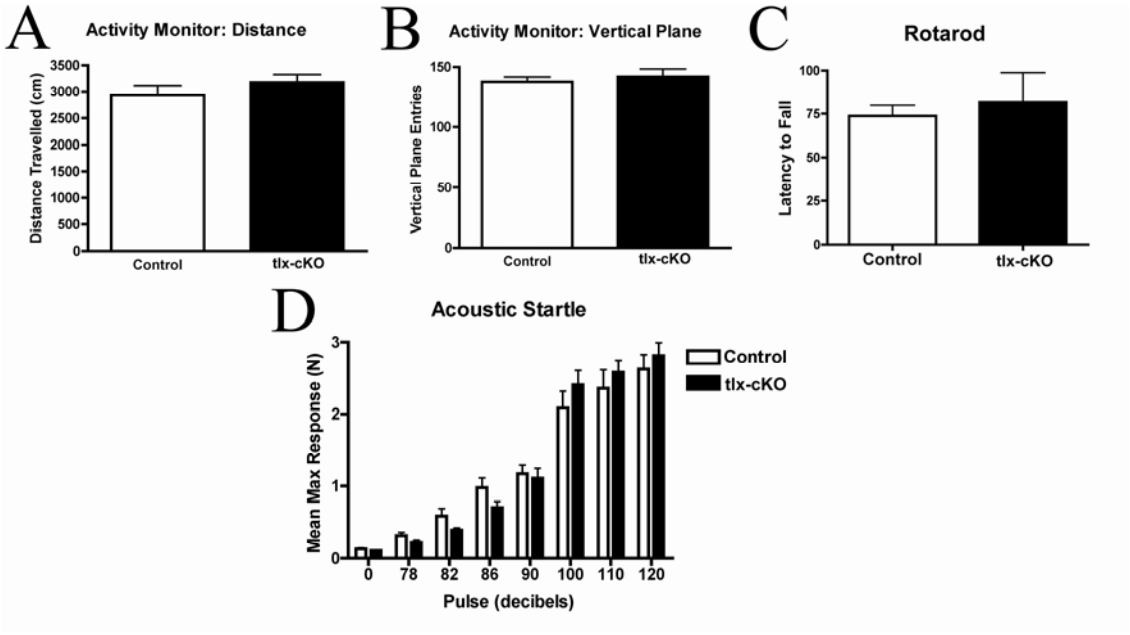

Figure 40. *Tlx*^{cKO} animals show no deficits in basic motor or sensory function

Tlx^{cKO} animals show no statistical difference from controls in either the distance traveled (A) or number of vertical plane entries (B) during fifteen minutes of activity monitoring in a dark chamber. No difference was observed in latency to fall on the rotarod task (C), indicating that *tlx*^{cKO} animals have no deficits in motor function. *tlx*^{cKO} animals showed similar responses to control animals in the acoustic startle task (D), indicating no differences in auditory function. Activity monitor, rotarod, n=19/genotype. Acoustic startle, n=18/genotype.

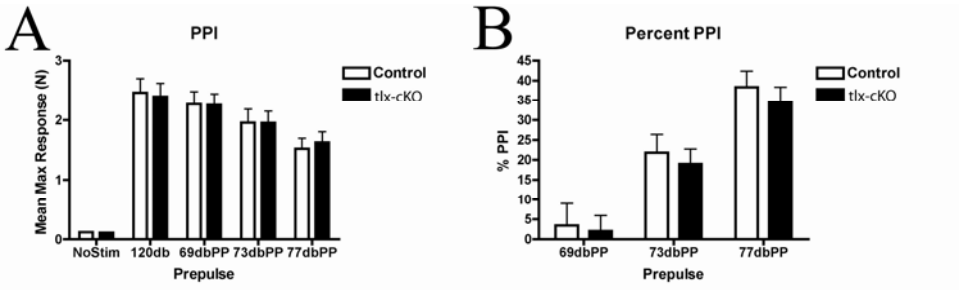

Figure 41. *Tlx*^{cKO} animals show no deficits in prepulse inhibition

Tlx^{cKO} animals show no statistical difference from controls in prepulse inhibition as shown by average startle magnitude (A) and percent prepulse inhibition (B). As expected, animals showed increased inhibition with increasing prepulse intensity. NoStim indicates trials with no pulse (background noise level only). 120db indicates trials with a 120 decibel pulse alone (no prepulse). 69dbPP indicates trials with the 120 decibel pulse preceded by a 69 decibel prepulse. N=18/genotype.

gating, a neural mechanism that inhibits processing of extraneous information. PPI, which can be experimentally measured in human subjects as well as in animal models, is reduced in patients with a variety of different cognitive disorders, including schizophrenia, bipolar disorder (during the manic phase), and several anxiety disorders (Geyer, 2006). *tlx*^{cKO} animals performed similarly to controls in the PPI paradigm, showing similar results for the average maximal startle response over different prepulse levels ($F_{1,34}$<0.001, p=0.99, n=18; Figure 41A) and for percent inhibition at different prepulse levels ($F_{1,34}$=0.308, p=0.58, n=18; Figure 41B). These findings suggest that sensorimotor gating is intact in the absence of *tlx* from dorsal progenitors.

5.3.6 Anxiety and depression-like behavior are reduced in *tlx*^{cKO} animals

Tlx has been shown by several groups to be required for the normal expression of anxiety, independent of vision (Roy et al., 2002; Young et al., 2002; Belz et al., 2007; Zhang et al., 2008). However, it is not known which deficits in the brain contribute to this reduced anxiety. In order to determine whether the brain abnormalities present in *tlx*^{cKO} animals are sufficient to cause this reduced anxiety, we tested anxiety in these animals using several paradigms. The light-dark box produces a natural conflict situation between the aversion of rodents to brightly illuminated areas and the tendency to explore (Bourin and Hascoet, 2003). The time spent in the light half of the box is indicative of the level of anxiety of the animal, with animals that are less anxious spending more time in the light. *Tlx*^{cKO} animals spent significantly more time in the aversive light half of the light-dark box, 42.6% ± 2.1% as compared to 33.4% ± 2.5% for controls (p<0.01, n=19; Figure 42A), which suggests that that these animals are less anxious than controls. We tested exploratory or novelty-seeking behavior by counting the number of nose pokes made by the animals into holes in the side of an open-field chamber. *Tlx*^{cKO} animals made significantly more

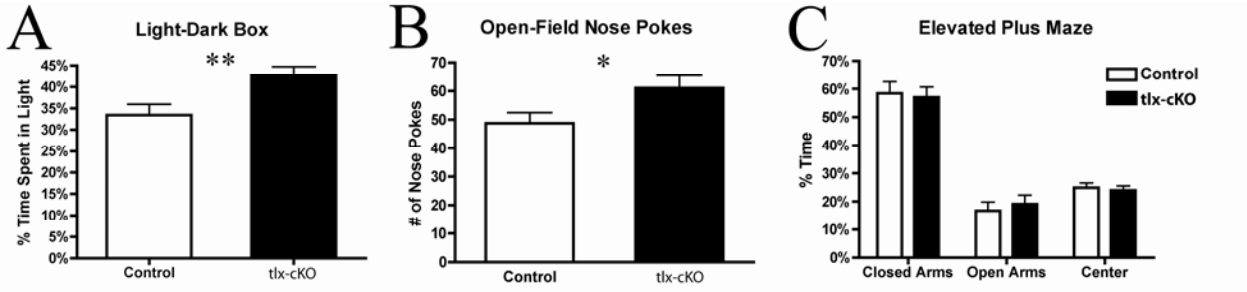

Figure 42. Anxiety is reduced in *tlx*^{cKO} animals

Tlx^{cKO} animals spent significantly more time than controls in the aversive light half of a light-dark chamber during a 5-minute test (A). *tlx*^{cKO} animals made significantly more nose-pokes into holes in the side of an open-field chamber during a 10-minute test (B). No significant differences were observed in time spent in open or closed arms of an elevated plus maze during a 5-minute test (C). * $p<0.05$; ** $p<0.01$. Light-dark, nose pokes, n=19/genotype. EPM n=18/genotype.

nose pokes, 61.0 ± 4.4 as compared to 48.7 ± 3.7 for controls ($p<0.05$, n=19; Figure 42B). Although this test does not directly address anxiety, a similar task examining head dipping in a novel environment fitted with a hole-board has been shown to be sensitive to anxiogenics and anxiolytics (Takeda et al., 1998). A second commonly used test of anxiety, the elevated plus maze, is based on the aversion of rodents to open spaces (Bourin et al., 2007). This maze is generally constructed as a raised "plus", with two opposing arms that are enclosed on the sides by walls and two opposing arms that are open. Mice generally prefer the closed arms; increased time spent in the open arms is used as a measure of reduced anxiety. *Tlx*^{cKO} animals did not show a significant difference from controls in time spent in closed ($p=0.80$, n=18) or open arms ($p=0.61$, n=18) (Figure 42C). Despite these results, we conclude based on the differences observed in the light-dark and nose poke tests that *tlx*^{cKO} animals exhibit reduced anxiety.

Although depression-like behaviors have not been tested in animals lacking functional *tlx* expression, anxiety and depression show high co-morbidity in humans and are thought to involve

many overlapping brain structures and circuits (Gorman, 1996). We examined depression-like behavior in our mice using the forced swim test. In this test animals are forced to swim in a small cylinder from which there is no escape; typically, after initial vigorous activity, animals will adapt a nearly immobile posture that is termed "behavioral despair", as it is thought to indicate that the animal has given up hope of escape (Porsolt et al., 2001). Treatment with antidepressants has been shown to reduce immobility, which suggests that time floating correlates with levels of "depression". *Tlx*^{cKO} animals spent significantly less time floating, 36.4% ± 4.4% as compared to 50.6% ± 2.9% for controls ($p<0.05$, n=18; Figure 43). These data suggest that *tlx*^{cKO} animals show both reduced anxiety and reduced depression.

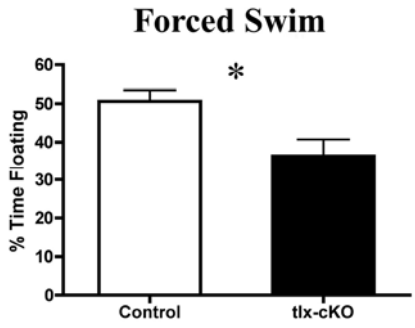

Figure 43. *Tlx*^{cKO} animals show reduced depressive-like behavior

Tlx^{cKO} animals spend significantly less time floating in the forced swim test. Results are shown for the last 4 minutes of a 6 minute test. * $p<0.05$. N=18/genotype.

5.3.7 *Tlx*^{cKO} animals show normal spatial learning but deficits in behavioral flexibility

Similar to *tlx* null animals, *tlx*^{cKO} animals have a significantly reduced hippocampus, and there is some indication that adult neurogenesis is impaired. Although the impaired vision in *tlx* null

animals has been shown to have a significant impact on their ability to perform the spatial learning task in the Morris water maze, there is evidence that *tlx* in the developing brain and in the adult does have a role in more challenging testing paradigms (Belz et al., 2007; Zhang et al., 2008). In order to determine whether the deficits in brain structure observed in tlx^{cKO} affect spatial learning in these animals we tested them using a hidden-platform version of the Morris water maze (Vorhees and Williams, 2006). We tested the second cohort of animals using a five-day training protocol followed by a probe trial 24 hours later on the sixth day, during which the hidden platform was removed and mice were tracked for 60 seconds. Tlx^{cKO} animals performed similarly to controls during training, as determined by two-way repeated measures ANOVA ($F_{1,8}$=2.34, p=0.16, n=5; Figure 44A) and showed significant memory retention for the platform location during the probe trial, with no difference between genotypes for time spent in the target quadrant (p=0.44, n=7; Figure 44B) or average distance from target (p=0.45, n=7). To examine the ability of these animals to extinguish their initial learning of the platform location in order to learn a new location (reversal learning), we then trained this same cohort for five days with the platform in the opposite quadrant followed by a probe trial on the sixth day. Again tlx^{cKO} animals performed similarly to controls during training ($F_{1,12}$=0.286, p=0.60, n=7; Figure 44C) and showed similar retention of the new platform location during the probe trial, with no difference between genotypes for the time spent in the new target quadrant (p=0.20, n=7; Figure 44D) or average distance from target (p=0.50, n=7). Overall the results from this initial cohort of animals indicated that despite the reduction in the hippocampus tlx^{cKO} animals are still capable of spatial and reversal learning.

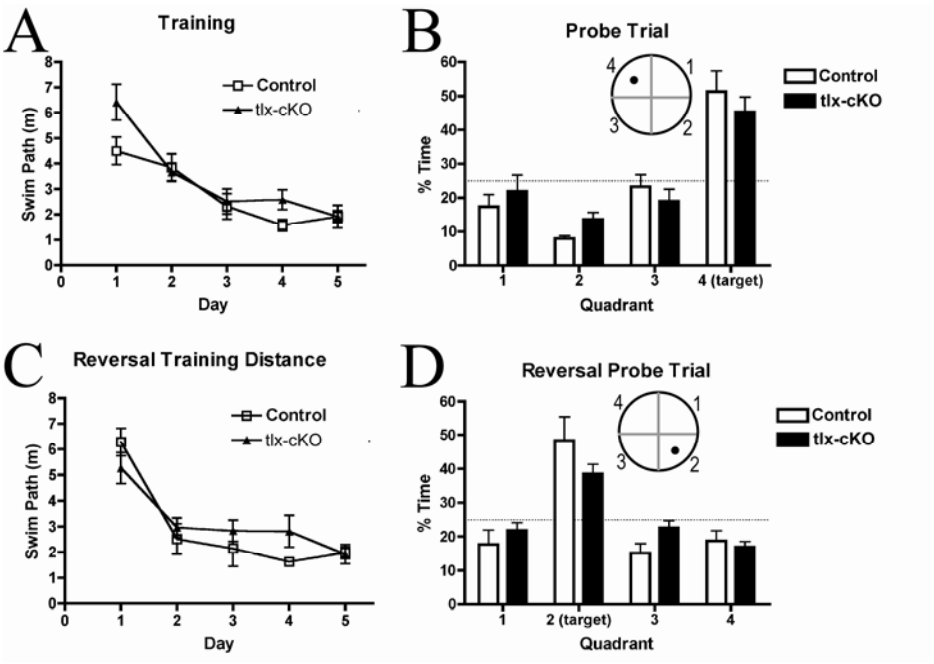

Figure 44. No deficits in spatial learning were observed using a one-probe water maze protocol

Tlx^{cKO} and control mice were trained on a hidden platform Morris water maze for 5 days (A). Memory was tested with a probe trial conducted on day 6 (B). No difference in spatial learning was observed, and animals of both genotypes showed a significant preference for the target quadrant during the probe trial (4; B, diagram). This was followed by 5 days of reversal training (C) with a probe trial conducted on day 6 (D). No significant differences were observed either during training or during the probe trial, with animals of both genotypes showing a preference for the target quadrant (2; D, diagram). Dotted lines indicate chance level (25%). N=7/genotype.

Experiments testing the role of *tlx* in adult neurogenesis showed that knocking out *tlx* in the adult using a tamoxifen-inducible Cre resulted in delays in spatial and reversal learning although these animals did show similar learning to controls by the end of training (Zhang et al., 2008). Therefore, with the third cohort of animals we used a longer water maze training paradigm with more probe trials conducted during the training period. Animals were trained for eight days, with probe trials conducted two hours before training on days 3, 5, and 7 with a final probe trial on day 9 (Figure 45A, arrows). *Tlx*^{cKO} animals performed similarly to controls during

training as determined by two-way repeated measures ANOVA ($F_{1,20}$=1.231, p=0.28, n=11; Figure 45A). Animals of both genotypes showed similar memory retention for the platform location during the final probe trial on day 9, with no significant difference in time spent in the target quadrant (p=0.73, n=11; Figure 45B) or average distance from target (p=0.64, n=11) (data shown here for the first 30 seconds of the probe trial). *tlx*^{cKO} animals also showed similar learning to controls as indicated by time spent in the target quadrant over successive probe trials (Figure 45C). Animals of both genotypes first showed significant memory retention for the platform location by day 7, as determined by paired t-test comparison of time spent in the target quadrant versus average time spent in non-target quadrants (control p<0.01, n=11; mutant p<0.05, n=11; data reported for full 60 seconds of probe trial).

This cohort of animals (cohort 3) was next tested for reversal learning using a six day training paradigm with a probe trial two hours before training on day 4 and a final probe trial on day 7. *tlx*^{cKO} animals showed significant overall impairment during reversal training ($F_{1,20}$=5.902, p<0.05, n=11; Figure 45D), although post-hoc contrasts did not indicate significant differences by genotype on any individual day. *tlx*^{cKO} animals did not appear to have learned the new target location by day 4, spending significantly less time in the target quadrant than controls (p<0.01, n=11; Figure 45E) and showing a greater average distance from the target (p<0.05, n=11) (data reported for the first 30 seconds of the probe trial). The reduced time spent in the new target quadrant was in part due to increased time spent in the old target location (quadrant 4), although this time was not significantly different from that of controls (p=0.17, n=11). By the final probe trial on day 7 *tlx*^{cKO} animals appeared to have successfully learned the new target location, as indicated by a similar amount of time spent in the target quadrant as compared to controls (p=0.23, n=11; Figure 45F). Animals of both genotypes spent significantly more time in

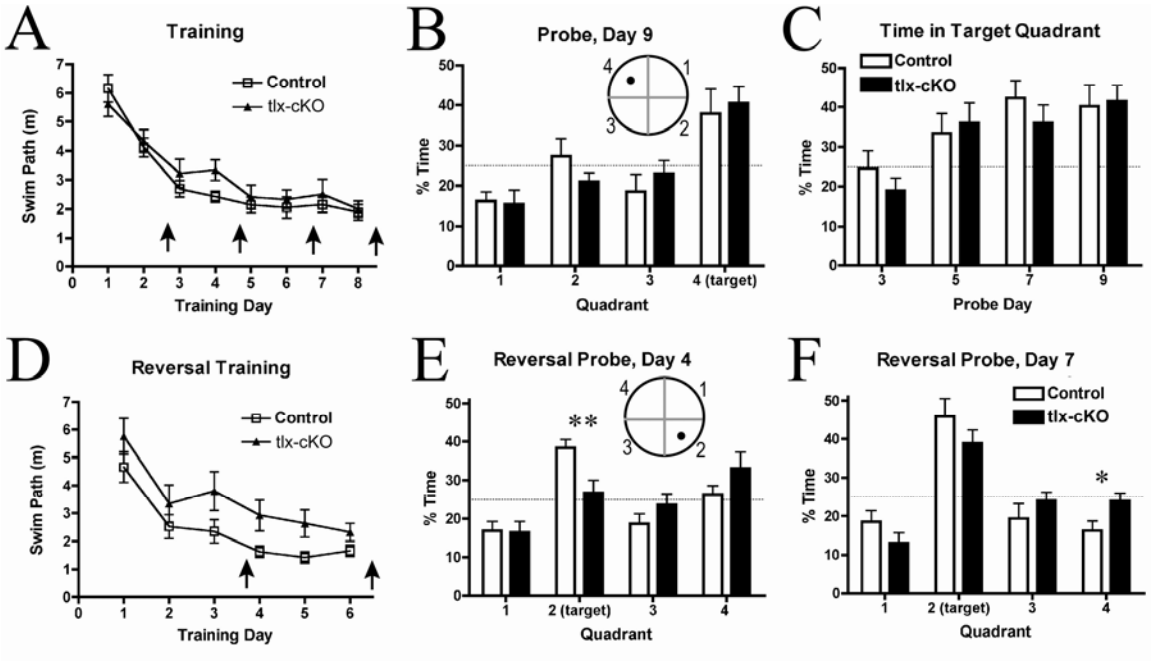

Figure 45. Spatial learning is normal but *tlx*^{cKO} animals show deficits in behavioral flexibility

Tlx^{cKO} and control mice were trained in a hidden platform Morris water maze for 8 days (A). Memory was tested with probe trials conducted 2 hours before training on days 3, 5, 7 with a final trial on day 9 (A, arrows). Animals of both genotypes showed significant preference for the target quadrant (4) by the final probe trial (B), and both showed similar improvements in memory over the different probe trials (C). This was followed by 6 days of reversal training (D) with probe trials conducted 2 hours before training on day 4 and on day 7 (arrows). *tlx*^{cKO} animals were significantly impaired in learning during reversal training as compared to controls ($p<0.05$). By the day 4 reversal probe trial (E) control animals spent significantly more time in the target quadrant (2) but *tlx*^{cKO} animals spent a chance amount of time. By the final reversal probe on day 7 (F) *tlx*^{cKO} animals spent a similar amount of time to controls in the target quadrant but still spent significantly more time in the previously learned target quadrant (4). The platform was located in quadrant 4 during training (B, diagram) and in quadrant 2 during reversal training (E, diagram). Dotted lines indicate chance level (25%). * $p<0.05$; ** $p<0.01$. N=11/genotype.

the target quadrant as compared to the average of the non-target quadrants (control $p<0.01$, n=11; mutant $p<0.01$, n=11). However, *tlx*^{cKO} animals spent significantly more time in the old target quadrant (quadrant 4) than controls during the day 7 probe trial ($p<0.05$, n=11; Figure 45F) and continued to show a greater average distance from the reversal target location ($p<0.05$, n=11). Overall, these results indicate that despite significant hippocampal reduction, *tlx*^{cKO} animals have intact spatial learning. These animals do however show impaired reversal learning.

We further examined spatial learning in *tlx*^{cKO} animals using a spontaneous alternation task. Spontaneous alternation is a measure of exploratory behavior but performance depends on spatial working memory (Lalonde, 2002). Lesion studies have implicated numerous brain regions in spontaneous alternation, including the prefrontal cortex, hippocampus, septum, striatum, and cerebellum (Lalonde, 2002). We used a variant of the task described by Ragozzino et al. (Ragozzino et al., 1998) in which mice are released into a 4-arm plus-maze and allowed to freely explore for 15 minutes, with the order of arm entries recorded. *tlx*^{cKO} animals showed no significant difference from controls in percent alternation, defined as the percent of 5-arm sets that include entries into all 4 arms ($p=0.28$, n=19; Figure 46A). We also analyzed perseverative or repetitive behavior, defined as the percent of 3-arm entries in which the same arm was entered twice (percent triplets). No significant difference in percent triplets was observed between genotypes ($p=0.043$, n=19; Figure 46B). These results support the conclusion that spatial learning is normal in *tlx*^{cKO} animals.

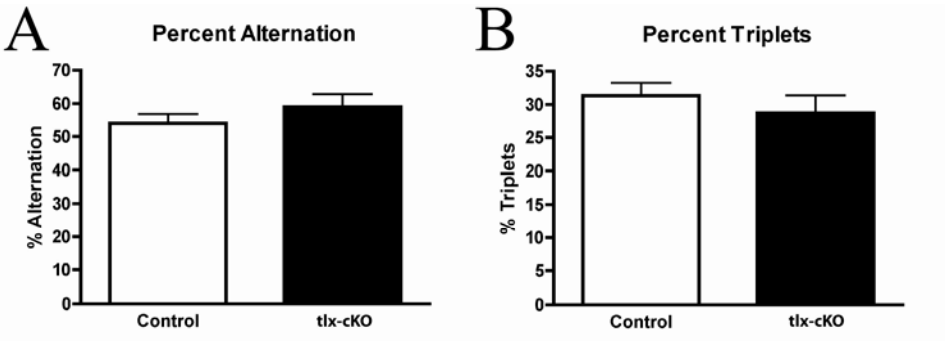

Figure 46. *Tlx*^{cKO} animals show no deficits in spontaneous alternation

Tlx^{cKO} and control animals were put into a 4-arm radial maze and allowed to freely explore for 15 minutes. The order of arm entry was recorded. *tlx*^{cKO} animals show no statistical difference from controls in percent alternation (A; sets of 5 arm entries that include entries into all 4 of the arms) or percent triplets (B; sets of 3 arm entries that only include entry into 2 different arms). N=19/genotype.

5.4 DISCUSSION

In this study we have used mice in which *tlx* has been specifically knocked out in dorsal progenitors from early stages of neurogenesis in order to examine the developmental connection between brain structure and behavior. Whereas mice completely lacking functional *tlx* expression exhibit a variety of structural and behavioral abnormalities, only a subset of these are observed when deletion of *tlx* is restricted to dorsal progenitors, as summarized in Table 2. *tlx*^{cKO} animals show reductions in many dorsally-derived structures, including the cerebral cortex, the hippocampus, the lateral/basolateral nuclei of the amygdala, the septum, and in fiber tracts, including the corpus callosum and the anterior commissure. Ventrally-derived cortical interneurons as well as structures including the striatum and the hypothalamus appear to be relatively unaffected. These animals show reduced anxiety and depression-like behavior but do not exhibit the severe aggression or hyperactivity characteristic of *tlx* null animals. *Tlx*^{cKO}

animals show normal spatial learning but some deficits in reversal learning, which suggests an impairment in behavioral flexibility. Our findings indicate that *tlx* has a role in dorsal progenitors in the development of specific brain structures and consequently the normal development of specific behaviors.

Table 2. Anatomical and behavioral deficits in *tlx* null versus *tlx*^{cKO} animals

Brain structure	Null	*tlx*^{cKO}	Behavior	Null	*tlx*^{cKO}
Cortex: surface area	↓	↓	Aggression	↑	--
Cortex: thickness	↓	↓	Maternal Instincts	↓	Not tested
Glutamatergic neurons	↓	↓	Hyperexcitable	↑	--
GABAergic neurons	↓/--	--	Motor coordination	Not tested	--
Glia	↑	↑	Anxiety	↓	↓
Hippocampus	↓	↓	Depression	Not tested	↓
Amygdala	↓	↓/--	Spatial learning	↓	--
Septum	↓↓	↓	Reversal learning	Not tested	↓
Striatum	↓	--	Fear conditioning	↓	Not tested
Hypothalamus	Disorganized	--	Acoustic startle	Not tested	--
Corpus callosum	↓	↓	PPI	Not tested	--
Olfactory bulbs	↓	↓	Epilepsy	↑	--
Eye	↓	--	Vision	↓	--

5.4.1 *Tlx* has an important role in the hippocampus for the normal development of anxiety

The hippocampus has been implicated in many behaviors, including spatial learning, anxiety, and depression, but it has become clear that different regions of the hippocampus have distinct roles in the expression of behavior coupled with differences in patterns of connectivity and

neuronal constitution (Moser and Moser, 1998; Bannerman et al., 2004b; Sahay and Hen, 2007). Here we have shown that in *tlx*^{cKO} animals the entire hippocampus is reduced in size, with the dentate gyrus particularly reduced at dorsal levels, but the overall size reduction more pronounced at ventral levels. Whereas the dorsal hippocampus (septal pole) has a preferential role in learning and memory, the ventral hippocampus (temporal pole) has been implicated in emotional behaviors such as anxiety and depression (Moser and Moser, 1998; Bannerman et al., 2004b; Sahay and Hen, 2007). Unlike the dorsal hippocampus, ventral hippocampus projects to prefrontal cortex. The ventral hippocampus is also closely connected to the lateral, basolateral, and central nuclei of the amygdala, the bed nucleus of the stria terminalis, and other structures associated with the hypothalamic-pituitary-adrenal (HPA) axis (Moser and Moser, 1998; Bannerman et al., 2004b; Sahay and Hen, 2007). Lesions of the ventral hippocampus have been shown to lead to a reduction in anxiety but have no effect on spatial learning (Moser et al., 1993; Kjelstrup et al., 2002; Bannerman et al., 2004b; McHugh et al., 2004). We have shown that *tlx* has a role in the normal development of the ventral hippocampus, and we propose that, in the absence of *tlx*, the reduction in this region contributes to the reduced anxiety observed in *tlx*^{cKO} animals in the light-dark box and open-field nose poke tasks.

Numerous lesion studies as well as studies using acute drug microinfusion have shown that the dorsal hippocampus has a preferential role in spatial learning in memory (Moser et al., 1993; Moser et al., 1995; Moser and Moser, 1998; Bannerman et al., 2004b). Despite significant changes in the dorsal hippocampus of *tlx*^{cKO} animals, spatial learning appeared to be intact as examined in the water maze and spontaneous alternation tasks. This is possibly due to some extent to intact vision in these conditional mutants, as it has previously been suggested that the deficiencies in spatial learning in the complete absence of *tlx* are due at least in part to blindness

of these animals, although these results are somewhat unclear (Belz et al., 2007; Zhang et al., 2008). However, it has also been shown using lesion studies in rats that as little as 26% of the dorsal hippocampus is sufficient to support learning in the water maze (Moser et al., 1995). Furthermore, whereas the reduction in the *tlx*^{cKO} hippocampus is most pronounced in the dentate gyrus, it has been suggested that the size of CA1 but not the dentate gyrus is crucial to spatial learning (Volpe et al., 1992; Olsen et al., 1994). Thus, our results support the conclusion that animals can show normal spatial learning with substantial dorsal hippocampal reduction.

Tlx has been shown to regulate the proliferation of adult neural stem cells, and deletion of *tlx* either from early developmental stages or acutely in the adult leads to loss of proliferation and neurogenesis (Shi et al., 2004; Liu et al., 2008; Zhang et al., 2008). Acute deletion of *tlx* from the adult brain using inducible Cre-mediated recombination results in delays in spatial learning (Zhang et al., 2008). As expected, neurogenesis is impaired in the dorsal hippocampus of *tlx*^{cKO} animals, indicated by a decreased number of GFAP-positive and calretinin-positive cells in the SGZ and an absence of Tbr2-positive cells. However, we did not observe any difference in spatial learning as compared to controls. The role of adult neurogenesis in spatial learning is somewhat unclear, as other studies have failed to find any impairment (Shors et al., 2002; Snyder et al., 2005; Saxe et al., 2006). Zhang and colleagues (Zhang et al., 2008) argue that the training protocol is critical in order to observe this subtle learning deficit as, in contrast to previous studies, hidden platform testing preceded visible platform testing in their protocol. In our study we similarly began with hidden platform testing, although other small differences in training, such as a longer trial duration (we used 1 minute as opposed to 40 seconds) could explain the normal learning observed with *tlx*^{cKO} animals. The most important difference between these studies, however, is that in *tlx*^{cKO} animals *tlx* is deleted in dorsal progenitors from an early

developmental stage, which allows for the possibility of developmental compensation in learning mechanisms.

Tlx^{cKO} animals showed delayed acquisition of the new platform location during the reversal phase of the water maze, exhibiting perseveration in the original platform location, which indicates a deficit in behavioral flexibility. Reversal learning has been shown to be impaired by lesions to orbitofrontal cortex or dorsal striatum (Divac et al., 1967; Ragozzino et al., 2002; Schoenbaum et al., 2002; McAlonan and Brown, 2003; Clarke et al., 2008). There is also evidence that the basolateral amygdala has a role downstream from orbitofrontal cortex in associative encoding, although lesions of the basolateral amygdala alone do not affect behavioral flexibility (Schoenbaum et al., 1999; Paton et al., 2006; Stalnaker et al., 2007). Since we have shown that the striatum appears relatively normal in *tlx*^{cKO} animals, we propose that the changes in the cerebral cortex and basolateral amygdala are sufficient to cause impaired behavioral flexibility.

5.4.2 The septum has a key role in mediating emotional behavior

The septum has a critical role in regulating both emotional and cognitive behavior (Chozick, 1985; Sheehan et al., 2004). "Septal rage syndrome", as demonstrated decades ago in rats with septal lesions (Brady and Nauta, 1953; King, 1958), manifests as a profile of hyperexcitability, aggression, and increased startle response very similar to the behavior observed in *tlx* null animals (Monaghan et al., 1997; Roy et al., 2002; Young et al., 2002). Further studies have confirmed these results and identified an important role for the septum in many other behaviors. The medial septum, which makes substantial cholinergic and GABAergic projections to the hippocampus, is important for spatial learning (Kelsey and Landry, 1988; Decker et al., 1995;

Bannerman et al., 2004a; Sheehan et al., 2004). The lateral septum mediates the aggressive behavior observed in septal lesion animals and has a critical role in fear and anxiety, but it is not clear exactly how the lateral septum regulates these behaviors (Decker et al., 1995; Treit and Menard, 1997; Bannerman et al., 2004a; Degroot and Treit, 2004; Sheehan et al., 2004). The lateral septum can be subdivided into different regions based on cytoarchitecture, connectivity, and neurotransmitter expression (Risold and Swanson, 1997b, a). However, most studies have failed to examine these different subregions, and the lesion studies that have established the role of the septum generally target the entire lateral septum, if not the medial septum as well. In this study we have identified a significant reduction in the size of the septum in the absence of *tlx*, with a lesser reduction in tlx^{cKO} animals. Although we have not yet identified the specific cell populations that are affected, we can speculate given that Emx1-driven Cre is not expressed in the medial septum (Gorski et al., 2002) that the lateral septum is reduced in tlx^{cKO} animals. We further predict that, similar to the cerebral cortex, later-born cells are specifically affected; the lateral septum is born after the medial septum and develops in an outside to inside manner (Bayer, 1979). Septal lesions produce anxiolytic effects similar to what we observed in tlx^{cKO} animals (Decker et al., 1995; Treit and Menard, 1997; Bannerman et al., 2004a; Degroot and Treit, 2004; Sheehan et al., 2004). This suggests that normal development of the lateral septum in conjuction with the ventral hippocampus is necessary for the normal expression of anxiety. Further analysis will allow us to identify specific populations of cells in the septum that are absent and therefore potentially involved in the normal expression of anxiety.

The septum and hypothalamus are two of the key regions that show differences between *tlx* null animals (which are very aggressive) and tlx^{cKO} animals (which do not show signs of aggression and have a normal startle response). It has been proposed that the rostral part of the

lateral septum (LSr) is specifically involved in mediating defensive as well as agonistic behaviors via inhibition of circuits mediating these actions (Risold and Swanson, 1997b). The LSr has dense bidirectional connections with the medial hypothalamus, in particular the anterior, dorsomedial ventromedial, and dorsal premammillary nuclei, which have been implicated in forms of aggressive behavior (Canteras et al., 1997; Risold and Swanson, 1997b; Haller et al., 2006). The medial hypothalamus could directly affect the motor components of defensive response through downstream projections to parts of the brainstem including the periaqueductal gray (Risold and Swanson, 1997b). Neurons in these hypothalamic nuclei show c-Fos immunoreactivity following defensive or agonistic behaviors, and bilateral lesions of the dorsal premammillary nucleus abolishes defensive responses in rats (Canteras et al., 1997; Haller et al., 2006). We propose that this circuit involving the LSr and the medial hypothalamus mediates the aggressive behavior observed in *tlx* null animals.

5.4.3 Contributions of other brain areas

Unlike the ventral hippocampus, the amygdala seems to be involved more in fear than in anxiety (Bannerman et al., 2004b). Lesion studies support a role for the amygdala in fear conditioning but not in anxiety (Treit et al., 1993a; Treit and Menard, 1997; Kjelstrup et al., 2002; McHugh et al., 2004), although studies involving localized drug infusions have yielded mixed results (Treit et al., 1993b; Pesold and Treit, 1995; Sajdyk et al., 2002a; Sajdyk et al., 2002b). Similarly, small lesions to specific amygdalar nuclei support a role for the amygdala in fear but find no effect on aggression (Oakes and Coover, 1997; Nader et al., 2001). *Tlx*^{cKO} animals show a reduction in the size of the lateral and basolateral nuclei of the amygdala, although the cellular composition of these regions seems similar to that of controls. Although we did not examine fear conditioning

in this study, we predict based on the findings that blindness is the cause of poor performance in both contextual and cued fear conditioning in *tlx* null animals (Belz et al., 2007; Zhang et al., 2008) that we would not observe any deficits in tlx^{cKO} animals. It is possible that the reduced number of cells present in the amygdala of tlx^{cKO} animals is sufficient to perform normally in the production of fear and anxiety. However, given the substantial connections between the lateral/basolateral nuclei and the ventral hippocampus (Pitkanen et al., 2000), we cannot rule out a contribution to the observed behavioral abnormalities.

In addition to reduced anxiety, tlx^{cKO} animals also showed a reduction in depression-like behavior, as shown by decreased time spent floating during the forced-swim test. Anxiety disorders and depression show high co-morbidity in human patients and can in many cases be treated with similar drugs, which suggests similar underlying neurobiological mechanisms (Gorman, 1996). Indeed, studies using animal models have identified numerous factors involved in both anxiety and depression, such as the serotonin transporter, brain-derived neurotrophic factor, and neuropeptide Y receptors (Holmes et al., 2003b; Holmes et al., 2003a; Lira et al., 2003; Chen et al., 2006b; Zhao et al., 2006; Painsipp et al., 2008). The ventral hippocampus, which we suggest is critical for the normal development of anxiety, contains many serotonergic, dopaminergic, and noradrenergic terminals (Gage and Thompson, 1980; Verney et al., 1985). Many other brain structures affected in tlx^{cKO} animals have also been implicated in depression, including the cerebral cortex, amygdala, and septum (Sheline, 2003; Sheehan et al., 2004; Sahay and Hen, 2007). Additionally, a reduction in astrocytes in the prefrontal and anterior cingulate cortex has been reported in human patients with major depression (Johnston-Wilson et al., 2000; Webster et al., 2001; Cotter et al., 2002), and it has recently been shown that pharmacological ablation of glia can produce depressive-like behavior in rats (Banasr and Duman, 2008). These

findings raise the intriguing possibility that the increased glia observed in *tlx*^{cKO} animals is somehow beneficial, contributing to the observed reduction in depression-like behavior.

5.4.4 Conclusions

We have identified a critical role for *tlx* in dorsal progenitors in the development of forebrain structures including the cerebral cortex, hippocampus, amygdala, and septum, and in the development of anxiety, depression, and behavioral flexibility. Our data support a role for the development of the ventral hippocampus and lateral septum in the normal expression of anxiety and possibly depression. Our studies also suggest that reductions in specific types of cells in the cerebral cortex and basolateral amygdala are sufficient to cause impairments in behavioral flexibility. The absence of severe aggression phenotype in *tlx*^{cKO} animals suggests that aggression is mediated by a distinct subregion of the septum in conjunction with the hypothalamus. Further studies to identify the specific cells in the septum that are affected in null and conditional *tlx* mutants will help to elucidate the precise role of septum in anxiety and aggression. Overall, this study provides a developmental model in which changes to specific regions of the brain can be correlated with behavioral abnormalities.

6.0 DISCUSSION

The development of the mature functioning brain is controlled by the precise regulation of the neural progenitor cells that give rise to all of the neurons and glia in the central nervous system. The normal development of adult behaviors depends upon these early processes, and changes in the proliferation, neurogenesis, or gliogenesis of PCs have a lasting impact on brain structure and behavior. Neural PCs are a heterogeneous population that matures over the course of development, tightly controlled by a complex system of intrinsic and extrinsic factors. The connection between this early regulation of PCs and the development of the adult brain and behavior is still not fully understood. Identifying early developmental processes that regulate specific behavioral changes will lend important insight into the pathology of human neuropsychiatric disorders. The transcription factor *tlx* is a highly conserved gene that is expressed in forebrain PCs and is critical for the normal development of the vertebrate brain, with loss of function resulting in significant structural and behavioral abnormalities. Here I have provided evidence that *tlx* is expressed in a subset of PCs in the developing forebrain, and has a role specifically within PCs of the dorsal telencephalon in the development of a specific set of brain structures and behaviors. This allows us to begin to make connections between early development and behavior.

I first characterized *tlx* expression in the developing forebrain. During neurogenesis *tlx* is expressed in PCs in regions that give rise to structures including the cortex, the hippocampus, the

septum, the striatum, and the hypothalamus, and in a subset of cells in the ventral differentiating field in the region of the developing amygdala, although further characterization will be needed to identify these cells. Within the dorsal telencephalon I showed that TLX protein is restricted primarily to radial glial cells (RGCs) in the VZ, overlapping significantly with RGC marker Pax6 (Gotz et al., 1998). In contrast TLX is only expressed in a subset of cells in the SVZ; although some TLX-expressing cells in the VZ and lower SVZ may also express the intermediate progenitor cell (IPC) marker Tbr2 (Englund et al., 2005) most Tbr2-positive cells in the SVZ do not express *tlx*. This pattern is reminiscent of the pattern of co-expression of Pax6 and Tbr2, which are thought to be expressed sequentially in early glutamatergic neurogenesis, with Pax6 downregulated in the transition from a RGC to an IPC (Englund et al., 2005). I propose that *tlx* is similarly down-regulated during the RGC to IPC transition. This raises the question of whether *tlx* has a role in the production of IPCs.

Although expression of *tlx* is restricted to RGCs, my findings demonstrate that in both *tlx* null and dorsal-specific conditional tlx^{cKO} mutants Tbr2-expressing IPCs are reduced throughout embryonic development, beginning as early as E12.5. This suggests that *tlx* acts within RGCs in the dorsal telencephalon to influence the production or maturation of IPCs. Furthermore, I showed that in both tlx^{cKO} and *tlx* null animals that the number of RGCs, estimated by absence of *Tbr2* at E12.5 and directly identified by Pax6 expression at E14.5 and E18.5, does not differ from that of controls. As shown in both this study in tlx^{cKO} animals and previous studies of *tlx* null animals (Roy et al., 2002; Roy et al., 2004), absence of *tlx* results in premature neurogenesis and an early increase in differentiated neurons relative to controls. This phenotype could be explained by a change in the type of division made by RGCs. IPCs are generated by asymmetric divisions of RGCs to produce an RGC and an IPC (Haubensak et al., 2004; Miyata et al., 2004;

Noctor et al., 2004; Attardo et al., 2008; Noctor et al., 2008). A shift from these IPC-producing divisions (RGC-IPC) to asymmetric neurogenic divisions (RGC-N) would increase the production of neurons and decrease the production of IPCs but should not affect the number of RGCs. IPCs add a secondary source of proliferating PCs (Haubensak et al., 2004; Miyata et al., 2004; Noctor et al., 2004), amplifying neuronal production particularly from mid-neurogenesis. Therefore, although a switch to neurogenic divisions would initially result in more neurons, as development progresses fewer neurons would ultimately be produced. Inactivation of Tbr2 has been suggested to favor such a shift in RGC divisions, and results in a phenotype strikingly similar to that observed in *tlx* null and conditional mutants (Arnold et al., 2008; Sessa et al., 2008). Although it does not explain the entire phenotype observed in the absence of *tlx*, my findings indicate that *tlx* promotes the production or maturation of IPCs, and in the absence of *tlx* RGCs undergo neurogenic divisions at the expense of IPC-producing divisions. This model is summarized in Figure 47.

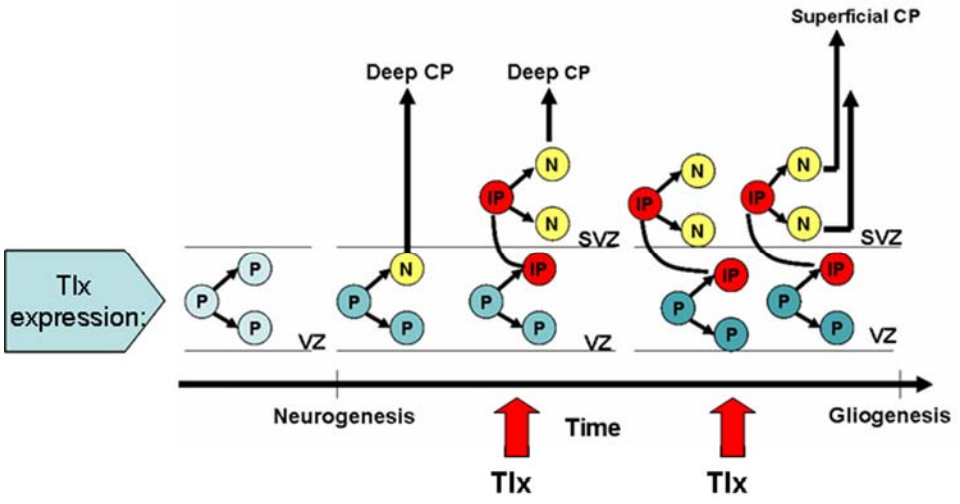

Figure 47. A role for *tlx* in the production of IPCs

Tlx has a role within radial glia progenitors (P) in promoting the production of intermediate progenitors (IP) throughout neurogenesis.

Within the dorsal VZ, *tlx* is expressed unevenly; *in situ* hybridization for *tlx* mRNA shows a columnar expression pattern, with subsets of cells that do not appear to express *tlx* mRNA, whereas TLX protein appears to be expressed in most RGCs but at varying levels. This expression pattern could reflect different subpopulations of RGCs with different properties. PCs responsive to CBF1-mediated Notch signaling show a columnar pattern similar to that of *tlx* mRNA that seems to reflect a role for this signaling pathway in maintaining progenitors as RGCs (Mizutani et al., 2007). Notch signaling through CBF1 activates pro-progenitor bHLH genes such as *hes1* and *hes5* (reviewed by (Yoon and Gaiano, 2005)). Data from our lab indicate that *tlx* regulates the transcription of *hes1* (Drill and Monaghan, unpublished results) which suggests a possible link between *tlx* and the Notch signaling pathway. Interestingly, unpublished data from our lab suggests that at E13.5 only a subset of RGCs express β-galactosidase, which is knocked into the *tlx* null locus and therefore expressed under the control of the *tlx* promoter, and that the proportion of RGCs that express β-galactosidase is increased in *tlx* null animals as compared to heterozygotes (Kuznicki and Monaghan, unpublished results). One possible explanation is that this β-galactosidase-negative population reflects those RGCs that have committed to IPC-producing divisions and downregulated *tlx* expression. Thus, in *tlx* null animals fewer RGCs undergo IPC-producing divisions and the β-galactosidase-negative population is reduced. Future studies could examine this hypothesis through clonal analysis in culture to identify differences in the progeny of β-galactosidase-positive PCs as compared to β-galactosidase-negative PCs. Cells would be collected from E13.5 dorsal cortex and FACS sorted for a general progenitor marker and the presence or absence of β-galactosidase, then each population cultured at clonal density for a week. IPCs have a more limited capacity for proliferation than RGCs; IPCs can undergo proliferative divisions to produce more IPCs, but

they mainly undergo symmetric divisions to produce neurons (Haubensak et al., 2004; Miyata et al., 2004; Noctor et al., 2004). Therefore, if the β-galactosidase-negative population corresponds to those PCs fated to produce IPCs I predict that this population will exhibit smaller clone sizes that include fewer glial cells as compared to the β-galactosidase-positive population.

My results suggest that *tlx* is necessary for the normal production of IPCs; but does *tlx* expression directly promote the production of IPCs? Overexpression of Tbr2 has been shown to promote an IPC fate and inhibit cell cycle exit (Sessa et al., 2008). Preliminary results from experiments in which I used *in utero* electroporation to overexpress *tlx* in the E13.5 dorsal telencephalon did not seem to promote an IPC fate in transfected cells, as determined by Tbr2 expression, instead affecting migration or maturation of neurons (Drill and Monaghan, unpublished results). However, these experiments were done using a constitutively active promoter to express *tlx*, and although our data suggest that *tlx* promotes divisions that produce IPCs, down-regulation of *tlx* might be an important step in the actual transition from an RGC to an IPC. Further experiments using *in utero* electroporation to overexpress *tlx* under the control of a progenitor-specific promoter such as the Nestin promoter (Zimmerman et al., 1994) or to knock down *tlx* using siRNA in a subset of cells at specific developmental stages could help identify the role of *tlx* in IPC development. *Tlx* might influence IPC production in conjunction with *pax6*, which is required cell autonomously for the normal expression of *tbr2* (Quinn et al., 2007). This proposed combined regulation of IPC development could explain the synergistic function of *tlx* and *pax6* in the formation of upper cortical layers (Schuurmans et al., 2004).

The data presented in this thesis demonstrate that *tlx* is important in the generation of IPCs. Currently, little is known about the specific role for IPCs in the normal development of adult brain structure and behavior; *tlx* mutants therefore provide a unique opportunity to link

perturbations in IPCs with an adult phenotype. In order to focus on specific aspects of the complex phenotype observed in null animals, I examined the anatomy and behavior of adult *tlx*^{cKO} animals in which *tlx* is deleted only from dorsal PCs. These conditional mutants exhibit a subset of the changes in brain structure that have been observed in *tlx* nulls, including reductions in the surface area and thickness of the cerebral cortex, the hippocampus, the lateral/basolateral nuclei of the amygdala, the septum, and the corpus callosum. Ventrally-derived cortical interneurons as well as structures including the striatum and hypothalamus appear to be relatively unaffected, which suggests a limited role for dorsal input in the gross development of ventral structures. A common theme of the abnormalities in *tlx*^{cKO} animals is the greater reduction in later born structures. Within the cerebral cortex, later-born superficial layers are specifically affected. Caudal functional cortical areas are disproportionately reduced, which could reflect the rostral to caudal gradient of neurogenesis within the cortex (Bayer and Altman, 1991). Although the hippocampus is reduced in overall size, the most severe change is observed in the dentate gyrus, specifically the infrapyramidal blade, which is born later than the suprapyramidal blade during early postnatal development (Altman and Bayer, 1990). The septum also develops in a precisely timed manner, with the medial septum born first, followed by the lateral septum generated in an outside to inside laminar pattern (Bayer, 1979). Although additional study will be necessary to identify the specific septal nuclei affected by the loss of *tlx*, we speculate that the medial septum is not affected given that Emx1-driven Cre recombination is only observed in the lateral septum (Gorski et al., 2002). I propose that this reduction in later-born cells and structures in *tlx* mutants is the result of the depletion of PCs, particularly IPCs, later during development, rather than a requirement for *tlx* in the direct specification of cells that contribute to these precise structures. In support of this hypothesis, Tbr2 conditional mutants

show similar reductions in the surface area and thickness of the cerebral cortex, specifically superficial cortical layers, and in the dentate gyrus, where the infrapyramidal blade shows the greatest reduction (Arnold et al., 2008).

IPCs have been primarily examined with respect to the development of the cerebral cortex. Interestingly, Tbr2, which is used as a molecular marker for IPCs in the dorsal telencephalon (Englund et al., 2005), is also expressed during development in a subset of cells in the dorsal part of the septum and in cells that give rise to pallial-derived nuclei of the amygdala (Bulfone et al., 1999). As I have shown, *tlx* expression is observed in these same regions. In *tlx*^{cKO} animals patchy expression of *tlx* is observed in the region corresponding to the ventral pallium, which sends cells to the amygdala, and preliminary results suggest that *tlx* expression may also be absent from the dorsal part of the septal neuroepithelium (data not shown). This raises the intriguing possibility that IPCs have a critical role in the development of these structures as well as the cerebral cortex. Together, these findings suggest that the deficits in the amygdala and the septum in *tlx*^{cKO} animals may be the result of deficits in IPCs in these regions, identifying a novel role for IPCs in telencephalic development.

The developmental and anatomical deficits in conditional *tlx* mutants lead to a relatively small set of behavioral abnormalities, specifically reduced anxiety and depressive-like behavior and deficits in behavioral flexibility. This allows us to make predictions about the structures and circuits involved in generating these behaviors. I propose that the reduced anxiety and depression in *tlx*^{cKO} animals results from deficits in the ventral hippocampus and the septum. Previous studies linking these regions with anxiety have generally used models derived from perturbation of the adult brain through lesions or localized drug injections (Moser and Moser, 1998; Bannerman et al., 2004b; Sheehan et al., 2004). In contrast, our study provides an

important model of the underlying developmental mechanisms. Anxiety and depression are symptoms associated with a wide variety of neuropsychiatric disorders. Anxiety disorders alone have a lifetime prevalence of 28.8% in the general population, and show high comorbidity with other disorders, including major depressive disorder and bipolar disorder (Gorman, 1996; McIntyre et al., 2006; Stein, 2006). Notably, the human *tlx* homologue *NR2E1* is significantly associated with bipolar disorder types I and II (Kumar et al., 2008).

Tlx^{cKO} animals do not display any signs of the aggression readily apparent in *tlx* null animals, although formal testing has not been done. This absence of aggression led us to hypothesize that the aggressive phenotype of null animals is mediated by brain structures or circuits unaffected in conditional mutants. I propose that this aggression is mediated by a circuit involving the septum, particularly the rostral part of the lateral septum, and the hypothalamus. Future studies using different Cre lines to generate additional conditional *tlx* mutants may be able to isolate this and other behaviors and provide important information about the underlying pathology. Aggression in humans is still poorly understood, and few animal models of aggression of developmental origin have been characterized (Miczek et al., 2007). Regulation of serotonin neurotransmission, and of the serotonin receptor 1A in particular, have been linked to both anxiety and aggression (Holmes et al., 2003a; Furmark et al., 2004; Zhao et al., 2006; Caramaschi et al., 2007; Miczek et al., 2007). Examination of serotonin transmission or receptor expression in *tlx* null and conditional mutants may help to further elucidate the mechanism of these altered behaviors.

Tlx null animals exhibit losses of distinct interneuron populations (Monaghan et al., 1997; Roy et al., 2002). However, no gross changes in interneuron populations were observed in *tlx*^{cKO} animals, which suggests that there is limited influence from the dorsal telencephalon in the

regulation of interneuron production and maturation. Although *NR2E1* has been linked with schizophrenia (Jackson et al., 1998; Kohn and Lerer, 2005; Kumar et al., 2008), *tlx*^{cKO} animals did not exhibit any deficits in pre-pulse inhibition, which is reduced in patients with schizophrenia and is a standard test for animal models of the disorder (Swerdlow et al., 2001; Geyer, 2006). Deficits in interneurons seem to be a critical component of human neuropsychiatric disorders such as schizophrenia (Lewis et al., 2005). To examine the potential link between *tlx* and schizophrenia, I propose that conditional mutant mice be generated in which *tlx* is deleted from the ventral telencephalon and tested for a schizophrenia-like phenotype in behavioral paradigms including pre-pulse inhibition. This could be done using a Cre line such as Nkx2.1-Cre (Xu et al., 2008), which will target interneurons derived from the MGE including parvalbumin- and somatostatin-expressing cells. Another Cre line that could be used is l12b-Cre, which drives expression of Cre recombinase under the control of a Dlx1/2 regulatory element thereby targeting most cortical interneurons as well as cells in the striatum and amygdala (Potter et al., 2009); however, as Cre expression in these animals is not detected in most cells until they have reached the SVZ, it is possible that *tlx* will not be deleted early enough to show an effect.

In this study I demonstrated that caudal and medial functionally-defined areas of the cortex in *tlx* null animals show a disproportionate reduction relative to the overall reduction in cortical surface area. In particular, primary visual cortex is specifically reduced; this same reduction is observed in the *tlx*^{cKO} animals, which have grossly normal vision and should have normal expression of *tlx* in the developing eye. This indicates that the reduction in visual cortex is therefore not due to the abnormal development of the optic nerve and retina in *tlx* null animals (Yu et al., 2000; Young et al., 2002; Miyawaki et al., 2004; Zhang et al., 2006). Rather, I

propose that this reduction in surface area is due to changes in the expansion of the PC population leading to the depletion of later-born caudal areas. However, additional markers will need to be examined to confirm that *tlx* does not interact with signaling molecules, such as FGFs or Wnts, to affect area specification, particularly in light of the observed reduction in the population of Wnt-expressing cells in the cortical hem. Overall, this raises the interesting question of whether a smaller visual cortex matters; does it have any effect on function? Although these animals show no gross visual deficits, more stringent tests of vision may still reveal subtle differences. Alternatively, it could be that the remaining cells in the smaller visual cortex are sufficient for normal function, perhaps implying redundancy in the normal adult visual system.

My findings described in this thesis suggest a role for *tlx* in the maturation of dorsal PCs and in the decisions they make during development. I propose that *tlx* acts within dorsal RGCs to promote divisions that produce IPCs, a secondary population of proliferating cells that have recently been shown to have an integral role in producing most of the neurons in the developing cerebral cortex. Normal expression of *tlx* in the dorsal telencephalon is important for the development of specific aspects of the adult brain and behavior. Association of *NR2E1* with human disorders suggests that this gene is important for human behavior, although interestingly, all mutations that have been identified appear to affect transcriptional regulation of *tlx* (Kumar et al., 2007; Kumar et al., 2008). Therefore, an important next step in elucidating the role of *tlx* in the development of behavior and in particular its relevance to neurological disorders will be to determine how it is regulated throughout development. One initial approach would be to determine whether any *Drosophila* genes that have been shown to regulate *tailless* expression have mammalian homologues and, if so, whether they have a similar role in regulating *tlx* in

mice. A second approach would be to use a DNA affinity capture assay (Gadgil et al., 2001; Park et al., 2005) to isolate and identify transcription factors or other associated proteins that bind to the *tlx* promoter in embryonic neural tissue. Characterization of identified transcription factors that regulate *tlx* in the developing mouse telencephalon will provide important insight into the mechanisms that underlie development in the human brain.

In this study, we have identified an important role for *tlx* in the production of intermediate progenitor cells in the dorsal cortex. Loss of *tlx* disrupts this specific subset of progenitors, leading to specific alterations in adult brain structure and behavior. Given that the primary developmental deficit in the absence of *tlx* is a reduction in intermediate progenitor cells, this suggests a potential novel role for this progenitor population in the development of structures outside of the cerebral cortex, including the hippocampus, basolateral amygdala, and lateral septum. Although we have not modeled a single human disorder, we have identified a developmental model of a behavioral endophenotype, anxiety, that is common to many neuropsychiatric disorders. With a model such as this, which goes from early neurogenesis to adult anatomy and behavior, we can begin to identify the processes that underlie both normal and pathological behaviors. Ultimately, improving our understanding of how behavior develops, and what happens when this system is perturbed early in life, will help us to better manage human developmental neuropsychiatric disorders.

APPENDIX A: ANTIBODIES USED FOR IMMUNOHISTOCHEMISTRY

Table 3. Antibodies used for immunohistochemistry

Target	Host	Company	Dilution	Cells/Structure Labeled	Reference
β-galactosidase (β-gal)	chicken	Abcam	1:500	Expressed under the control of the *tlx* promoter in the null allele	(Monaghan et al., 1997)
Calbindin	mouse	Sigma	1:1000	Cortical interneuron subpopulation; granule cell somata in the DG of the hippocampus; interneurons and some pyramidal cells in the amygdala; matric compartment of the striatum	(Gerfen et al., 1985; Sloviter, 1989; Kubota et al., 1994; Gonchar and Burkhalter, 1997; Kemppainen and Pitkanen, 2000)
Calretinin	rabbit	Chemicon	1:2500	Cortical interneuron subpopulation; immature postmitotic granule cells in the hippocampus	(Kubota et al., 1994; Liu et al., 1996; Gonchar and Burkhalter, 1997; Brandt et al., 2003)
CGRP (Calcitonin gene related peptide)	rabbit	Abcam	1:2000	Central nucleus of the amygdala	(Kawai et al., 1985; Yasui et al., 1991)
Ctip2 (COUP TF-interacting protein 2)	rat	Abcam	1:500	A subset of cells in cortical layer V	(Avram et al., 2000; Arlotta et al., 2005)
Cux1 (Cut-like homeobox 1)	rabbit	Santa Cruz	1:500 (Embryo) 1:1000 (Adult)	Upper cortical layers II/III and IV; IZ and SVZ in the embryo	(Nieto et al., 2004; Zimmer et al., 2004)

Target	Host	Company	Dilution	Cells/Structure Labeled	Reference
DARPP-32 (dopamine- and cAMP-regulated phosphoprotein)	rabbit	Chemicon	1:500	Interstitial nucleus and parts of the central nucleus of the amygdala; patch compartment of the striatum	(Ouimet et al., 1984)
GABA (γ-aminobutyric acid)	rabbit	Sigma	1:1000	Interneurons (general marker)	(Houser et al., 1983)
GFAP (Glial fibrillary acidic protein)	mouse	Sigma	1:400 (Embryo) 1:1000 (Adult)	Astrocytes; adult neural precursors in the dentate gyrus	(Bignami et al., 1972; Uyeda et al., 1972; Seri et al., 2001)
GFAP (Glial fibrillary acidic protein)	rabbit	Sigma	1:1000 (Adult)	Astrocytes; adult neural precursors in the dentate gyrus	(Bignami et al., 1972; Uyeda et al., 1972; Seri et al., 2001)
GLAST (Glutamate transporter)	guinea pig	Chemicon	1:4000	Radial glia progenitors	(Shibata et al., 1997; Hartfuss et al., 2001)
NeuN (Neuronal nuclei)	mouse	Chemicon	1:500	Mature neurons (general marker)	(Mullen et al., 1992)
Parvalbumin	mouse	Sigma	1:2000	Cortical interneuron subpopulation	(Kubota et al., 1994; Gonchar and Burkhalter, 1997)
Pax6 (Paired-box-containing gene 6)	rabbit	Covance	1:500	Radial glia progenitors	(Gotz et al., 1998)
Serotonin	rabbit	Immunostar	1:20,000	Terminations of thalamocortical axons in layer IV of primary sensory cortical areas (P8)	(Fujimiya et al., 1986)
Sox10 (SRY-box containing gene 10)	rabbit	CeMines	1:500	Precursors and oligodendrocytes	(Kuhlbrodt et al., 1998)
Tbr1 (T-box brain gene 1)	rabbit	Chemicon	1:1000 (Embryo) 1:2000 (Adult)	Glutamatergic cells in the subplate and layer VI of the cortex, weakly expressed by cells in	(Bulfone et al., 1995; Puelles et al., 2000; Hevner

Target	Host	Company	Dilution	Cells/Structure Labeled	Reference
				layers II/III and IV and a few cells in V; pallial-derived glutamatergic cells in the amygdala	et al., 2003; Kolk et al., 2005)
Tbr2 (T-box brain gene 2)	rabbit	Chemicon	1:1000 (Embryo) 1:2000 (Adult)	Intermediate progenitor cells in the embryonic cortex and adult hippocampus	(Englund et al., 2005; Hodge et al., 2008)
Tlx	rabbit	Gift from Y. Shi	1:1000	Tlx protein	(Li et al., 2008)
Tuj1 (Neuron-specific class III β-tubulin)	mouse	Sigma	1:1000	Early pan-neuronal marker	(Lee et al., 1990)
Vasopressin	rabbit	Chemicon	1:2000	Paraventricular nucleus of the hypothalamus	(Caffe and van Leeuwen, 1983)

BIBLIOGRAPHY

Abrahams BS, Kwok MC, Trinh E, Budaghzadeh S, Hossain SM, Simpson EM (2005) Pathological aggression in "fierce" mice corrected by human nuclear receptor 2E1. J Neurosci 25:6263-6270.

Abrahams BS, Mak GM, Berry ML, Palmquist DL, Saionz JR, Tay A, Tan YH, Brenner S, Simpson EM, Venkatesh B (2002) Novel vertebrate genes and putative regulatory elements identified at kidney disease and NR2E1/fierce loci. Genomics 80:45-53.

Allanson JE (2007) Noonan syndrome. Am J Med Genet C Semin Med Genet 145C:274-279.

Altman J, Bayer SA (1990) Migration and distribution of two populations of hippocampal granule cell precursors during the perinatal and postnatal periods. J Comp Neurol 301:365-381.

Alvarez-Buylla A, Garcia-Verdugo JM, Tramontin AD (2001) A unified hypothesis on the lineage of neural stem cells. Nat Rev Neurosci 2:287-293.

Anderson SA, Eisenstat DD, Shi L, Rubenstein JL (1997) Interneuron migration from basal forebrain to neocortex: dependence on Dlx genes. Science 278:474-476.

Anderson SA, Marin O, Horn C, Jennings K, Rubenstein JL (2001) Distinct cortical migrations from the medial and lateral ganglionic eminences. Development 128:353-363.

Angevine JB, Jr., Sidman RL (1961) Autoradiographic study of cell migration during histogenesis of cerebral cortex in the mouse. Nature 192:766-768.

Anthony TE, Klein C, Fishell G, Heintz N (2004) Radial glia serve as neuronal progenitors in all regions of the central nervous system. Neuron 41:881-890.

Arlotta P, Molyneaux BJ, Chen J, Inoue J, Kominami R, Macklis JD (2005) Neuronal subtype-specific genes that control corticospinal motor neuron development in vivo. Neuron 45:207-221.

Armentano M, Chou SJ, Tomassy GS, Leingartner A, O'Leary DD, Studer M (2007) COUP-TFI regulates the balance of cortical patterning between frontal/motor and sensory areas. Nat Neurosci 10:1277-1286.

Arnold SJ, Huang GJ, Cheung AF, Era T, Nishikawa S, Bikoff EK, Molnar Z, Robertson EJ, Groszer M (2008) The T-box transcription factor Eomes/Tbr2 regulates neurogenesis in the cortical subventricular zone. Genes Dev 22:2479-2484.

Attardo A, Calegari F, Haubensak W, Wilsch-Brauninger M, Huttner WB (2008) Live imaging at the onset of cortical neurogenesis reveals differential appearance of the neuronal phenotype in apical versus basal progenitor progeny. PLoS ONE 3:e2388.

Avram D, Fields A, Pretty On Top K, Nevrivy DJ, Ishmael JE, Leid M (2000) Isolation of a novel family of C(2)H(2) zinc finger proteins implicated in transcriptional repression mediated by chicken ovalbumin upstream promoter transcription factor (COUP-TF) orphan nuclear receptors. J Biol Chem 275:10315-10322.

Backman M, Machon O, Mygland L, van den Bout CJ, Zhong W, Taketo MM, Krauss S (2005) Effects of canonical Wnt signaling on dorso-ventral specification of the mouse telencephalon. Dev Biol 279:155-168.

Bai J, Ramos RL, Ackman JB, Thomas AM, Lee RV, LoTurco JJ (2003) RNAi reveals doublecortin is required for radial migration in rat neocortex. Nat Neurosci 6:1277-1283.

Banasr M, Duman RS (2008) Glial loss in the prefrontal cortex is sufficient to induce depressive-like behaviors. Biol Psychiatry 64:863-870.

Bani-Yaghoub M, Tremblay RG, Lei JX, Zhang D, Zurakowski B, Sandhu JK, Smith B, Ribecco-Lutkiewicz M, Kennedy J, Walker PR, Sikorska M (2006) Role of Sox2 in the development of the mouse neocortex. Dev Biol 295:52-66.

Bannerman DM, Matthews P, Deacon RM, Rawlins JN (2004a) Medial septal lesions mimic effects of both selective dorsal and ventral hippocampal lesions. Behav Neurosci 118:1033-1041.

Bannerman DM, Rawlins JN, McHugh SB, Deacon RM, Yee BK, Bast T, Zhang WN, Pothuizen HH, Feldon J (2004b) Regional dissociations within the hippocampus--memory and anxiety. Neurosci Biobehav Rev 28:273-283.

Barnabe-Heider F, Wasylnka JA, Fernandes KJ, Porsche C, Sendtner M, Kaplan DR, Miller FD (2005) Evidence that embryonic neurons regulate the onset of cortical gliogenesis via cardiotrophin-1. Neuron 48:253-265.

Bayer SA (1979) The development of the septal region in the rat. I. Neurogenesis examined with 3H-thymidine autoradiography. J Comp Neurol 183:89-106.

Bayer SA, Altman J (1991) Neocortical Development. New York: Raven Press.

Belz T, Liu HK, Bock D, Takacs A, Vogt M, Wintermantel T, Brandwein C, Gass P, Greiner E, Schutz G (2007) Inactivation of the gene for the nuclear receptor tailless in the brain preserving its function in the eye. Eur J Neurosci 26:2222-2227.

Berardi N, Pizzorusso T, Maffei L (2000) Critical periods during sensory development. Curr Opin Neurobiol 10:138-145.

Bertrand N, Castro DS, Guillemot F (2002) Proneural genes and the specification of neural cell types. Nat Rev Neurosci 3:517-530.

Bignami A, Eng LF, Dahl D, Uyeda CT (1972) Localization of the glial fibrillary acidic protein in astrocytes by immunofluorescence. Brain Res 43:429-435.

Bishop KM, Goudreau G, O'Leary DD (2000) Regulation of area identity in the mammalian neocortex by Emx2 and Pax6. Science 288:344-349.

Bond J, Roberts E, Mochida GH, Hampshire DJ, Scott S, Askham JM, Springell K, Mahadevan M, Crow YJ, Markham AF, Walsh CA, Woods CG (2002) ASPM is a major determinant of cerebral cortical size. Nat Genet 32:316-320.

Bond J, Scott S, Hampshire DJ, Springell K, Corry P, Abramowicz MJ, Mochida GH, Hennekam RC, Maher ER, Fryns JP, Alswaid A, Jafri H, Rashid Y, Mubaidin A, Walsh CA, Roberts E, Woods CG (2003) Protein-truncating mutations in ASPM cause variable reduction in brain size. Am J Hum Genet 73:1170-1177.

Bonni A, Sun Y, Nadal-Vicens M, Bhatt A, Frank DA, Rozovsky I, Stahl N, Yancopoulos GD, Greenberg ME (1997) Regulation of gliogenesis in the central nervous system by the JAK-STAT signaling pathway. Science 278:477-483.

Bourin M, Hascoet M (2003) The mouse light/dark box test. Eur J Pharmacol 463:55-65.

Bourin M, Petit-Demouliere B, Dhonnchadha BN, Hascoet M (2007) Animal models of anxiety in mice. Fundam Clin Pharmacol 21:567-574.

Brady JV, Nauta WJ (1953) Subcortical mechanisms in emotional behavior: affective changes following septal forebrain lesions in the albino rat. J Comp Physiol Psychol 46:339-346.

Brandt MD, Jessberger S, Steiner B, Kronenberg G, Reuter K, Bick-Sander A, von der Behrens W, Kempermann G (2003) Transient calretinin expression defines early postmitotic step of neuronal differentiation in adult hippocampal neurogenesis of mice. Mol Cell Neurosci 24:603-613.

Britz O, Mattar P, Nguyen L, Langevin LM, Zimmer C, Alam S, Guillemot F, Schuurmans C (2006) A role for proneural genes in the maturation of cortical progenitor cells. Cereb Cortex 16 Suppl 1:i138-151.

Bulfone A, Smiga SM, Shimamura K, Peterson A, Puelles L, Rubenstein JL (1995) T-brain-1: a homolog of Brachyury whose expression defines molecularly distinct domains within the cerebral cortex. Neuron 15:63-78.

Bulfone A, Martinez S, Marigo V, Campanella M, Basile A, Quaderi N, Gattuso C, Rubenstein JL, Ballabio A (1999) Expression pattern of the Tbr2 (Eomesodermin) gene during mouse and chick brain development. Mech Dev 84:133-138.

Butt SJ, Fuccillo M, Nery S, Noctor S, Kriegstein A, Corbin JG, Fishell G (2005) The temporal and spatial origins of cortical interneurons predict their physiological subtype. Neuron 48:591-604.

Bystron I, Blakemore C, Rakic P (2008) Development of the human cerebral cortex: Boulder Committee revisited. Nat Rev Neurosci 9:110-122.

Caffe AR, van Leeuwen FW (1983) Vasopressin-immunoreactive cells in the dorsomedial hypothalamic region, medial amygdaloid nucleus and locus coeruleus of the rat. Cell Tissue Res 233:23-33.

Cahana A, Escamez T, Nowakowski RS, Hayes NL, Giacobini M, von Holst A, Shmueli O, Sapir T, McConnell SK, Wurst W, Martinez S, Reiner O (2001) Targeted mutagenesis of Lis1 disrupts cortical development and LIS1 homodimerization. Proc Natl Acad Sci U S A 98:6429-6434.

Calegari F, Huttner WB (2003) An inhibition of cyclin-dependent kinases that lengthens, but does not arrest, neuroepithelial cell cycle induces premature neurogenesis. J Cell Sci 116:4947-4955.

Calegari F, Haubensak W, Haffner C, Huttner WB (2005) Selective lengthening of the cell cycle in the neurogenic subpopulation of neural progenitor cells during mouse brain development. J Neurosci 25:6533-6538.

Canteras NS, Chiavegatto S, Valle LE, Swanson LW (1997) Severe reduction of rat defensive behavior to a predator by discrete hypothalamic chemical lesions. Brain Res Bull 44:297-305.

Caramaschi D, de Boer SF, Koolhaas JM (2007) Differential role of the 5-HT1A receptor in aggressive and non-aggressive mice: an across-strain comparison. Physiol Behav 90:590-601.

Carney RS, Alfonso TB, Cohen D, Dai H, Nery S, Stoica B, Slotkin J, Bregman BS, Fishell G, Corbin JG (2006) Cell migration along the lateral cortical stream to the developing basal telencephalic limbic system. J Neurosci 26:11562-11574.

Casarosa S, Fode C, Guillemot F (1999) Mash1 regulates neurogenesis in the ventral telencephalon. Development 126:525-534.

Caviness VS, Jr., Takahashi T (1995) Proliferative events in the cerebral ventricular zone. Brain Dev 17:159-163.

Caviness VS, Jr., Takahashi T, Nowakowski RS (1999) The G1 restriction point as critical regulator of neocortical neuronogenesis. Neurochem Res 24:497-506.
Caviness VS, Jr., Goto T, Tarui T, Takahashi T, Bhide PG, Nowakowski RS (2003) Cell output, cell cycle duration and neuronal specification: a model of integrated mechanisms of the neocortical proliferative process. Cereb Cortex 13:592-598.
Chen B, Schaevitz LR, McConnell SK (2005) Fezl regulates the differentiation and axon targeting of layer 5 subcortical projection neurons in cerebral cortex. Proc Natl Acad Sci U S A.
Chen J, Lipska BK, Weinberger DR (2006a) Genetic mouse models of schizophrenia: from hypothesis-based to susceptibility gene-based models. Biol Psychiatry 59:1180-1188.
Chen YC, Lin SI, Chen YK, Chiang CS, Liaw GJ (2009) The Torso signaling pathway modulates a dual transcriptional switch to regulate tailless expression. Nucleic Acids Res 37:1061-1072.
Chen YJ, Chiang CS, Weng LC, Lengyel JA, Liaw GJ (2002) Tramtrack69 is required for the early repression of tailless expression. Mech Dev 116:75-83.
Chen ZY, Jing D, Bath KG, Ieraci A, Khan T, Siao CJ, Herrera DG, Toth M, Yang C, McEwen BS, Hempstead BL, Lee FS (2006b) Genetic variant BDNF (Val66Met) polymorphism alters anxiety-related behavior. Science 314:140-143.
Chenn A, Walsh CA (2002) Regulation of cerebral cortical size by control of cell cycle exit in neural precursors. Science 297:365-369.
Cholfin JA, Rubenstein JL (2007) Patterning of frontal cortex subdivisions by Fgf17. Proc Natl Acad Sci U S A 104:7652-7657.
Chozick BS (1985) The behavioral effects of lesions of the septum: a review. Int J Neurosci 26:197-217.
Christie BR, Li AM, Redila VA, Booth H, Wong BK, Eadie BD, Ernst C, Simpson EM (2006) Deletion of the nuclear receptor Nr2e1 impairs synaptic plasticity and dendritic structure in the mouse dentate gyrus. Neuroscience 137:1031-1037.
Chubb JE, Bradshaw NJ, Soares DC, Porteous DJ, Millar JK (2008) The DISC locus in psychiatric illness. Mol Psychiatry 13:36-64.
Clapcote SJ, Lipina TV, Millar JK, Mackie S, Christie S, Ogawa F, Lerch JP, Trimble K, Uchiyama M, Sakuraba Y, Kaneda H, Shiroishi T, Houslay MD, Henkelman RM, Sled JG, Gondo Y, Porteous DJ, Roder JC (2007) Behavioral phenotypes of Disc1 missense mutations in mice. Neuron 54:387-402.
Clarke HF, Robbins TW, Roberts AC (2008) Lesions of the medial striatum in monkeys produce perseverative impairments during reversal learning similar to those produced by lesions of the orbitofrontal cortex. J Neurosci 28:10972-10982.
Colas JF, Schoenwolf GC (2001) Towards a cellular and molecular understanding of neurulation. Dev Dyn 221:117-145.
Corbin JG, Gaiano N, Machold RP, Langston A, Fishell G (2000) The Gsh2 homeodomain gene controls multiple aspects of telencephalic development. Development 127:5007-5020.
Cotter PA, Mulligan OF, Landau S, Papadopoulos A, Lightman SL, Checkley SA (2002) Vasoconstrictor response to topical beclomethasone in major depression. Psychoneuroendocrinology 27:475-487.
Courchesne E, Pierce K, Schumann CM, Redcay E, Buckwalter JA, Kennedy DP, Morgan J (2007) Mapping early brain development in autism. Neuron 56:399-413.

D'Arcangelo G, Miao GG, Chen SC, Soares HD, Morgan JI, Curran T (1995) A protein related to extracellular matrix proteins deleted in the mouse mutant reeler. Nature 374:719-723.
de Carlos JA, Lopez-Mascaraque L, Valverde F (1996) Dynamics of cell migration from the lateral ganglionic eminence in the rat. J Neurosci 16:6146-6156.
Decker MW, Curzon P, Brioni JD (1995) Influence of separate and combined septal and amygdala lesions on memory, acoustic startle, anxiety, and locomotor activity in rats. Neurobiol Learn Mem 64:156-168.
Degroot A, Treit D (2004) Anxiety is functionally segregated within the septo-hippocampal system. Brain Res 1001:60-71.
Dehay C, Savatier P, Cortay V, Kennedy H (2001) Cell-cycle kinetics of neocortical precursors are influenced by embryonic thalamic axons. J Neurosci 21:201-214.
Dehay C, Giroud P, Berland M, Smart I, Kennedy H (1993) Modulation of the cell cycle contributes to the parcellation of the primate visual cortex. Nature 366:464-466.
Dehay C, Giroud P, Berland M, Killackey H, Kennedy H (1996) Contribution of thalamic input to the specification of cytoarchitectonic cortical fields in the primate: effects of bilateral enucleation in the fetal monkey on the boundaries, dimensions, and gyrification of striate and extrastriate cortex. J Comp Neurol 367:70-89.
Desai AR, McConnell SK (2000) Progressive restriction in fate potential by neural progenitors during cerebral cortical development. Development 127:2863-2872.
Divac I, Rosvold HE, Szwarcbart MK (1967) Behavioral effects of selective ablation of the caudate nucleus. J Comp Physiol Psychol 63:184-190.
Duan X, Kang E, Liu CY, Ming GL, Song H (2008) Development of neural stem cell in the adult brain. Curr Opin Neurobiol 18:108-115.
Dugas JC, Ibrahim A, Barres BA (2007) A crucial role for p57(Kip2) in the intracellular timer that controls oligodendrocyte differentiation. J Neurosci 27:6185-6196.
Durand B, Gao FB, Raff M (1997) Accumulation of the cyclin-dependent kinase inhibitor p27/Kip1 and the timing of oligodendrocyte differentiation. EMBO J 16:306-317.
Edwards MA, Yamamoto M, Caviness VS, Jr. (1990) Organization of radial glia and related cells in the developing murine CNS. An analysis based upon a new monoclonal antibody marker. Neuroscience 36:121-144.
Englund C, Fink A, Lau C, Pham D, Daza RA, Bulfone A, Kowalczyk T, Hevner RF (2005) Pax6, Tbr2, and Tbr1 are expressed sequentially by radial glia, intermediate progenitor cells, and postmitotic neurons in developing neocortex. J Neurosci 25:247-251.
Estivill-Torrus G, Pearson H, van Heyningen V, Price DJ, Rashbass P (2002) Pax6 is required to regulate the cell cycle and the rate of progression from symmetrical to asymmetrical division in mammalian cortical progenitors. Development 129:455-466.
Faedo A, Tomassy GS, Ruan Y, Teichmann H, Krauss S, Pleasure SJ, Tsai SY, Tsai MJ, Studer M, Rubenstein JL (2008) COUP-TFI coordinates cortical patterning, neurogenesis, and laminar fate and modulates MAPK/ERK, AKT, and beta-catenin signaling. Cereb Cortex 18:2117-2131.
Fairen A, Cobas A, Fonseca M (1986) Times of generation of glutamic acid decarboxylase immunoreactive neurons in mouse somatosensory cortex. J Comp Neurol 251:67-83.
Fan G, Martinowich K, Chin MH, He F, Fouse SD, Hutnick L, Hattori D, Ge W, Shen Y, Wu H, ten Hoeve J, Shuai K, Sun YE (2005) DNA methylation controls the timing of astrogliogenesis through regulation of JAK-STAT signaling. Development 132:3345-3356.

Featherstone RE, Rizos Z, Nobrega JN, Kapur S, Fletcher PJ (2007) Gestational methylazoxymethanol acetate treatment impairs select cognitive functions: parallels to schizophrenia. Neuropsychopharmacology 32:483-492.

Fish JL, Kosodo Y, Enard W, Paabo S, Huttner WB (2006) Aspm specifically maintains symmetric proliferative divisions of neuroepithelial cells. Proc Natl Acad Sci U S A 103:10438-10443.

Flagstad P, Glenthoj BY, Didriksen M (2005) Cognitive deficits caused by late gestational disruption of neurogenesis in rats: a preclinical model of schizophrenia. Neuropsychopharmacology 30:250-260.

Flagstad P, Mork A, Glenthoj BY, van Beek J, Michael-Titus AT, Didriksen M (2004) Disruption of neurogenesis on gestational day 17 in the rat causes behavioral changes relevant to positive and negative schizophrenia symptoms and alters amphetamine-induced dopamine release in nucleus accumbens. Neuropsychopharmacology 29:2052-2064.

Fode C, Ma Q, Casarosa S, Ang SL, Anderson DJ, Guillemot F (2000) A role for neural determination genes in specifying the dorsoventral identity of telencephalic neurons. Genes Dev 14:67-80.

Foley AC, Stern CD (2001) Evolution of vertebrate forebrain development: how many different mechanisms? J Anat 199:35-52.

Frantz GD, McConnell SK (1996) Restriction of late cerebral cortical progenitors to an upper-layer fate. Neuron 17:55-61.

Fujimiya M, Kimura H, Maeda T (1986) Postnatal development of serotonin nerve fibers in the somatosensory cortex of mice studied by immunohistochemistry. J Comp Neurol 246:191-201.

Fukuchi-Shimogori T, Grove EA (2001) Neocortex patterning by the secreted signaling molecule FGF8. Science 294:1071-1074.

Furmark T, Tillfors M, Garpenstrand H, Marteinsdottir I, Langstrom B, Oreland L, Fredrikson M (2004) Serotonin transporter polymorphism related to amygdala excitability and symptom severity in patients with social phobia. Neurosci Lett 362:189-192.

Furuta Y, Piston DW, Hogan BL (1997) Bone morphogenetic proteins (BMPs) as regulators of dorsal forebrain development. Development 124:2203-2212.

Gadgil H, Jurado LA, Jarrett HW (2001) DNA affinity chromatography of transcription factors. Anal Biochem 290:147-178.

Gage FH, Thompson RG (1980) Differential distribution of norepinephrine and serotonin along the dorsal-ventral axis of the hippocampal formation. Brain Res Bull 5:771-773.

Gaiano N, Kohtz JD, Turnbull DH, Fishell G (1999) A method for rapid gain-of-function studies in the mouse embryonic nervous system. Nat Neurosci 2:812-819.

Gaillard A, Nasarre C, Roger M (2003) Early (E12) cortical progenitors can change their fate upon heterotopic transplantation. Eur J Neurosci 17:1375-1383.

Galceran J, Miyashita-Lin EM, Devaney E, Rubenstein JL, Grosschedl R (2000) Hippocampus development and generation of dentate gyrus granule cells is regulated by LEF1. Development 127:469-482.

Gao FB, Durand B, Raff M (1997) Oligodendrocyte precursor cells count time but not cell divisions before differentiation. Curr Biol 7:152-155.

Garel S, Huffman KJ, Rubenstein JL (2003) Molecular regionalization of the neocortex is disrupted in Fgf8 hypomorphic mutants. Development 130:1903-1914.

Gauthier AS, Furstoss O, Araki T, Chan R, Neel BG, Kaplan DR, Miller FD (2007) Control of CNS cell-fate decisions by SHP-2 and its dysregulation in Noonan syndrome. Neuron 54:245-262.
Ge W, Martinowich K, Wu X, He F, Miyamoto A, Fan G, Weinmaster G, Sun YE (2002) Notch signaling promotes astrogliogenesis via direct CSL-mediated glial gene activation. J Neurosci Res 69:848-860.
Gerfen CR, Baimbridge KG, Miller JJ (1985) The neostriatal mosaic: compartmental distribution of calcium-binding protein and parvalbumin in the basal ganglia of the rat and monkey. Proc Natl Acad Sci U S A 82:8780-8784.
Geschwind DH, Levitt P (2007) Autism spectrum disorders: developmental disconnection syndromes. Curr Opin Neurobiol 17:103-111.
Geyer MA (2006) The family of sensorimotor gating disorders: comorbidities or diagnostic overlaps? Neurotox Res 10:211-220.
Geyer MA, Dulawa SC (2003) Assessment of murine startle reactivity, prepulse inhibition, and habituation. Curr Protoc Neurosci Chapter 8:Unit 8 17.
Gilmore EC, Ohshima T, Goffinet AM, Kulkarni AB, Herrup K (1998) Cyclin-dependent kinase 5-deficient mice demonstrate novel developmental arrest in cerebral cortex. J Neurosci 18:6370-6377.
Gitton Y, Cohen-Tannoudji M, Wassef M (1999) Specification of somatosensory area identity in cortical explants. J Neurosci 19:4889-4898.
Gonchar Y, Burkhalter A (1997) Three distinct families of GABAergic neurons in rat visual cortex. Cereb Cortex 7:347-358.
Gorman JM (1996) Comorbid depression and anxiety spectrum disorders. Depress Anxiety 4:160-168.
Gorski JA, Talley T, Qiu M, Puelles L, Rubenstein JL, Jones KR (2002) Cortical excitatory neurons and glia, but not GABAergic neurons, are produced in the Emx1-expressing lineage. J Neurosci 22:6309-6314.
Gotz M, Huttner WB (2005) The cell biology of neurogenesis. Nat Rev Mol Cell Biol 6:777-788.
Gotz M, Stoykova A, Gruss P (1998) Pax6 controls radial glia differentiation in the cerebral cortex. Neuron 21:1031-1044.
Gourevitch R, Rocher C, Le Pen G, Krebs MO, Jay TM (2004) Working memory deficits in adult rats after prenatal disruption of neurogenesis. Behav Pharmacol 15:287-292.
Graham V, Khudyakov J, Ellis P, Pevny L (2003) SOX2 functions to maintain neural progenitor identity. Neuron 39:749-765.
Grove EA, Tole S, Limon J, Yip L, Ragsdale CW (1998) The hem of the embryonic cerebral cortex is defined by the expression of multiple Wnt genes and is compromised in Gli3-deficient mice. Development 125:2315-2325.
Guillemot F, Molnar Z, Tarabykin V, Stoykova A (2006) Molecular mechanisms of cortical differentiation. Eur J Neurosci 23:857-868.
Gulisano M, Broccoli V, Pardini C, Boncinelli E (1996) Emx1 and Emx2 show different patterns of expression during proliferation and differentiation of the developing cerebral cortex in the mouse. Eur J Neurosci 8:1037-1050.
Gunhaga L, Jessell TM, Edlund T (2000) Sonic hedgehog signaling at gastrula stages specifies ventral telencephalic cells in the chick embryo. Development 127:3283-3293.

Gunhaga L, Marklund M, Sjodal M, Hsieh JC, Jessell TM, Edlund T (2003) Specification of dorsal telencephalic character by sequential Wnt and FGF signaling. Nat Neurosci 6:701-707.

Gupta A, Tsai LH, Wynshaw-Boris A (2002) Life is a journey: a genetic look at neocortical development. Nat Rev Genet 3:342-355.

Haller J, Toth M, Halasz J, De Boer SF (2006) Patterns of violent aggression-induced brain c-fos expression in male mice selected for aggressiveness. Physiol Behav 88:173-182.

Hamasaki T, Leingartner A, Ringstedt T, O'Leary DD (2004) EMX2 regulates sizes and positioning of the primary sensory and motor areas in neocortex by direct specification of cortical progenitors. Neuron 43:359-372.

Hartfuss E, Galli R, Heins N, Gotz M (2001) Characterization of CNS precursor subtypes and radial glia. Dev Biol 229:15-30.

Hartmann B, Reichert H, Walldorf U (2001) Interaction of gap genes in the Drosophila head: tailless regulates expression of empty spiracles in early embryonic patterning and brain development. Mech Dev 109:161-172.

Haubensak W, Attardo A, Denk W, Huttner WB (2004) Neurons arise in the basal neuroepithelium of the early mammalian telencephalon: a major site of neurogenesis. Proc Natl Acad Sci U S A 101:3196-3201.

He F, Sun YE (2007) Glial cells more than support cells? Int J Biochem Cell Biol 39:661-665.

He F, Ge W, Martinowich K, Becker-Catania S, Coskun V, Zhu W, Wu H, Castro D, Guillemot F, Fan G, de Vellis J, Sun YE (2005) A positive autoregulatory loop of Jak-STAT signaling controls the onset of astrogliogenesis. Nat Neurosci 8:616-625.

Heins N, Cremisi F, Malatesta P, Gangemi RM, Corte G, Price J, Goudreau G, Gruss P, Gotz M (2001) Emx2 promotes symmetric cell divisions and a multipotential fate in precursors from the cerebral cortex. Mol Cell Neurosci 18:485-502.

Heins N, Malatesta P, Cecconi F, Nakafuku M, Tucker KL, Hack MA, Chapouton P, Barde YA, Gotz M (2002) Glial cells generate neurons: the role of the transcription factor Pax6. Nat Neurosci 5:308-315.

Hevner RF (2006) From radial glia to pyramidal-projection neuron: transcription factor cascades in cerebral cortex development. Mol Neurobiol 33:33-50.

Hevner RF, Hodge RD, Daza RA, Englund C (2006) Transcription factors in glutamatergic neurogenesis: conserved programs in neocortex, cerebellum, and adult hippocampus. Neurosci Res 55:223-233.

Hevner RF, Daza RA, Englund C, Kohtz J, Fink A (2004) Postnatal shifts of interneuron position in the neocortex of normal and reeler mice: evidence for inward radial migration. Neuroscience 124:605-618.

Hevner RF, Daza RA, Rubenstein JL, Stunnenberg H, Olavarria JF, Englund C (2003) Beyond laminar fate: toward a molecular classification of cortical projection/pyramidal neurons. Dev Neurosci 25:139-151.

Hevner RF, Shi L, Justice N, Hsueh Y, Sheng M, Smiga S, Bulfone A, Goffinet AM, Campagnoni AT, Rubenstein JL (2001) Tbr1 regulates differentiation of the preplate and layer 6. Neuron 29:353-366.

Hirabayashi Y, Itoh Y, Tabata H, Nakajima K, Akiyama T, Masuyama N, Gotoh Y (2004) The Wnt/beta-catenin pathway directs neuronal differentiation of cortical neural precursor cells. Development 131:2791-2801.

Hirotsune S, Fleck MW, Gambello MJ, Bix GJ, Chen A, Clark GD, Ledbetter DH, McBain CJ, Wynshaw-Boris A (1998) Graded reduction of Pafah1b1 (Lis1) activity results in neuronal migration defects and early embryonic lethality. Nat Genet 19:333-339.

Hodge RD, Kowalczyk TD, Wolf SA, Encinas JM, Rippey C, Enikolopov G, Kempermann G, Hevner RF (2008) Intermediate progenitors in adult hippocampal neurogenesis: Tbr2 expression and coordinate regulation of neuronal output. J Neurosci 28:3707-3717.

Hollemann T, Bellefroid E, Pieler (1998) The *xenopus* homologue of the *drosophila* gene tailless has a function in early eye development. Development 125:2425-2432.

Holmes A, Murphy DL, Crawley JN (2003a) Abnormal behavioral phenotypes of serotonin transporter knockout mice: parallels with human anxiety and depression. Biol Psychiatry 54:953-959.

Holmes A, Lit Q, Murphy DL, Gold E, Crawley JN (2003b) Abnormal anxiety-related behavior in serotonin transporter null mutant mice: the influence of genetic background. Genes Brain Behav 2:365-380.

Houser CR, Hendry SH, Jones EG, Vaughn JE (1983) Morphological diversity of immunocytochemically identified GABA neurons in the monkey sensory-motor cortex. J Neurocytol 12:617-638.

Iacopetti P, Michelini M, Stuckmann I, Oback B, Aaku-Saraste E, Huttner WB (1999) Expression of the antiproliferative gene TIS21 at the onset of neurogenesis identifies single neuroepithelial cells that switch from proliferative to neuron-generating division. Proc Natl Acad Sci U S A 96:4639-4644.

Ishibashi M, Moriyoshi K, Sasai Y, Shiota K, Nakanishi S, Kageyama R (1994) Persistent expression of helix-loop-helix factor HES-1 prevents mammalian neural differentiation in the central nervous system. EMBO J 13:1799-1805.

Ishibashi M, Ang SL, Shiota K, Nakanishi S, Kageyama R, Guillemot F (1995) Targeted disruption of mammalian hairy and Enhancer of split homolog-1 (HES-1) leads to up-regulation of neural helix-loop-helix factors, premature neurogenesis, and severe neural tube defects. Genes Dev 9:3136-3148.

Jackson A, Panayiotidis P, Foroni L (1998) The human homologue of the Drosophila tailless gene (TLX): characterization and mapping to a region of common deletion in human lymphoid leukemia on chromosome 6q21. Genomics 50:34-43.

Jarriault S, Brou C, Logeat F, Schroeter EH, Kopan R, Israel A (1995) Signalling downstream of activated mammalian Notch. Nature 377:355-358.

Johnston-Wilson NL, Sims CD, Hofmann JP, Anderson L, Shore AD, Torrey EF, Yolken RH (2000) Disease-specific alterations in frontal cortex brain proteins in schizophrenia, bipolar disorder, and major depressive disorder. The Stanley Neuropathology Consortium. Mol Psychiatry 5:142-149.

Kandel ER, Schwartz JH, Jessell TM (1995) Essentials of neural science and behavior. Norwalk, CT: Appleton & Lange.

Kaneko N, Sawamoto K (2009) Adult neurogenesis and its alteration under pathological conditions. Neurosci Res 63:155-164.

Kawai Y, Takami K, Shiosaka S, Emson PC, Hillyard CJ, Girgis S, MacIntyre I, Tohyama M (1985) Topographic localization of calcitonin gene-related peptide in the rat brain: an immunohistochemical analysis. Neuroscience 15:747-763.

Kelsey JE, Landry BA (1988) Medial septal lesions disrupt spatial mapping ability in rats. Behav Neurosci 102:289-293.

Kemppainen S, Pitkanen A (2000) Distribution of parvalbumin, calretinin, and calbindin-D(28k) immunoreactivity in the rat amygdaloid complex and colocalization with gamma-aminobutyric acid. J Comp Neurol 426:441-467.

Kessaris N, Fogarty M, Iannarelli P, Grist M, Wegner M, Richardson WD (2006) Competing waves of oligodendrocytes in the forebrain and postnatal elimination of an embryonic lineage. Nat Neurosci 9:173-179.

King FA (1958) Effects of septal and amygdaloid lesions on emotional behavior and conditioned avoidance responses in the rat. J Nerv Ment Dis 126:57-63.

Kitambi SS, Hauptmann G (2007) The zebrafish orphan nuclear receptor genes nr2e1 and nr2e3 are expressed in developing eye and forebrain. Gene Expr Patterns 7:521-528.

Kjelstrup KG, Tuvnes FA, Steffenach HA, Murison R, Moser EI, Moser MB (2002) Reduced fear expression after lesions of the ventral hippocampus. Proc Natl Acad Sci U S A 99:10825-10830.

Koblar SA, Turnley AM, Classon BJ, Reid KL, Ware CB, Cheema SS, Murphy M, Bartlett PF (1998) Neural precursor differentiation into astrocytes requires signaling through the leukemia inhibitory factor receptor. Proc Natl Acad Sci U S A 95:3178-3181.

Kohn Y, Lerer B (2005) Excitement and confusion on chromosome 6q: the challenges of neuropsychiatric genetics in microcosm. Mol Psychiatry 10:1062-1073.

Kolk SM, Whitman MC, Yun ME, Shete P, Donoghue MJ (2005) A unique subpopulation of Tbr1-expressing deep layer neurons in the developing cerebral cortex. Mol Cell Neurosci 30:538-551.

Kornack DR, Rakic P (1998) Changes in cell-cycle kinetics during the development and evolution of primate neocortex. Proc Natl Acad Sci U S A 95:1242-1246.

Kosodo Y, Roper K, Haubensak W, Marzesco AM, Corbeil D, Huttner WB (2004) Asymmetric distribution of the apical plasma membrane during neurogenic divisions of mammalian neuroepithelial cells. EMBO J 23:2314-2324.

Kowalczyk T, Pontious A, Englund C, Daza RA, Bedogni F, Hodge R, Attardo A, Bell C, Huttner WB, Hevner RF (2009) Intermediate Neuronal Progenitors (Basal Progenitors) Produce Pyramidal-Projection Neurons for All Layers of Cerebral Cortex. Cereb Cortex.

Kubota Y, Hattori R, Yui Y (1994) Three distinct subpopulations of GABAergic neurons in rat frontal agranular cortex. Brain Res 649:159-173.

Kuhlbrodt K, Herbarth B, Sock E, Hermans-Borgmeyer I, Wegner M (1998) Sox10, a novel transcriptional modulator in glial cells. J Neurosci 18:237-250.

Kumar RA, Leach S, Bonaguro R, Chen J, Yokom DW, Abrahams BS, Seaver L, Schwartz CE, Dobyns W, Brooks-Wilson A, Simpson EM (2007) Mutation and evolutionary analyses identify NR2E1-candidate-regulatory mutations in humans with severe cortical malformations. Genes Brain Behav 6:503-516.

Kumar RA, McGhee KA, Leach S, Bonaguro R, Maclean A, Aguirre-Hernandez R, Abrahams BS, Coccaro EF, Hodgins S, Turecki G, Condon A, Muir WJ, Brooks-Wilson AR, Blackwood DH, Simpson EM (2008) Initial association of NR2E1 with bipolar disorder and identification of candidate mutations in bipolar disorder, schizophrenia, and aggression through resequencing. Am J Med Genet B Neuropsychiatr Genet 147B:880-889.

Lalonde R (2002) The neurobiological basis of spontaneous alternation. Neurosci Biobehav Rev 26:91-104.

Land PW, Monaghan AP (2003) Expression of the transcription factor, tailless, is required for formation of superficial cortical layers. Cereb Cortex 13:921-931.
Land PW, Monaghan AP (2005) Abnormal development of zinc-containing cortical circuits in the absence of the transcription factor Tailless. Brain Res Dev Brain Res 158:97-101.
Lavdas AA, Grigoriou M, Pachnis V, Parnavelas JG (1999) The medial ganglionic eminence gives rise to a population of early neurons in the developing cerebral cortex. J Neurosci 19:7881-7888.
Lee JK, Cho JH, Hwang WS, Lee YD, Reu DS, Suh-Kim H (2000a) Expression of neuroD/BETA2 in mitotic and postmitotic neuronal cells during the development of nervous system. Dev Dyn 217:361-367.
Lee MK, Tuttle JB, Rebhun LI, Cleveland DW, Frankfurter A (1990) The expression and posttranslational modification of a neuron-specific beta-tubulin isotype during chick embryogenesis. Cell Motil Cytoskeleton 17:118-132.
Lee SM, Tole S, Grove E, McMahon AP (2000b) A local Wnt-3a signal is required for development of the mammalian hippocampus. Development 127:457-467.
Lehmann U, Schmitz J, Weissenbach M, Sobota RM, Hortner M, Friederichs K, Behrmann I, Tsiaris W, Sasaki A, Schneider-Mergener J, Yoshimura A, Neel BG, Heinrich PC, Schaper F (2003) SHP2 and SOCS3 contribute to Tyr-759-dependent attenuation of interleukin-6 signaling through gp130. J Biol Chem 278:661-671.
Leingartner A, Thuret S, Kroll TT, Chou SJ, Leasure JL, Gage FH, O'Leary DD (2007) Cortical area size dictates performance at modality-specific behaviors. Proc Natl Acad Sci U S A 104:4153-4158.
Levers TE, Edgar JM, Price DJ (2001) The fates of cells generated at the end of neurogenesis in developing mouse cortex. J Neurobiol 48:265-277.
Levitt P, Barbe MF, Eagleson KL (1997) Patterning and specification of the cerebral cortex. Annu Rev Neurosci 20:1-24.
Levitt P, Eagleson KL, Powell EM (2004) Regulation of neocortical interneuron development and the implications for neurodevelopmental disorders. Trends Neurosci 27:400-406.
Lewis DA, Levitt P (2002) Schizophrenia as a disorder of neurodevelopment. Annu Rev Neurosci 25:409-432.
Lewis DA, Hashimoto T, Volk DW (2005) Cortical inhibitory neurons and schizophrenia. Nat Rev Neurosci 6:312-324.
Li W, Sun G, Yang S, Qu Q, Nakashima K, Shi Y (2008) Nuclear receptor TLX regulates cell cycle progression in neural stem cells of the developing brain. Mol Endocrinol 22:56-64.
Lian G, Sheen V (2006) Cerebral developmental disorders. Curr Opin Pediatr 18:614-620.
Liodis P, Denaxa M, Grigoriou M, Akufo-Addo C, Yanagawa Y, Pachnis V (2007) Lhx6 activity is required for the normal migration and specification of cortical interneuron subtypes. J Neurosci 27:3078-3089.
Lira A, Zhou M, Castanon N, Ansorge MS, Gordon JA, Francis JH, Bradley-Moore M, Lira J, Underwood MD, Arango V, Kung HF, Hofer MA, Hen R, Gingrich JA (2003) Altered depression-related behaviors and functional changes in the dorsal raphe nucleus of serotonin transporter-deficient mice. Biol Psychiatry 54:960-971.
Liu HK, Belz T, Bock D, Takacs A, Wu H, Lichter P, Chai M, Schutz G (2008) The nuclear receptor tailless is required for neurogenesis in the adult subventricular zone. Genes Dev 22:2473-2478.

Liu Y, Fujise N, Kosaka T (1996) Distribution of calretinin immunoreactivity in the mouse dentate gyrus. I. General description. Exp Brain Res 108:389-403.
Lodge DJ, Behrens MM, Grace AA (2009) A loss of parvalbumin-containing interneurons is associated with diminished oscillatory activity in an animal model of schizophrenia. J Neurosci 29:2344-2354.
Lukaszewicz A, Cortay V, Giroud P, Berland M, Smart I, Kennedy H, Dehay C (2006) The concerted modulation of proliferation and migration contributes to the specification of the cytoarchitecture and dimensions of cortical areas. Cereb Cortex 16 Suppl 1:i26-34.
Lukaszewicz A, Savatier P, Cortay V, Giroud P, Huissoud C, Berland M, Kennedy H, Dehay C (2005) G1 phase regulation, area-specific cell cycle control, and cytoarchitectonics in the primate cortex. Neuron 47:353-364.
Malatesta P, Hartfuss E, Gotz M (2000) Isolation of radial glial cells by fluorescent-activated cell sorting reveals a neuronal lineage. Development 127:5253-5263.
Malatesta P, Hack MA, Hartfuss E, Kettenmann H, Klinkert W, Kirchhoff F, Gotz M (2003) Neuronal or glial progeny: regional differences in radial glia fate. Neuron 37:751-764.
Mallamaci A, Stoykova A (2006) Gene networks controlling early cerebral cortex arealization. Eur J Neurosci 23:847-856.
Mallamaci A, Muzio L, Chan CH, Parnavelas J, Boncinelli E (2000) Area identity shifts in the early cerebral cortex of Emx2-/- mutant mice. Nat Neurosci 3:679-686.
Mallamaci A, Iannone R, Briata P, Pintonello L, Mercurio S, Boncinelli E, Corte G (1998) EMX2 protein in the developing mouse brain and olfactory area. Mech Dev 77:165-172.
Mangelsdorf DJ, Thummel C, Beato M, Herrlich P, Schutz G, Umesono K, Blumberg B, Kastner P, Mark M, Chambon P, Evans RM (1995) The nuclear receptor superfamily: the second decade. Cell 83:835-839.
Marin O, Rubenstein JL (2001) A long, remarkable journey: tangential migration in the telencephalon. Nat Rev Neurosci 2:780-790.
Marin O, Yaron A, Bagri A, Tessier-Lavigne M, Rubenstein JL (2001) Sorting of striatal and cortical interneurons regulated by semaphorin-neuropilin interactions. Science 293:872-875.
Marin O, Plump AS, Flames N, Sanchez-Camacho C, Tessier-Lavigne M, Rubenstein JL (2003) Directional guidance of interneuron migration to the cerebral cortex relies on subcortical Slit1/2-independent repulsion and cortical attraction. Development 130:1889-1901.
McAlonan K, Brown VJ (2003) Orbital prefrontal cortex mediates reversal learning and not attentional set shifting in the rat. Behav Brain Res 146:97-103.
McConnell SK (1988) Fates of visual cortical neurons in the ferret after isochronic and heterochronic transplantation. J Neurosci 8:945-974.
McConnell SK (1995) Constructing the cerebral cortex: neurogenesis and fate determination. Neuron 15:761-768.
McConnell SK, Kaznowski CE (1991) Cell cycle dependence of laminar determination in developing neocortex. Science 254:282-285.
McHugh SB, Deacon RM, Rawlins JN, Bannerman DM (2004) Amygdala and ventral hippocampus contribute differentially to mechanisms of fear and anxiety. Behav Neurosci 118:63-78.
McIntyre RS, Soczynska JK, Bottas A, Bordbar K, Konarski JZ, Kennedy SH (2006) Anxiety disorders and bipolar disorder: a review. Bipolar Disord 8:665-676.

Miczek KA, de Almeida RM, Kravitz EA, Rissman EF, de Boer SF, Raine A (2007) Neurobiology of escalated aggression and violence. J Neurosci 27:11803-11806.
Miller FD, Gauthier AS (2007) Timing is everything: making neurons versus glia in the developing cortex. Neuron 54:357-369.
Miller MW, Nowakowski RS (1988) Use of bromodeoxyuridine-immunohistochemistry to examine the proliferation, migration and time of origin of cells in the central nervous system. Brain Res 457:44-52.
Miyashita-Lin EM, Hevner R, Wassarman KM, Martinez S, Rubenstein JL (1999) Early neocortical regionalization in the absence of thalamic innervation. Science 285:906-909.
Miyata T, Kawaguchi A, Saito K, Kawano M, Muto T, Ogawa M (2004) Asymmetric production of surface-dividing and non-surface-dividing cortical progenitor cells. Development 131:3133-3145.
Miyawaki T, Uemura A, Dezawa M, Yu RT, Ide C, Nishikawa S, Honda Y, Tanabe Y, Tanabe T (2004) Tlx, an orphan nuclear receptor, regulates cell numbers and astrocyte development in the developing retina. J Neurosci 24:8124-8134.
Mizutani K, Saito T (2005) Progenitors resume generating neurons after temporary inhibition of neurogenesis by Notch activation in the mammalian cerebral cortex. Development 132:1295-1304.
Mizutani K, Yoon K, Dang L, Tokunaga A, Gaiano N (2007) Differential Notch signalling distinguishes neural stem cells from intermediate progenitors. Nature 449:351-355.
Molnar Z, Blakemore C (1995) How do thalamic axons find their way to the cortex? Trends Neurosci 18:389-397.
Molnar Z, Butler AB (2002) The corticostriatal junction: a crucial region for forebrain development and evolution. Bioessays 24:530-541.
Molyneaux BJ, Arlotta P, Hirata T, Hibi M, Macklis JD (2005) Fezl is required for the birth and specification of corticospinal motor neurons. Neuron 47:817-831.
Monaghan AP, Grau E, Bock D, Schutz G (1995) The mouse homolog of the orphan nuclear receptor tailless is expressed in the developing forebrain. Development 121:839-853.
Monaghan AP, Bock D, Gass P, Schwager A, Wolfer DP, Lipp HP, Schutz G (1997) Defective limbic system in mice lacking the tailless gene. Nature 390:515-517.
Moran E, Jimenez G (2006) The tailless nuclear receptor acts as a dedicated repressor in the early Drosophila embryo. Mol Cell Biol 26:3446-3454.
Mori T, Wanaka A, Taguchi A, Matsumoto K, Tohyama M (1995) Localization of novel receptor tyrosine kinase genes of the eph family, MDK1 and its splicing variant, in the developing mouse nervous system. Brain Res Mol Brain Res 34:154-160.
Morrow T, Song MR, Ghosh A (2001) Sequential specification of neurons and glia by developmentally regulated extracellular factors. Development 128:3585-3594.
Moser E, Moser MB, Andersen P (1993) Spatial learning impairment parallels the magnitude of dorsal hippocampal lesions, but is hardly present following ventral lesions. J Neurosci 13:3916-3925.
Moser MB, Moser EI (1998) Functional differentiation in the hippocampus. Hippocampus 8:608-619.
Moser MB, Moser EI, Forrest E, Andersen P, Morris RG (1995) Spatial learning with a minislab in the dorsal hippocampus. Proc Natl Acad Sci U S A 92:9697-9701.
Mullen RJ, Buck CR, Smith AM (1992) NeuN, a neuronal specific nuclear protein in vertebrates. Development 116:201-211.

Muzio L, Soria JM, Pannese M, Piccolo S, Mallamaci A (2005) A mutually stimulating loop involving emx2 and canonical wnt signalling specifically promotes expansion of occipital cortex and hippocampus. Cereb Cortex 15:2021-2028.

Muzio L, DiBenedetto B, Stoykova A, Boncinelli E, Gruss P, Mallamaci A (2002) Emx2 and Pax6 control regionalization of the pre-neuronogenic cortical primordium. Cereb Cortex 12:129-139.

Nader K, Majidishad P, Amorapanth P, LeDoux JE (2001) Damage to the lateral and central, but not other, amygdaloid nuclei prevents the acquisition of auditory fear conditioning. Learn Mem 8:156-163.

Nakagawa Y, Johnson JE, O'Leary DD (1999) Graded and areal expression patterns of regulatory genes and cadherins in embryonic neocortex independent of thalamocortical input. J Neurosci 19:10877-10885.

Nakahira E, Kagawa T, Shimizu T, Goulding MD, Ikenaka K (2006) Direct evidence that ventral forebrain cells migrate to the cortex and contribute to the generation of cortical myelinating oligodendrocytes. Dev Biol 291:123-131.

Nakashima K, Yanagisawa M, Arakawa H, Kimura N, Hisatsune T, Kawabata M, Miyazono K, Taga T (1999a) Synergistic signaling in fetal brain by STAT3-Smad1 complex bridged by p300. Science 284:479-482.

Nakashima K, Wiese S, Yanagisawa M, Arakawa H, Kimura N, Hisatsune T, Yoshida K, Kishimoto T, Sendtner M, Taga T (1999b) Developmental requirement of gp130 signaling in neuronal survival and astrocyte differentiation. J Neurosci 19:5429-5434.

Namihira M, Nakashima K, Taga T (2004) Developmental stage dependent regulation of DNA methylation and chromatin modification in a immature astrocyte specific gene promoter. FEBS Lett 572:184-188.

Naruse M, Nakahira E, Miyata T, Hitoshi S, Ikenaka K, Bansal R (2006) Induction of oligodendrocyte progenitors in dorsal forebrain by intraventricular microinjection of FGF-2. Dev Biol 297:262-273.

Nery S, Wichterle H, Fishell G (2001) Sonic hedgehog contributes to oligodendrocyte specification in the mammalian forebrain. Development 128:527-540.

Neuman T, Keen A, Zuber MX, Kristjansson GI, Gruss P, Nornes HO (1993) Neuronal expression of regulatory helix-loop-helix factor Id2 gene in mouse. Dev Biol 160:186-195.

Nieto M, Schuurmans C, Britz O, Guillemot F (2001) Neural bHLH genes control the neuronal versus glial fate decision in cortical progenitors. Neuron 29:401-413.

Nieto M, Monuki ES, Tang H, Imitola J, Haubst N, Khoury SJ, Cunningham J, Gotz M, Walsh CA (2004) Expression of Cux-1 and Cux-2 in the subventricular zone and upper layers II-IV of the cerebral cortex. J Comp Neurol 479:168-180.

Noctor SC, Martinez-Cerdeno V, Kriegstein AR (2008) Distinct behaviors of neural stem and progenitor cells underlie cortical neurogenesis. J Comp Neurol 508:28-44.

Noctor SC, Martinez-Cerdeno V, Ivic L, Kriegstein AR (2004) Cortical neurons arise in symmetric and asymmetric division zones and migrate through specific phases. Nat Neurosci 7:136-144.

Noctor SC, Flint AC, Weissman TA, Dammerman RS, Kriegstein AR (2001) Neurons derived from radial glial cells establish radial units in neocortex. Nature 409:714-720.

Noctor SC, Flint AC, Weissman TA, Wong WS, Clinton BK, Kriegstein AR (2002) Dividing precursor cells of the embryonic cortical ventricular zone have morphological and molecular characteristics of radial glia. J Neurosci 22:3161-3173.

Nowakowski RS, Lewin SB, Miller MW (1989) Bromodeoxyuridine immunohistochemical determination of the lengths of the cell cycle and the DNA-synthetic phase for an anatomically defined population. J Neurocytol 18:311-318.

O'Leary DD, Nakagawa Y (2002) Patterning centers, regulatory genes and extrinsic mechanisms controlling arealization of the neocortex. Curr Opin Neurobiol 12:14-25.

O'Leary DD, Sahara S (2008) Genetic regulation of arealization of the neocortex. Curr Opin Neurobiol 18:90-100.

Oakes ME, Coover GD (1997) Effects of small amygdala lesions on fear, but not aggression, in the rat. Physiol Behav 61:45-55.

Ohnuma S, Harris WA (2003) Neurogenesis and the cell cycle. Neuron 40:199-208.

Ohtsuka T, Ishibashi M, Gradwohl G, Nakanishi S, Guillemot F, Kageyama R (1999) Hes1 and Hes5 as notch effectors in mammalian neuronal differentiation. EMBO J 18:2196-2207.

Olivier C, Cobos I, Perez Villegas EM, Spassky N, Zalc B, Martinez S, Thomas JL (2001) Monofocal origin of telencephalic oligodendrocytes in the anterior entopeduncular area of the chick embryo. Development 128:1757-1769.

Olsen GM, Scheel-Kruger J, Moller A, Jensen LH (1994) Relation of spatial learning of rats in the Morris water maze task to the number of viable CA1 neurons following four-vessel occlusion. Behav Neurosci 108:681-690.

Ouimet CC, Miller PE, Hemmings HC, Jr., Walaas SI, Greengard P (1984) DARPP-32, a dopamine- and adenosine 3':5'-monophosphate-regulated phosphoprotein enriched in dopamine-innervated brain regions. III. Immunocytochemical localization. J Neurosci 4:111-124.

Painsipp E, Wultsch T, Edelsbrunner ME, Tasan RO, Singewald N, Herzog H, Holzer P (2008) Reduced anxiety-like and depression-related behavior in neuropeptide Y Y4 receptor knockout mice. Genes Brain Behav 7:532-542.

Park SS, Ko BJ, Kim BG (2005) Mass spectrometric screening of transcriptional regulators using DNA affinity capture assay. Anal Biochem 344:152-154.

Parrish M, Ott T, Lance-Jones C, Schuetz G, Schwaeger-Nickolenko A, Monaghan AP (2004) Loss of the Sall3 gene leads to palate deficiency, abnormalities in cranial nerves, and perinatal lethality. Mol Cell Biol 24:7102-7112.

Paton JJ, Belova MA, Morrison SE, Salzman CD (2006) The primate amygdala represents the positive and negative value of visual stimuli during learning. Nature 439:865-870.

Peduzzi JD (1988) Genesis of GABA-immunoreactive neurons in the ferret visual cortex. J Neurosci 8:920-931.

Pesold C, Treit D (1995) The central and basolateral amygdala differentially mediate the anxiolytic effects of benzodiazepines. Brain Res 671:213-221.

Pignoni F, Steingrimsson E, Lengyel JA (1992) bicoid and the terminal system activate tailless expression in the early Drosophila embryo. Development 115:239-251.

Pignoni F, Baldarelli RM, Steingrimsson E, Diaz RJ, Patapoutian A, Merriam JR, Lengyel JA (1990) The Drosophila gene tailless is expressed at the embryonic termini and is a member of the steroid receptor superfamily. Cell 62:151-163.

Pilz DT, Matsumoto N, Minnerath S, Mills P, Gleeson JG, Allen KM, Walsh CA, Barkovich AJ, Dobyns WB, Ledbetter DH, Ross ME (1998) LIS1 and XLIS (DCX) mutations cause

most classical lissencephaly, but different patterns of malformation. Hum Mol Genet 7:2029-2037.
Pitkanen A, Pikkarainen M, Nurminen N, Ylinen A (2000) Reciprocal connections between the amygdala and the hippocampal formation, perirhinal cortex, and postrhinal cortex in rat. A review. Ann N Y Acad Sci 911:369-391.
Polleux F, Dehay C, Kennedy H (1997a) The timetable of laminar neurogenesis contributes to the specification of cortical areas in mouse isocortex. J Comp Neurol 385:95-116.
Polleux F, Dehay C, Moraillon B, Kennedy H (1997b) Regulation of neuroblast cell-cycle kinetics plays a crucial role in the generation of unique features of neocortical areas. J Neurosci 17:7763-7783.
Polleux F, Whitford KL, Dijkhuizen PA, Vitalis T, Ghosh A (2002) Control of cortical interneuron migration by neurotrophins and PI3-kinase signaling. Development 129:3147-3160.
Porsolt RD, Brossard G, Hautbois C, Roux S (2001) Rodent models of depression: forced swimming and tail suspension behavioral despair tests in rats and mice. Curr Protoc Neurosci Chapter 8:Unit 8 10A.
Potter GB, Petryniak MA, Shevchenko E, McKinsey GL, Ekker M, Rubenstein JL (2009) Generation of Cre-transgenic mice using Dlx1/Dlx2 enhancers and their characterization in GABAergic interneurons. Mol Cell Neurosci 40:167-186.
Powell EM, Campbell DB, Stanwood GD, Davis C, Noebels JL, Levitt P (2003) Genetic disruption of cortical interneuron development causes region- and GABA cell type-specific deficits, epilepsy, and behavioral dysfunction. J Neurosci 23:622-631.
Price DJ, Aslam S, Tasker L, Gillies K (1997) Fates of the earliest generated cells in the developing murine neocortex. J Comp Neurol 377:414-422.
Puelles L, Kuwana E, Puelles E, Bulfone A, Shimamura K, Keleher J, Smiga S, Rubenstein JL (2000) Pallial and subpallial derivatives in the embryonic chick and mouse telencephalon, traced by the expression of the genes Dlx-2, Emx-1, Nkx-2.1, Pax-6, and Tbr-1. J Comp Neurol 424:409-438.
Qian X, Shen Q, Goderie SK, He W, Capela A, Davis AA, Temple S (2000) Timing of CNS cell generation: a programmed sequence of neuron and glial cell production from isolated murine cortical stem cells. Neuron 28:69-80.
Quinn JC, Molinek M, Martynoga BS, Zaki PA, Faedo A, Bulfone A, Hevner RF, West JD, Price DJ (2007) Pax6 controls cerebral cortical cell number by regulating exit from the cell cycle and specifies cortical cell identity by a cell autonomous mechanism. Dev Biol 302:50-65.
Ragozzino ME, Jih J, Tzavos A (2002) Involvement of the dorsomedial striatum in behavioral flexibility: role of muscarinic cholinergic receptors. Brain Res 953:205-214.
Ragozzino ME, Pal SN, Unick K, Stefani MR, Gold PE (1998) Modulation of hippocampal acetylcholine release and spontaneous alternation scores by intrahippocampal glucose injections. J Neurosci 18:1595-1601.
Rajan P, McKay RD (1998) Multiple routes to astrocytic differentiation in the CNS. J Neurosci 18:3620-3629.
Rakic P (1974) Neurons in rhesus monkey visual cortex: systematic relation between time of origin and eventual disposition. Science 183:425-427.
Rakic P (1988) Specification of cerebral cortical areas. Science 241:170-176.
Rakic P (2003) Elusive radial glial cells: historical and evolutionary perspective. Glia 43:19-32.

Rash BG, Grove EA (2006) Area and layer patterning in the developing cerebral cortex. Curr Opin Neurobiol 16:25-34.
Rice DS, Curran T (2001) Role of the reelin signaling pathway in central nervous system development. Annu Rev Neurosci 24:1005-1039.
Risold PY, Swanson LW (1997a) Chemoarchitecture of the rat lateral septal nucleus. Brain Res Brain Res Rev 24:91-113.
Risold PY, Swanson LW (1997b) Connections of the rat lateral septal complex. Brain Res Brain Res Rev 24:115-195.
Rockel AJ, Hiorns RW, Powell TP (1980) The basic uniformity in structure of the neocortex. Brain 103:221-244.
Roy K, Thiels E, Monaghan AP (2002) Loss of the tailless gene affects forebrain development and emotional behavior. Physiol Behav 77:595-600.
Roy K, Kuznicki K, Wu Q, Sun Z, Bock D, Schutz G, Vranich N, Monaghan AP (2004) The Tlx gene regulates the timing of neurogenesis in the cortex. J Neurosci 24:8333-8345.
Rubenstein JL, Anderson S, Shi L, Miyashita-Lin E, Bulfone A, Hevner R (1999) Genetic control of cortical regionalization and connectivity. Cereb Cortex 9:524-532.
Rush AJ (2003) Toward an understanding of bipolar disorder and its origin. J Clin Psychiatry 64 Suppl 6:4-8; discussion 28.
Sah P, Faber ES, Lopez De Armentia M, Power J (2003) The amygdaloid complex: anatomy and physiology. Physiol Rev 83:803-834.
Sahara S, Kawakami Y, Izpisua Belmonte JC, O'Leary DD (2007) Sp8 exhibits reciprocal induction with Fgf8 but has an opposing effect on anterior-posterior cortical area patterning. Neural Dev 2:10.
Sahay A, Hen R (2007) Adult hippocampal neurogenesis in depression. Nat Neurosci 10:1110-1115.
Sajdyk TJ, Schober DA, Gehlert DR (2002a) Neuropeptide Y receptor subtypes in the basolateral nucleus of the amygdala modulate anxiogenic responses in rats. Neuropharmacology 43:1165-1172.
Sajdyk TJ, Schober DA, Smiley DL, Gehlert DR (2002b) Neuropeptide Y-Y2 receptors mediate anxiety in the amygdala. Pharmacol Biochem Behav 71:419-423.
Saxe MD, Battaglia F, Wang JW, Malleret G, David DJ, Monckton JE, Garcia AD, Sofroniew MV, Kandel ER, Santarelli L, Hen R, Drew MR (2006) Ablation of hippocampal neurogenesis impairs contextual fear conditioning and synaptic plasticity in the dentate gyrus. Proc Natl Acad Sci U S A 103:17501-17506.
Schaeren-Wiemers N, Gerfin-Moser A (1993) A single protocol to detect transcripts of various types and expression levels in neural tissue and cultured cells: in situ hybridization using digoxigenin-labelled cRNA probes. Histochemistry 100:431-440.
Schoenbaum G, Chiba AA, Gallagher M (1999) Neural encoding in orbitofrontal cortex and basolateral amygdala during olfactory discrimination learning. J Neurosci 19:1876-1884.
Schoenbaum G, Nugent SL, Saddoris MP, Setlow B (2002) Orbitofrontal lesions in rats impair reversal but not acquisition of go, no-go odor discriminations. Neuroreport 13:885-890.
Schuurmans C, Guillemot F (2002) Molecular mechanisms underlying cell fate specification in the developing telencephalon. Curr Opin Neurobiol 12:26-34.
Schuurmans C, Armant O, Nieto M, Stenman JM, Britz O, Klenin N, Brown C, Langevin LM, Seibt J, Tang H, Cunningham JM, Dyck R, Walsh C, Campbell K, Polleux F, Guillemot

F (2004) Sequential phases of cortical specification involve Neurogenin-dependent and -independent pathways. Embo J 23:2892-2902.
Sehgal R, Sheibani N, Rhodes SJ, Adams TL (2009) BMP7 and SHH Regulate Pax2 in Mouse Retinal Astrocytes by Relieving TLX Repression. Dev Biol.
Serene JA, Ashtari M, Szeszko PR, Kumra S (2007) Neuroimaging studies of children with serious emotional disturbances: a selective review. Can J Psychiatry 52:135-145.
Seri B, Garcia-Verdugo JM, McEwen BS, Alvarez-Buylla A (2001) Astrocytes give rise to new neurons in the adult mammalian hippocampus. J Neurosci 21:7153-7160.
Sessa A, Mao CA, Hadjantonakis AK, Klein WH, Broccoli V (2008) Tbr2 directs conversion of radial glia into basal precursors and guides neuronal amplification by indirect neurogenesis in the developing neocortex. Neuron 60:56-69.
Sheehan TP, Chambers RA, Russell DS (2004) Regulation of affect by the lateral septum: implications for neuropsychiatry. Brain Res Brain Res Rev 46:71-117.
Sheline YI (2003) Neuroimaging studies of mood disorder effects on the brain. Biol Psychiatry 54:338-352.
Shen Q, Wang Y, Dimos JT, Fasano CA, Phoenix TN, Lemischka IR, Ivanova NB, Stifani S, Morrisey EE, Temple S (2006) The timing of cortical neurogenesis is encoded within lineages of individual progenitor cells. Nat Neurosci 9:743-751.
Sherr CJ, Roberts JM (1995) Inhibitors of mammalian G1 cyclin-dependent kinases. Genes Dev 9:1149-1163.
Shi Y, Chichung Lie D, Taupin P, Nakashima K, Ray J, Yu RT, Gage FH, Evans RM (2004) Expression and function of orphan nuclear receptor TLX in adult neural stem cells. Nature 427:78-83.
Shibata T, Yamada K, Watanabe M, Ikenaka K, Wada K, Tanaka K, Inoue Y (1997) Glutamate transporter GLAST is expressed in the radial glia-astrocyte lineage of developing mouse spinal cord. J Neurosci 17:9212-9219.
Shimogori T, Banuchi V, Ng HY, Strauss JB, Grove EA (2004) Embryonic signaling centers expressing BMP, WNT and FGF proteins interact to pattern the cerebral cortex. Development 131:5639-5647.
Shors TJ, Townsend DA, Zhao M, Kozorovitskiy Y, Gould E (2002) Neurogenesis may relate to some but not all types of hippocampal-dependent learning. Hippocampus 12:578-584.
Siegenthaler JA, Miller MW (2005) Transforming growth factor beta 1 promotes cell cycle exit through the cyclin-dependent kinase inhibitor p21 in the developing cerebral cortex. J Neurosci 25:8627-8636.
Siegenthaler JA, Tremper-Wells BA, Miller MW (2008) Foxg1 haploinsufficiency reduces the population of cortical intermediate progenitor cells: effect of increased p21 expression. Cereb Cortex 18:1865-1875.
Simeone A, Gulisano M, Acampora D, Stornaiuolo A, Rambaldi M, Boncinelli E (1992) Two vertebrate homeobox genes related to the Drosophila empty spiracles gene are expressed in the embryonic cerebral cortex. Embo J 11:2541-2550.
Sloviter RS (1989) Calcium-binding protein (calbindin-D28k) and parvalbumin immunocytochemistry: localization in the rat hippocampus with specific reference to the selective vulnerability of hippocampal neurons to seizure activity. J Comp Neurol 280:183-196.
Snyder JS, Hong NS, McDonald RJ, Wojtowicz JM (2005) A role for adult neurogenesis in spatial long-term memory. Neuroscience 130:843-852.

Spassky N, Goujet-Zalc C, Parmantier E, Olivier C, Martinez S, Ivanova A, Ikenaka K, Macklin W, Cerruti I, Zalc B, Thomas JL (1998) Multiple restricted origin of oligodendrocytes. J Neurosci 18:8331-8343.

Stalnaker TA, Franz TM, Singh T, Schoenbaum G (2007) Basolateral amygdala lesions abolish orbitofrontal-dependent reversal impairments. Neuron 54:51-58.

Stein MB (2006) An epidemiologic perspective on social anxiety disorder. J Clin Psychiatry 67 Suppl 12:3-8.

Stenman J, Yu RT, Evans RM, Campbell K (2003a) Tlx and Pax6 co-operate genetically to establish the pallio-subpallial boundary in the embryonic mouse telencephalon. Development 130:1113-1122.

Stenman JM, Wang B, Campbell K (2003b) Tlx controls proliferation and patterning of lateral telencephalic progenitor domains. J Neurosci 23:10568-10576.

Storm EE, Garel S, Borello U, Hebert JM, Martinez S, McConnell SK, Martin GR, Rubenstein JL (2006) Dose-dependent functions of Fgf8 in regulating telencephalic patterning centers. Development 133:1831-1844.

Stoykova A, Gruss P (1994) Roles of Pax-genes in developing and adult brain as suggested by expression patterns. J Neurosci 14:1395-1412.

Stoykova A, Treichel D, Hallonet M, Gruss P (2000) Pax6 modulates the dorsoventral patterning of the mammalian telencephalon. J Neurosci 20:8042-8050.

Strecker TR, Merriam JR, Lengyel JA (1988) Graded requirement for the zygotic terminal gene, tailless, in the brain and tail region of the Drosophila embryo. Development 102:721-734.

Sun G, Yu RT, Evans RM, Shi Y (2007) Orphan nuclear receptor TLX recruits histone deacetylases to repress transcription and regulate neural stem cell proliferation. Proc Natl Acad Sci U S A 104:15282-15287.

Sun Y, Nadal-Vicens M, Misono S, Lin MZ, Zubiaga A, Hua X, Fan G, Greenberg ME (2001) Neurogenin promotes neurogenesis and inhibits glial differentiation by independent mechanisms. Cell 104:365-376.

Sussel L, Marin O, Kimura S, Rubenstein JL (1999) Loss of Nkx2.1 homeobox gene function results in a ventral to dorsal molecular respecification within the basal telencephalon: evidence for a transformation of the pallidum into the striatum. Development 126:3359-3370.

Suzuki SC, Inoue T, Kimura Y, Tanaka T, Takeichi M (1997) Neuronal Circuits Are Subdivided by Differential Expression of Type-II Classic Cadherins in Postnatal Mouse Brains. Mol Cell Neurosci 9:433-447.

Swerdlow NR, Geyer MA, Braff DL (2001) Neural circuit regulation of prepulse inhibition of startle in the rat: current knowledge and future challenges. Psychopharmacology (Berl) 156:194-215.

Takahashi T, Nowakowski RS, Caviness VS, Jr. (1992) BUdR as an S-phase marker for quantitative studies of cytokinetic behaviour in the murine cerebral ventricular zone. J Neurocytol 21:185-197.

Takahashi T, Nowakowski RS, Caviness VS, Jr. (1995a) Early ontogeny of the secondary proliferative population of the embryonic murine cerebral wall. J Neurosci 15:6058-6068.

Takahashi T, Nowakowski RS, Caviness VS, Jr. (1995b) The cell cycle of the pseudostratified ventricular epithelium of the embryonic murine cerebral wall. J Neurosci 15:6046-6057.

Takahashi T, Goto T, Miyama S, Nowakowski RS, Caviness VS, Jr. (1999) Sequence of neuron origin and neocortical laminar fate: relation to cell cycle of origin in the developing murine cerebral wall. J Neurosci 19:10357-10371.

Takeda H, Tsuji M, Matsumiya T (1998) Changes in head-dipping behavior in the hole-board test reflect the anxiogenic and/or anxiolytic state in mice. Eur J Pharmacol 350:21-29.

Takizawa T, Nakashima K, Namihira M, Ochiai W, Uemura A, Yanagisawa M, Fujita N, Nakao M, Taga T (2001) DNA methylation is a critical cell-intrinsic determinant of astrocyte differentiation in the fetal brain. Dev Cell 1:749-758.

Talamini LM, Koch T, Luiten PG, Koolhaas JM, Korf J (1999) Interruptions of early cortical development affect limbic association areas and social behaviour in rats; possible relevance for neurodevelopmental disorders. Brain Res 847:105-120.

Tanaka D, Nakaya Y, Yanagawa Y, Obata K, Murakami F (2003) Multimodal tangential migration of neocortical GABAergic neurons independent of GPI-anchored proteins. Development 130:5803-5813.

Tarabykin V, Stoykova A, Usman N, Gruss P (2001) Cortical upper layer neurons derive from the subventricular zone as indicated by Svet1 gene expression. Development 128:1983-1993.

Tarui T, Takahashi T, Nowakowski RS, Hayes NL, Bhide PG, Caviness VS (2005) Overexpression of p27 Kip 1, probability of cell cycle exit, and laminar destination of neocortical neurons. Cereb Cortex 15:1343-1355.

Tekki-Kessaris N, Woodruff R, Hall AC, Gaffield W, Kimura S, Stiles CD, Rowitch DH, Richardson WD (2001) Hedgehog-dependent oligodendrocyte lineage specification in the telencephalon. Development 128:2545-2554.

Temple S, Raff MC (1986) Clonal analysis of oligodendrocyte development in culture: evidence for a developmental clock that counts cell divisions. Cell 44:773-779.

Tiveron MC, Rossel M, Moepps B, Zhang YL, Seidenfaden R, Favor J, Konig N, Cremer H (2006) Molecular interaction between projection neuron precursors and invading interneurons via stromal-derived factor 1 (CXCL12)/CXCR4 signaling in the cortical subventricular zone/intermediate zone. J Neurosci 26:13273-13278.

Tole S, Goudreau G, Assimacopoulos S, Grove EA (2000) Emx2 is required for growth of the hippocampus but not for hippocampal field specification. J Neurosci 20:2618-2625.

Toresson H, Potter SS, Campbell K (2000) Genetic control of dorsal-ventral identity in the telencephalon: opposing roles for Pax6 and Gsh2. Development 127:4361-4371.

Treit D, Menard J (1997) Dissociations among the anxiolytic effects of septal, hippocampal, and amygdaloid lesions. Behav Neurosci 111:653-658.

Treit D, Pesold C, Rotzinger S (1993a) Dissociating the anti-fear effects of septal and amygdaloid lesions using two pharmacologically validated models of rat anxiety. Behav Neurosci 107:770-785.

Treit D, Pesold C, Rotzinger S (1993b) Noninteractive effects of diazepam and amygdaloid lesions in two animal models of anxiety. Behav Neurosci 107:1099-1105.

Tronche F, Kellendonk C, Kretz O, Gass P, Anlag K, Orban PC, Bock R, Klein R, Schutz G (1999) Disruption of the glucocorticoid receptor gene in the nervous system results in reduced anxiety. Nat Genet 23:99-103.

Tseng KY, Chambers RA, Lipska BK (2008a) The neonatal ventral hippocampal lesion as a heuristic neurodevelopmental model of schizophrenia. Behav Brain Res.

Tseng KY, Lewis BL, Hashimoto T, Sesack SR, Kloc M, Lewis DA, O'Donnell P (2008b) A neonatal ventral hippocampal lesion causes functional deficits in adult prefrontal cortical interneurons. J Neurosci 28:12691-12699.
Uemura A, Kusuhara S, Wiegand SJ, Yu RT, Nishikawa S (2006) Tlx acts as a proangiogenic switch by regulating extracellular assembly of fibronectin matrices in retinal astrocytes. J Clin Invest 116:369-377.
Uyeda CT, Eng LF, Bignami A (1972) Immunological study of the glial fibrillary acidic protein. Brain Res 37:81-89.
Valcanis H, Tan SS (2003) Layer specification of transplanted interneurons in developing mouse neocortex. J Neurosci 23:5113-5122.
Verney C, Baulac M, Berger B, Alvarez C, Vigny A, Helle KB (1985) Morphological evidence for a dopaminergic terminal field in the hippocampal formation of young and adult rat. Neuroscience 14:1039-1052.
Voigt T (1989) Development of glial cells in the cerebral wall of ferrets: direct tracing of their transformation from radial glia into astrocytes. J Comp Neurol 289:74-88.
Volpe BT, Davis HP, Towle A, Dunlap WP (1992) Loss of hippocampal CA1 pyramidal neurons correlates with memory impairment in rats with ischemic or neurotoxin lesions. Behav Neurosci 106:457-464.
von Bohlen Und Halbach O (2007) Immunohistological markers for staging neurogenesis in adult hippocampus. Cell Tissue Res 329:409-420.
Vorhees CV, Williams MT (2006) Morris water maze: procedures for assessing spatial and related forms of learning and memory. Nat Protoc 1:848-858.
Wallace MN (1987) Histochemical demonstration of sensory maps in the rat and mouse cerebral cortex. Brain Res 418:178-182.
Ware CB, Horowitz MC, Renshaw BR, Hunt JS, Liggitt D, Koblar SA, Gliniak BC, McKenna HJ, Papayannopoulou T, Thoma B, et al. (1995) Targeted disruption of the low-affinity leukemia inhibitory factor receptor gene causes placental, skeletal, neural and metabolic defects and results in perinatal death. Development 121:1283-1299.
Webster MJ, Knable MB, Johnston-Wilson N, Nagata K, Inagaki M, Yolken RH (2001) Immunohistochemical localization of phosphorylated glial fibrillary acidic protein in the prefrontal cortex and hippocampus from patients with schizophrenia, bipolar disorder, and depression. Brain Behav Immun 15:388-400.
Wichterle H, Alvarez-Dolado M, Erskine L, Alvarez-Buylla A (2003) Permissive corridor and diffusible gradients direct medial ganglionic eminence cell migration to the neocortex. Proc Natl Acad Sci U S A 100:727-732.
Wichterle H, Turnbull DH, Nery S, Fishell G, Alvarez-Buylla A (2001) In utero fate mapping reveals distinct migratory pathways and fates of neurons born in the mammalian basal forebrain. Development 128:3759-3771.
Wiesel TN, Hubel DH (1963) Single-Cell Responses In Striate Cortex Of Kittens Deprived Of Vision In One Eye. J Neurophysiol 26:1003-1017.
Wilkinson DG (1992) Whole mount in situ hybridization of vertebrate embryos. In: In situ hybridization: a practical approach (Wilkinson DG, ed), pp 75-83. New York, NY: Oxford University Press.
Williams BP, Price J (1995) Evidence for multiple precursor cell types in the embryonic rat cerebral cortex. Neuron 14:1181-1188.

Wilson SW, Rubenstein JL (2000) Induction and dorsoventral patterning of the telencephalon. Neuron 28:641-651.
Woods CG, Bond J, Enard W (2005) Autosomal recessive primary microcephaly (MCPH): a review of clinical, molecular, and evolutionary findings. Am J Hum Genet 76:717-728.
Wrobel CN, Mutch CA, Swaminathan S, Taketo MM, Chenn A (2007) Persistent expression of stabilized beta-catenin delays maturation of radial glial cells into intermediate progenitors. Dev Biol 309:285-297.
Xu Q, Wonders CP, Anderson SA (2005) Sonic hedgehog maintains the identity of cortical interneuron progenitors in the ventral telencephalon. Development 132:4987-4998.
Xu Q, Tam M, Anderson SA (2008) Fate mapping Nkx2.1-lineage cells in the mouse telencephalon. J Comp Neurol 506:16-29.
Xu Q, Cobos I, De La Cruz E, Rubenstein JL, Anderson SA (2004) Origins of cortical interneuron subtypes. J Neurosci 24:2612-2622.
Yasui Y, Saper CB, Cechetto DF (1991) Calcitonin gene-related peptide (CGRP) immunoreactive projections from the thalamus to the striatum and amygdala in the rat. J Comp Neurol 308:293-310.
Yokoyama A, Takezawa S, Schule R, Kitagawa H, Kato S (2008) Transrepressive function of TLX requires the histone demethylase LSD1. Mol Cell Biol 28:3995-4003.
Yoon K, Gaiano N (2005) Notch signaling in the mammalian central nervous system: insights from mouse mutants. Nat Neurosci 8:709-715.
Young KA, Berry ML, Mahaffey CL, Saionz JR, Hawes NL, Chang B, Zheng QY, Smith RS, Bronson RT, Nelson RJ, Simpson EM (2002) Fierce: a new mouse deletion of Nr2e1; violent behaviour and ocular abnormalities are background-dependent. Behav Brain Res 132:145-158.
Younossi-Hartenstein A, Green P, Liaw GJ, Rudolph K, Lengyel J, Hartenstein V (1997) Control of early neurogenesis of the Drosophila brain by the head gap genes tll, otd, ems, and btd. Dev Biol 182:270-283.
Yu RT, McKeown M, Evans RM, Umesono K (1994) Relationship between Drosophila gap gene tailless and a vertebrate nuclear receptor Tlx. Nature 370:375-379.
Yu RT, Chiang MY, Tanabe T, Kobayashi M, Yasuda K, Evans RM, Umesono K (2000) The orphan nuclear receptor Tlx regulates Pax2 and is essential for vision. Proc Natl Acad Sci U S A 97:2621-2625.
Yue T, Xian K, Hurlock E, Xin M, Kernie SG, Parada LF, Lu QR (2006) A critical role for dorsal progenitors in cortical myelination. J Neurosci 26:1275-1280.
Yun K, Potter S, Rubenstein JL (2001) Gsh2 and Pax6 play complementary roles in dorsoventral patterning of the mammalian telencephalon. Development 128:193-205.
Yun ME, Johnson RR, Antic A, Donoghue MJ (2003) EphA family gene expression in the developing mouse neocortex: regional patterns reveal intrinsic programs and extrinsic influence. J Comp Neurol 456:203-216.
Zeitlin SG, Barber CM, Allis CD, Sullivan KF (2001) Differential regulation of CENP-A and histone H3 phosphorylation in G2/M. J Cell Sci 114:653-661.
Zembrzycki A, Griesel G, Stoykova A, Mansouri A (2007) Genetic interplay between the transcription factors Sp8 and Emx2 in the patterning of the forebrain. Neural Dev 2:8.
Zhang CL, Zou Y, Yu RT, Gage FH, Evans RM (2006) Nuclear receptor TLX prevents retinal dystrophy and recruits the corepressor atrophin1. Genes Dev 20:1308-1320.

Zhang CL, Zou Y, He W, Gage FH, Evans RM (2008) A role for adult TLX-positive neural stem cells in learning and behaviour. Nature 451:1004-1007.

Zhao C, Sun G, Li S, Shi Y (2009) A feedback regulatory loop involving microRNA-9 and nuclear receptor TLX in neural stem cell fate determination. Nat Struct Mol Biol 16:365-371.

Zhao S, Edwards J, Carroll J, Wiedholz L, Millstein RA, Jaing C, Murphy DL, Lanthorn TH, Holmes A (2006) Insertion mutation at the C-terminus of the serotonin transporter disrupts brain serotonin function and emotion-related behaviors in mice. Neuroscience 140:321-334.

Zhou C, Tsai SY, Tsai MJ (2001) COUP-TFI: an intrinsic factor for early regionalization of the neocortex. Genes Dev 15:2054-2059.

Zimmer C, Tiveron MC, Bodmer R, Cremer H (2004) Dynamics of Cux2 expression suggests that an early pool of SVZ precursors is fated to become upper cortical layer neurons. Cereb Cortex 14:1408-1420.

Zimmerman L, Parr B, Lendahl U, Cunningham M, McKay R, Gavin B, Mann J, Vassileva G, McMahon A (1994) Independent regulatory elements in the nestin gene direct transgene expression to neural stem cells or muscle precursors. Neuron 12:11-24.